Measurement and Modelling of the Fire Behaviour of Composite Laminates

This thesis is submitted with the requirements of Newcastle University
for the degree of Doctor of Philosophy.

By

Awad Elsaber Elmughrabi

Centre for Composite Materials Engineering,
School of Mechanical and Systems Engineering,
Newcastle University.

November 2008

NEWCASTLE UNIVERSITY LIBRARY
207 32598 2
Thesis L8955

Acknowledgements

Firstly, I wish to express my thanks to the Libyan Higher Education Secretary and the Culture Affairs Department of the Libyan People's Bureau in London for providing the managerial and financial support during my PhD study at Newcastle University.

I am heartily grateful to Professor A.G. Gibson for his supervision, continued support enthusiasm and invaluable help during the research. I also would like to thank Professor Mark Robinson for his comments and advice.

I would like to thank all staff in the School of Mechanical and System Engineering and Centre for Composite Material Engineering at Newcastle University, Mr. R. Jensen, Dr. Yongshu Wu and Dr. N. Dodds for their help.

Lastly, but not least, appreciation and many thanks is extended to my wife and my children for their continued support, overwhelming encouragement and patience during the period of my research.

Abstract

This thesis describes the measurement and modelling of the fire reaction and resistance properties of fibre glass polyester and vinyl ester composite laminates.

A new small-scale loading frame was designed and fabricated to apply tensile and compressive stresses in a cone calorimeter under a constant heat flux of 75 kW/m^2. It was found, for the first time, that stress has a small but significant effect on the fire reaction properties. Increasing tensile stress increased heat release rate and smoke production, while shortening the time-to-ignition. Compressive stress had the reverse effect. This was attributed to the fact that tensile stress promotes the formation of matrix microcracks, facilitating the evolution of flammable volatiles. This hypothesis is further supported by the observation that stress has the greatest effect on the early heat and smoke release peaks, with a lower effect on the final 'run-out' values.

Another new small scale testing rig was developed along with a calibrated conical radiant heater, which resembles the cone calorimeter's heater, to allow testing composite laminates at high tensile and compressive stresses. Stress rupture (time-to-failure) curves were produced. It was shown that, in tension, the behaviour was fibre dominated, with failure times roughly ten times those in compression. Compressive failure involved resin dominated local fibre kinking initiated near the cold face and was controlled by the matrix glass transition temperature.

The existing thermal model was upgraded to include the mass flux effect into the net total energy on the hot face of the composite laminate at flashover. This novel approach has resulted in very good predictions of the most important fire reaction properties obtained from the cone calorimeter such as time-to-ignition, mass loss rate, heat release rate and flame-out time. In addition, the predicted temperature and resin content profiles combined with the temperature dependent properties values were used to model the failure times by applying a suitable empirical relationship. Good agreement was found.

TABLE OF CONTENTS

ABSTRACT **1**

CHAPTER 1 INTRODUCTION **7**

CHAPTER 2 LITERATURE REVIEW **12**

2.1 General overview **12**

2.2 Reinforcing glass fibres **12**

2.3 Resin systems **15**

2.3.1 Polyester resin 16

2.3.2 Vinyl ester resins 17

2.4 Composite combustion process **18**

2.5 Fire damage of composites **19**

2.6 Characteristics of fire performance of composites **20**

2.6.1 Fire reaction 20

2.6.1.1 Cone calorimeter test (ISO 5660-1) *21*

2.6.1.2 Limiting Oxygen Index (LOI) ISO 4589, ASTM D 2863 ..... *22*

2.6.1.3 N.B.S. Smoke Chamber Test (ISO 5659-2, ASTM E 662) *23*

2.6.1.4 Radiant Panel Test (ASTM E 162) *24*

2.6.1.5 SBI (BS EN13823) / Room calorimeter test (ISO 9705) *25*

2.6.2 Fire resistance.....27

2.6.2.1 Furnace test.....*27*

2.6.2.2 Pool fire test.....*29*

2.6.2.3 Jet fire test.....*30*

2.7 Temperature effect on mechanical properties.....32

2.8 Modelling the composites behaviour in fire.....37

2.8.1 Heat conduction modelling.....38

2.8.2 Fire response modelling of composites.....39

2.8.2.1 Henderson model.....*40*

2.8.2.2 Simplified version of Henderson model.....*42*

2.9 Modelling fire behaviour of laminates under load.....44

2.9.1 The two layer model.....44

2.9.2 Laminate theory.....47

CHAPTER 3 EXPERIMENTAL METHODS.....52

3.1 Materials used.....52

3.2 Volume fraction determination.....52

3.3 Thermo-gravimetric Tests (TGA).....55

3.4 Cone calorimeter.....56

3.4.1 Main components 59

3.5 Small scale loading rig 60

3.6 Fire tests under high load 65

CHAPTER 4 RESULTS & DISCUSSION 69

4.1 Fire reaction properties 69

4.1.1 General 69

4.1.2 Time-to-ignition 69

4.1.3 Heat release rate 70

4.1.4 Smoke production 72

4.1.5 CO and CO_2 production 73

4.1.6 Mass loss 74

4.1.7 Effective heat of combustion.....74

4.2 Testing composite laminates under load using the cone calorimeter 76

4.2.1 Mechanical-thermal effect on fire reaction properties 76

4.2.1.1 Mechanical- thermal effect on heat release rate and time-to-ignition.....76

4.2.1.2 Mechanical-thermal effect on smoke evolution.....83

4.2.1.3 Time-to-failure 86

4.3 Fire resistance properties 90

4.3.1 Thermal insulation (rear face measurement).....90

4.3.2 Fire testing under load.....92

4.3.2.1 Tensile tests.....92

4.3.2.2 Compression tests.....95

4.3.2.3 Thermal forces and moments.....99

CHAPTER 5 MODELLING.....103

5.1 Preparation for thermal modelling.....103

5.1.1 Volume fraction determination.....103

5.1.2 Thermo-gravimetric Analysis (TGA).....103

5.2 Thermal model.....110

5.3 Effect of mass flux on the hot face at flashover.....114

5.4 Fire reaction modelling.....116

5.4.1 Mass loss.....116

5.4.2 Heat release rate.....119

5.4.3 Time-to-ignition.....124

5.5 Fire resistance modeling.....126

5.5.1 Temperature dependent properties.....126

5.5.2 Modelling time-to-failure.....127

5.5.3 Prediction of flame-out time 131

CHAPTER 6 CONCLUSIONS.....132

6.1 Fire reaction measurements 132

6.2 Fire reaction properties as function of stress.....132

6.3 Fire under load tests.....132

6.4 Modelling.....133

CHAPTER 7 FUTURE WORK 134

7.1 Thermal model.....134

7.2 Fire protection techniques 134

7.3 Equipment modification 134

7.4 Heat flux measurement.....135

REFERENCES.....136

LIST OF PUBLICATIONS.....151

APPENDIX 152

1 **Fitting with Gnuplot, Multi-branch fitting procedure 152**

2 **Thermal properties for glass vinyl ester and glass polyester composites....153**

3 **Engineering drawing of the small scale testing rig.....154**

Chapter 1 Introduction

Fibre reinforced polymers have been used in last few decades in various applications. They are used in many building, offshore platforms, transport and other infrastructure applications, both as light weight structural and non-structural components owing to their long term cost effectiveness, low thermal expansion, corrosion and chemical resistance, and high specific strength (tensile strength/density).

Despite the fact that composites will not replace the most used engineering materials like steel and aluminium alloys due to their anisotropic properties and poor impact damage tolerance, they pose a main challenge for these materials in many applications like aircraft, boat building, bridges, civil infrastructure and chemical industry. The driving force for the research in composite materials is to improve their structural performance, and reduce their total cost.

An inbuilt problem with composite materials is their poor performance in fire. This behaviour is related to the combustibility of their organic matrix and the connected risk from fire [1, 2]. Polyester, vinyl ester and epoxies are the most often used resins in structural applications. These polymers loose much of their stiffness and strength when they reach the glass transition temperature, which often lies in the range of 80 to 150°C. Higher temperatures, typically in excess of 400°C, result in decomposition and produce products that may burn. These products release heat, which contributes to fire growth. In addition, smoke and toxic fumes may be released, limiting visibility, hindering escape and thus constituting a further hazard and making fire-fighting a difficult task [3]. Also, this behaviour has led to concerns about the structural integrity of composite materials and the reduction in mechanical properties during and after fire.

Although the use of composites in applications where fire can occur, such as in aircraft cabins, ships, offshore drilling platforms, marine applications and transportation, is seriously affected by this behaviour, research has shown that polymer composite materials have good properties such as slow burn-through and excellent thermal insulation [4-6]. These properties take place as a result of the low thermal conductivity

and diffusivity of composites, the low thermal conductivity of the residual glass depleted of resin, the endothermic effect of the matrix decomposition, and the convectional cooling flow of volatiles towards the hot face. The heat absorption in the enothermic pyrolysis of the polymeric matrix can be considered as the most important factor contributing to composites integrity in fire.

In addition to these inherited properties, different methods have been shown to improve composites fire properties either by chemical modification of the polymer chains (reactive flame retardants) or by using additives [7]. The use of halogenated resins instead of the traditional resins can delay ignition [3, 8], but this can result in the possible production of toxic and corrosive smoke. Also, the addition of phosphorous promotes char formation [3]: the char holds the fire damaged laminates together, keeps the oxygen and heat away from resin, reduces the amount of volatile fumes and reduces decomposition endotherm. However, it can result in increased carbon monoxide levels at long times. Furthermore, the addition of alumina trihydrate (ATH) improves the fire performance [3, 9] and can mitigate the response of composites to fire: ATH decomposes at temperatures in the range of (200-400°C) producing water which provides an intumescing effect and blanket against oxygen, and the decomposition process itself is endothermic. Research demonstrated that the addition of ATH at a concentration of 60 parts per 100 parts of polyester resin almost doubled the time-to-ignition, reduced heat release rate to 50%, and cut smoke production by 25% [8]. Another strategy is to use polymers with high main chain aromatic content or phenolics [10]; they generally have longer ignition times, lower heat release rates and lower toxic products than the styrene based resins and a higher proportion of the resin remains as a carbonaceous char. The fire performance of composites can be improved further through surface modifications by using paints, gelcoats and intumescent paints [3] or by the use of very light weight protection layers.

The limitation of most of these methods is that the improvement to one fire property, such as ignitability, is usually accompanied by adverse effects to others such as toxic product generation, processability, appearance and mechanical properties [3, 11].

There is another issue related to the assessment of the organic matrix combustibility, which is normally carried out by a number of qualification tests. This assessment includes effects on ignitability, heat release, and production of smoke and toxic products (fire reaction properties). Also these tests are utilized to investigate the effects of heat flux and load on the thermal and mechanical integrity of composite structures (fire resistance properties). Fire resistance tests are generally larger in scale than fire reaction tests, and they are often required to characterise the performance over longer periods of time, often an hour or more, sometimes under load. Useful information, however, can be gained from the results of testing composites after fire exposure [1, 2, 12, 13]. The high cost of fire resistance tests is an important issue because they are usually used to qualify finished products in a large scale such as BS 476 [14]. This issue restricts industry to invest in product development research in order to find root solutions at early stages of design and material selection.

Recently it has been suggested, by a number of workers [13, 15-21] that fundamental information about fire resistance can be gained from relatively low cost, small-scale tests on samples under constant load, subject to constant one sided heat flux. Validating these tests with mathematical thermal and mechanical modelling may be sufficient to replace more expensive test methods.

A large amount of research has been performed to investigate and classify the flammability properties and structural behaviour of composites in fire, for example [5, 11, 13, 15, 19, 22-36]. It has been found possible to generate 'stress rupture' curves (i.e. curves relating the applied stress to the time-to-failure) for structures in fire, similar to the relationships more commonly employed for other types of environmental exposure, albeit with a shorter time scale.

Hitherto it has been assumed that thermal and mechanical effects on composites are separable. In other words, if the temperature and decomposition history of the material can be modelled using, say the Henderson Equation [4, 6] approach, and if properties can be modelled as a function of temperature and decomposition, then it should be possible to model the behaviour of the structure by summing, in an appropriate fashion,

the contribution of its parts. This assumption is equivalent to regarding the fire reaction behaviour of a structure as independent of the presence of stress. To date, however. there have been no reports on the effect of the applied stress on the fire reaction properties.

The work presented here allows the testing of composite laminate samples in a modified cone calorimeter under tensile and compressive loading, with the aim of measuring the effect of stress on fire reaction properties. Also, it shows the testing of small scale composite laminates under high loads using a specially designed apparatus under a fume extractor, with a calibrated conical radiant heater producing a constant heat flux.

The main objectives of this research are:

- To validate the newly developed loading rig that has been fitted to the cone calorimeter to test composite laminates in tension or compression.

- To study the effect of the tensile and compressive loads on fire reaction properties of glass reinforced polyester and vinyl ester laminates.

- To test small scale glass reinforced polyester and vinyl ester samples under high loads and constant calibrated radiant heat flux using a higher load testing rig.

- To model the most important fire reaction and fire resistance properties.

In this thesis, the literature is reviewed in chapter 2. This includes: a general view of composite materials and their constituents, the fire damage of composite materials, their fire performance on the basis of fire reaction and resistance properties, the effect of high temperature on the mechanical behaviour of composites, and the development of thermal and mechanical models to predict the behaviour of fibre reinforced composites in fire. Chapter 3 describes the cone calorimeter, its components and working principle. the newly developed small-scale loading rig, the materials used in the research and the

determination of the volume fraction, the kinetic parameters, and the higher loads testing rig. Chapter 4 presents the results of characterising vinyl ester and polyester laminates in terms of their fire reaction properties, the measurement of these properties as a function of applied tensile or compressive loads, and the determination of the fire resistance. The modelling of the main fire reaction and resistance properties is carried out in chapter 5. In Chapter 6 conclusions are drawn and recommendations for future work are suggested in Chapter 7.

Chapter 2 Literature Review

2.1 General overview

A composite material is a material system consisting of a mixture or a combination of two or more different materials which are insoluble in each other [37, 38].

Fibre reinforced composite materials are classified into four categories based on the matrix system used [39]. They are metal matrix composites, ceramic matrix composites, carbon-carbon composites and polymer matrix composites. Polymer matrix composites are made of thermoplastic and thermoset resins reinforced with fibres such as glass, carbon or boron.

2.2 Reinforcing glass fibres

Fibres have a small diameter ranging from 5-15 micrometers. In addition to their low density, fibres are stronger and stiffer than those used in bulk form. Flaws are likely to be present in the bulk form and mostly absent in fibre form. This reflects the lower strength of bulk glass. Approximately 90% of the structural applications are based on glass fibres [40].

The surrounding matrix enables fibres to contribute to the major part of the tensile, compressive, flextural or shear strength and stiffness of FRP composites. The "composite action" between the reinforcement and the matrix works to distribute loads evenly through the whole material.

Glass fibers are made by a direct melting process using silica sand, limestone, fluorspar, boric acid and clay. Different glass grades, such as E-glass, C-glass, S-glass, can be obtained by varying the amount of raw materials and processing parameters.

This research is concerned with E-glass fibre as the reinforcement material. Some of E-glass properties are listed in Table 2.1.

Table 2.1 Typical properties of E-glass [37]

	Typical diameter (μm)	*Specific gravity*	*Tensile modulus (GPa)*	*Tensile strength (GPa)*	*Ultimate elongation %*	*Thermal expansion coefficient 10^{-6}/°C*
E-glass	10	2.54	72.4	3.45	4.8	5

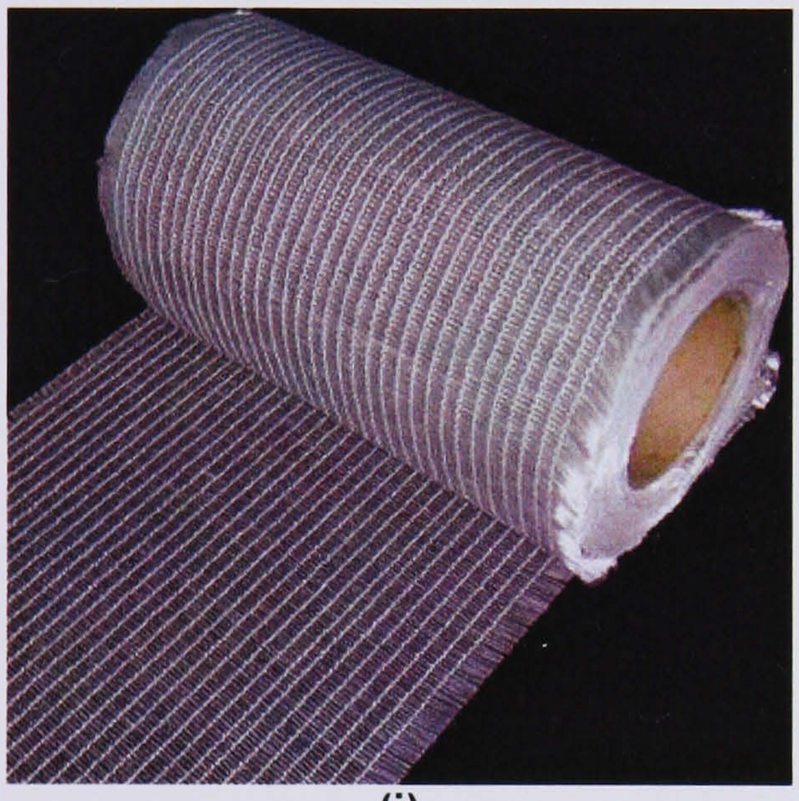
E-glass fibres have low strength to weight ratio and are inexpensive to produce compared with other fibres. However, these fibres like other glass fibres, could suffer from the environmental effects. Schutte [41] reviewed the effect of environmental moisture attack on the properties of glass fibres. He concluded that this attack can degrade the glass fibre strength: plasticize, swell, or microcrack the resin, and affect the fibre-resin bond. The failure of glass fibres under environmental exposure depends on the presence of stress, type of stress, temperature, length of exposure time and glass composition. Hale et al. [42] found that the immersion of E-glass fibres in water at a temperature of 70°C caused some degradation of the fibres. In addition, other researchers [32] demonstrated that the exposure of glass fibres to high temperature (150°C till 650°C) reduces their strength significantly, even in the absence of stress. Corrosion is a plausible cause.

Stress corrosion is the combined effect of the corrosive environment and applied stress. It occurs more rapidly in alkaline or acidic media and the two proposed mechanisms for this phenomenon are [43, 44]: -

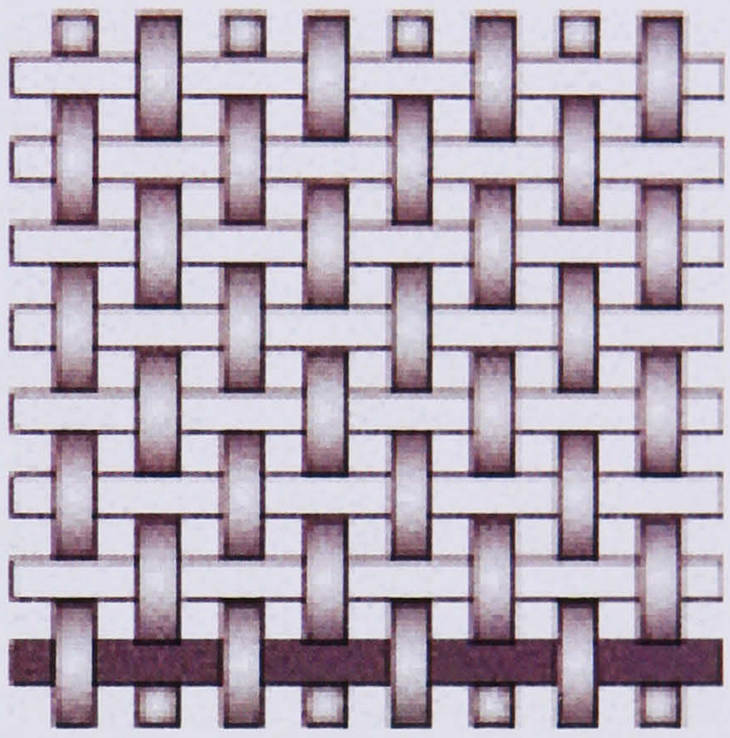
1. An ion exchange mechanism, where hydrogen from the surrounding medium substitutes the alkali ions in the glass, in particular Na^+.
2. The degradation and dissolution of silica network in the glass structure.

Agrawal & Broutman [44] explained the first mechanism as follows: the small singly charged hydrogen ions penetrate the glass fibres from the surrounding environment untill they find sodium ions. Then the sodium ions move to the surface and leave the glass. The volume of hydrogen ion is smaller than that of sodium it replaces and this leads to contraction in the molar volume. As a result of this contraction, the affected surface layer is prevented from shrinkage, by the bulk of glass fibres, which are not affected by the ion exchange. Consequently, tensile stresses are generated on the surface layer and then failure takes place, especially if the component is under stress already.

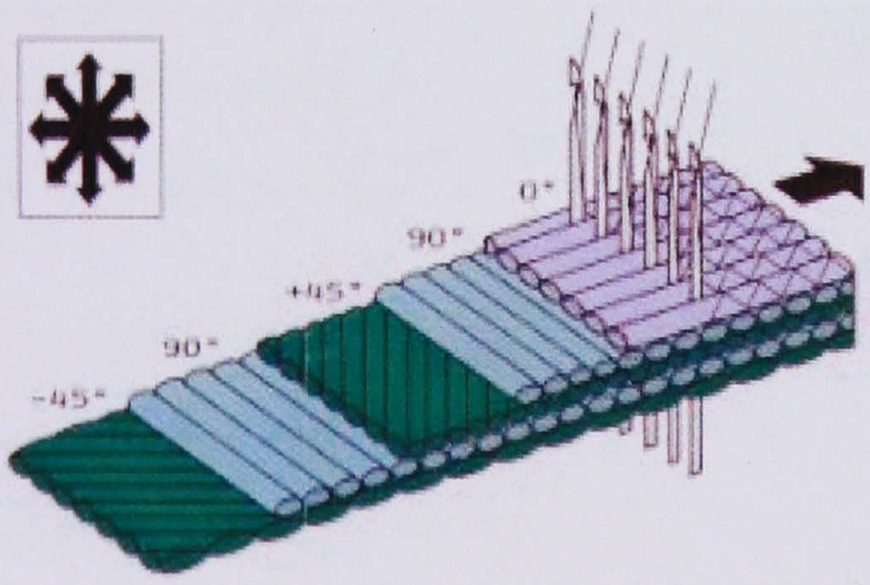
Almenara & Thornburrow [43] proposed that for short periods of time and at low concentrations and temperature the first mechanism dominates and it is mainly controlled by diffusion. After longer periods of time, and at high temperature and acid concentration, the silica network can dissolve. Therefore, resistance to stress corrosion can be improved by using glass fibres, which are resistance to chemical attack. It has been reported that AR-glass (Alkai Resistant Glass) are more corrosion-resistant than other types of glass [43]. Continuous fibres are available in four main forms as shown in Figure 2.1. Fibre orientation is used to categorise the fabric type.



(i)



(ii)



(iii)



(iv)

Figure 2.1 Main forms of continuous glass fibre (i) Unidirectional fibre glass cloth [45] (ii) Plain woven roving [46] (iii) Multiaxial fabrics [46] (iv) Roving [47]

2.3 Resin systems

The resin system used in composite materials has several tasks, such as binding the fibres together and keeping them in a proper position, transfer and distribute loads to fibres, and protect fibres from abrasion.

To carry out the above tasks, the resin system should have the following properties: -

1. Good mechanical properties.
2. Good adhesive properties.
3. Good toughness properties.
4. Good resistance to environmental degradation.

Polymers are classified into two main types: thermosetting and thermoplastic polymers according to the effect of heat on their processing and properties.

Thermosetting polymers are formed as a result of the chemical reaction, which takes place between the resin and the hardener (catalyst). The curing process is a non-reversible molecular cross-linking process to form a tightly bound rigid product. Cured thermosetting resins do not melt if heated, but their mechanical properties degrade if they are heated to a temperature above the glass transition temperature. In this case, the molecular structural behavior of thermoset resins change from a rigid glassy polymer to amorphous polymer.

In contrast, thermoplastics differ from thermosets in that they do not cure or set under heat [48]. They merely soften or melt when heated, and harden and solidify upon cooling the mould, and take the shape of the mould to get the required item. This process can be repeated as often as desired without any appreciable effect on the material properties in either state.

2.3.1 Polyester resin

Unsaturated polyester resins have a wide range of usage due to their low cost, good mechanical properties and chemical resistance [49, 50]. Polyester resins are unsaturated polymers of relatively low molecular weight containing carbon-carbon double bonds (or unsaturation) in the back-bone chain dissolved in an unsaturated monomer, which is usually styrene [15]. The styrene solvent performs the crucial function of enabling the resin to cure from liquid to a solid by cross-linking the molecular chain of the polyester. Also, the addition of sufficient amounts of styrene helps to make the resin easier to handle [51]. Polyesters can be produced by the reaction of alcohols, such as glycol and di-basic acids.

The most common types of polyester are orthophthalic and isophthalic. The orthophthalic polyester resins are used as general purpose economic resins. They are relatively prone to chemical attack and have lower mechanical properties. They are used in structural applications where the corrosion resistance is not an essential requirement. On the other hand, the isophthalic polyesters are frequently used in industries such as marine and oil industries due to their superior water resistance and mechanical properties [50].

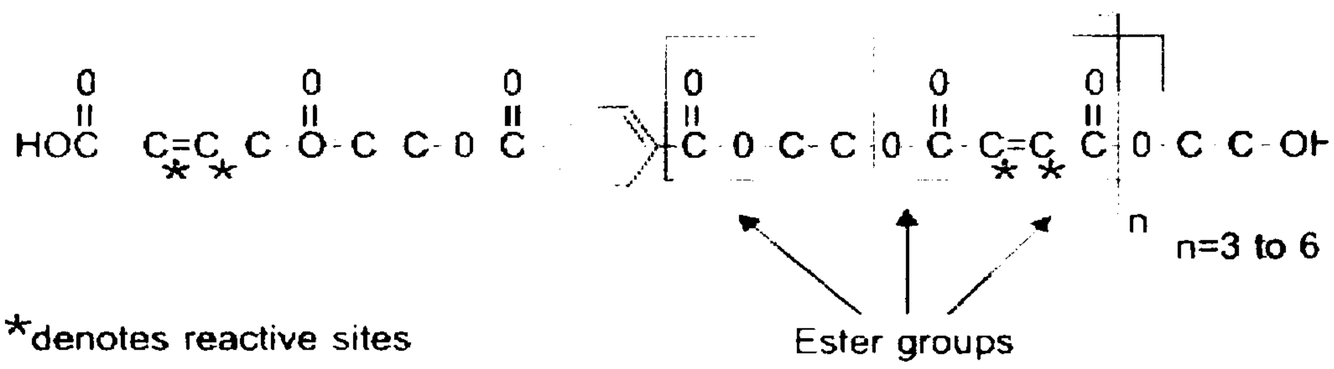


Figure 2.2 Idealised chemical structure of a typical isophthalic polyester [52]

2.3.2 Vinyl ester resins

The cost of vinyl esters is higher than polyester resins, although the molecular structure for both resin systems is similar. The location of the reactive sites is positioned at the ends of the molecular chains, which is different from that of polyesters. This makes vinyl esters tougher than polyesters as the whole length of the molecular chain exists to absorb shock loadings [52]. They also have better corrosion resistance than polyesters due to a lower number of ester groups, which are susceptible to water degradation by hydrolysis. See Figure 2.3. These properties allow vinyl ester resins to be frequently used in corrosion resistance applications such as pipelines, chemical storage tanks and marine industry.

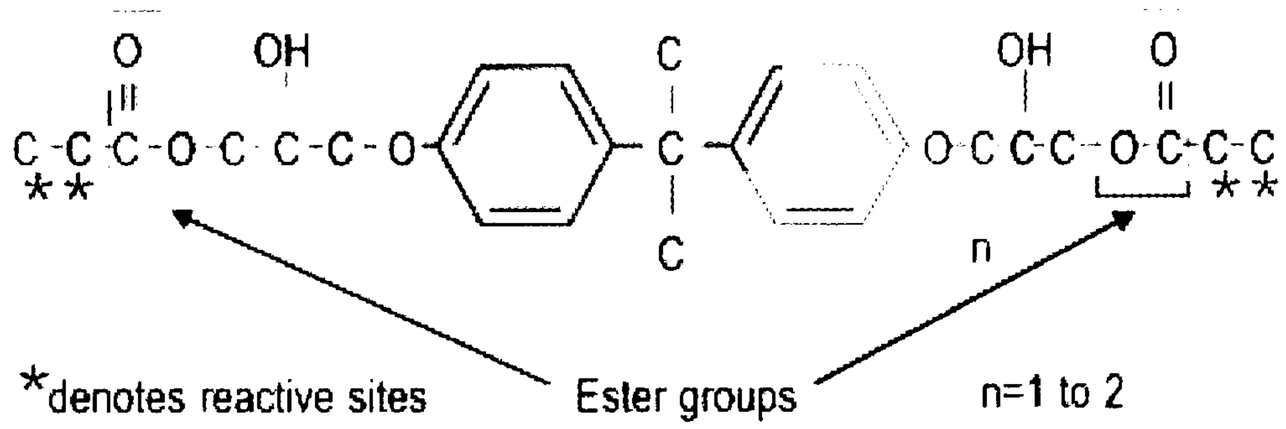


Figure 2.3 Idealised chemical structure of a typical epoxy based vinyl ester [52]

2.4 Composite combustion process

The initial decomposition and ignition of the polymeric matrix is driven by the applied heat, for example a fire [53]. This fire may come from any ignition source like an electric fault, overheated surfaces, burning debris, etc. The overall combustion process occurs as a result of coupled events: heating of the composite surface, decomposition, ignition and combustion.

At the beginning, the polymeric matrix is heated to a temperature at which it starts to decompose producing gaseous products. Some of these gaseous products enter the fire and undergo combustion in the gas phase and therefore more heat is liberated. Some of the heat is then transferred back to the polymeric matrix to accelerate the decomposition rate and produce more volatiles to sustain the combustion cycle. Figure 2.4 explains the mechanism controlling the fire behaviour of polymer composites.

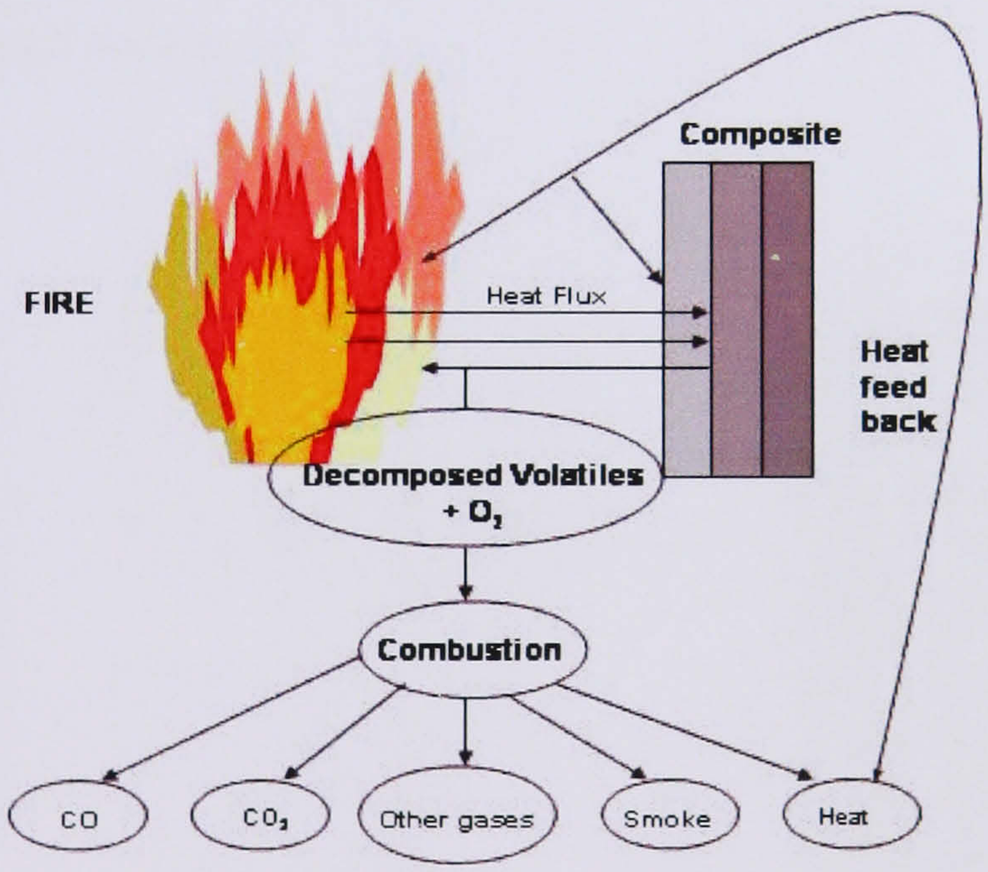


Figure 2.4 Mechanisms involved in the thermal decomposition of polymer composites

2.5 Fire damage of composites

Char formation, softening and degradation of the matrix and organic fibres, and delamination of plies, and matrix cracking, are the major types of fire damage [15]. Figure 2.5 shows a section for a fire damaged thick charring laminate (12 mm thick). As it can be seen, the resin/glass surface layer which is directly exposed to fire, is the first to suffer thermal degradation and is revealed as a black layer due to complete degradation of the matrix and the formation of char. Below this layer is the pyrolysis front region where the polymer matrix has been heated to above the decomposition reaction temperature but below the char formation temperature. In this region the matrix is partially degraded but the matrix has not been reduced to char and there has no evolution of combustion gases. Delamination cracks between the plies and fine matrix cracks within the plies are found below the decomposition zone [13]. Near the cold face area is the virgin material region where the laminate has not been affected by the fire because the temperature is too low to cause any softening or decomposition of the matrix. Progressive movement of the decomposition and char zones towards the cold face is noticed with increasing exposure time to fire. As a result, the composite matrix will be completely degraded to char.

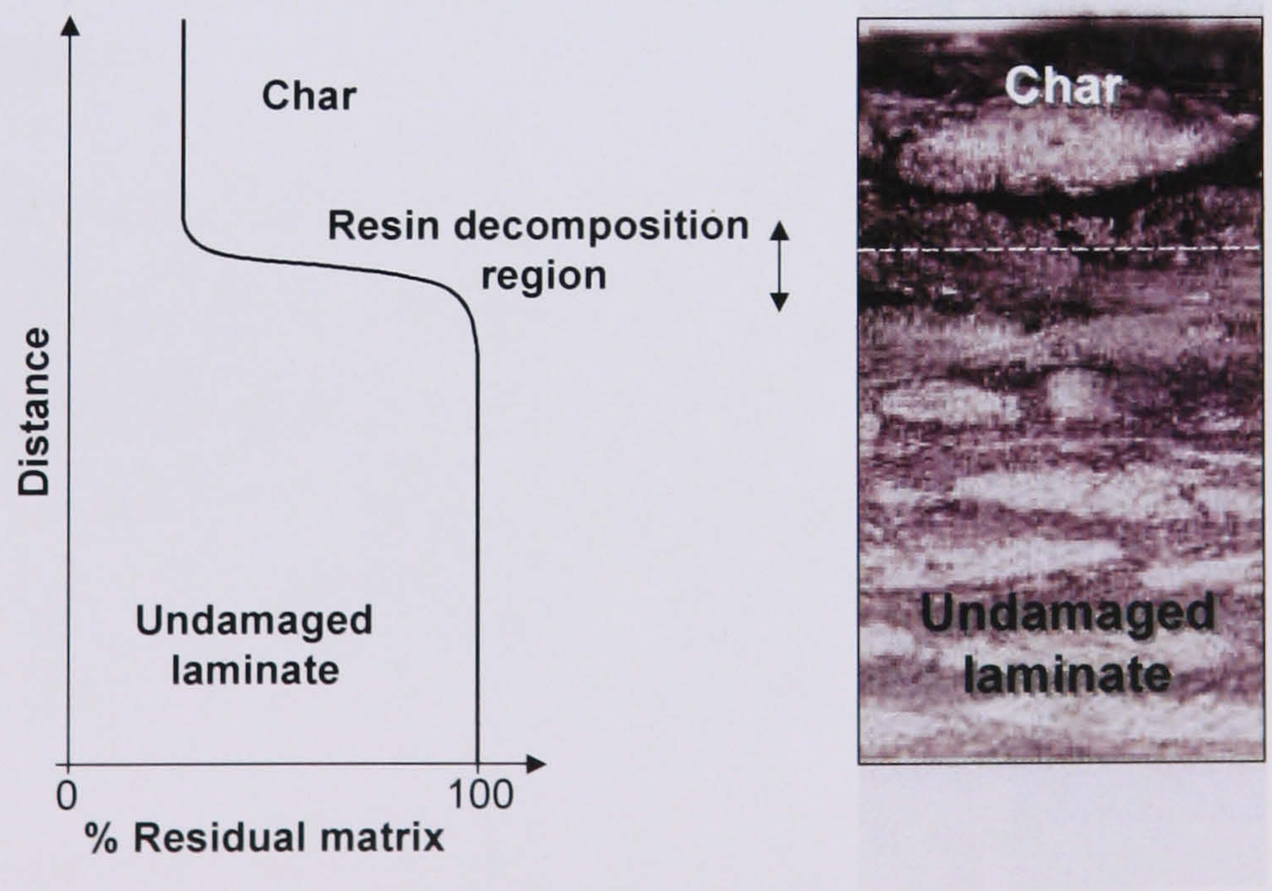


Figure 2.5 Section of a fire-damaged thick laminate showing the different damage zones. The variation in resin content through the laminate is shown schematically [15]

2.6 Characteristics of fire performance of composites

Fire performance of composites is normally classified on the basis of the fire reaction and fire resistance properties. Table 2.2 outlines these properties: -

Table 2.2 Summary of properties and tests relating to the fire performance of materials in structural applications [3]

Fire reaction properties	
Start up and progress of fire	Oxygen index Combustibility Time-to-ignition Surface spread of flame Peak heat release Average heat release
Human survivability	Smoke generation Toxicity index
Fire resistance properties	
	Pool fire tests Burner tests Furnace tests Jet fire tests

2.6.1 Fire reaction

Fire reaction defines the flammability and the response of composite materials to the fire particularly at its early stages, generally from ignition to flashover, and their effects on the surrounding environment. It considers the properties that are related to the start up and propagation of the fire, and the properties that are connected to human survivability as in the case of evolution of smoke and toxic gases that limit visibility and pose a safety hazard respectively [3, 15].

Bench scale tests are the main methods for fire reaction measurement. They are quick, inexpensive and usually provide consistent, reproducible data. These tests include the cone calorimeter, Ohio State University (OSU) heat release rate test, limiting oxygen

index (LOI) test, National Bureau of Standards (N.B.S.) smoke chamber. radiant panel. and smoke toxicity tests.

A drawback of many bench-scale tests is that they ignore the effects due to fire growth. Instead, they are said to relate "only to a snapshot of part of the overall fire behaviour of the test material" [54]. Another disadvantage is that the simulation of actual fires using bench-scale techniques (for example, heat release rate, air movements and the oxygen/fuel ratio that exist in actual fires) are often different to those in bench-scale fire tests, and this can substantially affect the measured fire reaction properties [55]. A further remark on bench-scale tests is that the entire sample is often completely consumed, whereas in real fires this may not happen, due to the reduced oxygen levels encountered within enclosed unventilated spaces. Properties such as flame spread need another equipment for testing; they can not be measured along with other properties such as heat release rate using the same equipment as in the cone calorimeter tests. However, fire reaction properties of large components can be measured using large scale tests such as single burning item test, intermediate scale cone calorimeter and room fire calorimeter test.

2.6.1.1 Cone calorimeter test (ISO 5660-1)

A large number of fire reaction properties can be determined using the cone calorimeter [56, 57]. Relatively small samples (100mm × 100mm × thickness up to 50 mm) are used for the test. It measures average heat release rate, peak heat release rate, time-to-ignition, effective heat of combustion, smoke density, mass loss rate and CO and CO_2 yields. It uses the oxygen consumption principle; the amount of oxygen consumed is directly proportional to heat release rate.

Materials can be fire tested at incident heat fluxes up to 100 kW/m^2. In this test the specimen is allowed to burn untill all the resin has decomposed and stopped flaming. The fire intensity scales from small bin fire for a heat flux of 25 kW/m^2 to significant room fire and hydrocarbon fire for 75 kW/m^2 and 100 kW/m^2, respectively. Detailed description of the cone calorimeter is discussed in section 3.4.

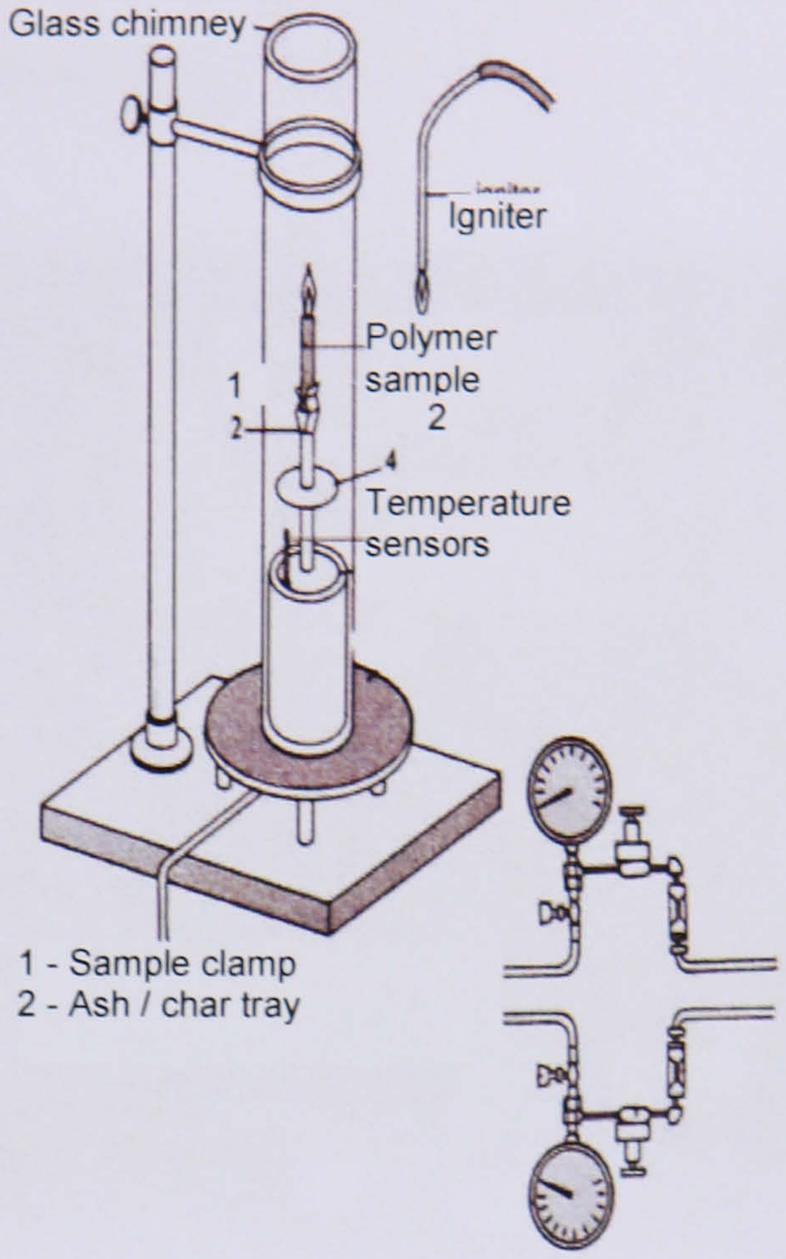


Figure 2.6 The cone calorimeter

2.6.1.2 Limiting Oxygen Index (LOI) ISO 4589, ASTM D 2863

The Limiting oxygen index [58] is measured by exposing the sample to an ignition source in a transparent glass chimney under different controlled oxygen levels. Rectangular samples of 7mm width by 120mm length and by 3mm thickness are used in this technique. The minimum oxygen percentage that enables the sample to burn with a candle like flame for 3 minutes is determined. Therefore, LOI can be considered as the minimum concentration of oxygen in an oxygen–nitrogen mixture, required to just support the downward burning of a vertically mounted test specimen [59, 60]. Despite the fact that the oxygen index is often used to describe the relative inflammability of polymers, it does not test the sample in a real fire environment [61]. A high limiting oxygen index represents a more difficult ignitable and flammable material (better flame retardancy). This test is not suitable for testing composite materials due to the presence of glass fibres, which can influence the burning of the tested sample and hence affecting the results.





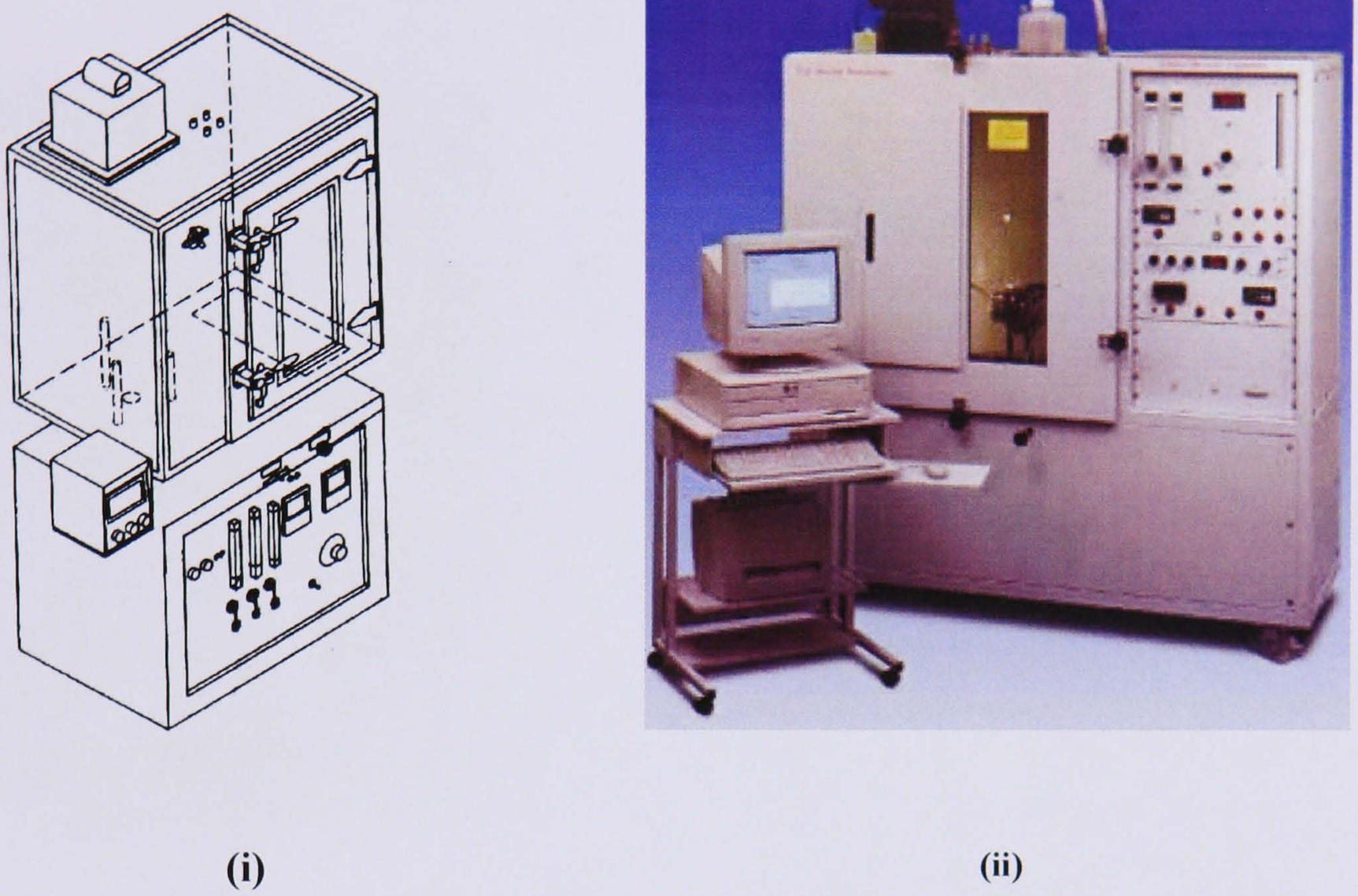
(i) **(ii)**

Figure 2.7 (i) Photograph [62], and (ii) Schematic diagram of the Limiting Oxygen Index test Equipment [63]

2.6.1.3 N.B.S. Smoke Chamber Test (ISO 5659-2, ASTM E 662)

A smoke unit is defined in ASTM E-176 [64] as "the concentration of smoke particulates in a cubic metre of air that reduces the percent transmission of light through 1-m path to 10%. SMOKE = standard metric optical kinetic emission". This test was developed at the National Bureau of Standards. Small scale samples (76.2mm × 76.2mm × up to 25.4mm thickness) are used in this technique. It is regarded as one of the most practical procedures to measure smoke obscuration [65]. The specimen is mounted in the vertical position, in a flaming or smoldering mode to allow the produced smoke to accumulate in the smoke collection chamber, facing an electric radiant heater that generates an incident heat flux of 25 kW/m^2. The heater of some N.B.S. Smoke

Chamber is modified so tests can be performed at variable heat fluxes up to 50 kW/m^2. The smoke optical density is measured over time using monochromatic laser light.



(i) (ii)

Figure 2.8 (i) Schematic diagram of the NBS smoke density chamber [66] and (ii) Photograph [67]

2.6.1.4 Radiant Panel Test (ASTM E 162)

A radiant panel test is used to determine the rate at which a flame front spreads down the surface of a burning specimen [68]. A flat sample is exposed to a heat flux produced by a (300mm × 460mm) gas-fired radiant heat source. The test panel is (150mm wide × 460mm height), and is inclined at an angle of 45° to the heating element. Ignition takes place at the upper edge of the specimen, and the time taken for the flame to travel down the panel is recorded along with the temperature rise in the stack. A flame spread index is calculated from this information in order to quantify the test material.

This test can be used to measure the flame spread for composite materials [69] and the most likely actual flame spread mode in composite materials is the rapid upward flame spread , which is different than the slower downward movement of the flame in the radiant panel testing. This observation poses a question as to the practical relevance of

this test to represent the actual scenario as the material that has a good flame spread resistance when tested in the downward mode may not have the same performance in actual upward spread [15].

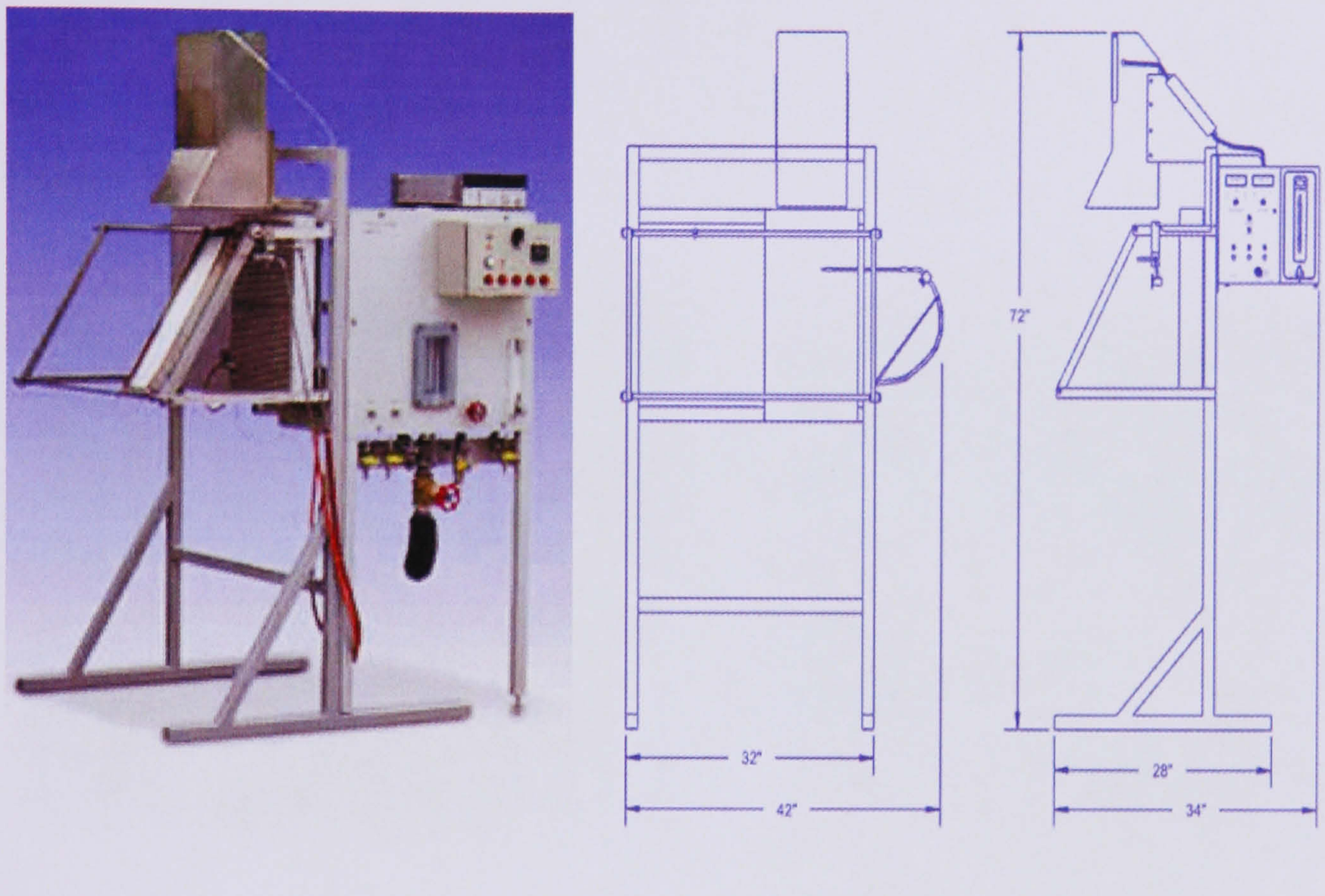
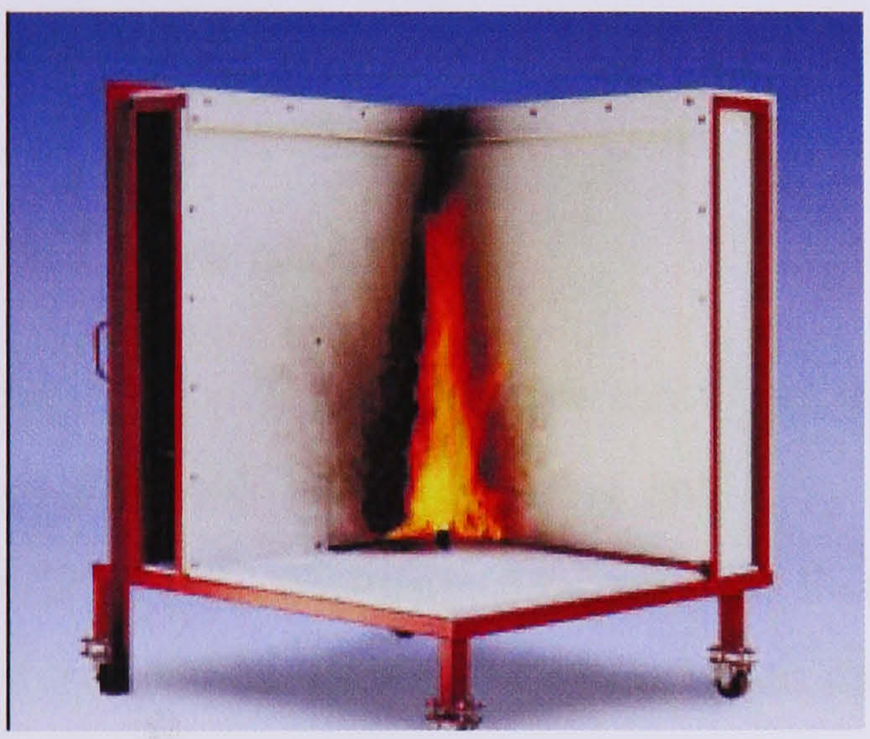


Figure 2.9 Photograph and schematic digram of the radiant panel test equipment [70]

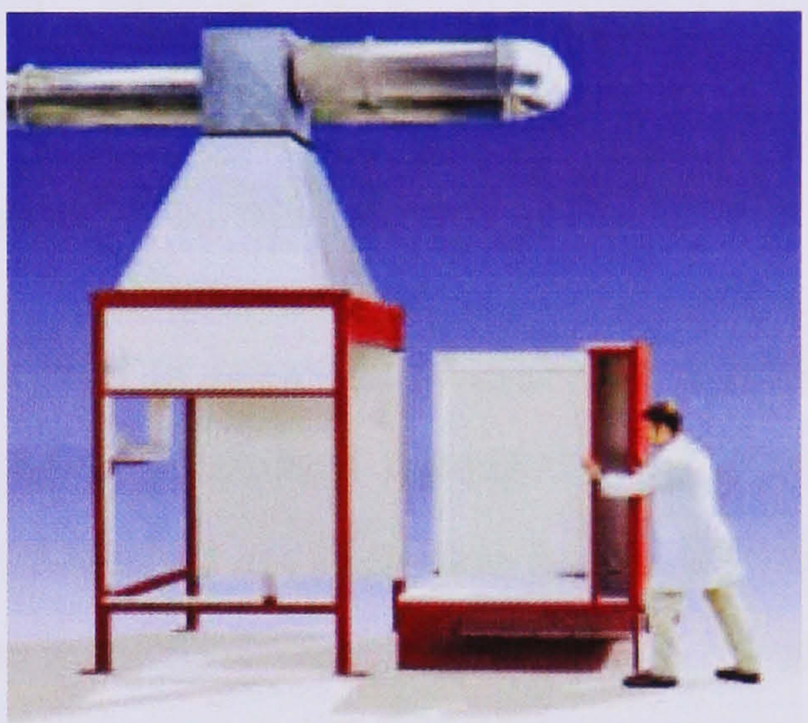
2.6.1.5 SBI (BS EN13823) / Room calorimeter test (ISO 9705)

Extrapolating the results of bench scale data such as the cone calorimeter to full scale items such as fire compartments and walls has been considered as a problem. This has lead to the development of intermediate scale tests. Single burning item test (SBI) [71] is mostly used to study the fire reaction properties of construction products (except floorings) including composite materials in their end use conditions as far as possible. It consists of two wall panels made of the test material (Figure 2.10 i and ii). One wall is 1.5m height × 1m wide and the second narrow wall is 1.5m height × 0.5m wide. A heat flux of 30 kW/m^2 is generated using a propane gas burner located in the corner, which

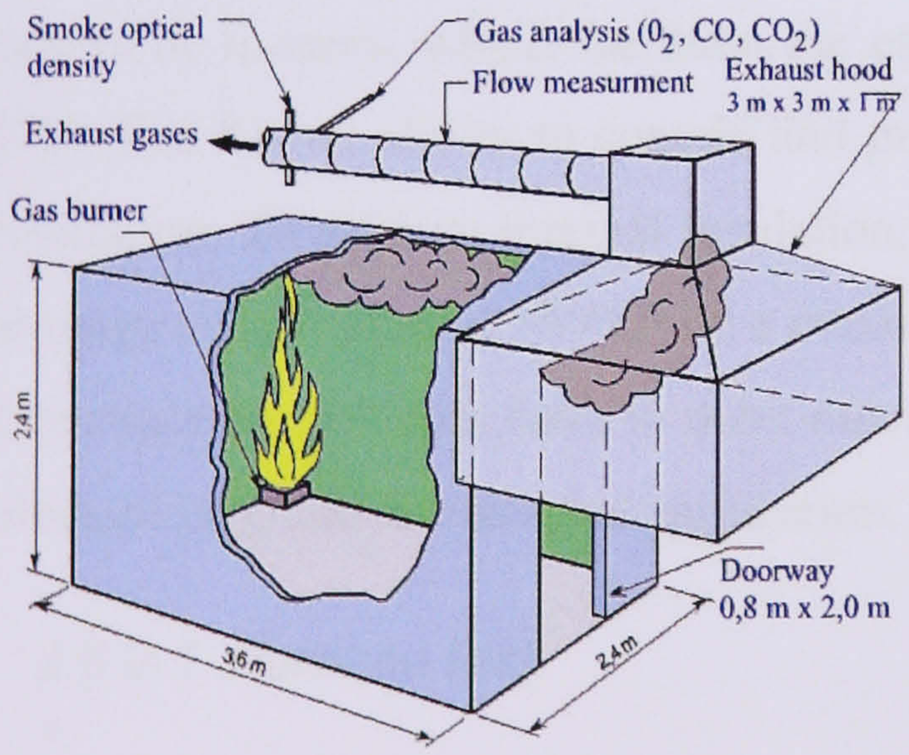
simulates the burning of a waste paper basket. The specimen is placed on a trolley beneath an exhaust system. There is a non-combustible floor but no ceiling. The fire reaction properties of the specimen are measured by physical and instrumental means. Heat release rate is calculated from the oxygen consumed during burning of the wall materials using the oxygen consumption principle. The time-to-ignition and flame spread rate are determined by visual observation. The temperature, air-flow rate, smoke density, O_2 and CO_2 concentrations are measured continuously using sensors inside the exhaust duct.



(i)



(ii)



(iii)



(iv)

Figure 2.10 (i & ii) General view of the SBI test [67], (iii & iv) Room calorimeter test [72]

ISO 9705 [73] outlines the procedure of conducting the room calorimeter test (Figure 2.10 iii and iv), which is one of the room fire tests. The fire room size is 3.6m long, 2.4m wide and 2.4m high. This room has an open doorway at one of the wall sides and there is a fume extractor just outside the doorway. The test panels are placed on the remaining side walls and the ceiling, as in the end use conditions. A propane burner is placed at one of the corners. This burner provides a heat flux of 100 kW/m^2 for the first ten minutes of the test and then increased to 300 kW/m^2 for another ten minutes. The fire reaction properties are measured in the same way as in SBI test.

The main drawbacks of these tests are the cost and the fact that they are not suitable for pultruded sections, pipes and different shapes other than flat sheets or panels.

2.6.2 Fire resistance

Fire resistance describes the capability of a material or structure to maintain mechanical and physical integrity during and after fire and to limit heat damage to other remote surfaces [3]. Stability, integrity and thermal insulation are the three failure criteria for fire resistance testing [74]. In order to meet the stability criterion, the structural element must bear the applied load during the test, without any sign of structural collapse. The requirement to meet the integrity criterion is that the test sample must not develop any cracks or fissures, which facilitate the escape of hot gases sufficient to cause ignition [75]. The barrier ability to contain and prevent fire spread is a measure of integrity and insulation. To achieve thermal insulation, the cold face temperature must not exceed an average temperature of 140°C and a maximum temperature of 180°C.

Construction elements have to meet one or more of the three criteria depending on the element type and its intended application.

2.6.2.1 Furnace test

In this technique [76], composite panels between 1 m^2 and 10 m^2 depending on the furnace size, are placed at the open end of a gas or electric furnace with thermocouples attached to the rear face. Controlled time-temperature heating curves are normally used in this test in order to measure the fire resistance of composites. Figure 2.11 shows the

cellulosic (ISO 834) [77] and hydrocarbon (BS 476-20/21) [14] heating curves that are often used.

The fire resistance of combustible materials is often defined by the time taken for the rear face temperature to reach 160°C at a single point, at which the fire is likely to spread to neighbouring rooms. Also, it is defined by the burn-through resistance, which represents the time taken by the fire to penetrate the composite material. Panels are tested in the end-use condition with the appropriate surface coatings, joints and other structural details to ensure a realistic test for the fire behaviour of a full-size composite structure. Furnace tests are also used to determine the structural integrity of loaded composite panels when exposed to fire. During fire testing the panel is subjected to a compressive and/or bending load.

Despite the fact that the furnace testing represents an actual fire scenario, it suffers from reproducibility as different results can be obtained from different furnaces and testing institutions [20, 78]. Figure 2.12 shows a photograph of furnace test facility.

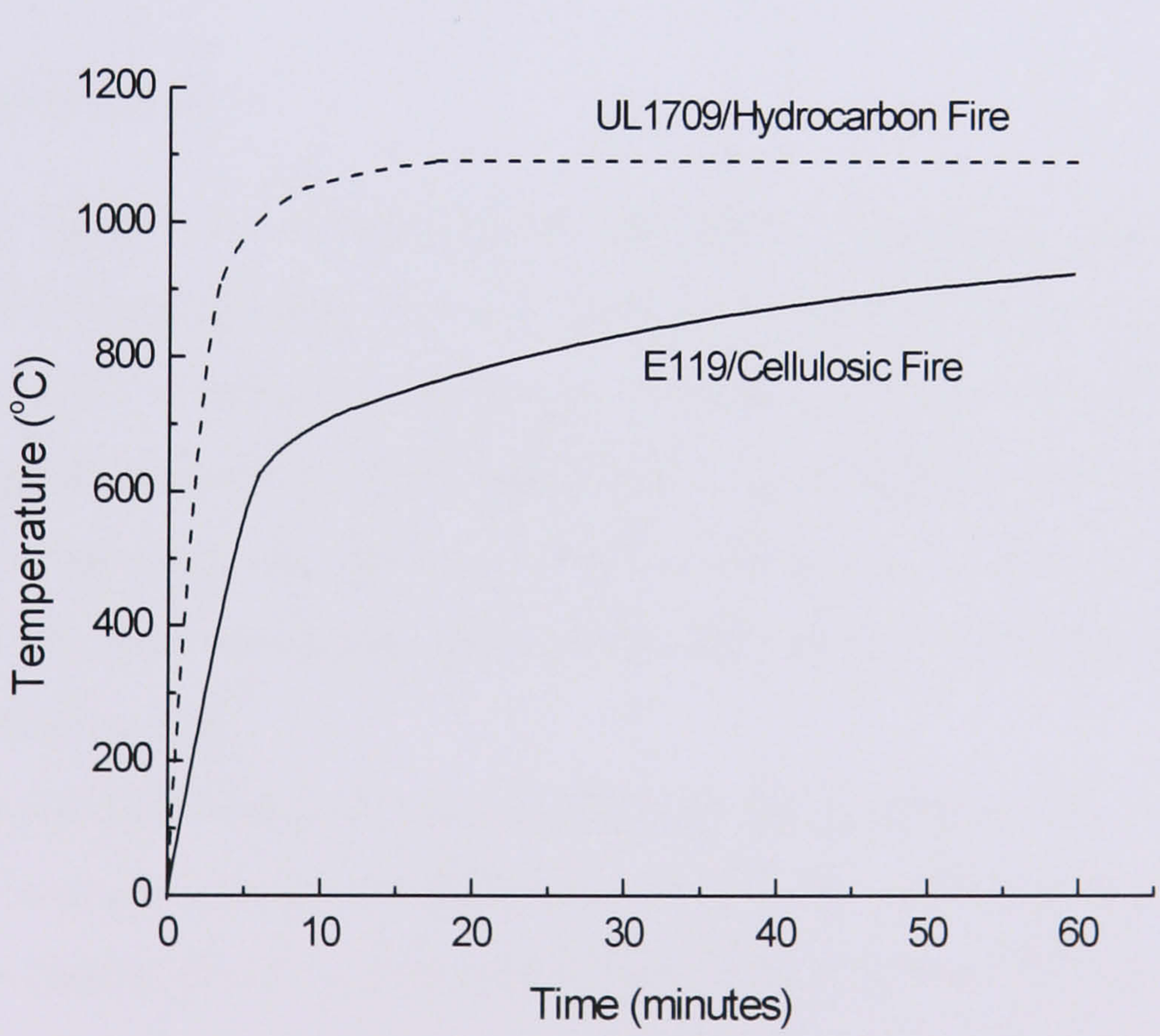


Figure 2.11 Standard test curves for furnace fire testing, according to the hydrocarbon fire and the cellulosic fire specifications [3, 14]

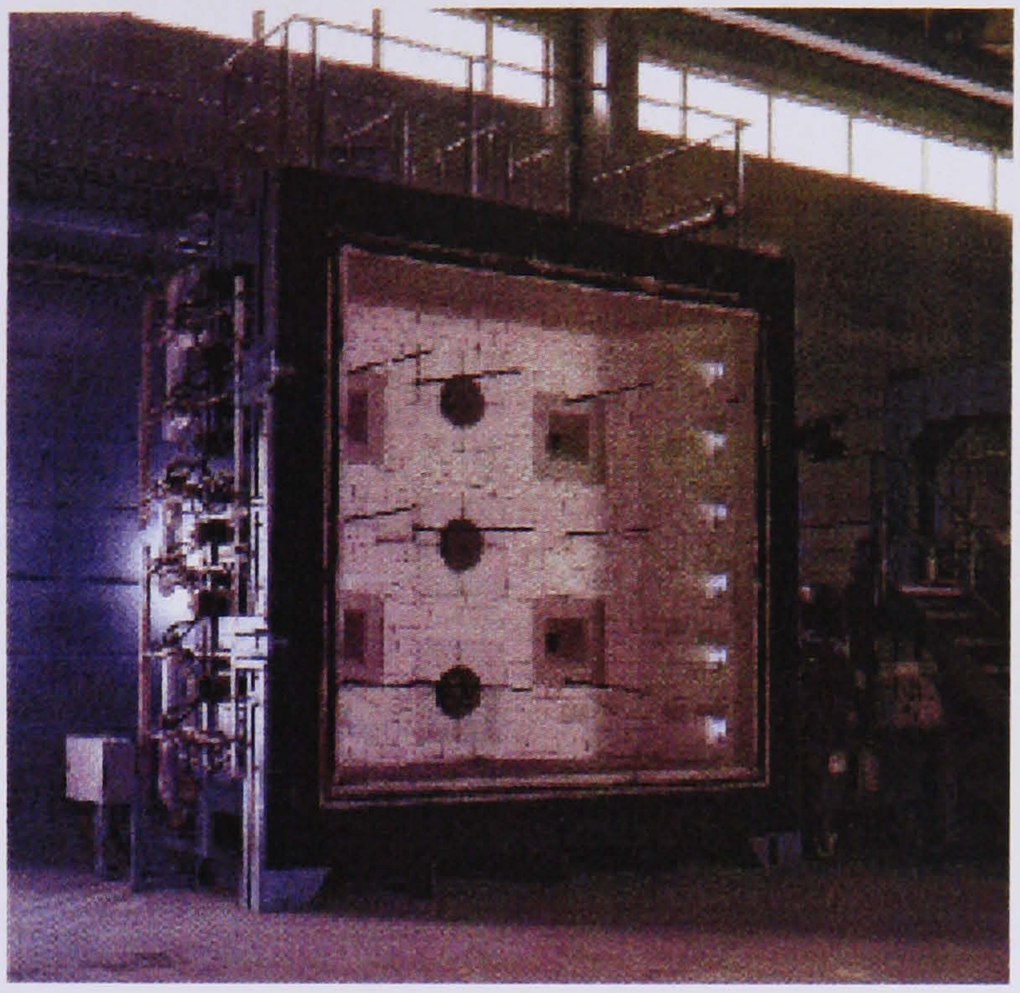


Figure 2.12 Photograph of the furnace test facility [79]

2.6.2.2 Pool fire test

Pool fire tests, Figure 2.13, are designed to simulate an accidental ignition that results from combustible liquid spillage or exposure of an open fuel tank to an ignition source. Pool fire tests consist of placing a section, sometimes under load, over a tray of a highly inflammable liquid, depending on the application. Heat transfer and structural integrity are measured throughout the test. It is enclosed because the smoke and hot gases accumulate at the wall boundaries and radiate heat back towards the fuel and hence increasing the burning rate.

It has been found that pool fires can exhibit two distinct flashovers. The initial one occurs at low temperature and the second hotter one takes place, when the heat of the fire begins to reflect back on itself, rapidly heating the remaining fuel [36].

A major drawback of the pool fire test is the difficulty in maintaining a steady heat from the fire. In addition, the presence of air streams and convectional currents will pose concerns on reproducibility.



Figure 2.13 Pool fire test [80]

2.6.2.3 Jet fire test

It is a very important burn-through fire resistive test. The rupture of a fuel container or gas pipe that produces high pressure flame can be simulated using jet fire test [59]. It is more severe and more damaging than pool fire test because it generates a high heat flux, which has an erosive effect due to the high gas velocity. Usually, the burn-through time or the time taken to loose the integrity and the increase in temperature of protected surfaces are measured in this test. The United States Navy considers the test material to have adequate fire resistance when the back-face temperature remains below 120°C after thirty minutes exposure [15]. Figure 2.14 show the largest jet fire rig, which is operated by British Gas, and is capable of directing a 20 meter long horizontal flame of burning natural gas onto the component under test. The test article is located about half-way down the flame length where it is subjected to a combination of high heat flux (~300 kW/m^2) and high gas jet velocity (~50 m/s) [15]. The specimen is exposed to the jet fire for a fixed time, and after testing the functionality and burn-through of the test article are assessed.



Figure 2.14 Jet fire test at British Gas Spadeadam facility [81], capable of directing a 20 meter long horizontal flame, producing a heat flux of ~300 kW/m^2 and 50 m/s velocity

Because full scale jet fire testing is extremely expensive, small to medium sized jet fire resistance tests, such as the propane burner test, have been developed [20, 82, 83]. These tests enable the test materials to be subjected to high heat flux and gas velocity at low cost. Figure 2.15 shows a small scale propane burner test.

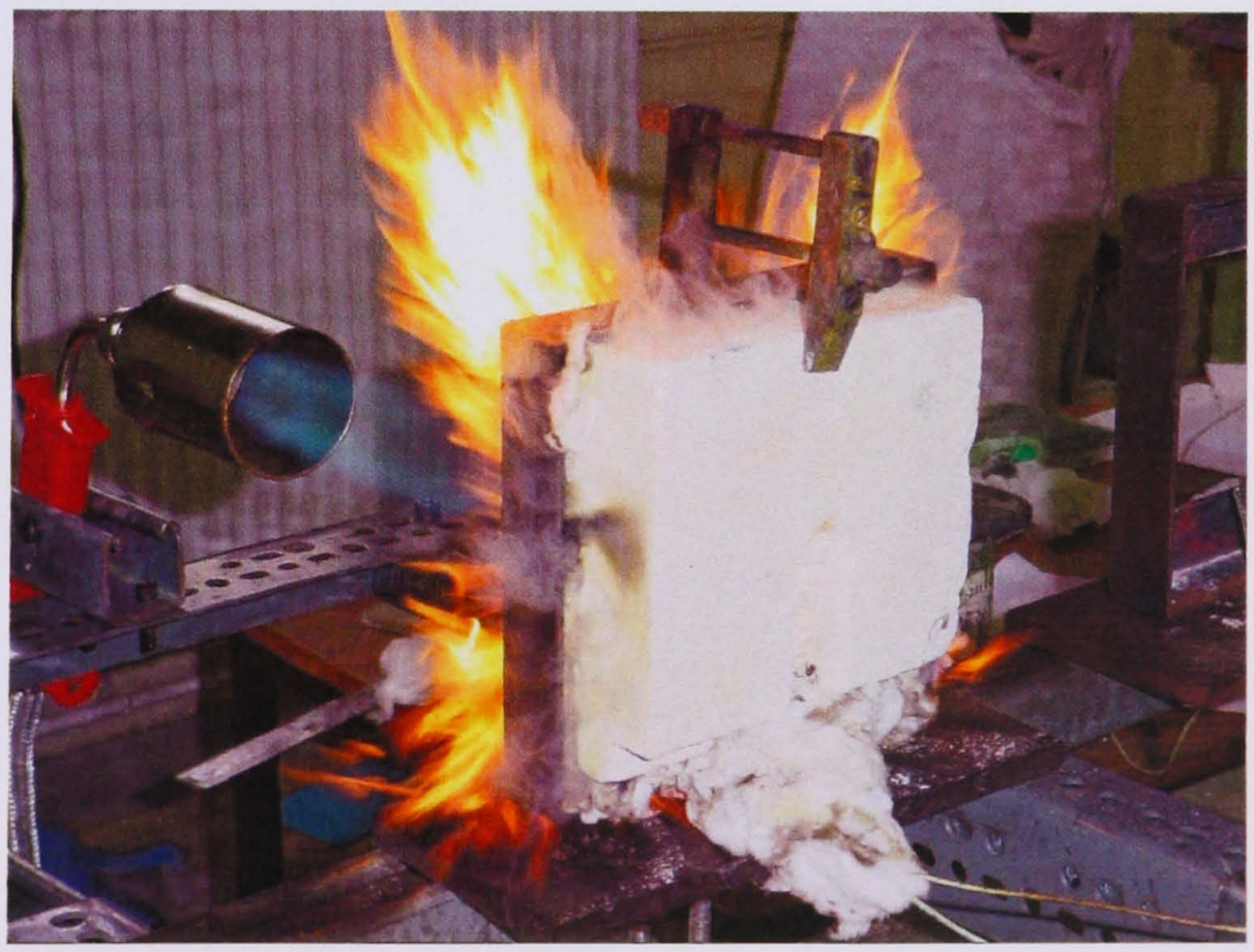


Figure 2.15 Small scale jet fire test (propane burner test) used for small scale samples and can produce a heat flux up to 200 kW/m^2 [20]

2.7 Temperature effect on mechanical properties

Mechanical properties of polymer composites, such as Young's modulus, shear modulus and compressive strength exhibit the behaviour shown in Figure 2.16, when exposed to temperature under isothermal conditions (ie. constant temperature through the material thickness) [15]. The unrelaxed property value (P_u) remains constant as at room temperature until it reaches the critical softening temperature (T_{cr}). Above the softening temperature the property decreases until it reaches the relaxed value (P_R). This decay in the property value occurs as a result of the thermal softening of the polymer matrix which occurs at lower temperature than the glass transition temperature. The glass transition temperature is the temperature at which the material changes its behaviour from glassy to rubbery behaviour. At temperatures above (T_m) the properties actually decrease very gradually below P_R due to further softening and (eventually) pyrolysis of the polymer.

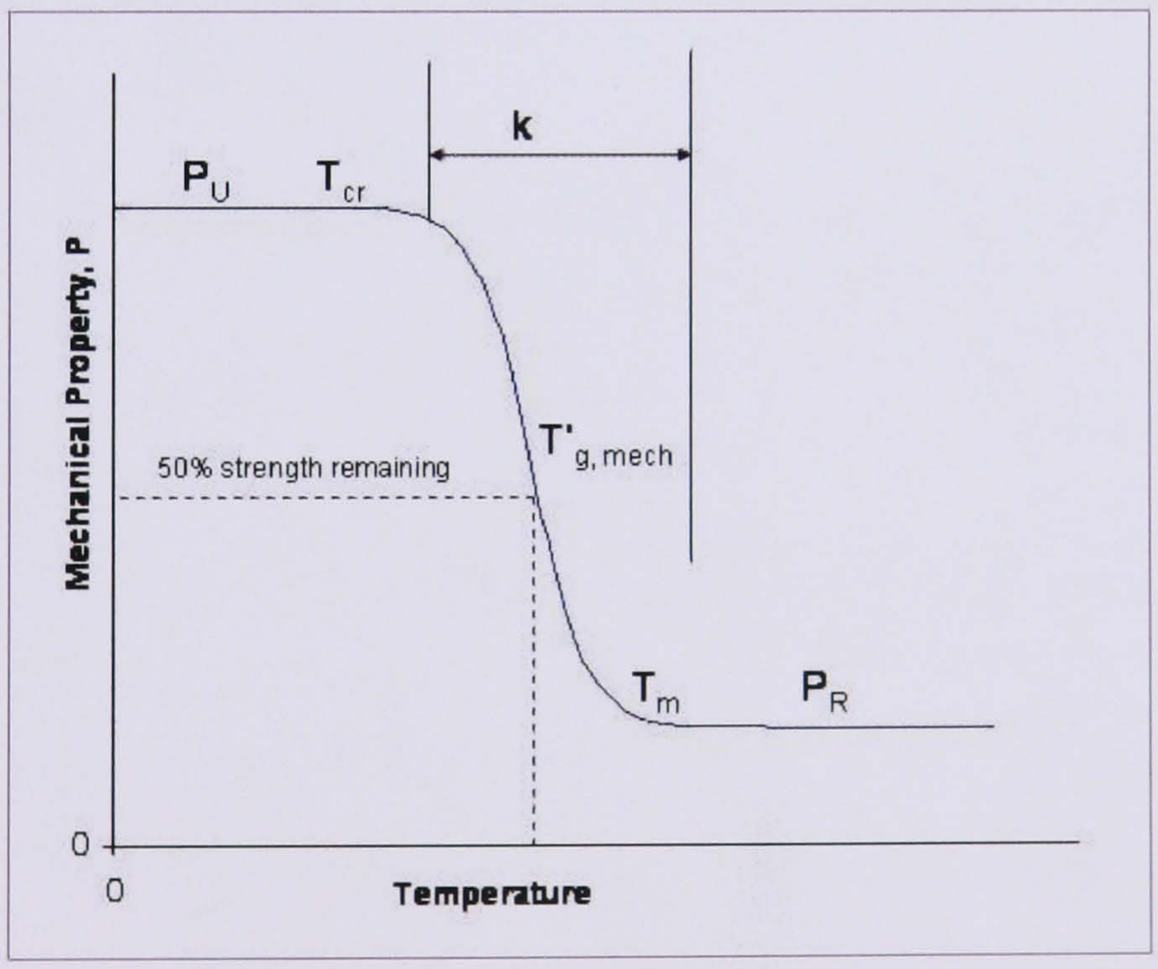


Figure 2.16 Schematic of the effect of temperature on the mechanical property of a laminate [15]. Increasing the temperature to and beyond the glass transition temperature reduces the mechanical strength

It has been assumed that all mechanical properties, including strength, for most thermosetting amorphous polymer composites follow the relationship presented in Figure 2.16. On heating, these materials undergo one transition before decomposition (ie. the glass transition temperature). The main task, therefore, was to find a relationship that can fit this transformation region in order to model all mechanical properties.

A polynomial in temperature would be a good method to represent the mechanical property, flextural modulus for example, in the transition region [12, 84]. Some workers [21, 85, 86] used the polynomial in temperature over a narrow thermal range to describe properties like young's modulus. However, this approach is found to be not suitable sometimes due to the need of polynomial of order five or six to describe the property as a function of temperature with sufficient accuracy. In addition, this approach would perform well within the range of fitted data only as demonstrated in Figure 2.17.

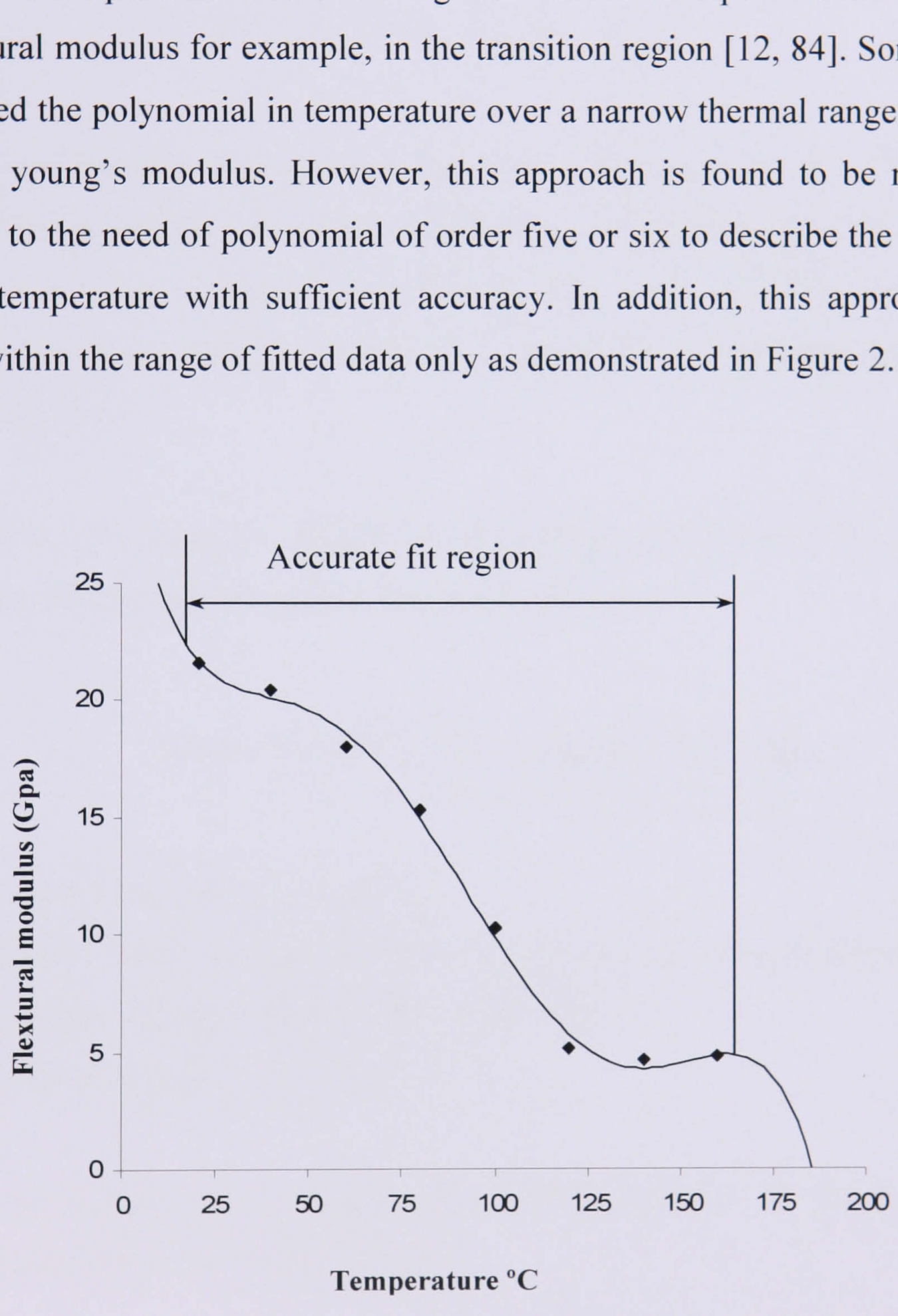


Figure 2.17 Flexural modulus results over a range of temperatures for a glass/polyester laminate. The fitted curve is a 5th order polynomial in temperature. Note that outside the measured data range, the polynomial fit loses accuracy [35]

Mahieux and Reifsnider [87, 88] assumed that temperature increase has the effect of increasing the breakage of intermolecular bonds in the resin. Cumulative Weibull distribution was used to model the bond strength as a function of temperature. They proposed the following relationship:

$$P(T) = P_R + (P_U - P_R)\,exp\left(-\left(\frac{T}{T_0}\right)^m\right) \qquad (2.1)$$

where, $P(T)$ is a particular property as a function of temperature, P_U and P_R are the unrelaxed (low temperature) and relaxed (high temperature) values of that property, respectively, T_0 is the relaxation temperature, and m is the Weibull exponent. Temperature is in Kelvin. Properties could be fit reasonably for most thermosets with m values in the range 9-21.

Gibson et al. [15, 19] found an empirical relationship based on the hyperbolic tanh function to fit the transformation region. The relationship is:

$$P(T) = P_R + \left(\frac{P_U - P_R}{2}\right) \cdot \left\{1 - \tanh\left[k \cdot \left(T - T_g\right)\right]\right\} \qquad (2.2)$$

where: $P(T)$ is a particular material property,

P_U and P_R are the un-relaxed and the relaxed property values respectively,

k is a constant relating to the breadth of the transition,

T_g is the glass transition temperature (°C).

To count for the residual resin content (RRC) using Equation 2.2, each mechanical property was modified by a power law factor.

$$P(T) = P_R + \left(\frac{P_U - P_R}{2}\right) \cdot \left\{1 - \tanh\left[k \cdot \left(T - T_g\right)\right]\right\} \cdot R^n \qquad (2.3)$$

where, R^n is the power law factor to count for resin decomposition.

Properties like compressive strength, shear modulus and Young's modulus clearly dependent on resin content of the composite materials. On the other hand, tensile strength is not resin dependent and mainly reflects the reinforcing fibre`s strength. It has been found [19] that the degradation in resin dependent properties was fitted using $n=1$, whereas for tensile strength $n=0$, which in turn brings Equation 2.3 back to Equation 2.2.

It has been reported [15, 35] that some composite materials have two relaxation stages when heated, such as polypropylene. Therefore, the proposed relationships in Equations 2.2 could not be used. Instead the above equation was modified to incorporate the two relaxation stages as shown in the following equation:

$$P(T) = P_R + \left(\frac{P_U - P_I}{2}\right)\cdot\{1 - \tanh[k_1\cdot(T - T_1')]\} + \left(\frac{P_I - P_R}{2}\right)\cdot\{1 - \tanh[k_2(T - T_2')]\} \quad \textbf{(2.4)}$$

where: P_U, P_I and P_R are the high (un-relaxed), intermediate and low (relaxed) temperature property values respectively,

T_{g1} and T_{g2} are the high and low temperatures around which each transition occurs.

k_1 and k_2 are the breadth of the high and low transition regions respectively.

Figure 2.18 and Figure 2.19 show the fitted property curves for glass vinylester, polyester and polypropylene composites.

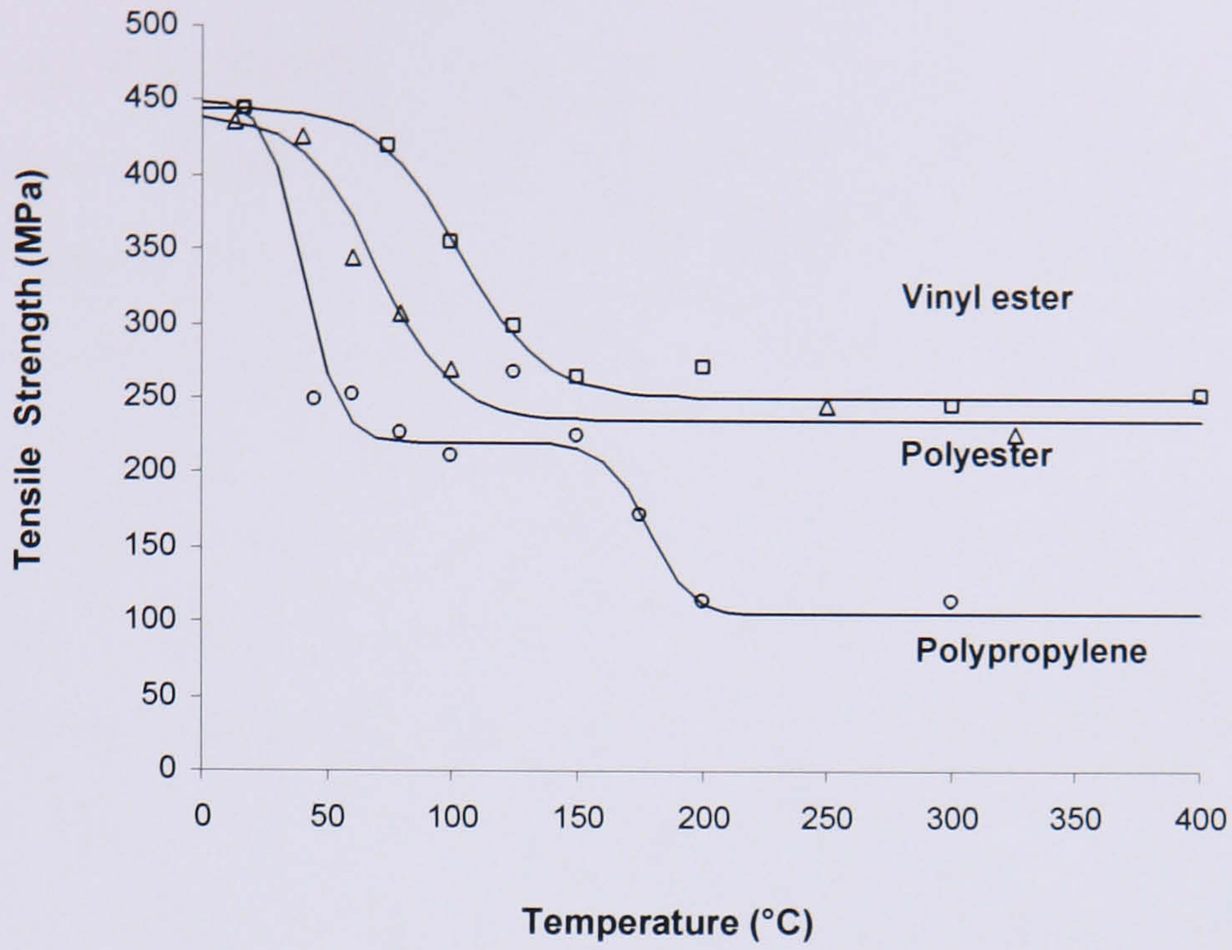
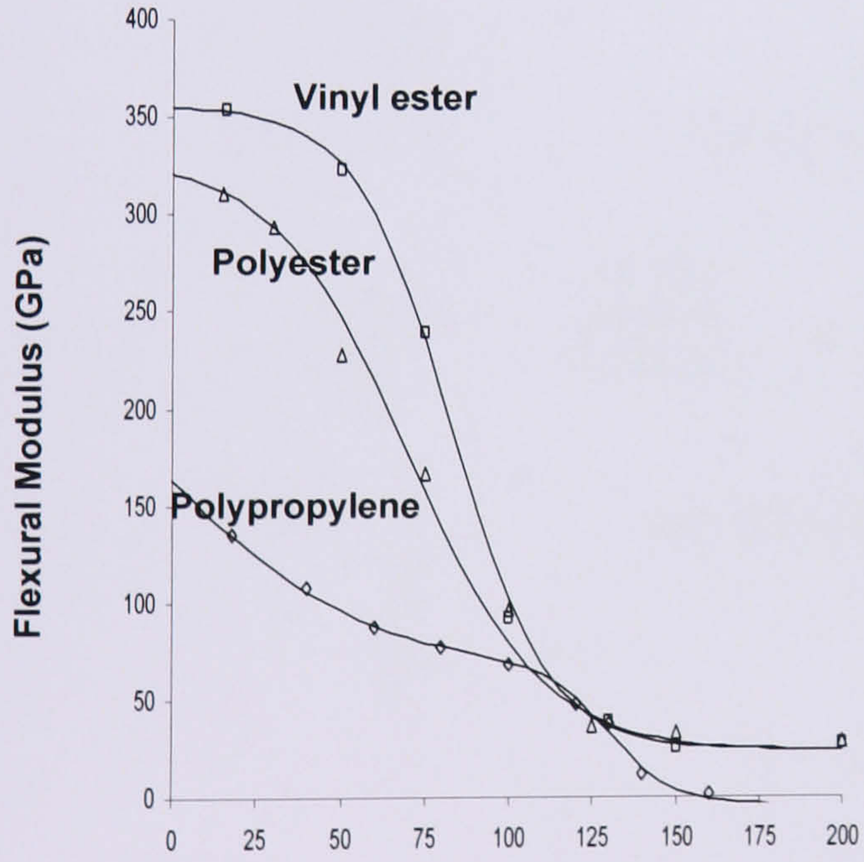
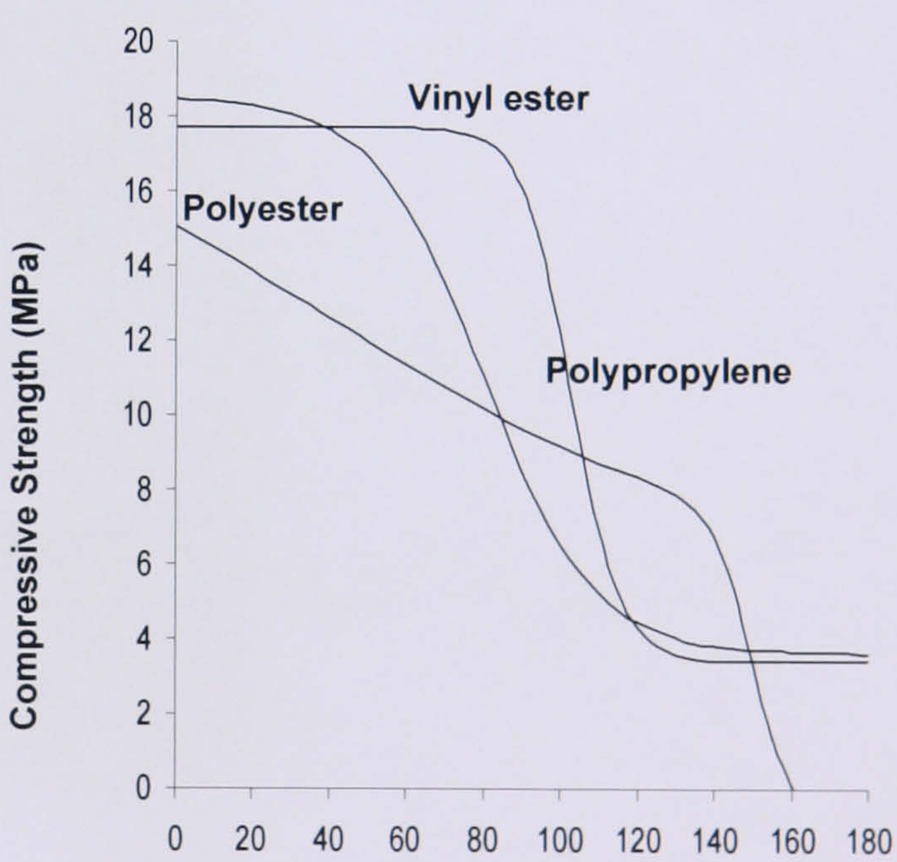


Figure 2.18 Tensile strength results for vinyl ester (□), polyester (Δ) and polypropylene (○) laminates [15]



(i)



(ii)

Figure 2.19 Resin dependent properties as a function of temperature for three laminate systems. (i) Flextural Modulus. (ii) Compressive strength [15]

2.8 Modelling the composites behaviour in fire

Prediction of the fire behaviour of composites in high temperature applications necessitates thermal modelling. These models are important because they demonstrate the different processes that control the behaviour of fibre reinforced polymers in fire. Also, they can be used as a design tool for the development of new composite structures and reduce the cost of expensive fire tests [89].

Modelling the pyrolysis of wood in a fire environment was the basis for development of composites thermal models [90-93]. Wood burning was modelled based on the assumption that it has two-phases: the residual char and the undamaged material. These phases are explained in Figure 2.20. Kung [91], Kansa et al. [90], and Fredlund [94], have developed thermal-chemical models that consider the processes of transient heat conduction, endothermic decomposition of wood, convection flow of volatiles and the gaseous combustion of these volatiles at or near the surface.

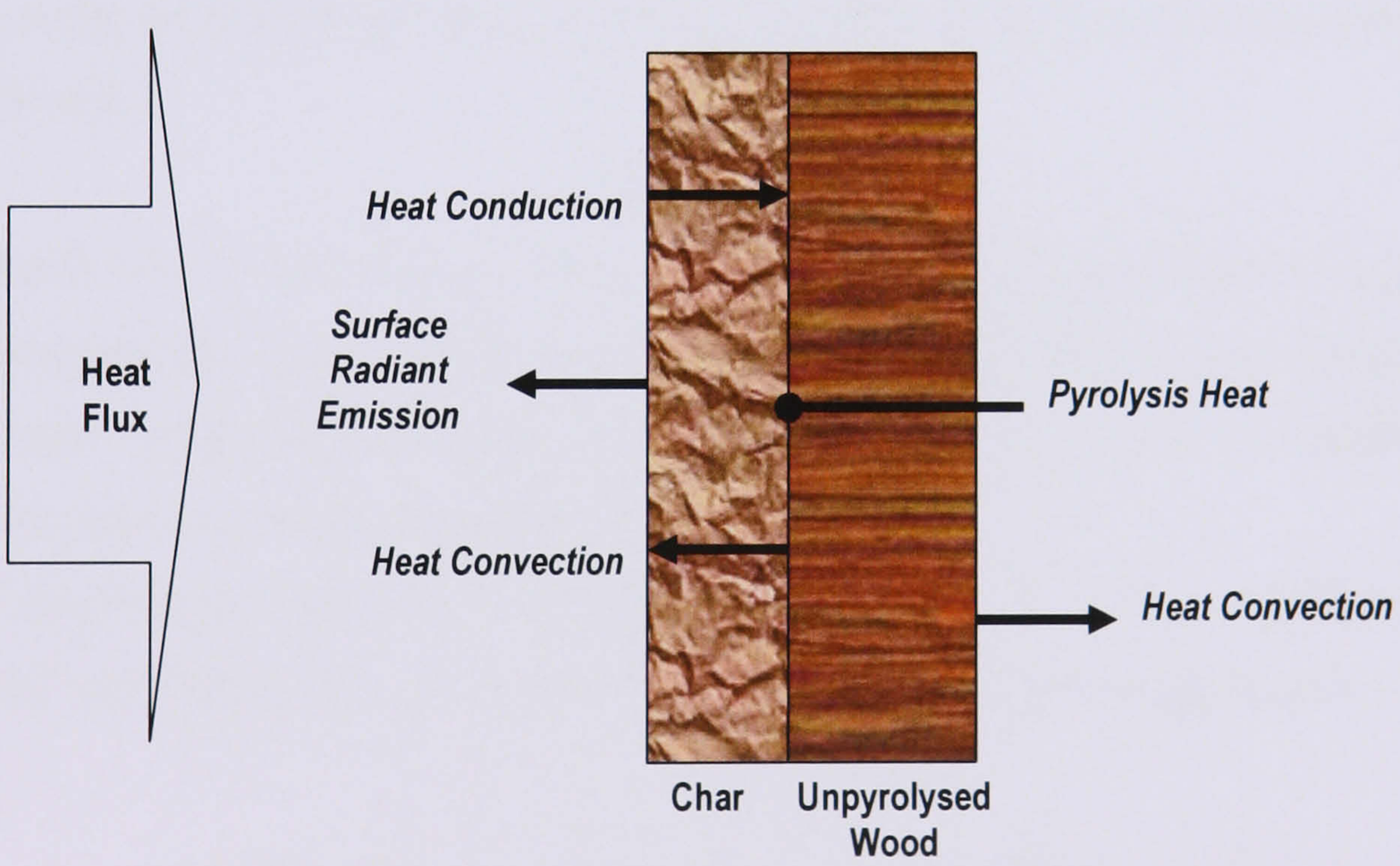


Figure 2.20 Thermal decomposition of wood

2.8.1 Heat conduction modelling

The effect of heat conduction through the composite material thickness is the most effective heat transfer mode. Heat of conduction is expressed as a one dimensional model [95] under the conditions of one-sided heating as

$$\rho C_p \frac{\partial T}{\partial t} = \frac{\partial}{\partial x}\left[k_x \frac{\partial T}{\partial x}\right] \tag{2.5}$$

Where:

T is the temperature (K),

t is time (s),

x is the distance below the hot surface,

ρ is the composite density (kg/m^3),

C_p is the specific heat of the composite (J/kg.K),

k_x is the thermal conductivity of the composite in the through-thickness direction (W/m.K).

The left hand side of the equation considers the change in total thermal energy per unit volume whereas the right hand side is the heat conduction energy flux. Specific heat (C_p), thermal conductivity (k) and density (ρ) are assumed to be independent of temperature, which is not the actual case.

This one dimensional model was studied by Asaro et al. [96], Milke and Vizzini [97], and Charles and Wilson [98] , and extended to give a three dimensional model:

$$\rho C_p \frac{\partial T}{\partial t} = \frac{\partial}{\partial x}\left[k_x(T)\frac{\partial T}{\partial x}\right] + \frac{\partial}{\partial y}\left[k_y(T)\frac{\partial T}{\partial y}\right] + \frac{\partial}{\partial z}\left[k_z(T)\frac{\partial T}{\partial z}\right] \tag{2.6}$$

where: x is the through thickness direction and y and z are the planar directions, $k_x(T)$, $k_y(T)$ and $k_z(T)$ are the thermal conductivities in the x,y and z directions.

Again, it was assumed that the specific heat, density and thermal conductivity are not temperature dependent.

It can be seen that both equations do not consider the polymer decomposition and also the flow of gaseous volatiles from cold face to hot face. For these reasons these equations are only perfect for the prediction of temperature profiles of low heat fluxes that do not cause combustion or degradation of the organic matrix. For most types of polymer composites, the heat flux limit below which pyrolysis does not occur is in the range of 10 to 20 kW/m^2 [15].

2.8.2 Fire response modelling of composites

The change in total thermal energy in a material due to the combined effect of heat conduction and polymeric matrix decomposition was modelled for the first time by Pering, Farrel and Springer [99]. They proposed the following equation:

$$\rho C_p \frac{\partial T}{\partial t} = \frac{\partial}{\partial x}\left[k_x \frac{\partial T}{\partial x}\right] + \frac{\partial m}{\partial t} Q_p \qquad (2.7)$$

$\frac{\partial m}{\partial t}$ is the vapour mass rate generated by unit volume (kg/s),

Q_p is the heat of decomposition (J).

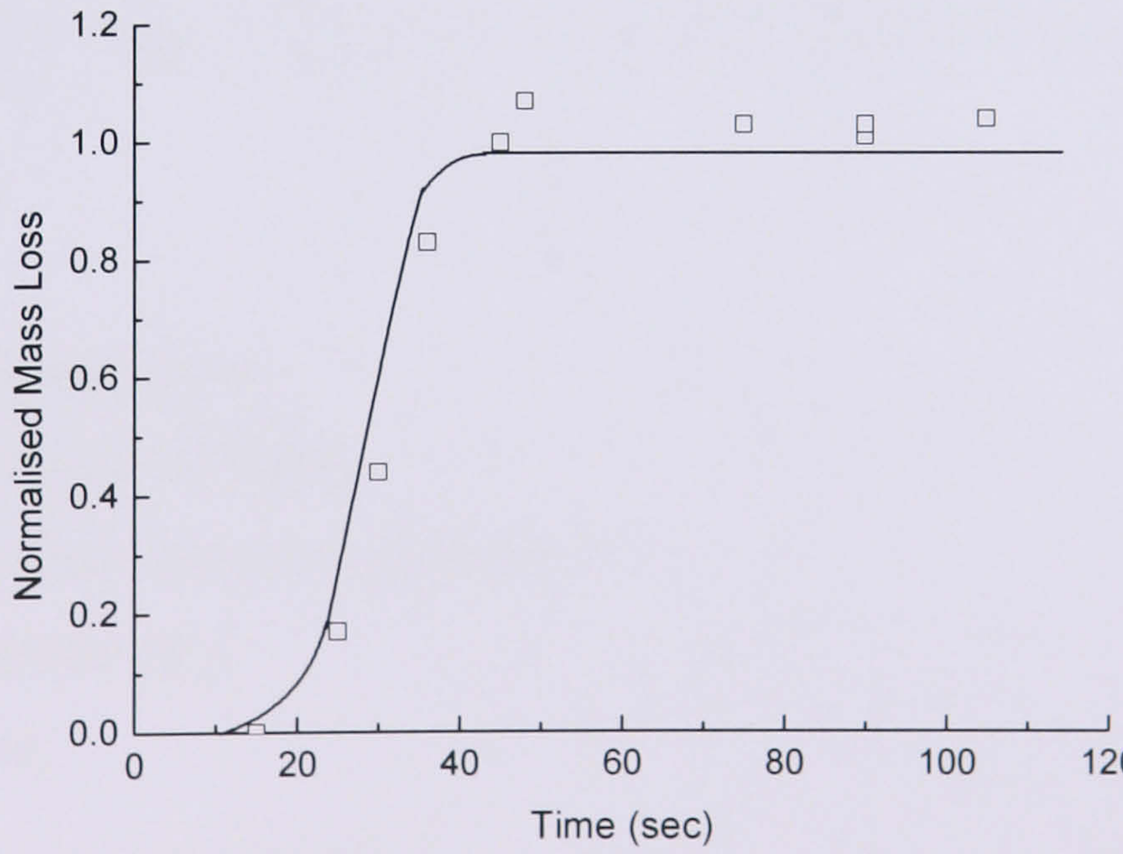


Figure 2.21 Measured against calculated mass loss of carbon/epoxy composite at flame fire of 540°C temperature [99]

Figure 2.21 shows the results of the work done by Pering et al [99] on carbon-epoxy composite exposed to gas flame temperature of 540°C. The normalized mass loss is equal to the polymer matrix mass loss resulting from decomposition divided by the matrix original mass. A good agreement was found between the theoretical mass loss (curve) and the measured mass loss (data points).

It can be noticed that some of the normalized data points exceeded the maximum value of 1. This is may be because the samples should be burned for several hours to allow full decomposition of the matrix as the presence of carbon fibres can hinder this process.

In addition, Browne [35] commented that the calculation of the normalized mass loss was implemented using the theoretical fibre volume fraction value, while the actual value may have a significant variation from it. This could yield an error in calculating the mass loss value.

2.8.2.1 Henderson model

Henderson et. al. [4, 6] derived a 1 D equation for the prediction of thermal response of glass reinforced polymer laminates. It was based on the work done on the decomposition of wood by Kung [91] and Kansa et al. [90]. Henderson model can be expressed as:

$$\rho C_p \frac{\partial T}{\partial t} = k \frac{\partial^2 T}{\partial x^2} + \frac{\partial k}{\partial x}\frac{\partial T}{\partial x} - \dot{M}_G C_{pg} \frac{\partial T}{\partial x} - \frac{\partial \rho}{\partial t}\left(Q + h_C - h_g\right) \qquad \textbf{(2.8)}$$

where:

ρ is the density (kg/m^3).

C_p is specific heat (J/kg.K).

k is the thermal conductivity (W/mK).

T is temperature (K).

t is time (s).

$\dot{M}_G$ is the mass flux (kg/m^{2}s).

C_{Pg} is the specific heat (J/kgK) of the volatile gases.

Q is the heat of decomposition (J/kg).

h_C is the enthalpy of the solid composite (J/kg).

h_G is enthalpy of the volatile gas (J/kg).

The first and second terms of the right hand side of the equation refers to the heat of conduction. This equation takes into account the change of thermal conductivity of the composite with temperature, which is different to Equations 2.6 and 2.7. The third term in Henderson equation considers the effect of volatiles flow through and out of the damaged material. Because it has a cooling effect, it is provided with a negative sign. The fourth term is the rate of heat generation or consumption resulting from matrix decomposition and the char-glass fibre reactions. It is negative for endothermic reactions that absorb heat and is positive for exothermic reactions. In this term, the decomposition reaction rates are determined from the mass loss rate using the Arrhenius kinetic rate equation:

$$\frac{\partial m}{\partial t} = -A_i m_o \left[\left(m - m_f \right) / m_o \right]^{n_i} e^{(-E/RT)} \qquad \textbf{(2.9)}$$

where:

m_o, m_f and m are the initial, final and instantaneous mass of the material, respectively (kg).

A_i is the pre-exponential factor (s^{-1}),

E is the activation energy (J/mol),

n_i is the order of the reaction,

R is the universal gas constant (8.314 J/mol.K),

T is the temperature (K).

Figure 2.22 shows the measured and the calculated temperature profile for 3 cm glass phenolic composite at a heat flux of 280 kW/m^2 using Equation 2.8. As it can be seen. good agreement was found between the measurements and model predictions at different layers through the laminate thickness. The high heat flux used allowed complete resin decomposition and glass/char reactions.

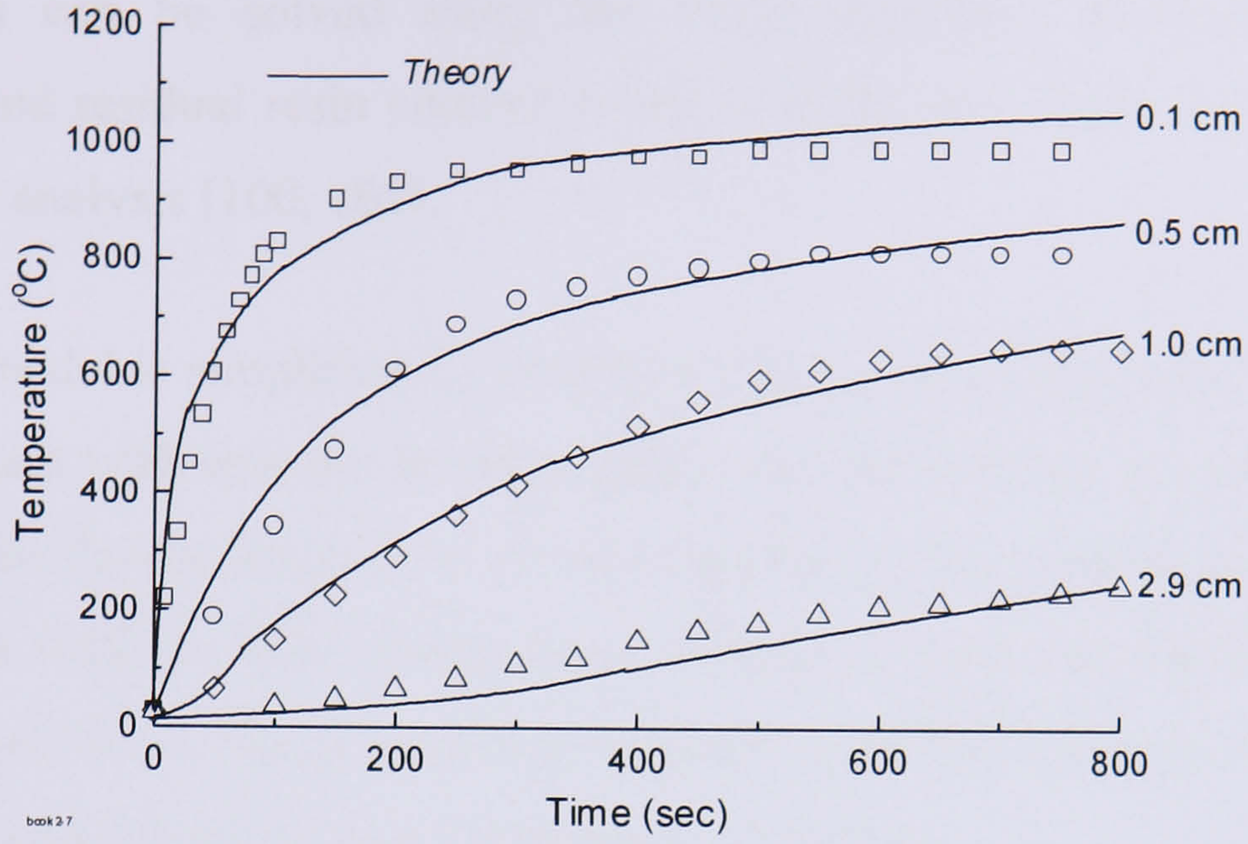


Figure 2.22 Theoretical and experimental temperature profile for 3cm thick glass/phenolic at 280 kW/m^2 heat flux [6]

2.8.2.2 Simplified version of Henderson model

A modified version of Henderson equation [6] was formulated by Gibson et al. [5] to predict the thermal response of glass reinforced polymer laminates exposed to one-sided heating.

$$\rho C_P \frac{\partial T}{\partial t} = \frac{\partial}{\partial x}\left(k \frac{\partial T}{\partial x}\right) - \dot{M}_G \frac{\partial}{\partial x} h_G - \rho A \left[\frac{(m - m_f)}{m_o}\right]^n e^{\frac{E}{RT}} \left(Q_P + h_c - h_g\right) \qquad \textbf{(2.10)}$$

As shown in Equation 2.10, the model incorporates the three main processes that occur in a composite exposed to fire. First process is the conductive heat transfer through the material, which causes the temperature rise. Second term is the convective mass flow of volatile products generated by the decomposition of the matrix from the reaction zone to the hot fire/composite interface. It is convective because the initial temperature of decomposition gases is lower than the temperature of the char surface/fire interface. The third term represents the endothermic or exothermic decomposition processes of the

polymeric matrix, which result in heat absorption or generation, respectively. Most polymers used in laminates have an endothermic decomposition nature.

The equation can be solved using the finite difference methods to predict the temperature and residual resin content evolution with time. It can be also solved using finite element analysis [100, 101].

The thermal model is simplified by assuming that the thermal conductivity and specific heat are constant with increase in temperature, and thermal and gas transport properties remain constant during the process of decomposition. The ambient temperature values are used in the analysis. Rule of mixture is employed to calculate the thermal properties. The decomposition reaction is modelled using the Arrhenius Equation 2.9 and the matrix density is updated during the thermal analysis accordingly

$$\rho_{comp} = V_f \rho_f + V_m \rho_m \qquad \textbf{(2.11)}$$

$$1/K_{comp} = \left(V_f/K_f\right) + \left(V_m/K_m\right) \qquad \textbf{(2.12)}$$

$$C_p)_{comp} = [(C_p)_f \rho_f V_f + (C_p)_m \rho_m V_m] / (\rho_f V_f + \rho_m V_m) \qquad \textbf{(2.13)}$$

Where:

ρ_f and ρ_m are the density of the fibre and matrix respectively.

V_f and V_m are the volume fraction of the fibre and matrix respectively.

K_f and K_m are the thermal conductivities of the fibre and matrix respectively.

The fibres mass loss is not accounted for in the model as the fibres are assumed to remain inert in the analysis.

Although this model does not account for char formation which is beneficial for the composite integrity, or for the fibres falling away from the hot surface after prolonged exposure to fire, it has nevertheless made accurate predictions for many types of thermosetting composite systems [5, 11, 31, 100, 101] as shown in Figure 2.23.

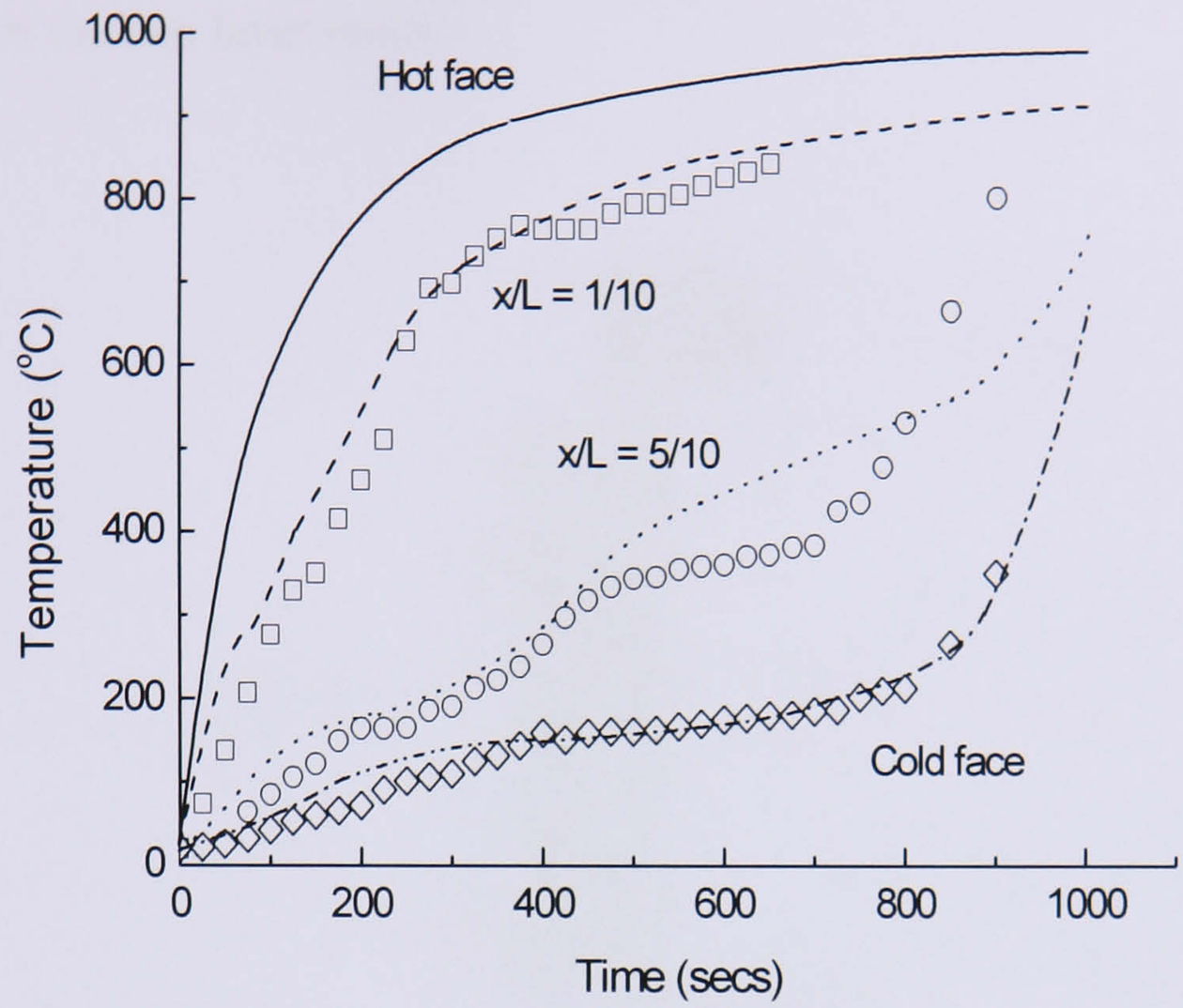


Figure 2.23 Measured and predicted temperature profiles for a 10.9mm thick glass/polyester laminate exposed to a one-sided hydrocarbon fire[15]. The term *x/L* represents the distance below the hot surface (*x*) divided by the specimen thickness (*L*)

2.9 Modelling fire behaviour of laminates under load

The two-layer model and the laminate model are extensively used to model the fire response of loaded composite laminates.

2.9.1 The two layer model

This model [1, 2, 12, 13, 102] assumes that the damaged laminate by fire consists of two layers: a fully degraded region that is simplified as having little or negligible mechanical properties and unaffected layer that is assumed to have the same properties as virgin material before exposure to fire. A major drawback of this model is that it fails to consider the change in mechanical properties by changing temperature. These properties degrade near the char/virgin boundary and increase toward the unheated surface. However, this model can be used to calculate the residual tensile properties after fire. The tensile strength of the virgin layer is assumed to be constant and has the same value

as in the room temperature. Figure 2.24 shows schematic diagram of laminate exposed to fire based on the two layer model.

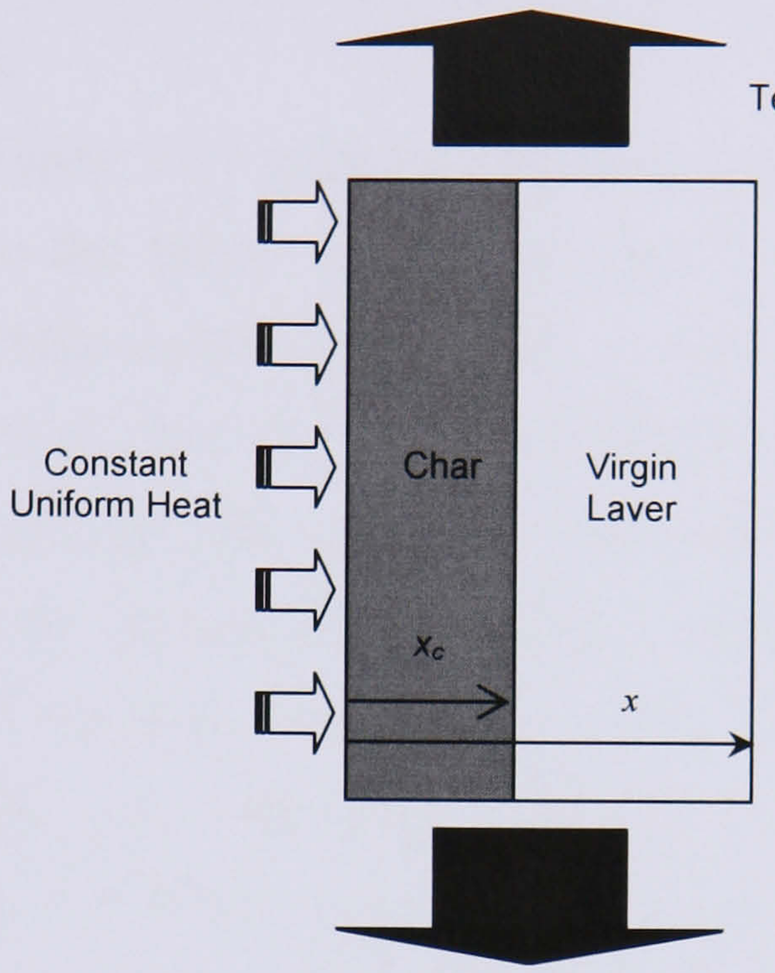


Figure 2.24 Schematic showing the two layer model. X_C is the char depth and X is the depth of original material [15]

Residual tensile strength (σ_T) is calculated using the following equation:

$$\sigma_T = \left(\frac{x_\circ - x_c}{x_\circ}\right)\cdot\sigma_{T(\circ)} + \left(\frac{x_c}{x_\circ}\right)\cdot\sigma_{T(c)} \qquad \textbf{(2.14)}$$

Where:

$\sigma_{T(o)}$ is the original tensile strength of the material at room temperature (MPa),

$\sigma_{T(c)}$ is the tensile strength of the char layer, which is assumed to be negligible in this case based on experimental data.

x_o is the total thickness of the laminate (m),

x_c is the thickness of char (m).

x_c is a location in the through-thickness direction at which the predicted temperature of the laminate reaches the temperature at which the matrix will decompose to char. It is calculated using Equation 2.10, and at this point the temperature is still high enough for

the polymer matrix to decompose to char. The charring temperature is determined using thermo-gravimetric analysis. The sample is considered to fail when the applied tensile stress σ_T, calculated using the above equation, exceeds the residual tensile strength of the laminate. Therefore, the time to failure is the time taken to bring the residual strength below the applied stress.

Theoretical curves in Figure 2.25 were constructed using the two layer model. Good agreement was found to the failure times of 50 and 75 kW/m^2. However, the model overestimated the remaining tensile strength values when exposed to a heat flux of 25 kW/m^2. The graph shows that the laminate preserved its original strength for more than three hours. This is because the decomposition temperature to form char based on TGA analysis was 440°C and at this heat flux the laminate does not reach this temperature. Therefore, according to the two layer model no char has formed and therefore the strength does not degrade. Also, due to the longer exposure of glass fibres to the heat flux, it is reported that they fail by creep rupture and the two layer model does not account for this [12, 103]. The use of this model should be restricted to applications where creep effects do not exist.

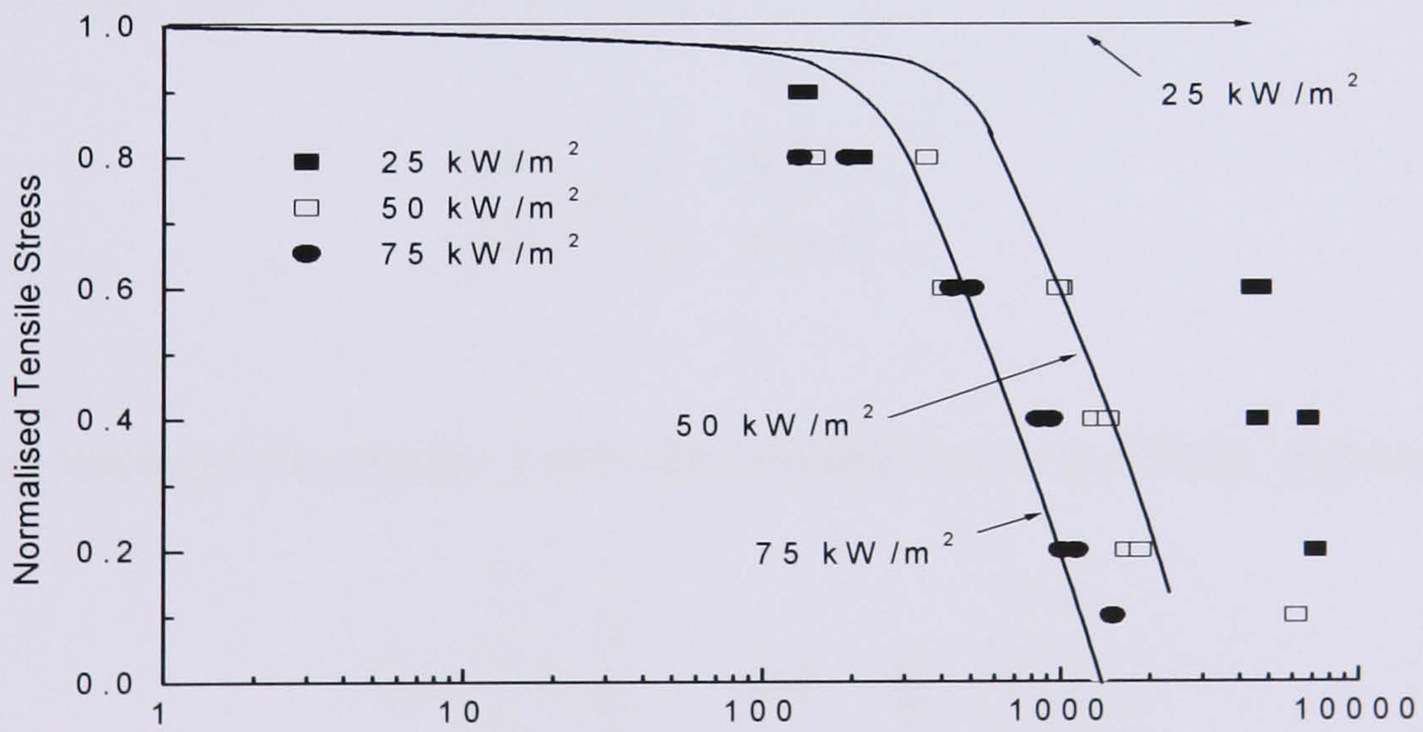


Figure 2.25 Comparison of the calculated and measured times for a woven glass/vinyl ester laminate under tensile loading and one-sided heat flux. The curves were calculated using the two-layer model [104]

2.9.2 Laminate theory

Laminate theory is a well known mathematical technique that is used to determine the strength and stiffness of a laminate [38, 40, 44, 105]. Figure 2.26 shows the required inputs for fire resistance modeling.

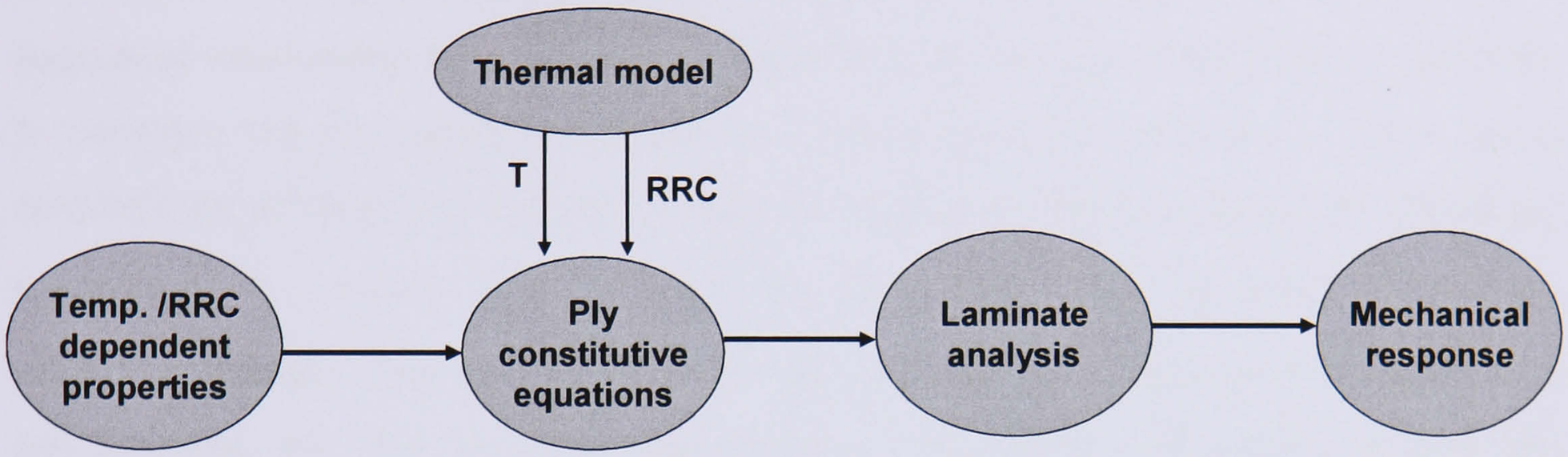


Figure 2.26 Schematic diagram showing the steps for coupling the thermal model outputs and the temperature dependent properties, which are used to construct the ply constitutive equations, with the laminate analysis to predict the mechanical response of loaded composite laminates in fire [35]

Under isothermal conditions, applied forces and bending moments are related to the resultant mid-plane strains and curvatures by,

$$\begin{bmatrix} \widetilde{N} \\ \widetilde{M} \end{bmatrix} = \begin{bmatrix} \widetilde{A} & \widetilde{B} \\ \widetilde{B} & \widetilde{D} \end{bmatrix} \begin{bmatrix} \widetilde{\varepsilon}_o \\ \widetilde{\kappa} \end{bmatrix} \tag{2.15}$$

$\widetilde{N}$ and $\widetilde{M}$ are matrices for normal loads and bending moments in the laminate

$$\widetilde{N} = \begin{bmatrix} N_x \\ N_y \\ N_{xy} \end{bmatrix} \quad \text{and} \quad \widetilde{M} = \begin{bmatrix} M_x \\ M_y \\ M_{xy} \end{bmatrix} \tag{2.16}$$

and $\widetilde{\varepsilon}_o$ and $\widetilde{\kappa}$ are the mid-plane strains and curvatures:

$$\tilde{\varepsilon} = \begin{bmatrix} \varepsilon_x \\ \varepsilon_y \\ \varepsilon_{xy} \end{bmatrix} \quad \text{and} \quad \tilde{\kappa} = \begin{bmatrix} \kappa_x \\ \kappa_y \\ \kappa_{xy} \end{bmatrix} \tag{2.17}$$

The temperature profile and residual resin content (RRC) through the laminate thickness are calculated using the thermal model Equation 2.10. The laminate model requires a functional relationship for mechanical properties as a function of temperature and RRC to construct the ply constitutive equations. Laminate matrix analysis is then used to calculate the stiffness and strength of each ply layer in the laminate at the calculated ply temperature at a certain point of time. The transformed stiffness matrix $\overline{Q}$ of a ply within a laminate may be found from the temperature dependent properties of a unidirectional ply. For an orthotropic laminate, with 0°/90° orientation of plies and woven roving laminates, loaded in the principal axes, they do not exhibit shear strains. The transformed stiffness matrix, $\overline{Q}$, will be simplified to the following form due to the absence of shear extensional coupling.

$$\overline{Q} = \begin{bmatrix} \overline{Q}_{11} & \overline{Q}_{12} & 0 \\ \overline{Q}_{12} & \overline{Q}_{22} & 0 \\ 0 & 0 & \overline{Q}_{66} \end{bmatrix} \tag{2.18}$$

where:
$$\overline{Q}_{11} = Q_{11}c^4 + 2(Q_{12} + 2Q_{66})s^2c^2 + Q_{22}s^4$$
$$\overline{Q}_{12} = (Q_{11} + Q_{22} - 4Q_{66})s^2c^2 + Q_{12}(s^4 + c^4)$$
$$\overline{Q}_{22} = Q_{11}s^4 + 2(Q_{12} + 2Q_{66})s^2c^2 + Q_{22}c^4$$
$$\overline{Q}_{16} = (Q_{11} - Q_{12} - 2Q_{66})sc^3 + (Q_{12} - Q_{22} + 2Q_{66})s^3c$$
$$\overline{Q}_{26} = (Q_{11} - Q_{12} - 2Q_{66})s^3c + (Q_{12} - Q_{22} + 2Q_{66})sc^3$$
$$\overline{Q}_{66} = (Q_{11} + Q_{22} - 2Q_{12} - 2Q_{66})s^2c^2 + Q_{66}(s^4 + c^4)$$

(c and s denote sinθ and cosθ, respectively), and

$$Q_{11}=\frac{E_1}{1-\nu_{12}\nu_{21}},\quad Q_{22}=\frac{E_2}{1-\nu_{12}\nu_{21}},\quad Q_{12}=\frac{\nu_{12}E_2}{1-\nu_{12}\nu_{21}}=Q_{21},\quad Q_{16}=Q_{26}=0,\quad Q_{66}=G_{12}$$

where: E_1 is the modulus of the material in the 1-direction (longitudinal),

E_2 is the modulus of the material in the 2-direction (transverse),

υ_{12} is Poisson's ratio (referring to the strains produced in the 2-direction when the lamina is stressed in the 1-direction).

υ_{21} is Poisson's ratio (referring to the strains produced in the 1-direction when the lamina is stressed in the 2-direction).

G_{12} is the shear modulus of the material.

The laminate **A, B**, and **D** matrices may be calculated using the $\overline{Q}$ matrix to give a representation of overall laminate response. Due to temperature and property variation through each ply, the conventional summation procedure is supplemented by a numerical integration from layer to layer, so that:

$$A=\sum_{k=1}^{n}\int_{h_{k-1}}^{h_k}\overline{Q}dz \qquad B=\sum_{k=1}^{n}\int_{h_{k-1}}^{h_k}\overline{Q}zdz \qquad D=\sum_{k=1}^{n}\int_{h_{k-1}}^{h_k}\overline{Q}z^2dz \qquad \textbf{(2.19)}$$

The **A** matrix Figure 2.27(a), which describes the laminate in-plane stiffness, falls continuously due to the general deterioration of the elastic properties with increasing temperature and resin degradation.

The laminate interaction term, **B** Figure 2.27(b), describes the interaction between in-plane loads and out of plane bending. B initially starts at zero because of the symmetry of the laminate about its centreline. The imbalance of moduli in regions on either side of the laminate centreline causes B to rise rapidly when a heat flux is initially applied. As the deterioration of the elastic properties continues, B falls.

The **D** matrix Figure 2.27(c) describes the laminate bending resistance which falls with increasing temperature. It is very interesting to notice that the shoulder in this term corresponds to the peak in the B matrix. This reflects the asymmetry about the laminate centreline.

An inverted version of Equation 2.16 may be used when the input parameters are the loads: At first, the matrices are partially inverted:

$$\begin{bmatrix} \varepsilon_o \\ k \end{bmatrix} = \begin{bmatrix} A* & B* \\ C* & D* \end{bmatrix} \cdot \begin{bmatrix} N \\ M \end{bmatrix} \tag{2.20}$$

where:

$$[A^*] = [A^{-1}]$$

$$[B^*] = -[A^{-1}][B]$$

$$[C^*] = [B][A^{-1}] = [B^*]^T$$

$$[D^*] = [D] - [B][A^{-1}][B]$$

Then, the fully inverted matrices are calculated by applying the following operations:

$$[A'] = [A^*] - [B^*]\,[D^{*-1}]\,[C^*] = [A^*] + [B^*][D^{*-1}][B^*]^T$$

$$[B'] = [B^*][D^{*-1}]$$

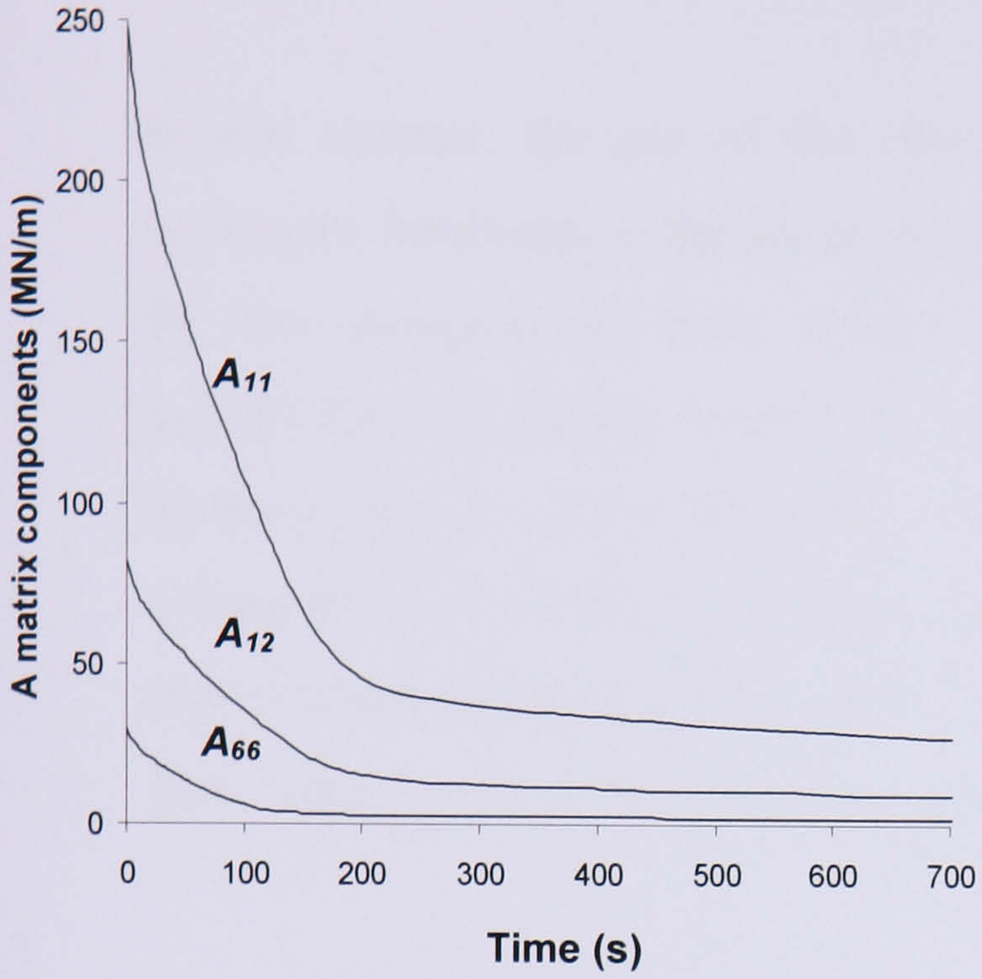
$$[C'] = -\,[D^{*-1}]\,[C^*] = [B^*]^T = [B']$$

$$[D'] = [D^{*-1}]$$

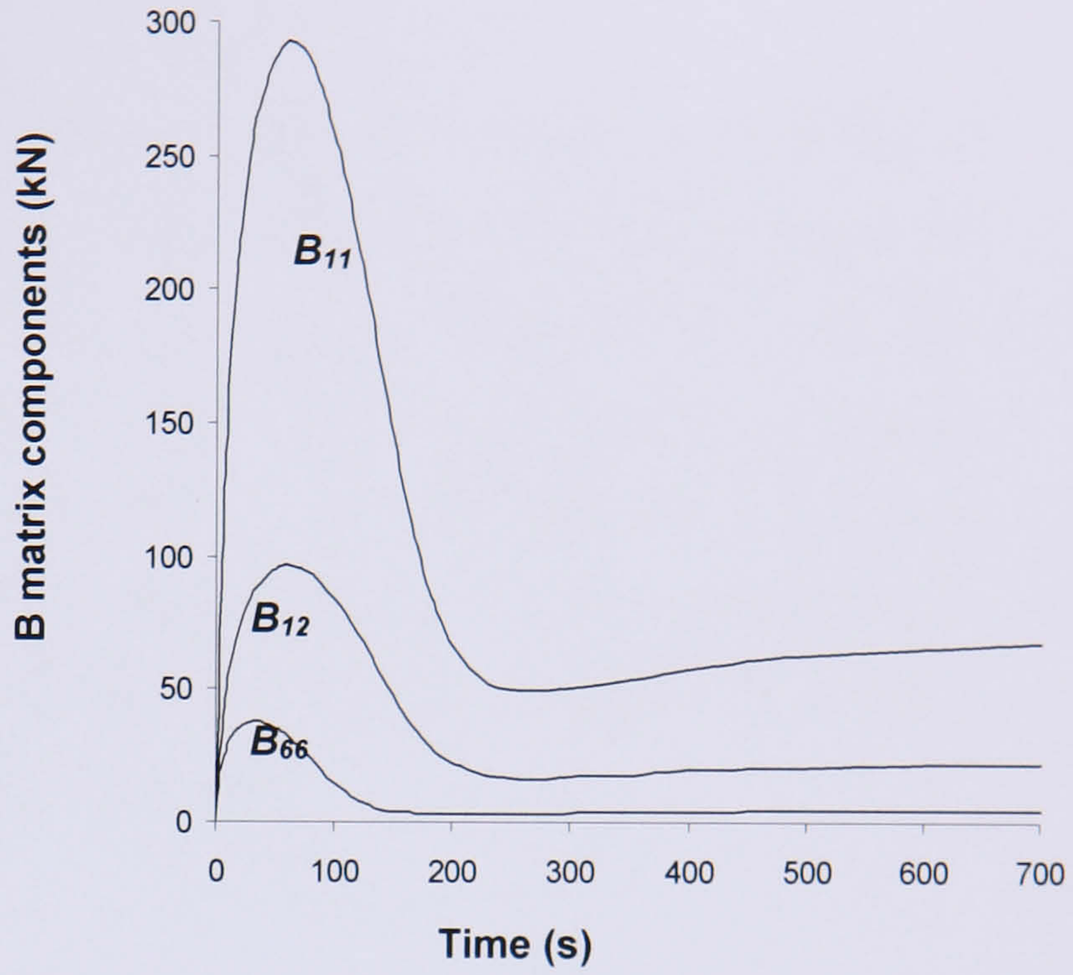
The inverted form of the ***A***, ***B***, and ***D*** matrices allow analysis of laminate structures when the input parameters are the loads:

$$\begin{bmatrix} \varepsilon_o \\ \kappa \end{bmatrix} = \begin{bmatrix} A' & B' \\ B' & D' \end{bmatrix} \begin{bmatrix} N \\ M \end{bmatrix} \tag{2.21}$$

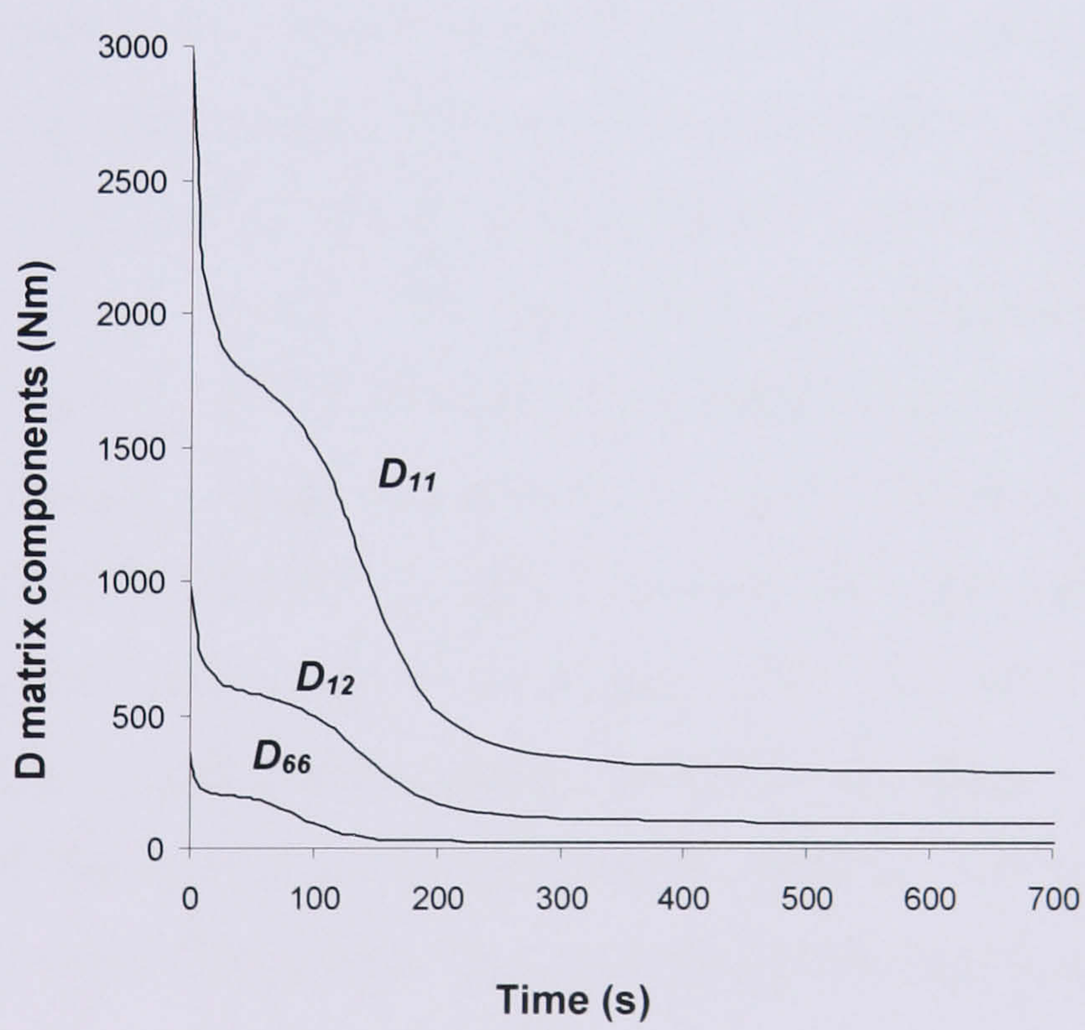
Once the A, B and D matrices are solved, they can be used to calculate the deformation and buckling failure of simple flat structures.



(a)



(b)



(c)

Figure 2.27 Laminate model for a glass/vinyl ester laminate: predicted variation of the components of the laminate A, B and D matrices with time for a heat flux of 75 kW/m^2 (a) A, (b) B and (c) D matrix components [106]

Chapter 3 Experimental Methods

In this chapter, the use of the cone calorimeter to characterise the flammability of composite laminates in the loaded and unloaded condition is described with emphasis on the new designed and built small scale loading rig. Also, the high constant heat flux provided by the radiant heater was employed to study the fire resistance of small scale samples and to investigate the burn through effect by measuring the back face temperature. The design of a higher load testing rig with a source for constant heating is also explained. Measurement of the kinetic parameters and determination of density, fibre volume fraction and void content are also discussed.

3.1 Materials used

The composite samples used in this investigation were vinyl ester and polyester-based laminates of the type commonly employed in marine structures. The materials were 11.8 mm thick vinyl ester and 11.6 mm thick polyester glass plates, prepared by hand laminating onto a flat mould. The laminates were supplied by the Composite Technology Centre (CTC) of VT Halmatic, Portchester, a manufacturer of large marine craft. The reinforcement was non-crimp stitched E-Glass fabric, with equal numbers of layers in the 0° and 90° directions. 24 plies in total of the glass fabric were used in each laminate. The resins were Dow 411-45 vinyl ester and Scott Bader Crystic 489 isophthalic polyester, cured with organic peroxides according to the manufacturers' specifications. The laminates were not post-cured, which is quite common for composite parts used in large marine structures. They were, however, stored at ambient temperature for approximately 12 months prior to testing.

3.2 Volume fraction determination

Determination of glass volume fraction was based on the standard ASTM D 792-00 [107]. This standard determines the fibre mass by burning a known mass of composite laminate sample in a furnace. The matrix resin melts and evaporates while the fibre

remains. After weighing the remaining fibre and dividing it by the initial mass of the laminate, the mass fraction and volume fraction can be calculated as percentages. Approximately 5 (g) samples were used in this test. Each sample was weighed in air and water. Samples mass in water was measured by using $100mm^3$ density bottles. The samples' density was determined as per the following equation:

$$\rho_C = \frac{m_{in\,air} * \rho_{water}}{m_{in\,air} - m_{inwater}} \tag{3.1}$$

where,

$m_{in\,air}$ is the mass of the composite in air (in grams).

$m_{in\,water}$ is the mass of the composite in water (in grams).

ρ_{water} is the water density, which equals 0.9975 (g/cm^3).

Small crucibles were labelled and weighed both with and with out samples, and then placed inside an electric furnace for 4-5 hours at 550°C (Figure 3.1). After complete burning, the fibre mass was determined by subtracting the mass of empty crucible from the total mass of the crucible with fibres. The fibre and matrix volume fractions, V_f and V_m, respectively were determined by the following equations:

$$V_f = \frac{m_f \rho_C}{m_C \rho_f} \times 100\% \tag{3.2}$$

$$V_m = (1 - V_f) \tag{3.3}$$

where:

m_f *and* m_c are the masses of remaining fibre and sample respectively.

ρ_f and ρ_C are the density of the glass fibres (~2.54 g/cm^3), and the density of the composite sample, respectively.

The void content can be calculated by the following equation:

$$V_v = \left(\frac{\rho_{theoritical} - \rho_{measured}}{\rho_{theoritical}}\right) \times 100\% \qquad \textbf{(3.4)}$$

where:

$\rho_{theoritical}$ and $\rho_{measured}$ are the theoretical and measured densities respectively.

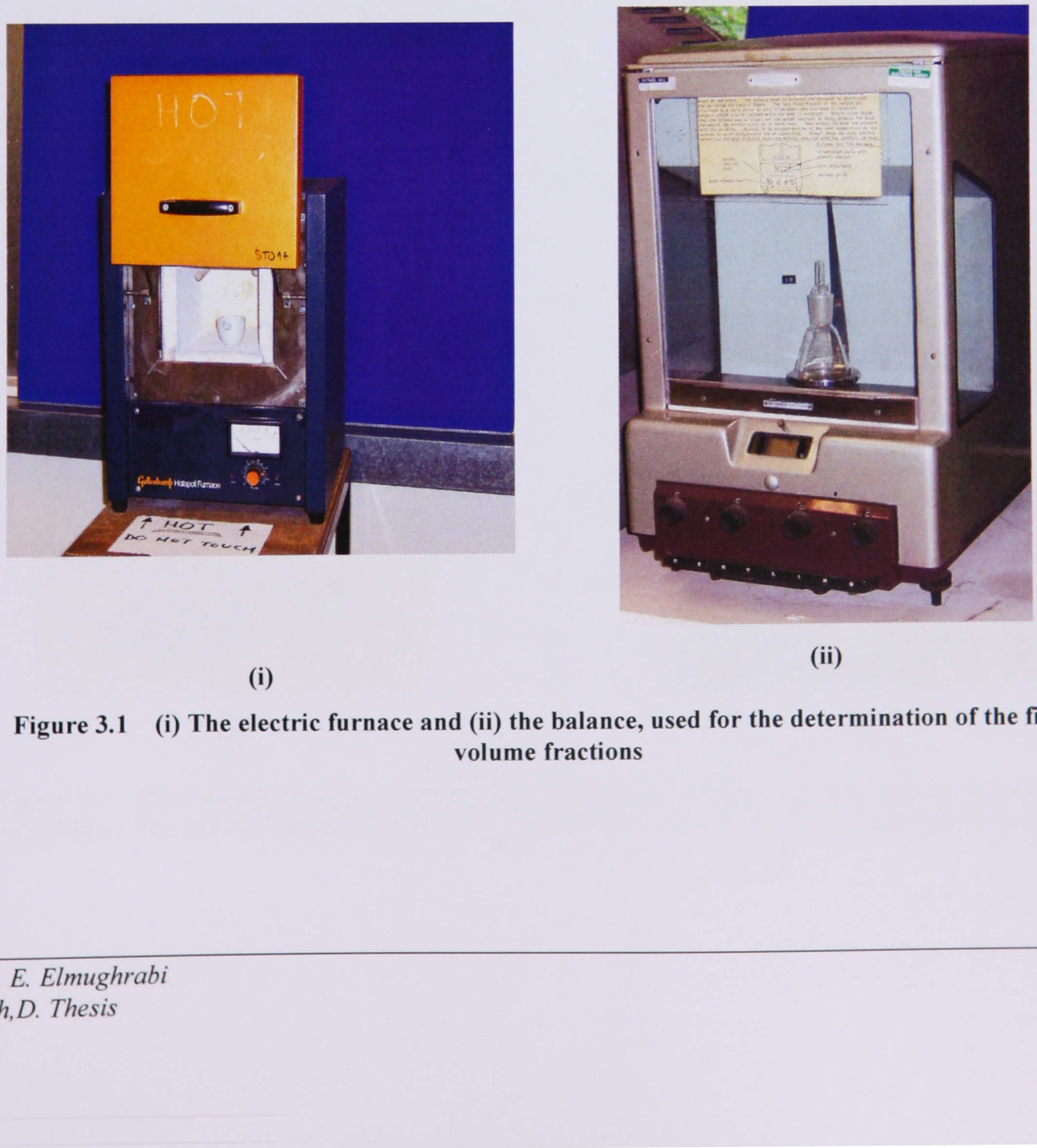
The rule of mixture can be employed to calculate the theoretical density assuming zero void content.

$$\rho_{theoretical} = V_f \rho_f + V_m \rho_m \qquad \textbf{(3.5)}$$

where:

ρ_f and ρ_m are the fibre and matrix densities respectively,

V_f and V_m are the fibre and matrix volume fractions respectively.



(i) (ii)

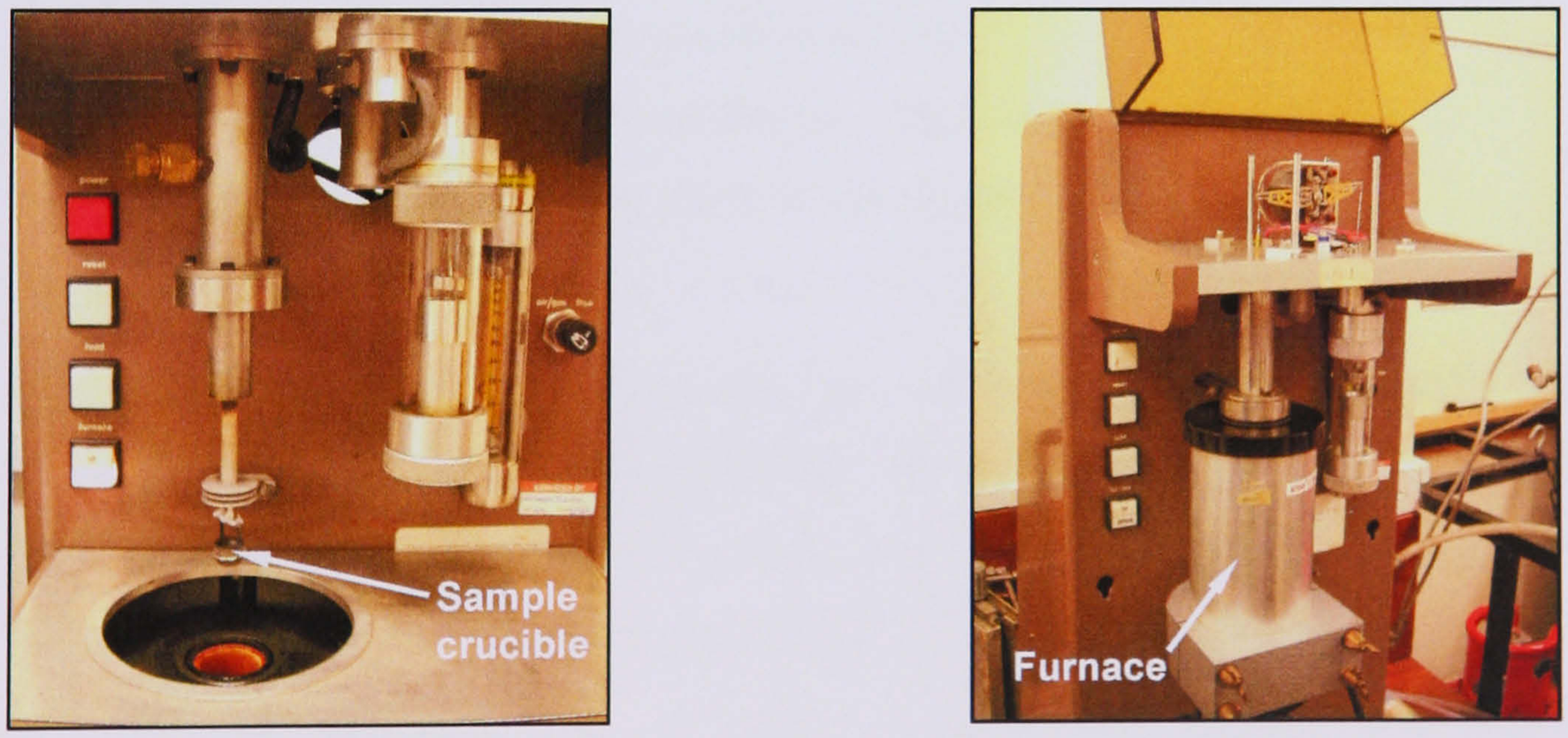
Figure 3.1 (i) The electric furnace and (ii) the balance, used for the determination of the fibre volume fractions

3.3 Thermo-gravimetric Tests (TGA)

In addition to volume fraction, the thermal model requires certain kinetic parameters to calculate the resin decomposition rate. Thermo-gravimetric analysis measures the mass loss of the material with increasing temperature.

TGA tests were implemented using 50 mg small samples from each laminate system. Figure 3.2 shows the small furnace that was used to heat the samples under constant heating rates. The test was conducted in an inert (N_2) to prevent samples from igniting and also to simulate the actual decomposition scenario in fire: the resin decomposes in absence of oxygen because the air flow from the surrounding to the decomposition zone is counteracted by the volatiles flow from the cold face to the surface/fire front. The rate of mass change with increasing temperature was recorded up to 900°C. The test was repeated two times and good agreement was found between the results.

25°C/min. and 40°C min. heating rates were used to accurately predict the degradation parameters. Two different heating rates were chosen to mimic the actual decomposition scenario of polymer composites as they undergo different heating rates when exposed to fire due to their low thermal conductivity. The main kinetic parameters obtained from TGA analysis were A, the rate factor and E, the activation energy for each material. Detailed TGA analysis will be discussed in Chapter five.



(i) (ii)

Figure 3.2 TGA testing furnace. A constant heating rate was applied to the samples in a nitrogen atmosphere. The rate of change of mass with increasing temperature was measured using a load cell

3.4 Cone calorimeter

The backbone of the experimental work was the cone calorimeter (as supplied by Fire Testing Technology (FTT Ltd), East Grinstead, West Sussex, UK) in conformance with ISO 5660 [56, 57], see Figure 3.3 for details. At the core of the instrument there is an electrically heated cone element produces a near-constant heat flux over the 100mm square surface of the test specimen. All the combustion products are drawn, with an excess of air, through the hood extraction system. The air flow rate, temperature and oxygen concentration are measured, enabling a continuous record of heat release to be calculated. Large number of fire reaction properties can be determined in one cone calorimeter test. Heat release during the burning process can be measured simultaneously along with the values of peak heat release and average heat release rates. Time-to-ignition, effective heat of combustion, smoke obscuration, mass loss rate, and CO and CO2 yields are also measured, with the addition of appropriate sensors. The heating element can irradiate heat fluxes ranging from (0 to 100) kW/m^2.

This technique can be used to [108]:

- compare and rank the fire performance of different materials,
- pass or fail a material according to a certain fire criteria (eg. maximum heat release rate value or smoke obscuration level),
- assess the likely response of a material when exposed to a large fire,
- generate fire reaction data to validate fire models.

The cone calorimeter has many advantages; the specimens used in the cone calorimeter are small compared to other fire tests like the SBI test or room corner tests. Also, the amount of exhaust gases is smaller than in the SBI test: the gas flow in cone calorimeter is 24l/s whereas in the SBI test and Room Corner Test it is 600l/s and 2500l/s respectively. In addition, this technique enables reproducible and consistent measurement of heat release and other fire reaction properties.

The sample is inserted into a sample holder and placed on a load cell for measurement of mass loss rate throughout the test. The principle of oxygen consumption is employed to calculate the heat release rate, which makes measurements dependent solely on precise oxygen concentration and flow [109, 110]. Hugget [109] observed that the heat of combustion for most organic materials commonly encountered in fires is approximately the same. He found that this value is ≈13.1 MJ/kg and explained this further: as the process of combustion of these products is mainly the oxidation of C—C and C—H bonds which release approximately the same amount of energy. Therefore. the heat release rate can be calculated using the expression:

$$\dot{q} = \frac{\Delta h_c}{r_o}\left(\dot{m}o_{2,\alpha} - \dot{m}o_2\right) \tag{3.6}$$

where:

Δh_c is the net heat of combustion.

r_o is the stoichiometric oxygen/fuel mass ratio.

$\dot{m}o_{2,\alpha}$ is the total mass flow of oxygen from the air.

$\dot{m}o_2$ is the total mass flow of oxygen into the fire.

Oxygen concentration in the exhaust stream is measured with an oxygen analyzer capable of an accuracy of 50 ppm., and the heat release rate is determined by comparing the oxygen concentration with the value obtained when no sample is burning. This method enabled an accurate and more convenient way to calculate heat release rate and it holds for a broad range of materials, including polymer based ones.

The cone calorimeter contains a smoke measurement device, consisting of a helium-neon laser beam and a beam detector for determination of a specific extinction area (SEA) of the smoke being released from the burning sample. This beam shines a monochromatic light through the smoke over a fixed distance. Before the light reaches the smoke, it is split into two beams, one of which is directed to a compensation detector

without crossing the smoke. A reference signal is generated by this detector to compensate for any laser power out-fluctuation. The second beam passes through the smoke and its power intensity is measured by a silicon photodiode.

Smoke obscuration is defined by the extinction coefficient (k):

$$k = \left(\frac{1}{L}\right) \ln \frac{I_o}{I} \qquad (3.7)$$

where:

I_o = power intensity measured by the compensating detector.

I = power intensity measured by the smoke detector.

L = the light path length.

The average smoke extinction area $\sigma_{f(avg)}$ is equal to:

$$\sigma_{f(avg)} = \frac{\sum V_i k_i \Delta t_i}{m_i - m_f} \qquad (3.8)$$

where:

V_i is the volume exhaust flow rate, m_i is the initial specimen mass and m_f is the final specimen mass.

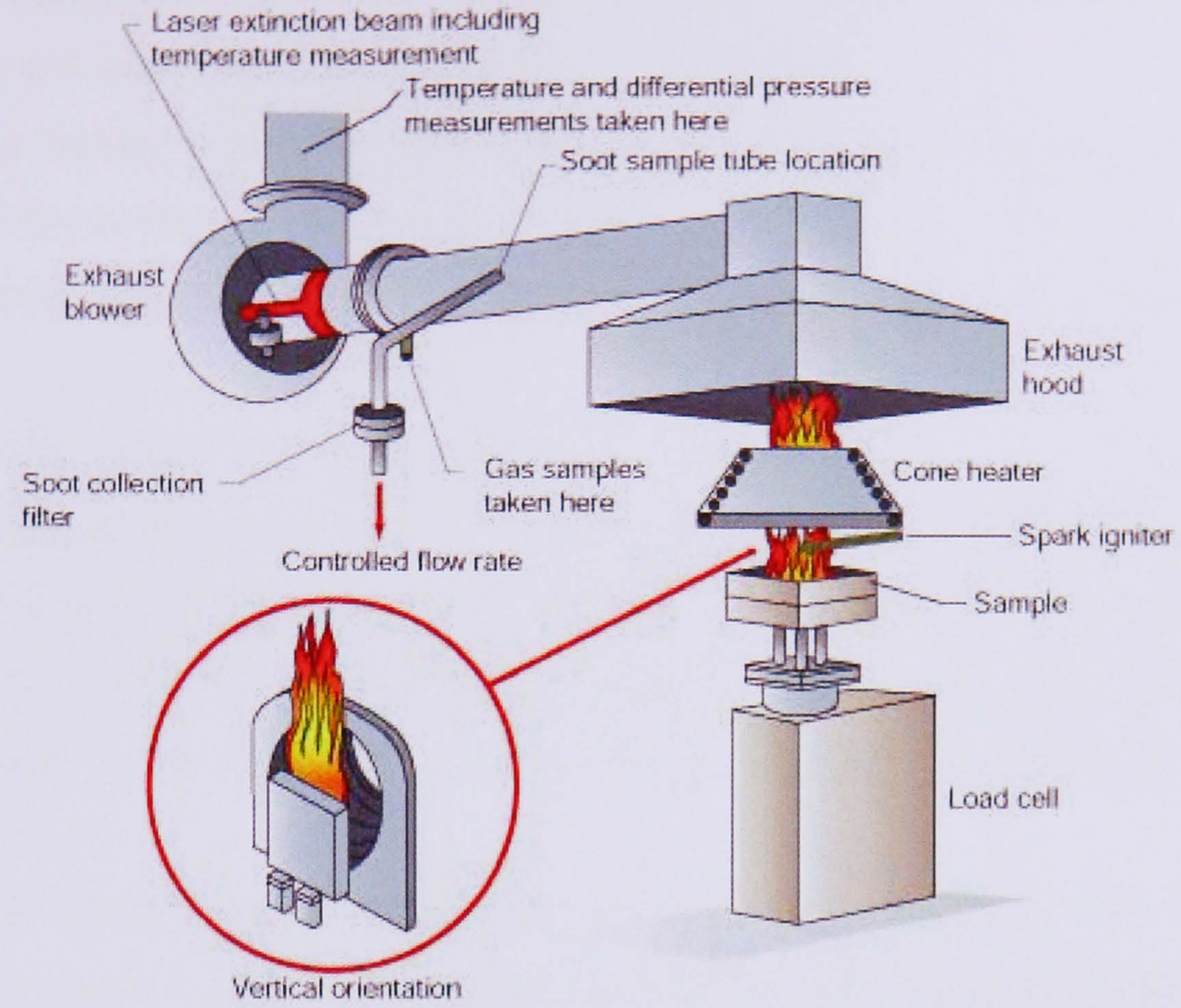


Figure 3.3 The main components of the cone calorimeter [111]

The software package "CONECALC-d" supplied with the cone calorimeter is used to calculate all parameters: mass loss rate, smoke production (smoke extinction area), effective heat of combustion, heat release rate and CO/CO_2 yield. Also, the events that are observed during the test can be documented

3.4.1 Main components

The **conical heater** wound in the form of a truncated cone, is rated 5000 W at 230 V with a heat output up to an equivalent to 100 kW/m^2 and for use horizontally and vertically. It consists of a heater element of resistive wire packed in magnesium oxide refractory, which is sheathed in an incoloy tube. The heater element is mounted internally on a double skinned insulated truncated cone. Temperature control is achieved by three type K- thermocouples fixed in direct contact with the heater element.

A split shutter mechanism protects the sample area before the beginning of the test. It gives the operator time to check the system before testing and also allows the load cell to

stabilize. This added time is very important for easily-ignitable samples, which often ignite irreproducibly if a shutter mechanism is not in place.

A specimen holder is used for specimens of 100 mm squared area and up to 50 mm thick, in the horizontal and vertical orientation.

The load cell can measure up to total weight of 2 kg, with a quick electronic tare facility.

Spark ignition uses a 10 kV spark generator

The exhaust system is manufactured from Stainless steel for long life. It comprises a hood, a gas sampling ring probe, an exhaust fan and an orifice plate flow measurement (thermocouple and differential pressure transducer), which is 24 l/s in normal operation.

Gas sampling comprises the ring sampler, refrigerated cold trap, pump, drying columns and flow control.

Smoke obscuration is measured with a laser system, using photodiodes. A small 0.5 mW helium-neon laser beam is projected across the exhaust duct. The detector system uses both main and compensation detectors, overcoming the stability problems of the helium-neon laser. Output is provided directly as an extinction coefficient.

A heat flux meter is used for setting the irradiance on the surface of specimen.

A calibration burner calibrates the rate of heat release measured by the apparatus using methane of 99.5% purity.

3.5 Small scale loading rig

A small scale loading rig was designed and used, for the first time, to facilitate the testing of glass polyester and vinyl ester samples under tension and compression loads at constant heat flux (see Figure 3.4 for details).

The loading rig consisted of a pressure cylinder and loading frame comprising three 25 mm diameter steel bars. An electronic load cell was fitted on the pressure cylinder plunger to measure the load applied to the samples. To minimize thermal effects this was situated just outside the area affected by the radiant heat flux from the cone element.

Some compromises were required to enable the rig to fit in the restricted space under the cone element in the standard type of instrument. It was necessary, for instance, to

remove the mass loss measuring transducer, so no mass loss measurement were possible in the tests reported here. The 25 mm gap between the cone element and the sample was kept the same as in a conventional test.

The limited working area under the cone restricted the space available for sample grips, so it was necessary to reduce the exposed area of the sample from the standard 100 mm square, down to 100 mm × 30mm. The grips are shown in Figure 3.5. The tensile specimens were given a 15 mm corner radius at either end of the gauge length. The small difference in area resulting from this was allowed for when computing the heat release per unit area. The sample edges were insulated with Kaowool, to ensure as far as possible that heat was applied to only one side, giving near one-dimensional heat flow in the sample.

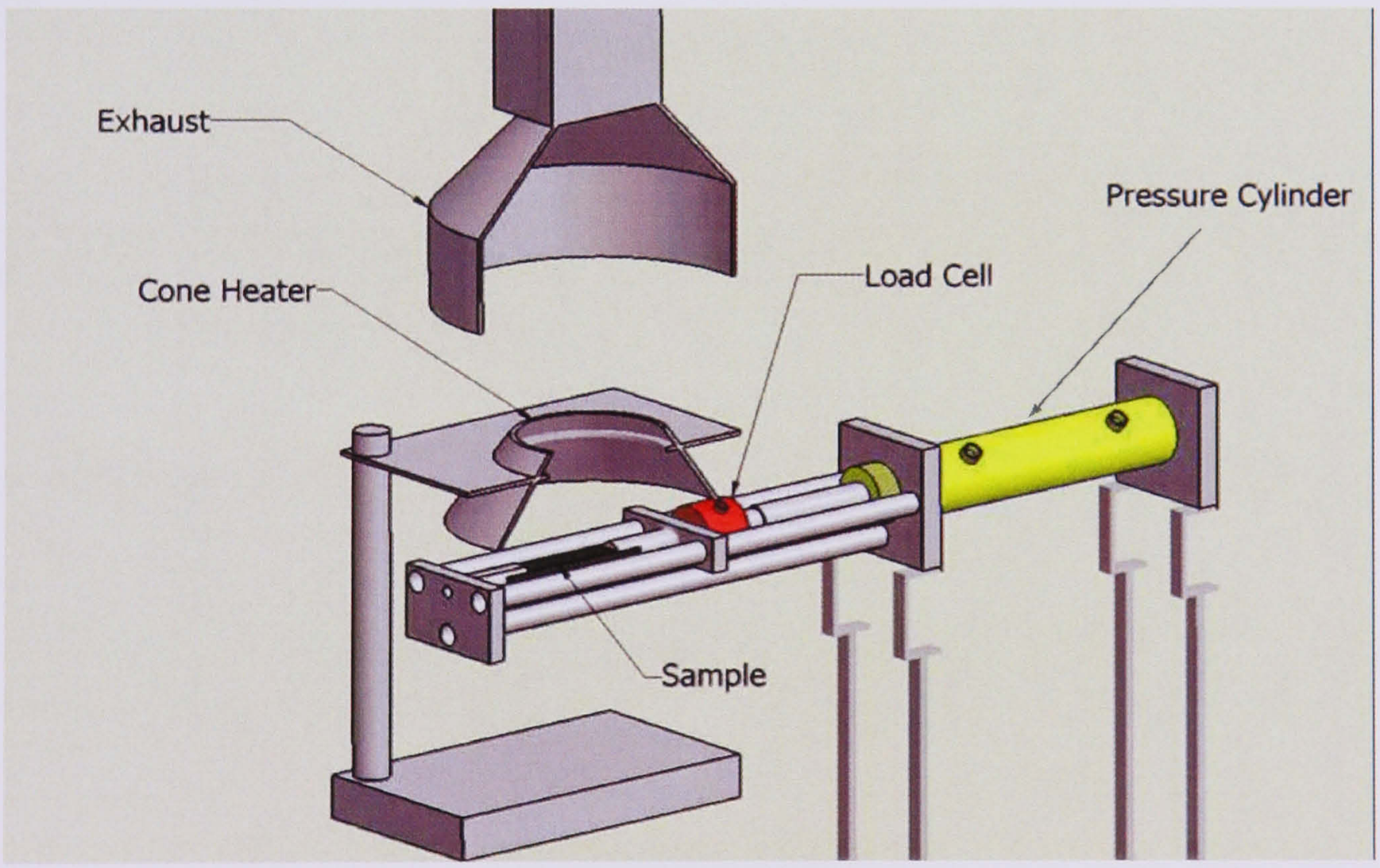


Figure 3.4 Small scale loading rig designed to fit into the cone calorimeter, in order to measure the fire reaction properties as function of the applied load

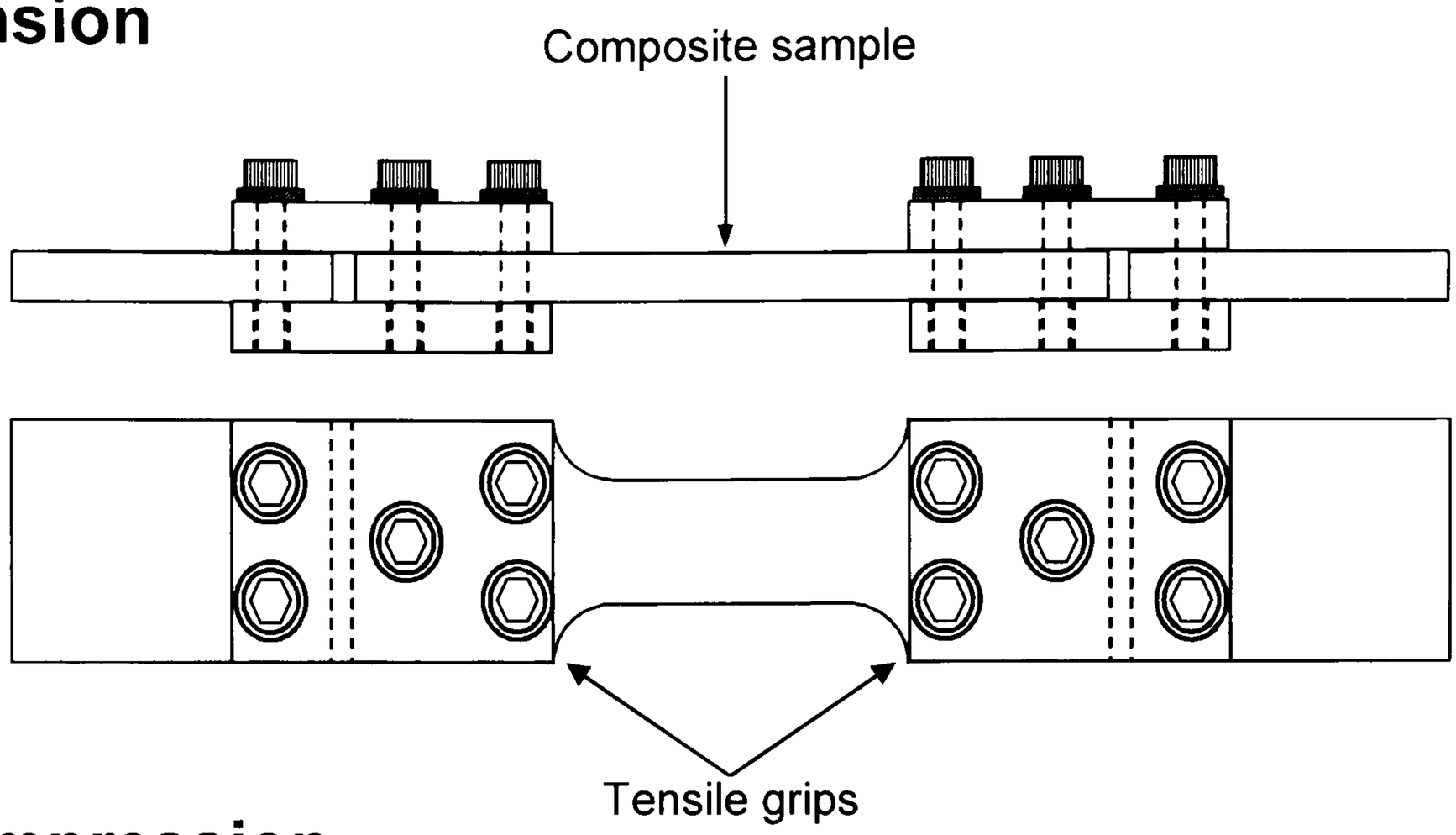


Figure 3.5 Specimen grips for tension and compression. In each case the heat-exposed sample dimensions were 100 mm long by 30 mm wide

The change in sample dimensions will have had the effect of decreasing the accuracy of the fire reaction measurements and there may also have been some effects due to the increased area of the sample edges, compared to those in a conventional test. Nevertheless, tests carried out with zero load on the sample produced very similar heat release profiles to those measured with conventional sample dimensions. This was attained by incorporating the actual exposed surface area in the test information before measuring the HRR using Cone-Calc. software. Figure 3.6 and Figure 3.7 show the measured HRR profiles for the standard cone calorimeter samples compared to the modified ones with reduced size of (100mm ×30mm). The slight increase in the average HRR in the reduced samples compared to the standard samples is mainly due to the edge effect and the exposure of more surface area to the heat flux as it was more difficult to insulate the modified samples than the standard ones using the conventional picture frame. Ritchie S. [112] studied the effect of the sample diameter (size) on the heat release rate of horizontal wood and found that it has a little effect. He explained that the lack of size effect was due to influence of the formed insulating char layer, which reduced the gasification rate. It would, nevertheless, be desirable, for future instruments of this type, to modify the design a little, in order to permit full-size specimens to be placed under the cone heater.

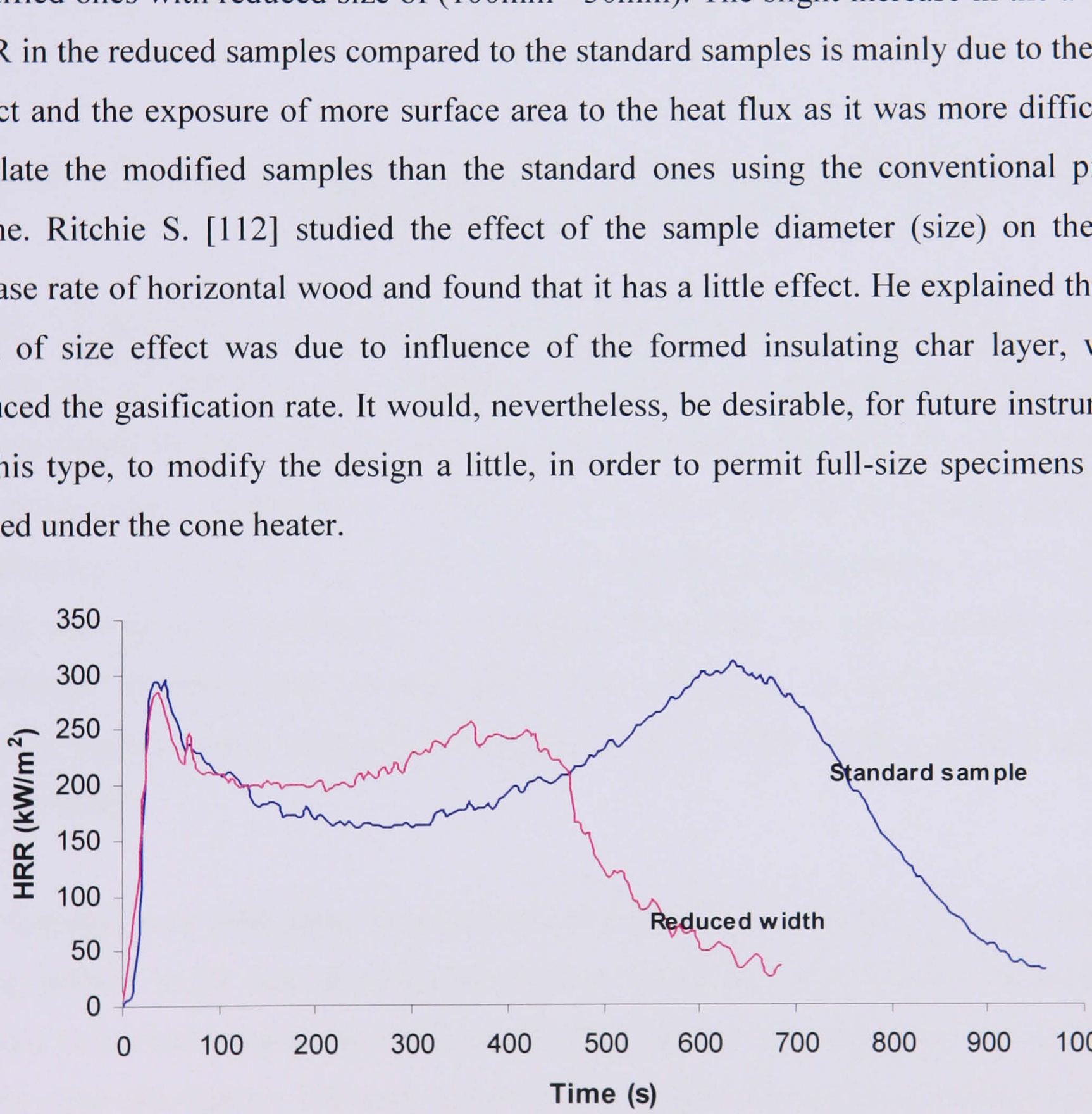


Figure 3.6 Comparison of the HRR profiles of conventional standard sample and the modified one for glass vinyl ester composite at 75 kW/m^2

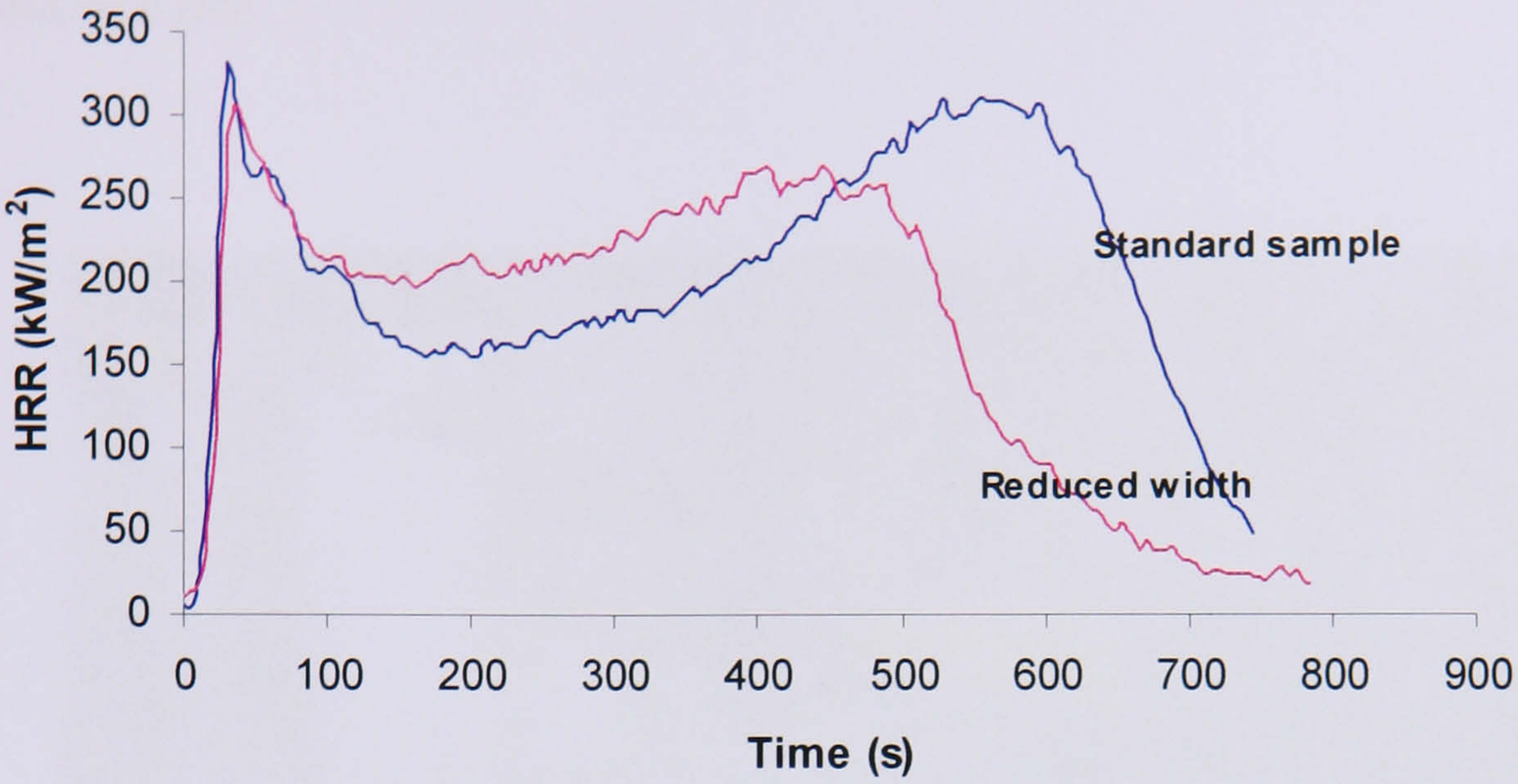


Figure 3.7 Comparison of the HRR profiles of conventional standard sample and the modified one for glass polyester composite at 75 kW/m^2

Figure 3.8 shows the loading frame in place under the cone calorimeter heating element. A heat flux of 75 kW/m^2 was employed in this study, corresponding to a fairly severe fire, as might be encountered in a compartment fire on a ship. This is equivalent to a minimum source temperature of about 840°C, according to the Stefan-Boltzmann relationship. This heat flux is higher than the more commonly employed of 50 kW/m^2, which corresponds approximately to a typical room fire. As with conventional cone calorimeter measurements a spark igniter was employed, to ensure the ignition of evolved decomposition products. The elapsed time to visible ignition of these products was recorded.

The samples were held under load until mechanical failure occurred, the time-to-failure being defined as the time at which the laminate could no longer support the externally applied load. Heat release rate and smoke production rate were measured simultaneously by the cone calorimeter. The peak values of heat release and smoke generation rate were reported. It is also common to report average values of these parameters, computed over a period, often of 300 seconds. In the present study, however, this was not possible, as the samples failed after different time periods depending on the stress level. Instead, values of the heat and smoke release rate immediately prior to failure were recorded.

These will be referred to as the minimum heat release rate and the minimum smoke production rate.

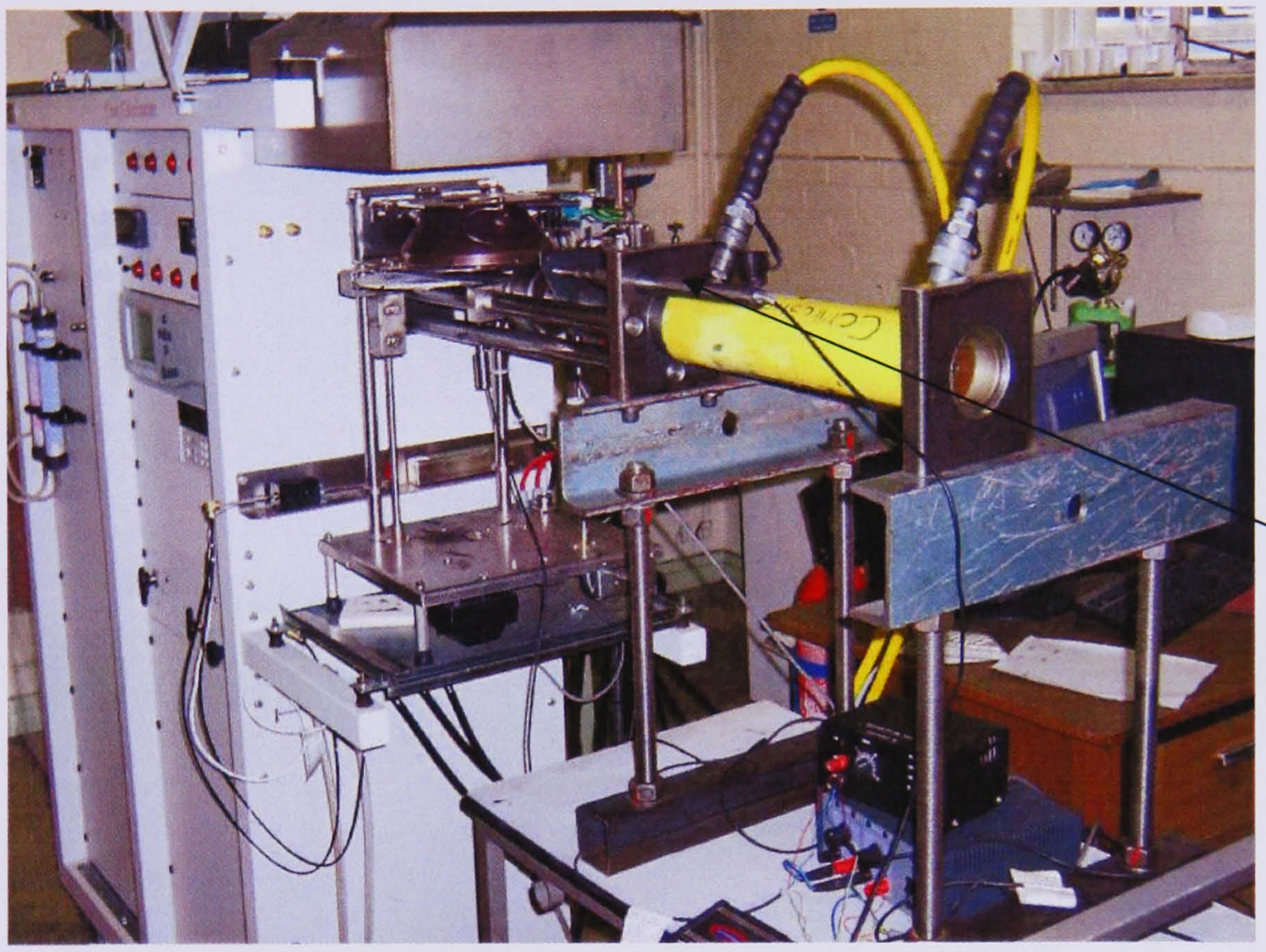


Figure 3.8 Small scale loading rig which was fitted under the cone calorimeter heating element

3.6 Fire tests under high load

Another small scale new rig was designed to test composite laminate under high load. It is capable of testing samples up to 280 kN load (Figure 3.9 and Figure 3.10). The rig was fitted with a fume hood to extract the smoke and hot gases Rectangular tensile samples of 500 mm length× 75 mm width and compression samples of 200 mm length × 100 mm width were tested under constant load and constant heat flux of 75 kW/m^2. The time-to-failure was recorded for every stress. Special grips were designed for tensile and compressive loads (Figure 3.11). The compression grips were designed in such a way to prevent local buckling of the tested specimens. LVDT was positioned at the back face of the sample to measure the out-of-plane deflection during compression loading. The loaded laminate was exposed to radiant heat flux from a specially designed conical

heater (5000 W), which resembles the cone calorimeter's heater (Figures 3.12 and 3.13). The new radiant heater was calibrated using the existing Schmidt-Boelter heat flux gauge, which is attached to the cone calorimeter. Time-to-failure curves were constructed for tested composite laminates.

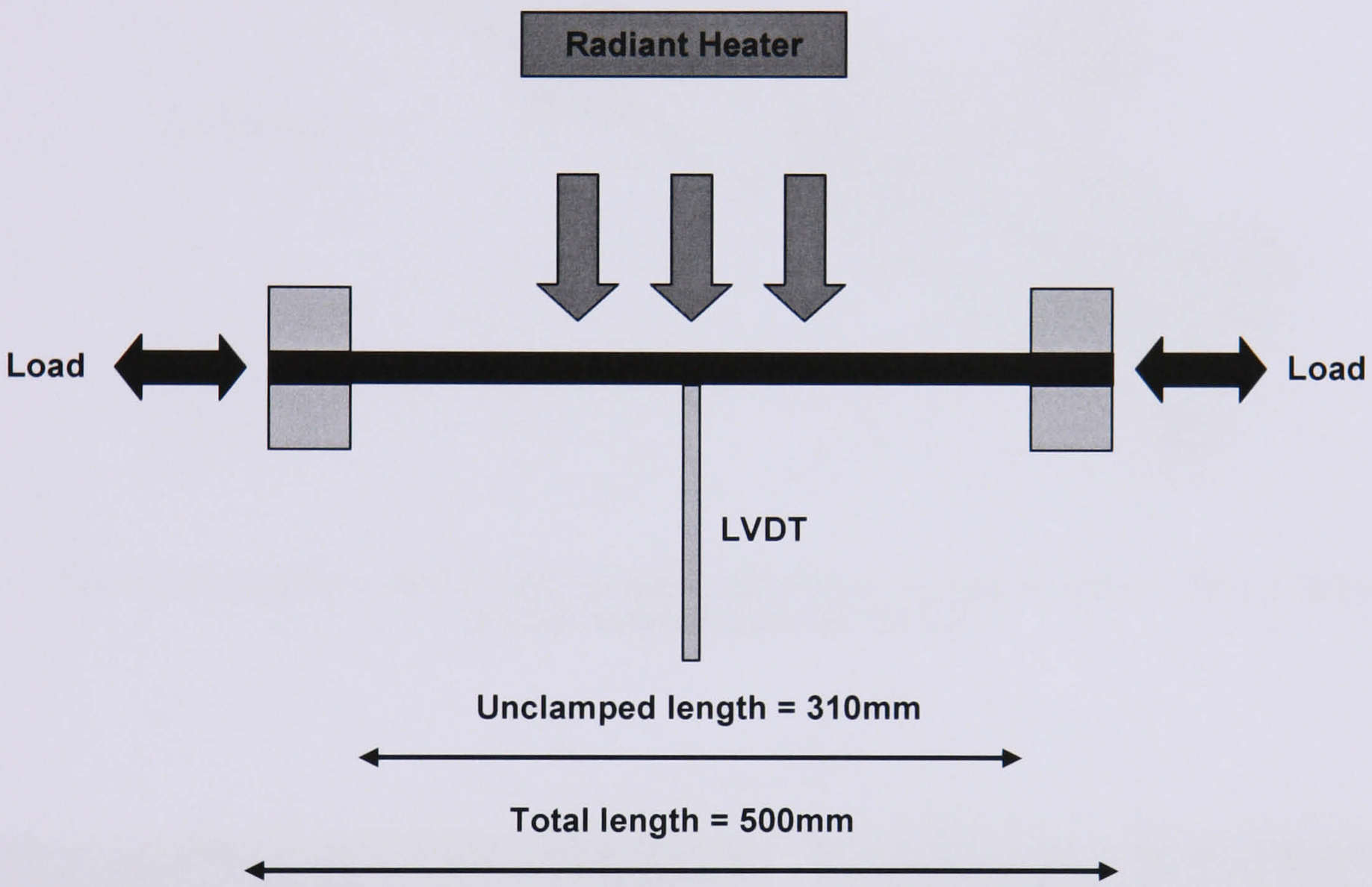


Figure 3.9 Schematic showing the testing arrangement

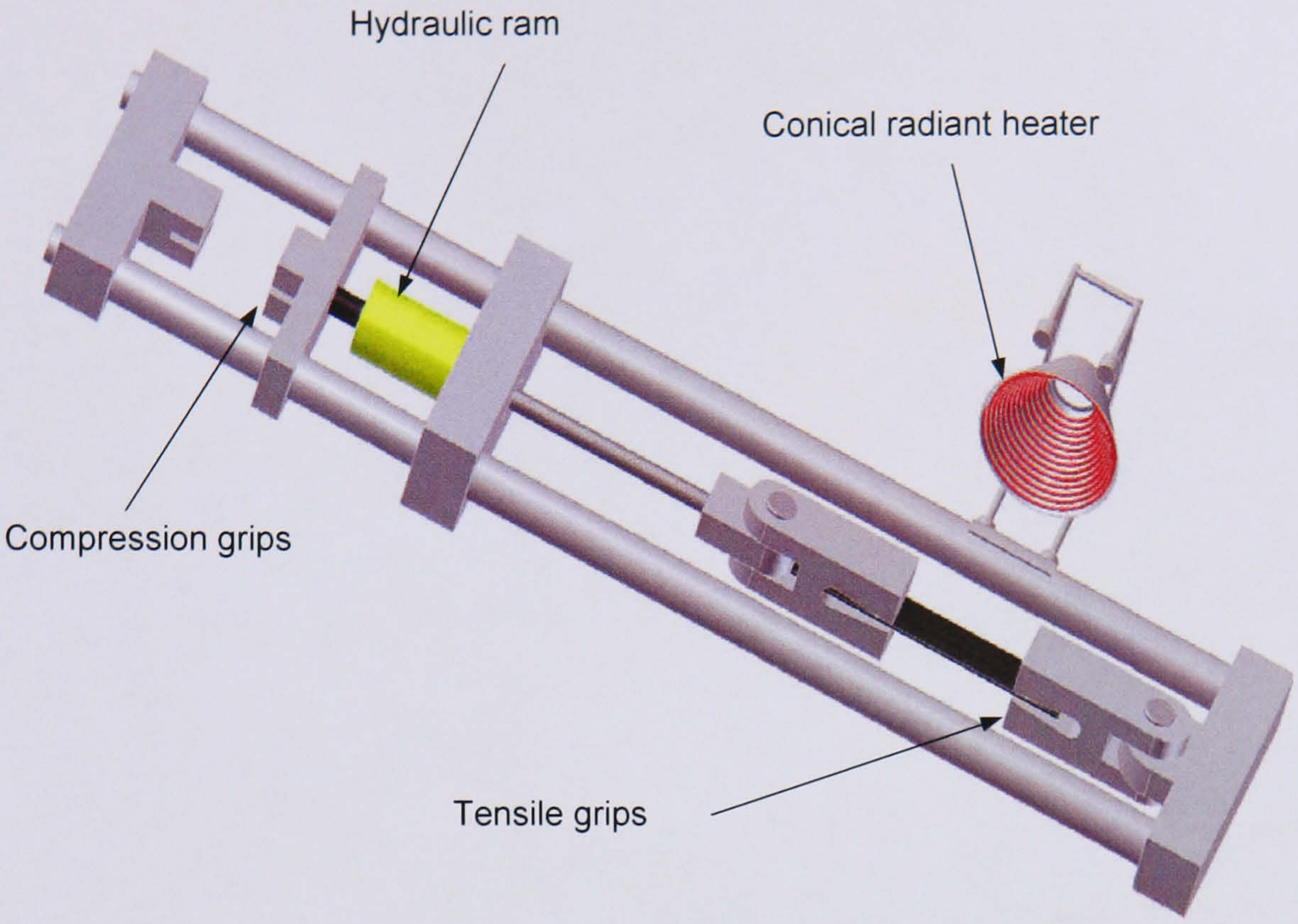
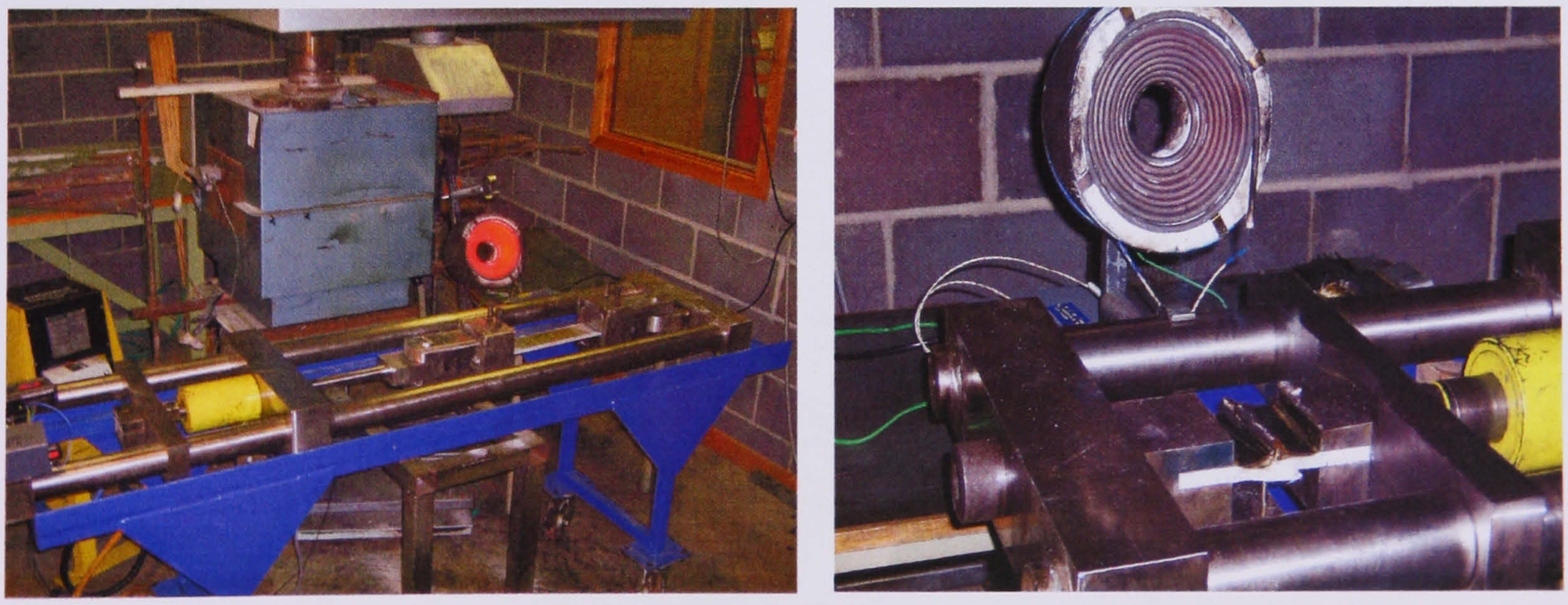


Figure 3.10 High load testing rig. It is capable of testing composite samples at 280 kN and a constant heat flux up to 100 kW/m^2



(i) **(ii)**

Figure 3.11 High load testing rig. (i) Tensile side. (ii) Compression side

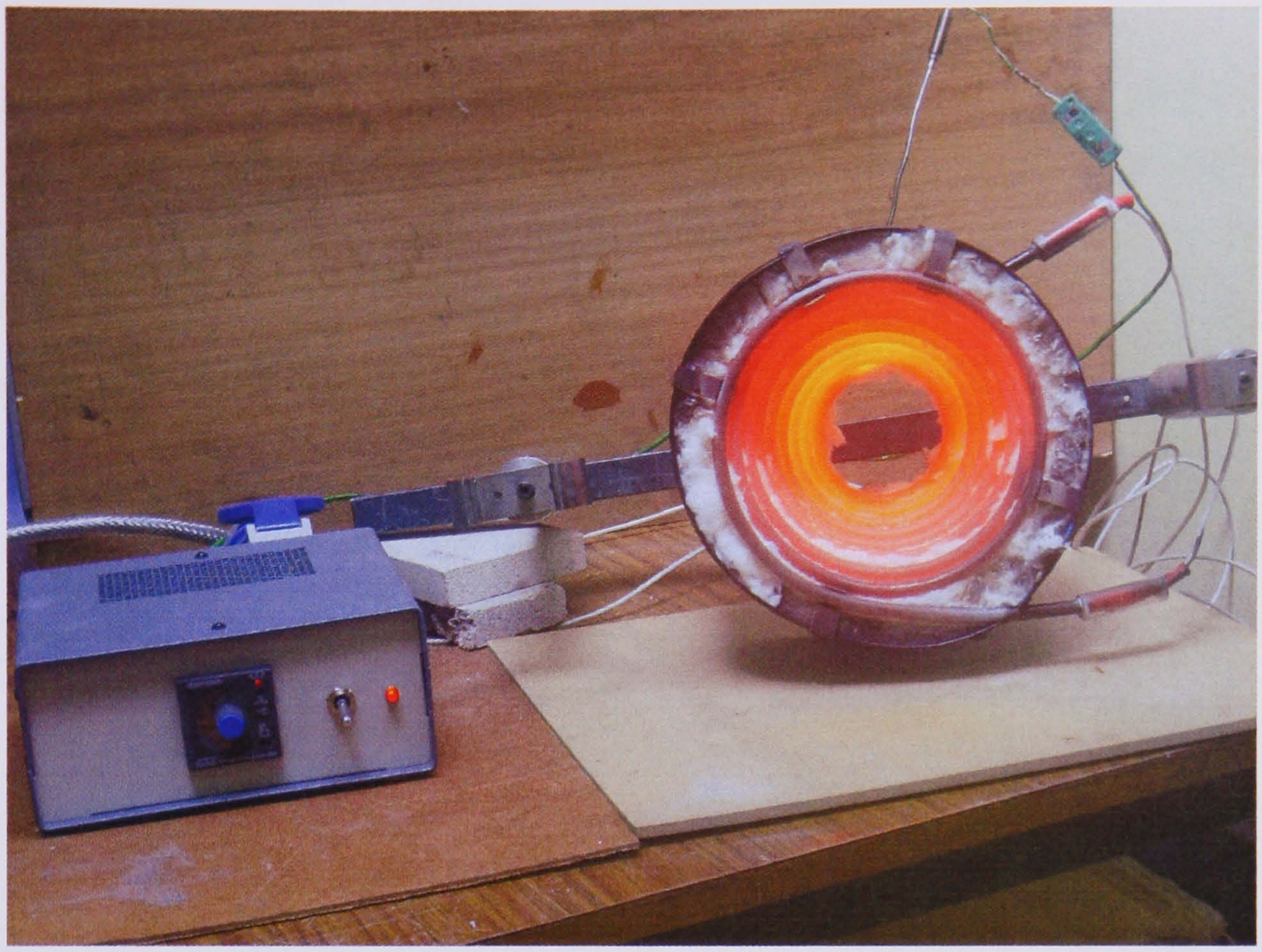


Figure 3.12 The calibrated radiant conical heater. It is calibrated to provide a heat flux upto 100 kW/m^2

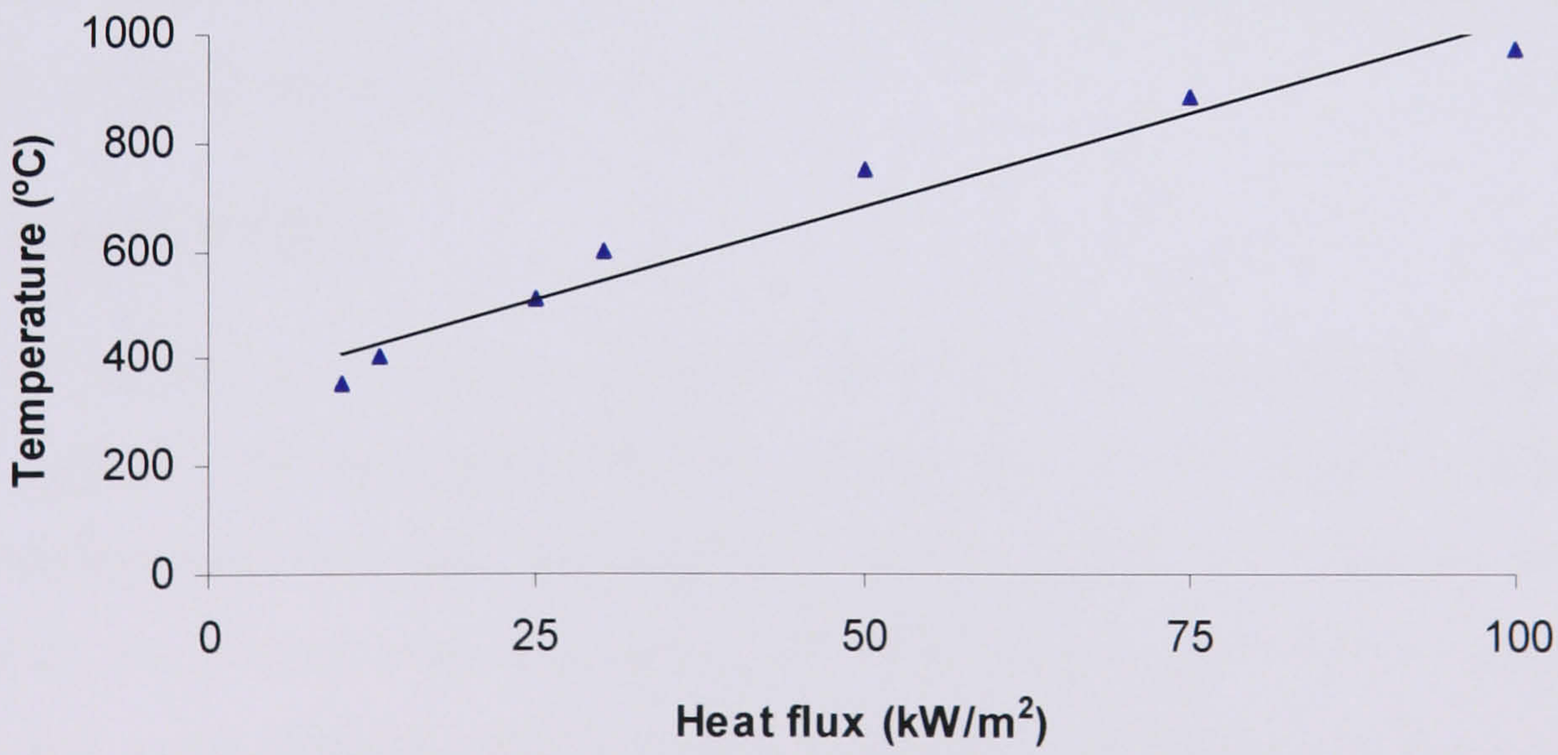


Figure 3.13 The heater calibration curve. The curve shows the temperature required to provide a heat flux from 10-100 kW/m^2

Chapter 4 Results & Discussion

The experimental results for testing glass fibre reinforced vinyl ester and polyester composite laminates are reported in this chapter. These results are used to characterise the fire behaviour of these materials in terms of their fire reaction and fire resistance properties. In addition, the effect of tensile and compressive stresses on main fire reaction properties is discussed.

4.1 Fire reaction properties

4.1.1 General

In the cone calorimeter test, the exposed surface of the material begins producing decomposition gases (outgassing) within a few seconds of exposure to the radiant heater. This outgassing is typically followed by an initial delamination within the surface of the laminate. Prior to sustained ignition, at least one flash of flame above the sample surface occurs. Heat fluxes of 50 kW/m^2 and 75 kW/m^2 were chosen as they represent the intensity of a room fire and a ship compartment fire, respectively. Two tests were performed in a horizontal position for every condition and the average values have been reported for each property. The back face and edges were thermally insulated using Kaewool in order to minimize edge effects.

4.1.2 Time-to-ignition

The start of flaming combustion is defined by the time-to-ignition. It is reported that the onset of ignition can be characterized in several ways: critical ignition temperature, critical incident heat flux onto the material's surface, rapid rate of rise in the surface temperature, and critical mass loss rate [15]. Many models assume that ignition takes place as soon as the material surface reaches the ignition temperature of the material and the concentration of flammable volatiles released by the decomposing matrix reach a critical value [113]. The measured time-to-ignition values for glass polyester composite were 39 seconds and 17 seconds, and for glass vinyl ester 46 seconds and 18 seconds at

50 kW/m^2 and 75 kW/m^2, respectively. It can be noticed that the higher the irradiance level is, the earlier time-to-ignition because of the faster decomposition rates.

4.1.3 Heat release rate

Heat release rate (HRR) is the most important key measurement required to assess the fire development of materials and products, and it is considered as the driving force for fire spread [30, 61, 108]. It provides an indication of the fire size, rate of the fire growth, the time available for escape and the type of effective suppressive action.

HRR is the thermal energy produced per unit area of flammable materials' surface and is controlled by the amount of combustion gas products resulting from matrix decomposition. These gaseous decomposition products may themselves reduce the heat release rate because they are endothermic. Also, the flow of gases from the cold face to the hot face has a cooling effect.

Peak heat release rate (PHRR) indicates the maximum flammability of the material and this takes place a short time after ignition. Average heat release rate (AHRR) is the mean total heat released over a certain burning time (usually three to five minutes).

The HRR properties for vinyl ester and polyester composites tested at 50 and 75 kW/m^2, using the cone calorimeter, are shown in Table 4.1 and Figure 4.1. At these heat fluxes the surface temperature of the specimens is sufficiently high (more than 600°C) to allow for complete decomposition for the resin [15, 23, 30, 32, 33]. The average heat release rate values are presented over the first five minutes (300 seconds) as after this time the AHRR value has dropped considerably below the peak value. This makes 300s a convenient time period for determining AHRR [57, 114, 115].

Table 4.1 Average and peak HRR for glass vinyl ester and polyester composites at 50 and 75 kW/m^2

	Heat flux of 50 kW/m^2		Heat flux of 75 kW/m^2	
	Peak HRR (kW/m^2)	Average HRR (kW/m^2)	Peak HRR (kW/m^2)	Average HRR (kW/m^2)
Glass/polyester	262 ± 7	137 ± 3	335 ± 5	182 ± 8
Glass/vinyl ester	249 ± 2	145 ± 1	298 ± 3	183 ± 5

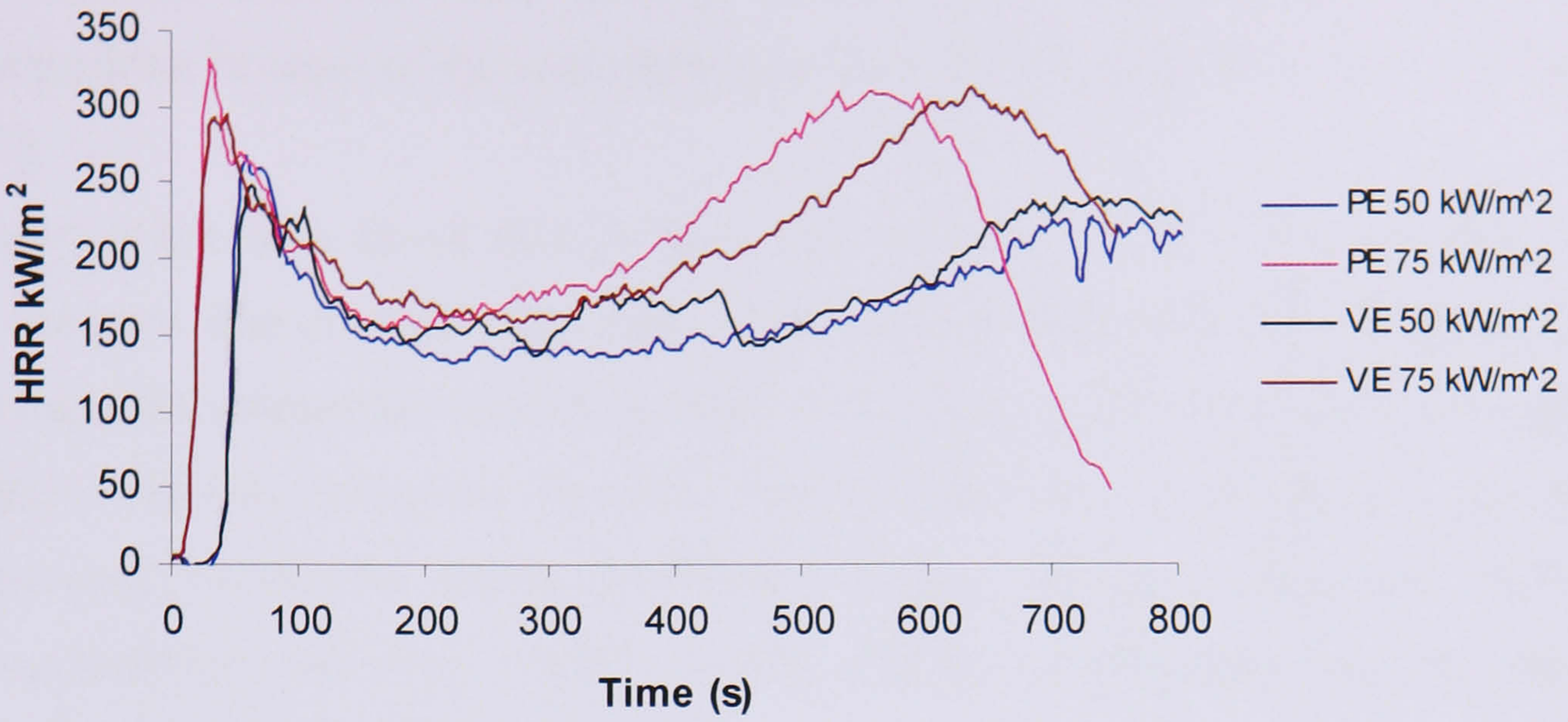


Figure 4.1 Heat release rate profiles for glass vinyl ester and polyester exposed to a constant heat flux of 50 and 75 kW/m^2

The HRR profiles oscillate with exposure time because of different chemical and thermal events that take place. Firstly, the composite does not release any heat (induction period) which means that volatilisation decomposition temperature has not reached yet. Secondly, sudden increase in HRR due to the ignition of the material surface resin rich layer, which indicate high gasification rates, until it reaches its' peak. Thirdly, HRR declines progressively with time due to the formation and growth of char. Char reduces the release of heat by delaying the heat transfer into the underlying material and also hindering the gas transfer from the decomposition front. The second increase in HRR after this period is mainly due the presence of some resin attached to the back surface of the sample, which by that time becomes thin and burns very quickly. Also, the insulation in the back face of the material forces the temperature to increase and thus enhances the decomposition rate. Fourthly, the heat release curve goes down to a very low value, which is an indication of complete resin degradation.

Because the composite used is a woven laminate, the profile fluctuates with a series of peaks and troughs over time, which reflects an erratic burning. This behaviour is mainly due to the fact that woven composites have different layered structure as they have resin-rich regions between the ply layers. During exposure to fire, the burning rate of the resin-rich layer produces more volatiles, which causes the peaks, while burning less resin glass layers results in lower HRR and as a consequence troughs are obtained. It has

been reported that the HRR profile for chopped fibre laminates has steady decomposition because of the reasonable distribution of resin between the glass layers [15, 27].

Moreover, it has been found that the heat flux has a significant effect on HRR. The graph indicates that the HRR rises with increasing heat flux especially the peak value. due to rapid decomposition reaction at higher heat fluxes. This effect was also reported for other composite laminates by other authors [26, 116]. In contrast, it has been demonstrared [15] that the AHRR and PHRR of high performance thermoset laminates, such as phenolics, are less sensitive to the increase of external heat flux due to temperature induced char formation.

4.1.4 Smoke production

The importance of characterising the smoke production comes from the fact that it can be a safety hazard, especially if it is dense, reducing visibility, causing disorientation and making fire fighting a complex task. The specific extinction area (SEA) is used to quantify the smoke density. It measures the effectiveness of converting a given mass of volatiles into smoke.

Table 4.2 shows a comparison of average and peak SEA (300 seconds) of glass vinyl ester and polyester composites at two different heat fluxes. From this Table, it can be seen that the increase in fire intensity (heat flux) leads to a slight increase in smoke obscuration. This is probably due to the increase in soot particles production. In contrast to the reported smoke density for highly aromatic polymer composites; it decreased with the increase of heat flux due to their high char yield, which restricts the flow of soot and decomposed gases to the surface [116]. Also, it is clearly noticed that the smoke production in vinyl ester is slightly higher than in polyester due to the higher styrene content in vinyl ester composites, 44% compared to 35% in polyester [15]. A strong direct correlation was reported between smoke density and HRR [30] because both properties depend on the endothermic decomposition rate.

Table 4.2 Average and peak SEA for glass vinyl ester and polyester composites at 50 and 75 kW/m^2

	Heat flux of 50 kW/m^2		Heat flux of 75 kW/m^2	
	Peak SEA (m^2/kg)	**Average SEA (m^2/kg)**	**Peak SEA (m^2/kg)**	**Average SEA (m^2/kg)**
Glass/polyester	2742 ± 140	1010 ± 50	2852 ± 155	1178 ± 30
Glass/vinyl ester	2908 ± 160	1249 ± 60	3433 ± 220	1577 ± 29

4.1.5 CO and CO_2 production

The production of toxic gases such as CO from burning the polymer composite are a major safety concern for human survival [117]. It has been reported that death in humans takes place within an hour when the concentration of CO or CO_2 reaches 1500 and 100,000 ppm, respectively [15].

Table 4.3 indicates that the amount of CO produced by a composite is directly related to the heat release rate, whereas the correlation between heat release rate and average CO_2 yield is unclear [30]. This is because of the stronger dependence of CO_2 on the oxygen available in the atmosphere than on the decomposition rate, which controls the HRR. It can be concluded that in applications where CO hazard has to be a minimum value, composites with low AHRR have to be selected.

Table 4.3 CO/CO_2 yields and AHRR for glass vinyl ester and polyester composites at constant heat fluxes of 50 and 75 kW/m^2

	Heat flux of 50 kW/m^2			Heat flux of 75 kW/m^2		
	ACOY (kg/kg)	**ACO_2Y (kg/kg)**	**AHRR (kW/m^2)**	**ACOY (kg/kg)**	**ACO_2Y (kg/kg)**	**AHRR (kW/m^2)**
Glass/polyester	0.00013	2.5	163	0.043	2.14	206
Glass/vinyl ester	0.0004	2.5	145	0.052	2.28	209

4.1.6 Mass loss

The weight change of glass vinyl ester and polyester composite laminates was measured as shown in Figure 4.2 using the load cell attached to the cone calorimeter. The remaining mass fraction is the instantaneous mass divided by the original mass of the composite.

It is clear that the graph shows different regions for each mass loss profile. These regions correspond to the same events that occur in HRR curves (Figure 4.1). This indicates that the mass loss measurement is an accurate tool to determine the amount and rate of decomposition and it controls the heat release rate.

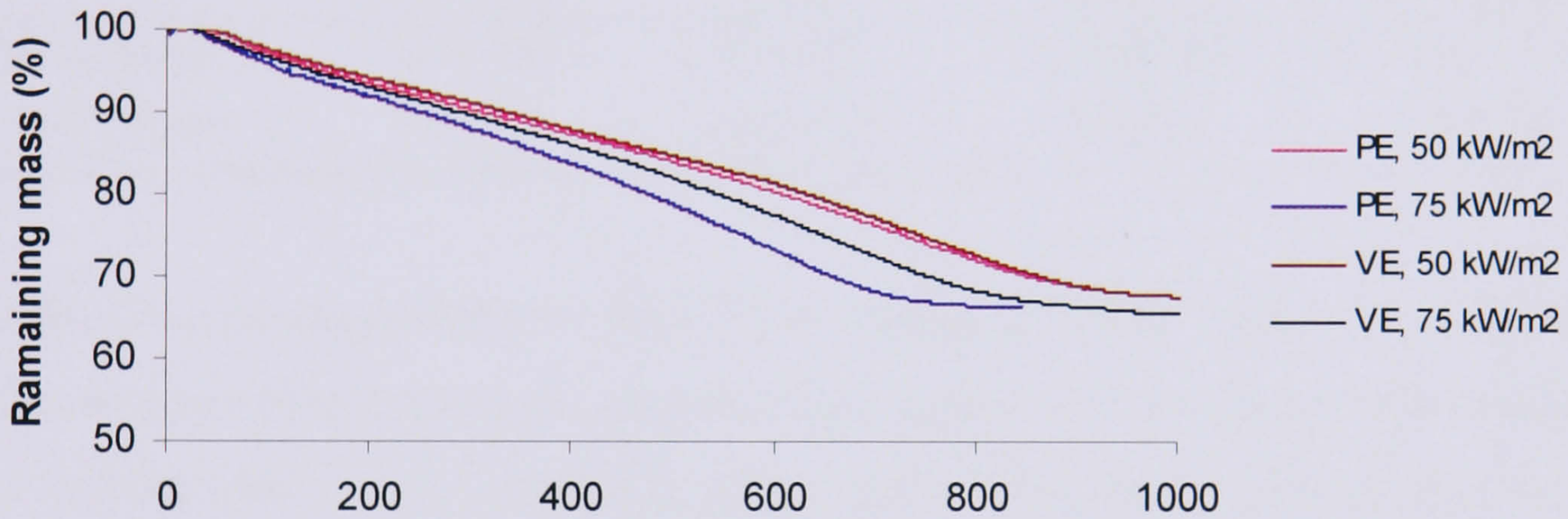


Figure 4.2 Mass loss curves for glass vinyl ester and polyester composites at constant heat fluxes of 50 & 75 kW/m^2

4.1.7 Effective heat of combustion

The amount of heat released by the combustion of a unit quantity of fuel is known to be the effective heat of combustion (EHC) [118]. It is derived by dividing the energy released by the mass loss rate. The CONECALC software calculates the effective heat of combustion for the material being tested and includes it in the output file.

Table 4.4 shows the measured values for peak and average heat of combustion for glass vinyl ester and polyester samples at two different heat fluxes. It is clear that the peak values generally occur after the sample has burned for several minutes and the heat release rate had decreased considerably, whereas the average EHC over a time period of

300s and the EHC for the entire burn period were almost the same. For this reason the EHC for the entire burning was chosen for reporting purposes.

Table 4.4 shows that average EHC values were approximately the same regardless of the level of applied heat flux because the potential energy to produce volatiles is the same. This finding reinforces the published literature [115, 119].

Table 4.4 Peak and average heat of combustion for glass polyester and vinyl ester composite laminates at 50 & 75 kW/m^2 irradiance levels

	Heat flux of 50 kW/m^2		Heat flux of 75 kW/m^2	
	Peak EHC (MJ/kg)	**Average EHC (MJ/kg)**	**Peak EHC (MJ/kg)**	**Average EHC (MJ/kg)**
Glass/polyester	73 at 730s	23 ± 0.5	69 at 695s	21.5 ± 0.5
Glass/vinyl ester	61at 900s	24.5 ± 0.2	53at 880s	25 ± 0.2

The effective heat of gasification (EHG) is the heat required to produce a unit mass of gaseous volatiles from a unit mass of solid [120]. Quintiere [121] described a method to derive it: peak HRR values are plotted against applied heat flux and the slope of the line represents the quotient of EHC/EHG and hence, EHG can be determined. By applying this method, the effective heat of gasification, EHG, is found to be 9.3 MJ/kg & 7.8 MJ/kg for glass polyester and vinyl ester, respectively. These two values should be treated with caution because only two flux values were used to draw the slope line.

4.2 Testing composite laminates under load using the cone calorimeter

The results below represent the measurement of the fire reaction properties as function of the applied stress and study the mechanical-pyro effects on glass vinyl ester and polyester composite laminates. A heat flux of 75 kW/m^2 was employed in this study, corresponding to a fairly severe fire, as might be encountered in a compartment fire on a ship. A lower heat flux such as 25 kW/m^2 was not used to avoid heating the grips due to longer exposure periods, which may affect the results.

4.2.1 Mechanical-thermal effect on fire reaction properties

4.2.1.1 Mechanical- thermal effect on heat release rate and time-to-ignition

The full heat release rate profiles, up to sample failure, for glass vinyl ester and polyester are shown in Figure 4.3 and Figure 4.4, respectively, as functions of the applied tensile stress at constant heat flux. The main effect of increasing tensile stress was to shorten the time taken to failure, an effect that will be discussed later. It can also be seen that increasing the tensile stress has a small, but significant effect on the heat release rate: increasing it. In the case of compressive stress, shown in Figure 4.5 and Figure 4.6, the failure times were shorter and the heat release decreased slightly with increasing stress.

All the heat release rate profiles showed similar characteristics: a short delay, corresponding to the observed time-to-ignition, a rapid increase up to the peak heat release rate, then a slow decline to a steady, almost constant 'minimum' release rate that lasted up to the point of sample failure.

It is interesting to note that there was little change in the heat release profiles at the point of sample failure, either in tension or compression. This may be because, when failure occurred, the peak heat release rate had already passed, with the heat release rate having fallen to the lower almost steady value mentioned above. At this stage a significant proportion of the resin will have already been burnt out from the sample surface layers.

The heat release profiles and the size of the stress effect can be seen to be fairly similar for the vinyl ester and the polyester-based laminates. This is probably to be expected, as both resins are based on 'solvent monomer' systems, in which styrene is an important component. In the present case the heat release rate of the vinyl ester samples was slightly lower than that of the polyester, which is in contrast to previous work [15], where the reverse was reported. It is probable that the heat release of these resins depends to some extent on the particular grade of vinyl ester or polyester and, most especially, on the actual styrene content and chemical differences between the species present in the main chain backbone. As reported previously [15], the thermal decomposition characteristics of vinyl ester and polyester resins are similar, in that they both generally decompose almost completely into volatile products, leaving only a small percentage of char, often of the order of 4% of the original resin mass. This almost complete decomposition is again likely to be due to the resin styrene content. Such behaviour is in marked contrast to resins such as phenolic, which contain complex highly crosslinked aromatic species, that can produce a substantial yield of carbonaceous char on decomposition [1, 2, 15, 17, 18, 30, 122].

The vinyl ester is a little more thermally stable than the polyester [15]. For instance, thermogravimetric analysis (TGA), detailed in the next Chapter, at a heating rate of 25 °C/min in N_2 shows a maximum decomposition rate at 450°C for vinyl ester, compared to 425°C for polyester (see Figure 5.3 and Figure 5.4).

The details of the important initial heat release peaks are difficult to distinguish in Figure 4.3 to Figure 4.6, so the information was re-plotted over a shorter timescale of 120 seconds, in Figure 4.7 and Figure 4.8, for the two resin types, with the data for tensile and compressive stress combined. There were no tensile failures within 120 seconds, but some compressive samples did fail within this period. This has been indicated in Figure 4.7 and Figure 4.8 by placing a cross on the curves in question at the point of failure. It is acknowledged that the levels of variation in heat release rate, time-to-ignition and smoke production rates were within the range of scatter normally expected between cone calorimeter measurements. However, it should be borne in mind

that these results were generated within a single run of experiments for each resin type, with the calorimeter calibration being checked at both the beginning and end of the run. Despite a certain level of scatter, which is fairly typical for this type of measurement, a clear pattern can be discerned, in which the release profiles decrease fairly progressively in magnitude going from the highest tensile stress, down to the lowest compressive one. This decrease is accompanied by an increase in the induction time for the onset of heat release, which is roughly the same as the observed time to ignition.

The physical processes involved when composites are exposed to heat have been discussed by Mouritz and co-workers [15, 23, 32, 33]. First the laminate surface is heated by the incoming heat flux. The surface temperature increases, resulting in decomposition of the resin, producing volatile, often flammable, by-products, which generate a pressure within the resin phase [4, 6]. This leads eventually to the formation of a network of cracks in the resin phase. These resin cracks will form predominantly normal to the plane of the laminate, permitting the easier escape of volatiles. When the laminate surface temperature reaches a particular value, depending on the heat flux [15, 23, 32, 33], the volatile evolution rate is sufficient to allow ignition and sustained combustion to occur. This critical surface temperature for the onset of ignition has been estimated for vinyl ester resin to be about 600 °C for the present heat flux of 75 kWm^{-2} [15, 23, 30, 32, 33].

The present results show the onset of ignition to be significantly affected by stress. The most probable mechanism is that tensile stress promotes the formation of resin cracks, shortening the time-to-ignition. Conversely, compressive stress can be expected to inhibit cracking, giving the opposite effect.

As mentioned, the laminates in this study are thermally 'thick': which means that there can be a significant temperature difference between the heat-exposed and rear surfaces. A 'front' of decomposing resin passes through the thickness of the laminate, generating flammable volatile products that migrate to the laminate surface, where they burn. The speed at which this decomposition front passes through the laminate is controlled to a

certain extent by heat transfer, and the endothermic nature of the resin decomposition process. The heat release profiles demonstrate that an almost steady-state condition is achieved, with near constant release rate, which persists through to the point of mechanical failure.

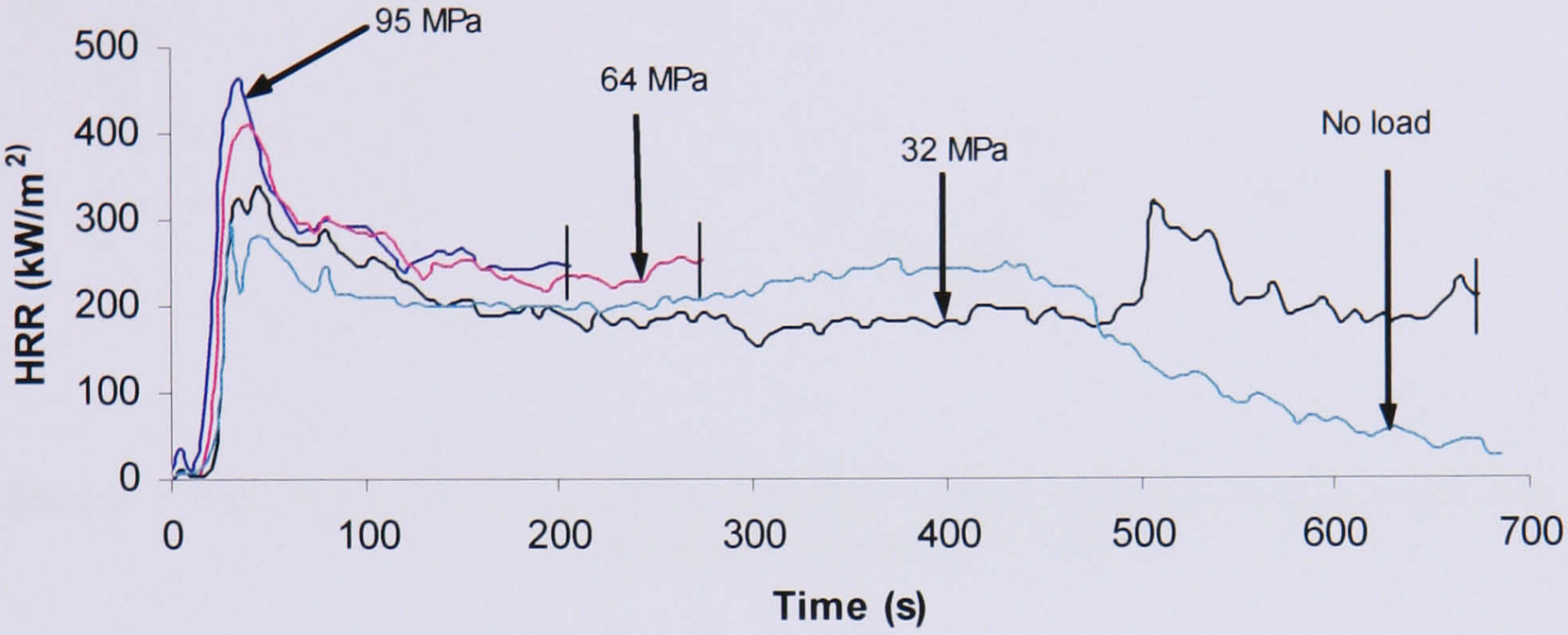


Figure 4.3 Full heat release rate profiles for glass vinyl ester laminates under tensile stress at a constant heat flux of 75 kW/m^2

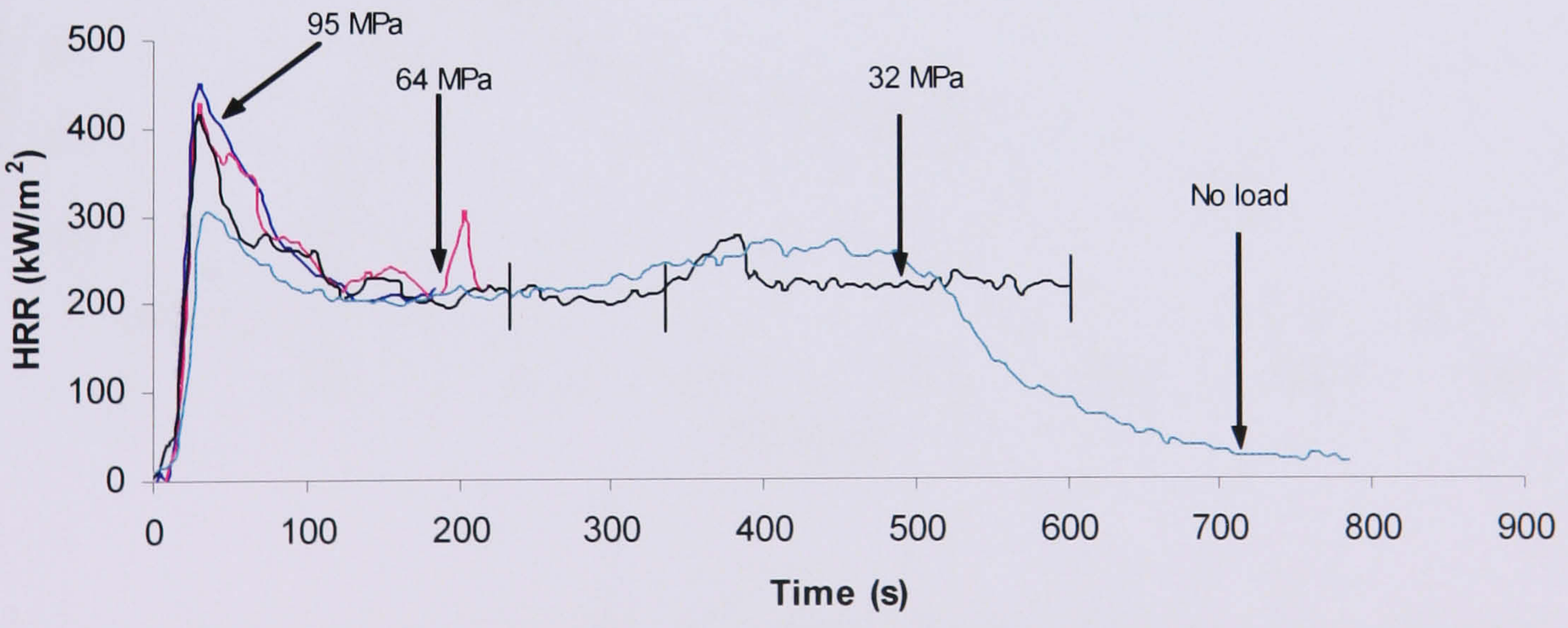


Figure 4.4 Full heat release rate profiles for polyester laminates under tensile stress at a constant heat flux of 75 kW/m^2

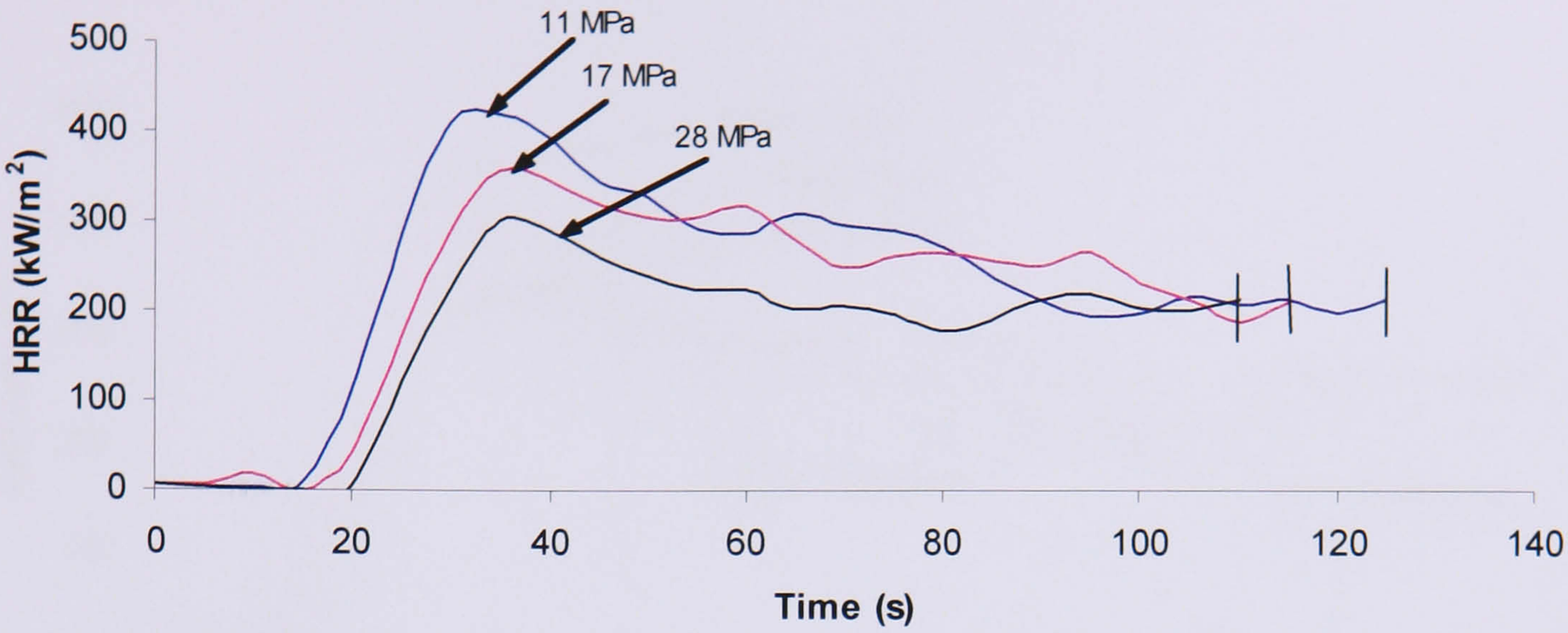


Figure 4.5 Full heat release rate profiles for glass vinyl ester laminates under compressive stress at a constant heat flux of 75 kW/m^2

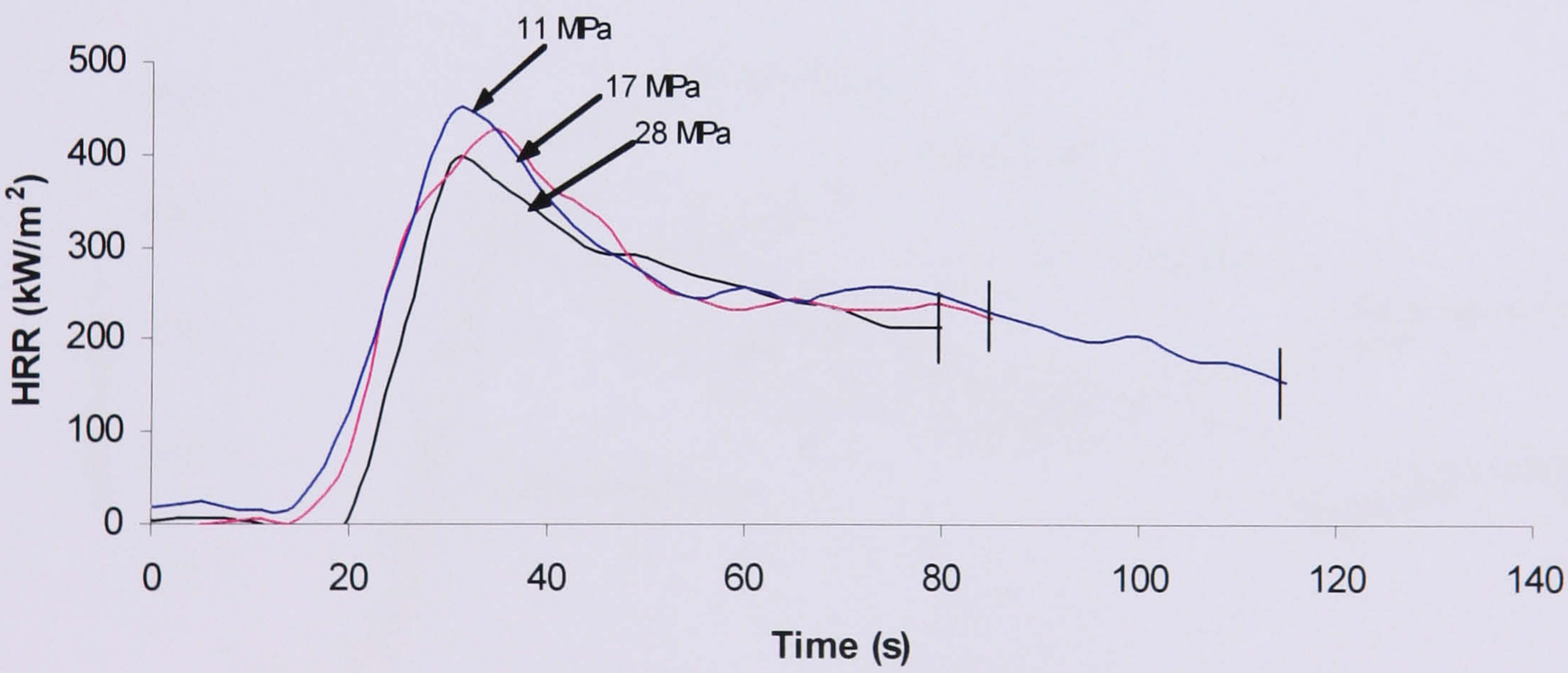


Figure 4.6 Full heat release rate profiles for glass polyester laminates under compressive stress at a constant heat flux of 75 kW/m^2

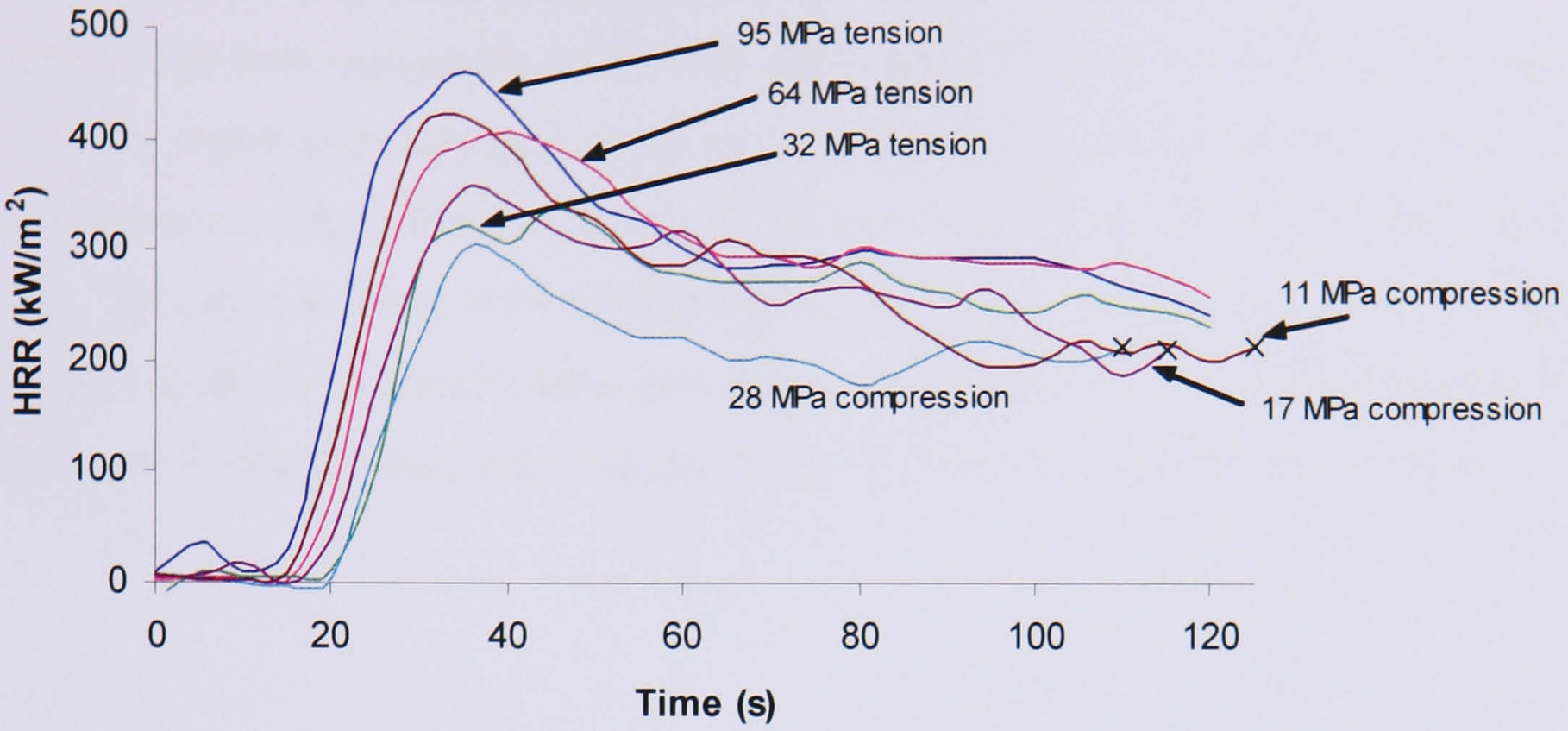


Figure 4.7 Heat release rate of glass vinylester under tensile & compression loads at a constant heat flux of 75 kW/m^2

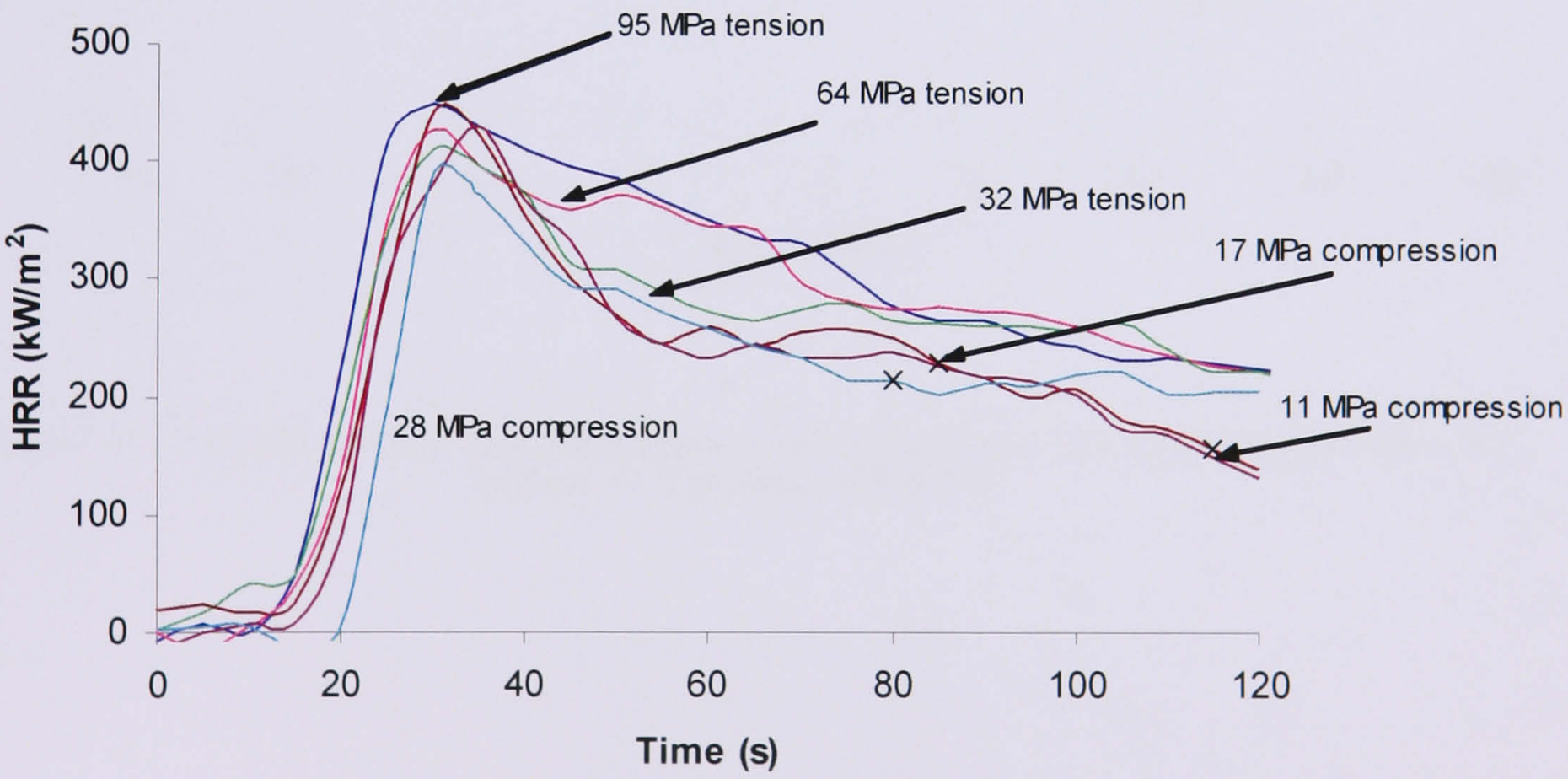


Figure 4.8 Heat release rate of glass polyester under tensile & compression loads at a constant heat flux of 75 kW/m^2

Figure 4.9 shows the peak heat release rates (PHRR) and minimum release rates (MHRR) at failure as a function of stress. Also, it shows the same property values at zero stress for both composite resins. The stress effect is clear on the peak heat release rate curves, again emphasising the increased release rate for tensile stress and vice versa for compressive. The effect can be seen to be rather less for the minimum heat release at failure. This is in keeping with the hypothesis that stress predominantly affects matrix cracking and the initial heat release response. It is probably to be expected that the heat release rate during the later stages of exposure would be less significantly affected.

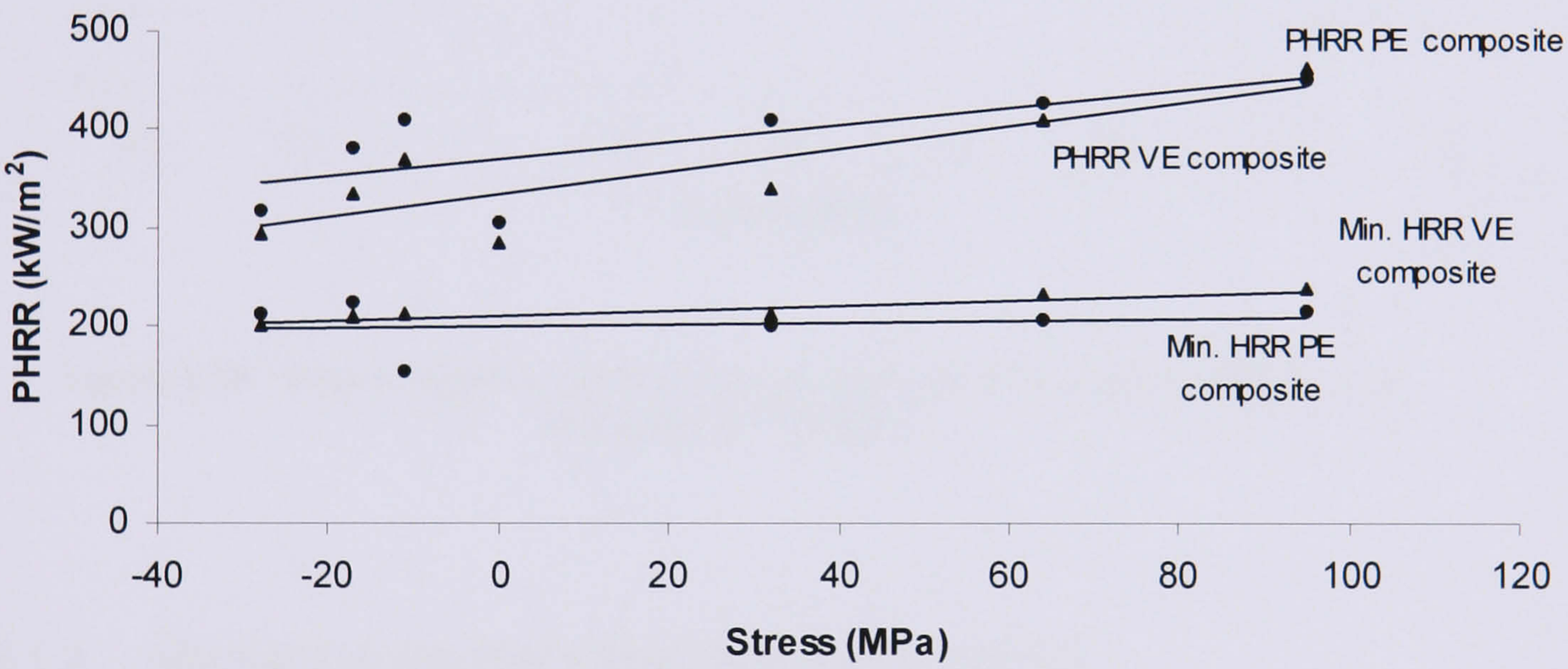


Figure 4.9 Peak and minimum heat release rates versus stress for glass vinyl ester and glass polyester laminates at a heat flux of 75 kW/m^2

Figure 4.10 shows the variation of the time-to-ignition also with stress, which is progressive, decreasing with increasing tensile stress and increasing with compressive stress. Both resin types behave similarly, with the vinyl ester showing slightly longer times-to-ignition as it shown at zero stress value.

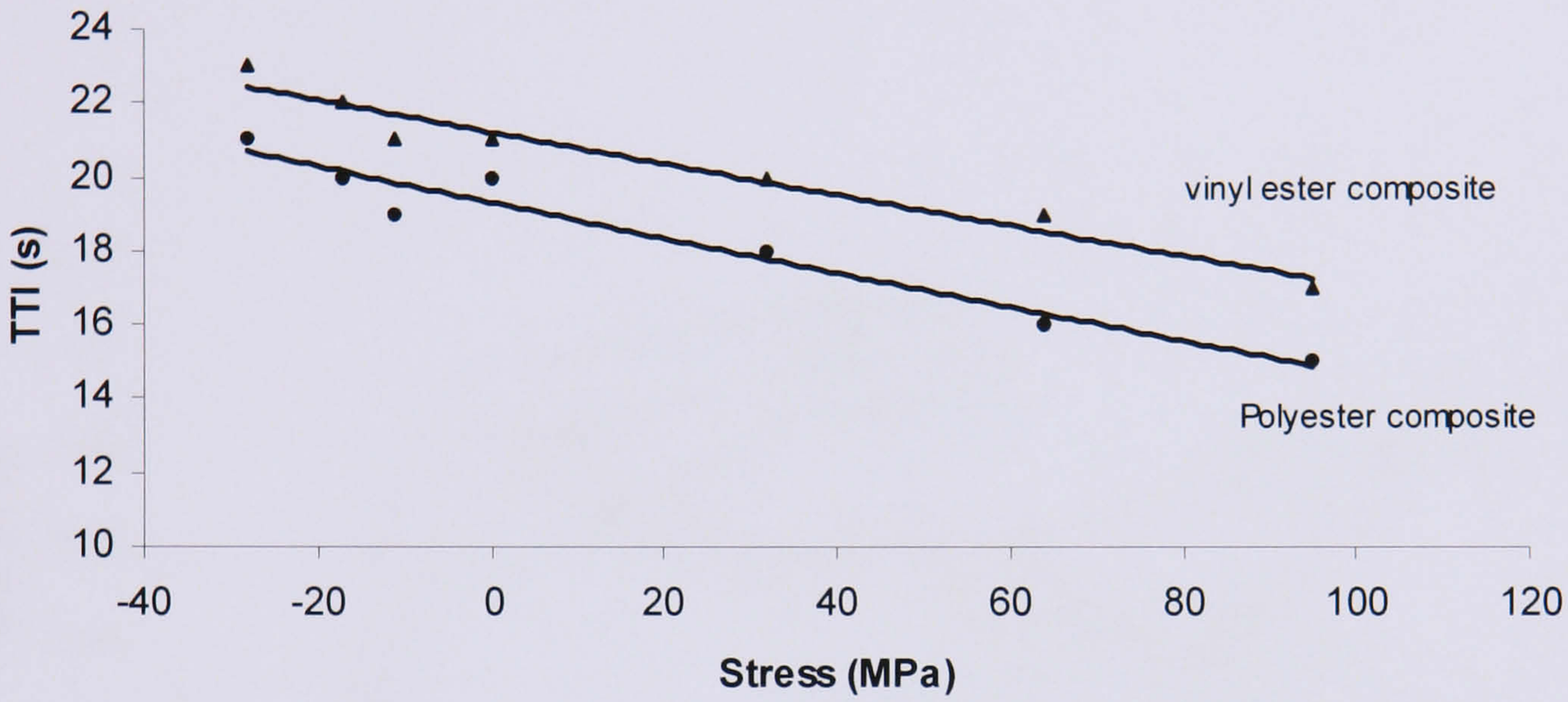


Figure 4.10 Time-to-ignition versus stress for glass vinyl ester and glass polyester laminates, at 75 kW/m^2

4.2.1.2 Mechanical-thermal effect on smoke evolution

Figure 4.11 and Figure 4.12 show the effect of stress on the smoke generation profiles over a 120 second period. These are rather similar in shape to the heat release profiles already discussed, albeit with greater superimposed fluctuations. The vinyl ester smoke generation is somewhat greater than that for the polyester laminates due to its higher styrene content. As with heat release, a significant effect of stress can be observed. Figure 4.13 shows the peak smoke generation (PSPR) rate and the minimum smoke generation rate (MSPR) at sample failure. As with heat release the stress effect can be seen, the curves being rather similar to those in Figure 4.9 for peak heat release rate. The close relationship between heat release and smoke generation for composite systems of

this type has been discussed previously [30]. However, the final value of smoke production rate at failure, which shows quite a lot of scatter, actually declines a little with increasing stress. The probable reason may be that much of the smoke is evolved during the initial peak, so increasing this peak will result in a decline smoke during the later stages of exposure.

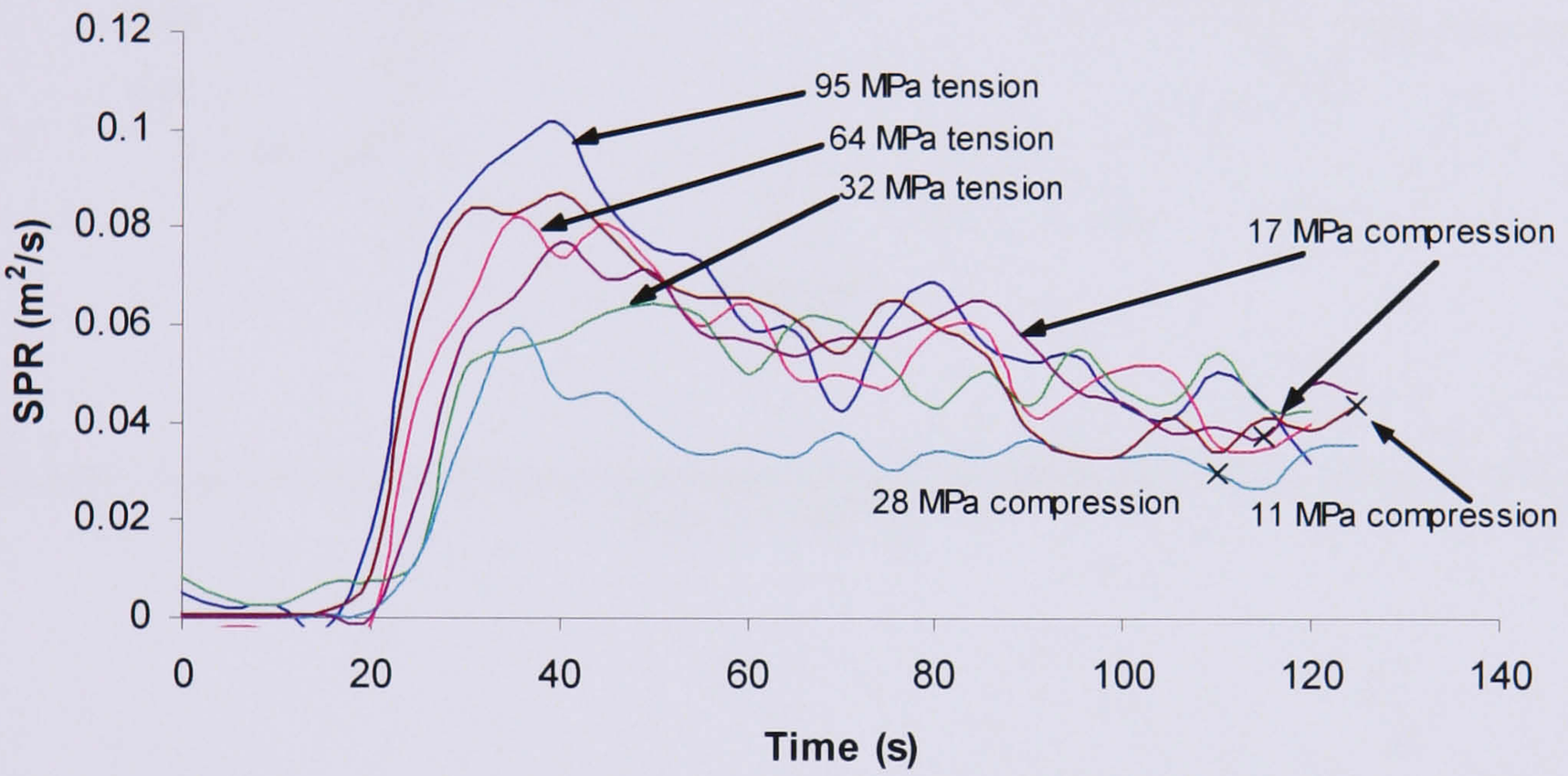


Figure 4.11 Smoke production rate profiles for glass vinyl ester laminates under tensile and compression stress, at 75 kW/m^2

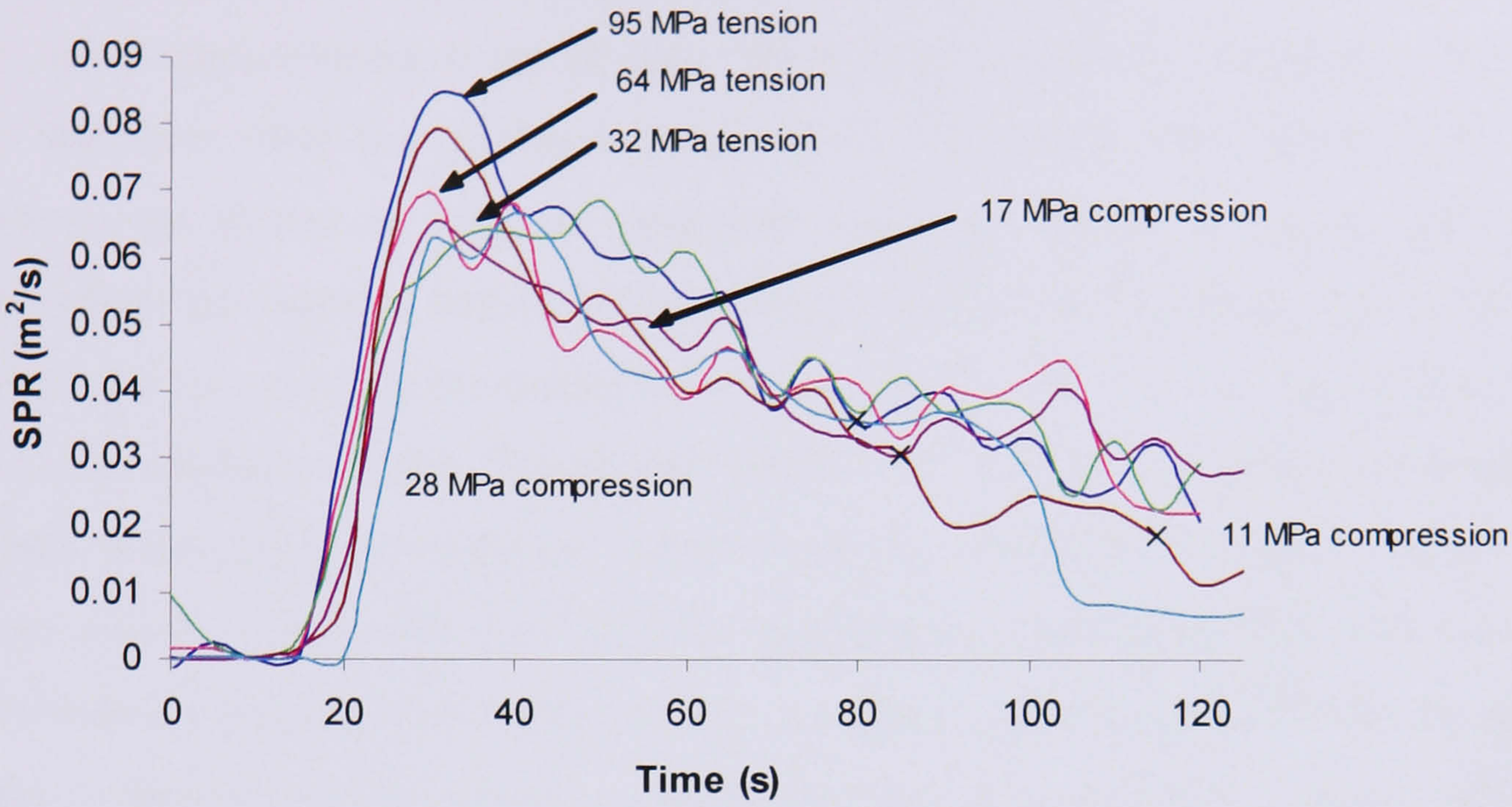


Figure 4.12 Smoke production rate profiles for glass polyester laminates under tensile and compression stress, at 75 kW/m^2

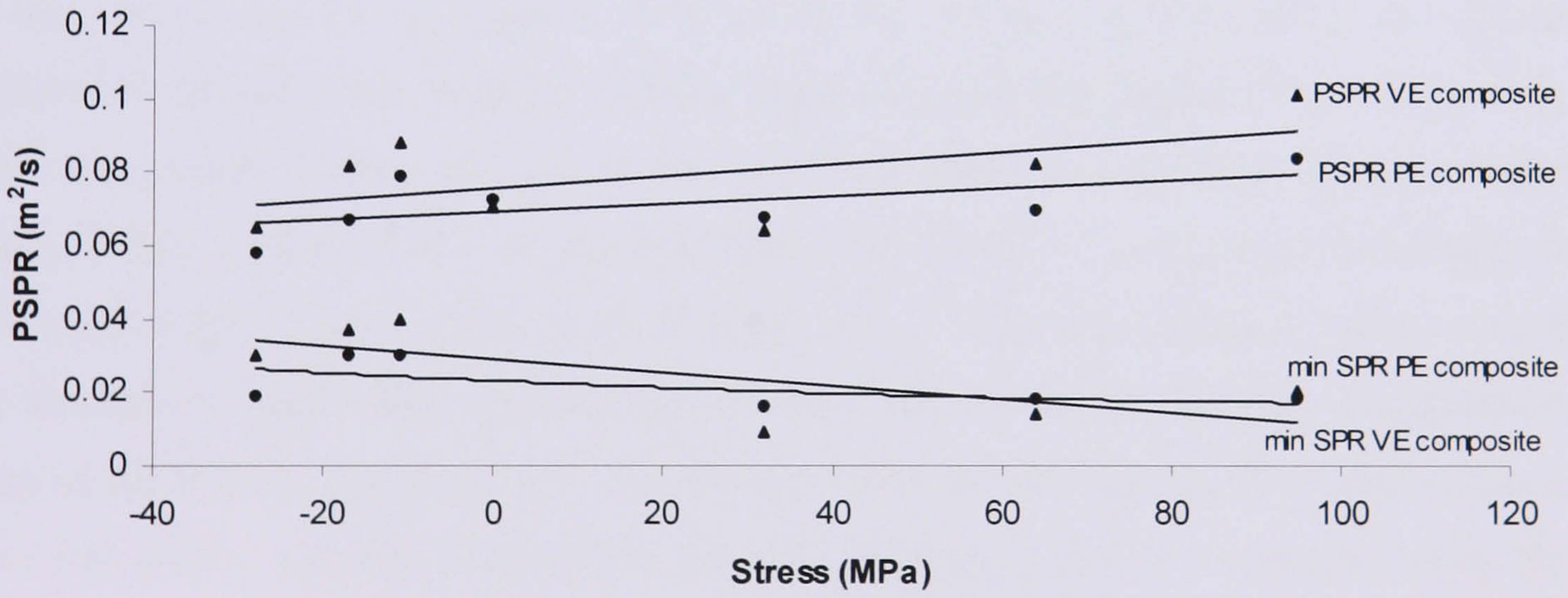


Figure 4.13 Peak and minimum smoke production rate versus stress, for glass vinyl ester and glass polyester laminates at 75 kW/m^2

4.2.1.3 *Time-to-failure*

Figure 4.14 and Figure 4.15 show 'stress rupture' plots of tensile and compressive stresses, respectively. These curves relate the time-to-failure, shown on the horizontal axis, to the applied stress. It can be seen that in both tension and compression the failure time decreases when the applied stress increases. The failure times under tensile stress, however, are almost an order of magnitude larger than those for compressive stress. This reflects the fact that tensile failure is largely determined by the strength of the glass fibres, whereas compressive failure is resin dominated. The tension failure data for the two resin systems are rather close to one another, the vinyl ester system performing only slightly better than the polyester, again reflecting the fibre dominated nature of the failure process. The curves in this figure were fitted on the assumption of a power law relationship between tensile stress and time-to-failure. A point was added corresponding to the undamaged tensile strength, 440 MPa, which was assumed to correspond to an arbitrary time-to-failure of 10 seconds. The strengths for the undamaged samples were actually carried out, not in stress rupture, but at a testing speed of 10 mm/min. The exact timescale of the strength point corresponding to zero fire exposure is probably debatable.

In the tensile case it is possible, over about 10 minutes (600 seconds) to support composite stresses of the order of 30 MPa. Neglecting any contribution from the matrix, this corresponds to fibre stresses in excess of 130 MPa in those plies that are under stress. While significant, this is quite low, compared to the room temperature strength of commercial glass fibres, which is about 1,800 MPa. It has been reported, however, that the strength of glass fibres declines significantly and irreversibly at high temperatures, even in the absence of stress [32]. Debate continues on the origin of this phenomenon. First Possibility includes a corrosion process involving absorbed moisture from the atmosphere. Second possibility is the onset of devitrification (crystallization): glass undergoes a variety of physicochemical transitions that change the initially largely amorphous structure into one having elements of order/crystallinity. The formed crystals are weak and brittle. The 130 MPa stress value at 600 seconds corresponds fairly closely to the diminished strength value at elevated temperature predicted by the model reported in [32, 33].

Figure 4.16 shows a sample after failure in tension. The black appearance indicates a significant amount of residual decomposed resin. Fibre failure was distributed throughout the gauge length of the sample, with multiple points of fracture. The specimen did not separate into two clear parts, because pumping to the hydraulic cylinder was terminated when the load fell to zero.

Figure 4.17 shows one of the samples that failed in compression. The compressive failure mode involved localised kinking of the plies, followed by more extensive crumpling, accompanied by delamination of some of the hot surface plies. The kinking effect is similar to that described by Budiansky and Fleck [123] for isothermal compressive failure of unidirectional samples. This model assumes that some local region of material, in which the fibres are imperfectly oriented, initiates a shear-dominated local collapse. Despite the greater complexity of the present case, which is non-isothermal and which does not involve a unidirectional composite, the mechanism is clearly rather similar to this. The resin shear-dominated nature of the failure accounts for why it occurs at such a short time, or low average laminate temperature. Again a power law relationship was assumed when plotting the curves. Undamaged compressive strength values were 355 MPa and 310 MPa for vinyl ester and polyester, respectively. Again these were assumed to correspond to a time-to-failure of 10 seconds.

The longer-term stress that could be supported, at less than 10 MPa, is certainly lower than that observed in the tension case. It reflects the substantial softening of the resin at its glass transition temperature. The most pronounced kinking of the sample is near to the rear (cold) face. Due to the non-isothermal regime of the cone calorimeter test this cool region will concentrate most of the compressive stress, due to the fall in Young's modulus of the layers nearer to the laminate hot surface. Compressive failure probably initiates in this region.

The times to failure in tension and compression are somewhat shorter than those reported previously for similar laminates [1, 12, 13, 15]. The reason is probably the smaller sample size used here and the greater edge area. Although the edge region was

well-insulated during the tests it is known that there is an 'edge' effect, due mainly to the greater ease with which the volatiles can escape from this region. The shorter times to failure in the present work do not affect the main conclusions with regard to the effect of stress. Indeed it is possible the specimen edges reduced the apparent stress effect.

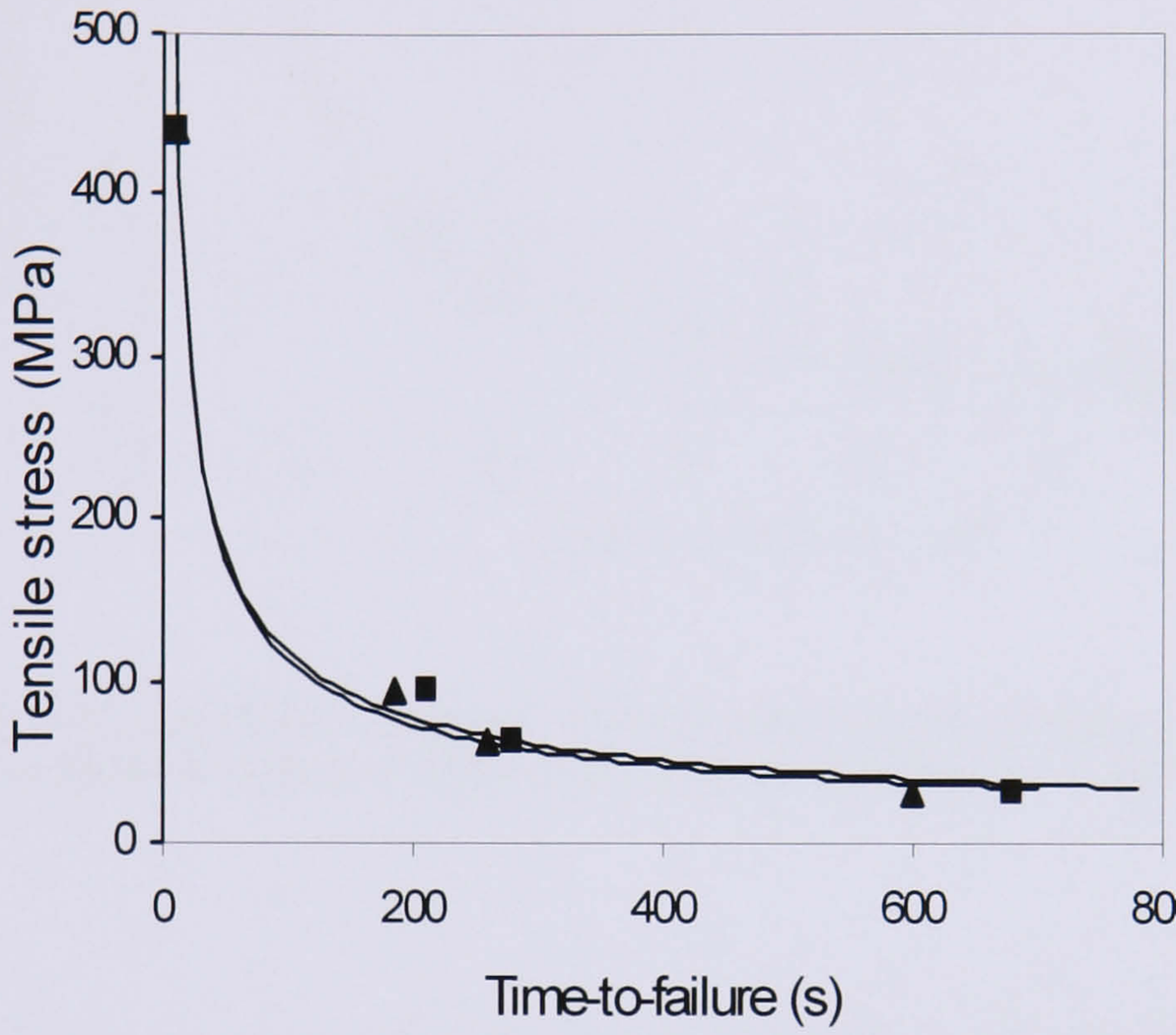


Figure 4.14 Tensile stress rupture curves (stress vs time-to-failure) for glass vinyl ester laminates (squares) and glass polyester laminates (triangles) at a heat flux of 75 kW/m^2

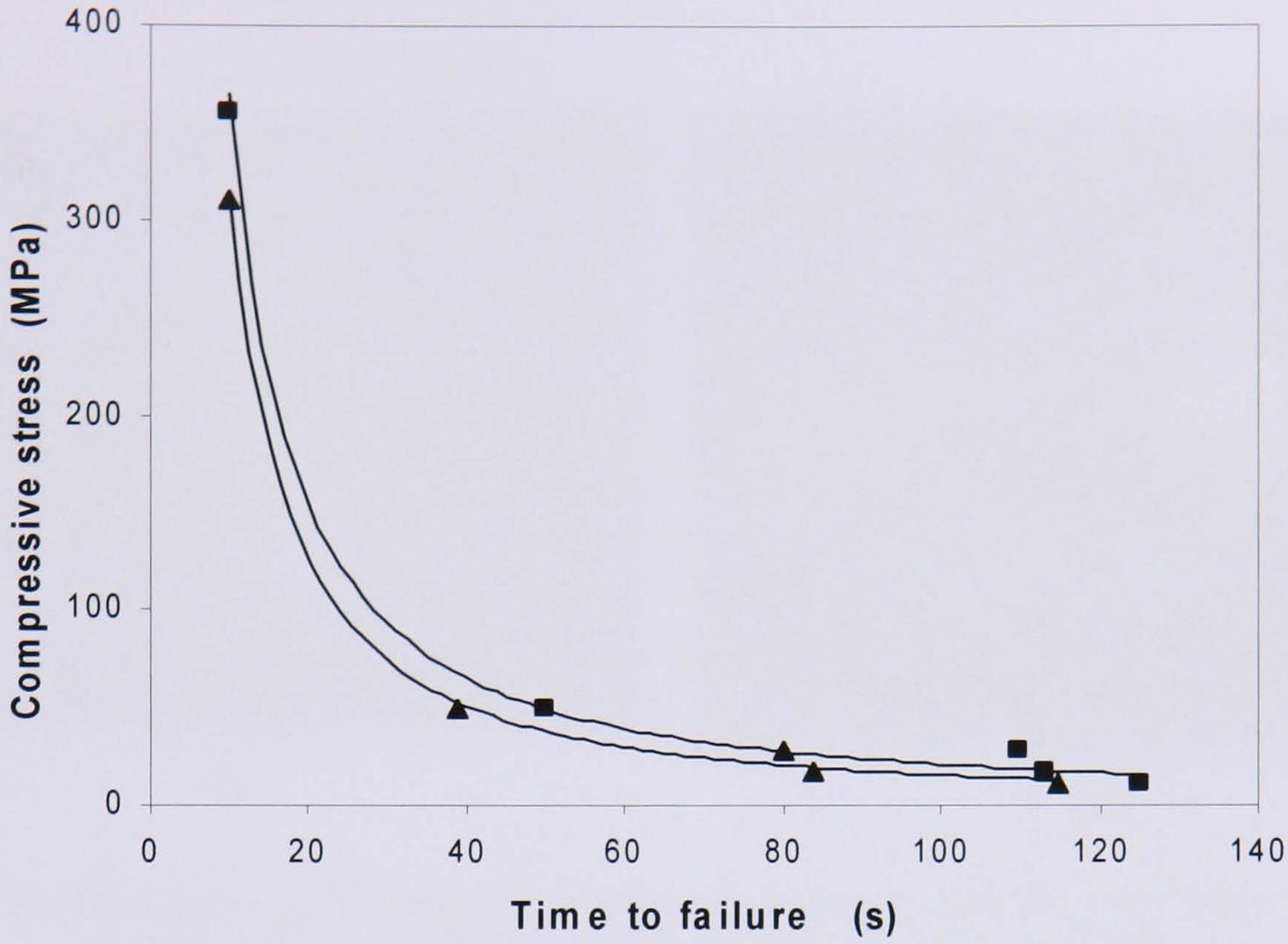


Figure 4.15 Compressive stress rupture curves (stress vs time-to-failure) for glass vinyl ester laminates (squares) and glass polyester laminates (triangles) at a heat flux of 75 kW/m^2

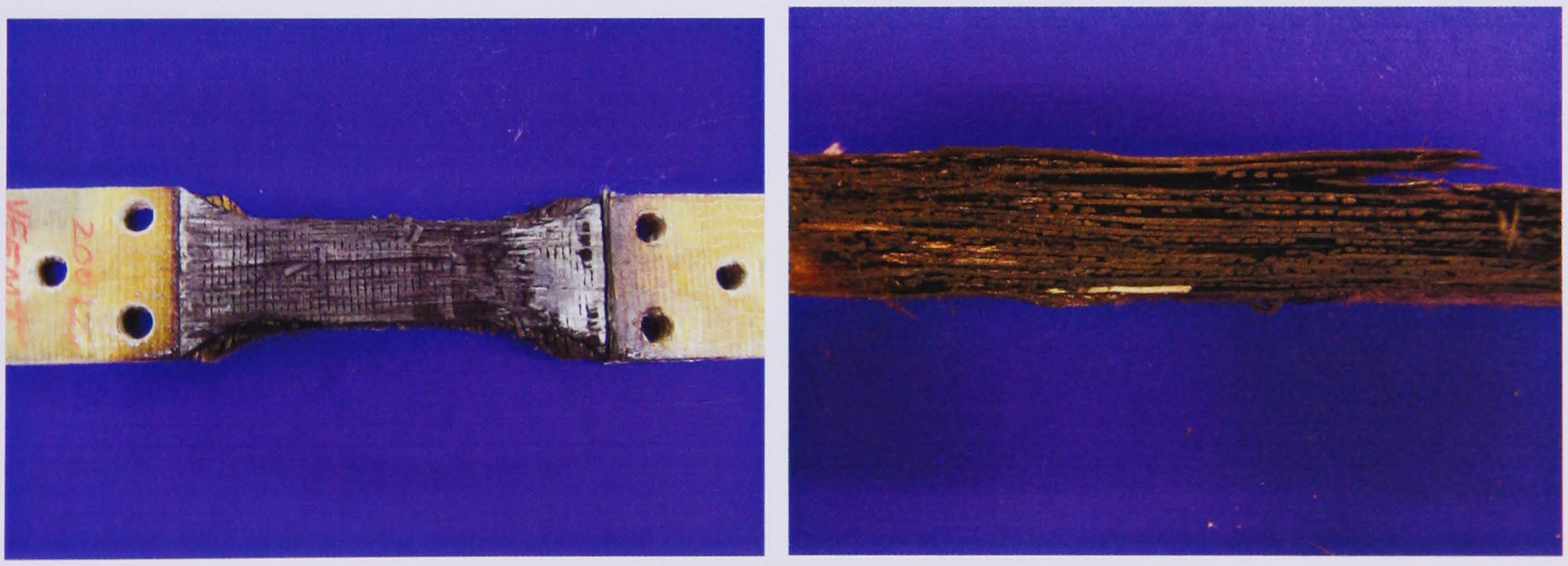


Figure 4.16 Samples failed under tensile loading and a constant heat flux of 75 kW/m^2



(i) (ii)

Figure 4.17 Samples failed under compressive load and a constant heat flux of 75 kW/m^2. (i) Kinking in the cold face. (ii) The hot face moves toward the heating element

4.3 Fire resistance properties

Fire resistance is mainly concerned with the physical and mechanical integrities of composite laminates. Stability, integrity and thermal insulation are the three failure criteria for fire resistance [74].

4.3.1 Thermal insulation (rear face measurement)

The main purpose of these measurements is to study the fire resistance of vinyl ester and polyester laminates subjected to constant heat fluxes of 50 and 75 kW/m^2 using the cone calorimeter.

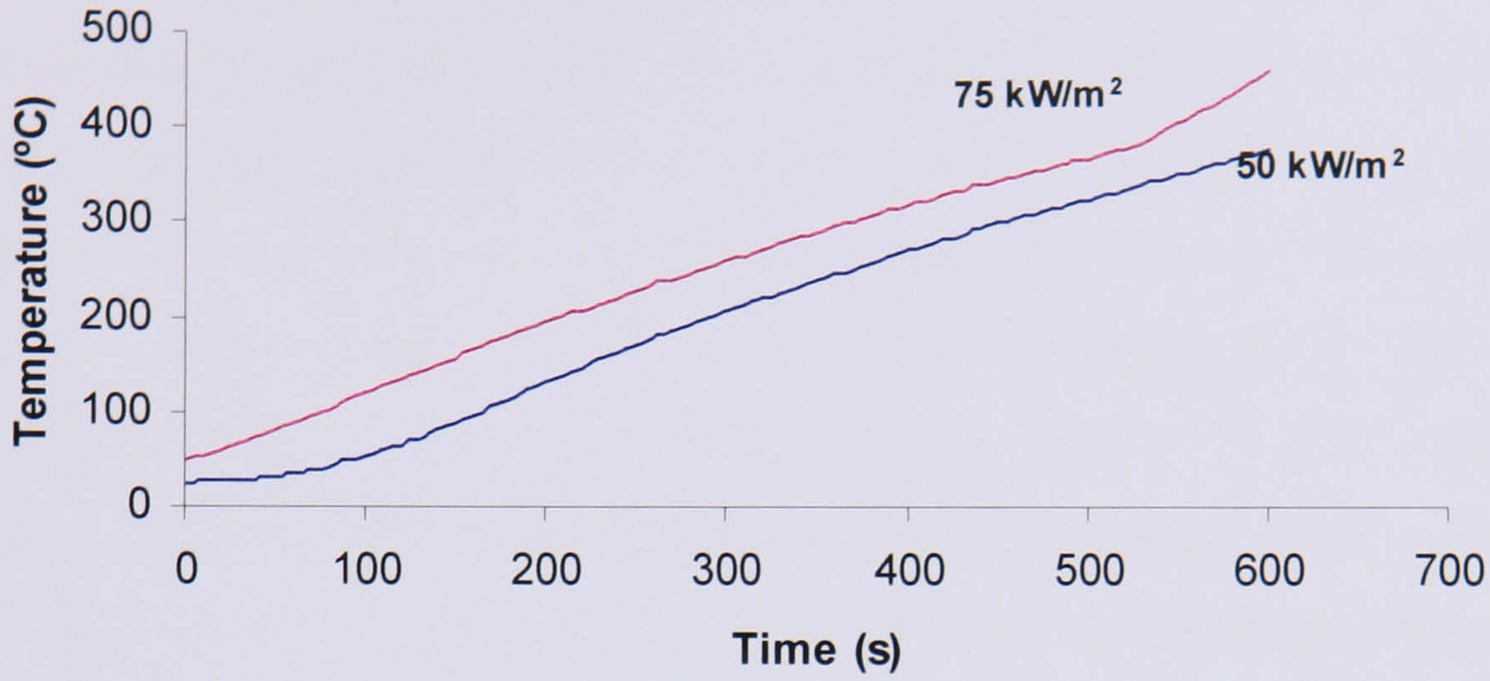


Figure 4.18 Rear face temperature profiles of glass polyester at constant heat fluxes of 50 & 75 kW/m^2

Figure 4.19 Rear face temperature profiles of glass vinyl ester at constant heat fluxes of 50 and 75 kW/m^2

The thermal resistance is assessed by the time taken to heat the unexposed surface (rear face) to 160°C. It is believed that the fire spreads to adjacent rooms when it reaches this temperature. From Figure 4.18 and Figure 4.19 the effect of heat flux on the rear face profile can be clearly seen, as the higher the heat flux is the less time to reach 160°C, i.e. lower the fire resistance. Also it has been observed that the thermal insulation provided by glass vinyl ester is ≈ 25% better than glass polyester laminates. This reinforces the finding that the time-to-failure for glass vinyl ester is higher than for glass polyester under the same loading conditions as in Figure 4.14 and Figure 4.15. The probable cause of this result is the decomposition temperature of both resin systems. From TGA results, detailed in next chapter in section 5.1.2, it can be seen that glass polyester started to decompose earlier than glass viny ester. This explains why polyester has thermal insulation than vinyl ester.

4.3.2 Fire testing under load

Small scale fire tests were conducted on glass vinyl ester and glass polyester specimens loaded in tension or compression at higher testing loads. A heat flux of 75 kW/m^2 was provided by a calibrated conical radiant heater to preloaded samples. The time to failure (TTF) was recorded for every given load. The testing arrangement was shown in Chapter 3 (Figure 3.9).

4.3.2.1 Tensile tests

Figure 4.20 shows the failure curves of glass polyester and vinyl ester laminates under tensile loads. Two main factors control the tensile failure: thermal resin softening followed by decomposition and rupture of the glass fibres. This phenomena was also observed by other researchers [32, 104] who compared the tensile strength of glass fibres, with composite laminates having the same type of fibres and subjected to the same testing conditions. They found that there was no major difference in failure time, which indicates that tensile failure is fibre dominated. Therefore, the composite laminate fails when the applied stress reaches or exceeds the fibres' strength.

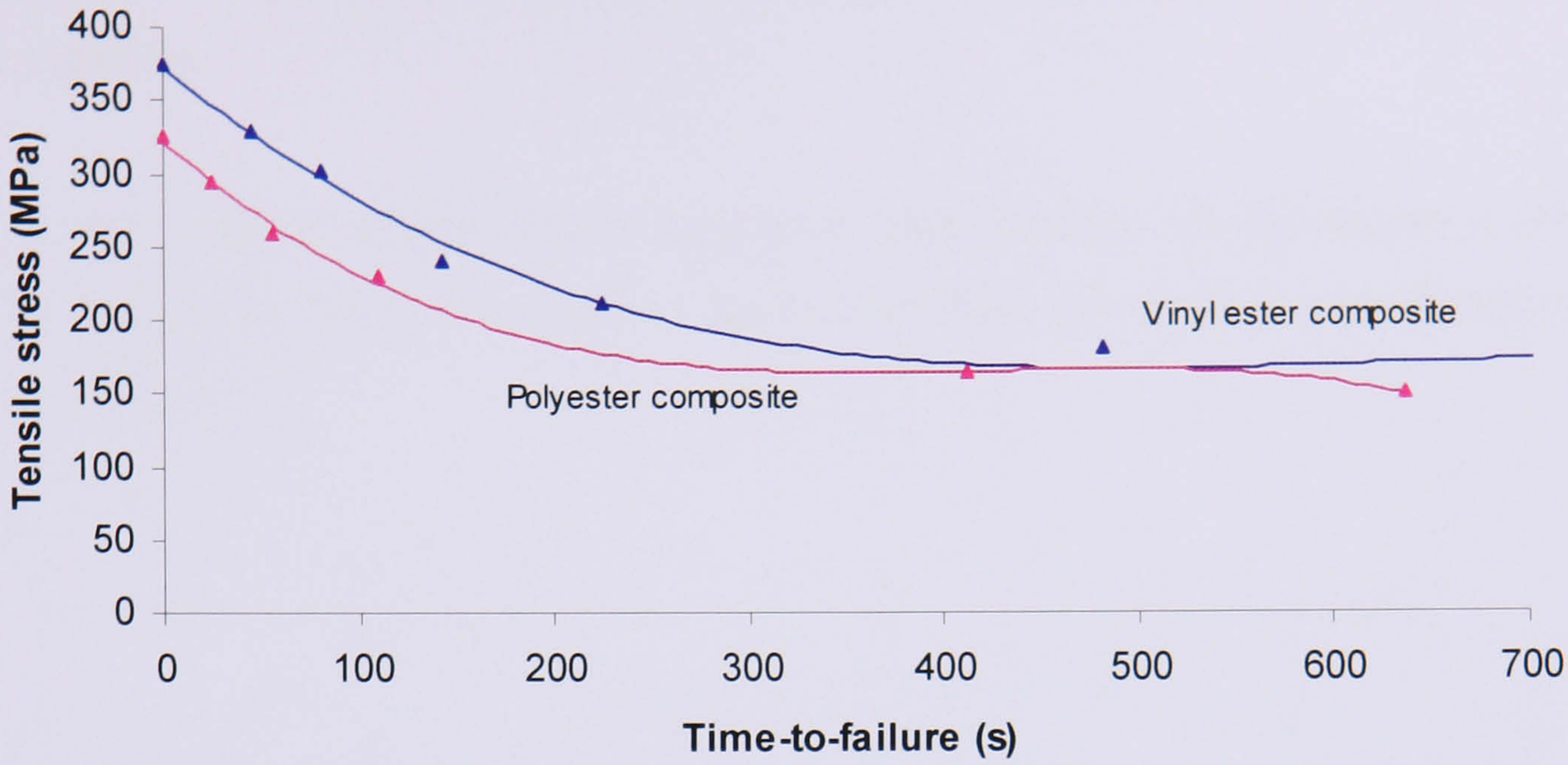


Figure 4.20 Glass polyester and vinylester subjected to tensile loading and a constant radiant heat flux of 75 kW/m^2. The curves shown are the best fit

To investigate the correlation between resin decomposition and tensile failure, another graph relating normalised heat release rate and normalised tensile strength, to failure time was generated (Figure 4.21 and Figure 4.22).

The heat release rate curves below show that decomposition of the matrices mostly occur over the period between 25 and 800 seconds, and this is the time range over which the laminate failed under tensile loads above 50%. This indicates that decomposition and volatalisation of the polymeric matrix, which is reflected by heat release rate, contributes to the tensile failure event. Matrix degradation is responsible for the loss of the 'composite action', which means that the load on glass fibres is not distributed evenly. As a consequence, fibres fail one after the other.

Before this time range, it can be seen that tensile failure occurs as a result of high tensile loads (> 90%). This demonstrates that despite the softening of the matrix resulting from heating the laminate to the glass transition temperature, it is still functioning and holds the fibres together in order to support the applied loads.

At lower load levels, the composite laminates were able to retain their strength for prolonged periods because of the residual strength of the hot fibres, even after resin full decomposition.

The abrupture failure of glass fibres might have occurred due to the deterioration of their fracture toughness. The reasons behind this deterioration have been discussed previously in section 4.2.1.3.

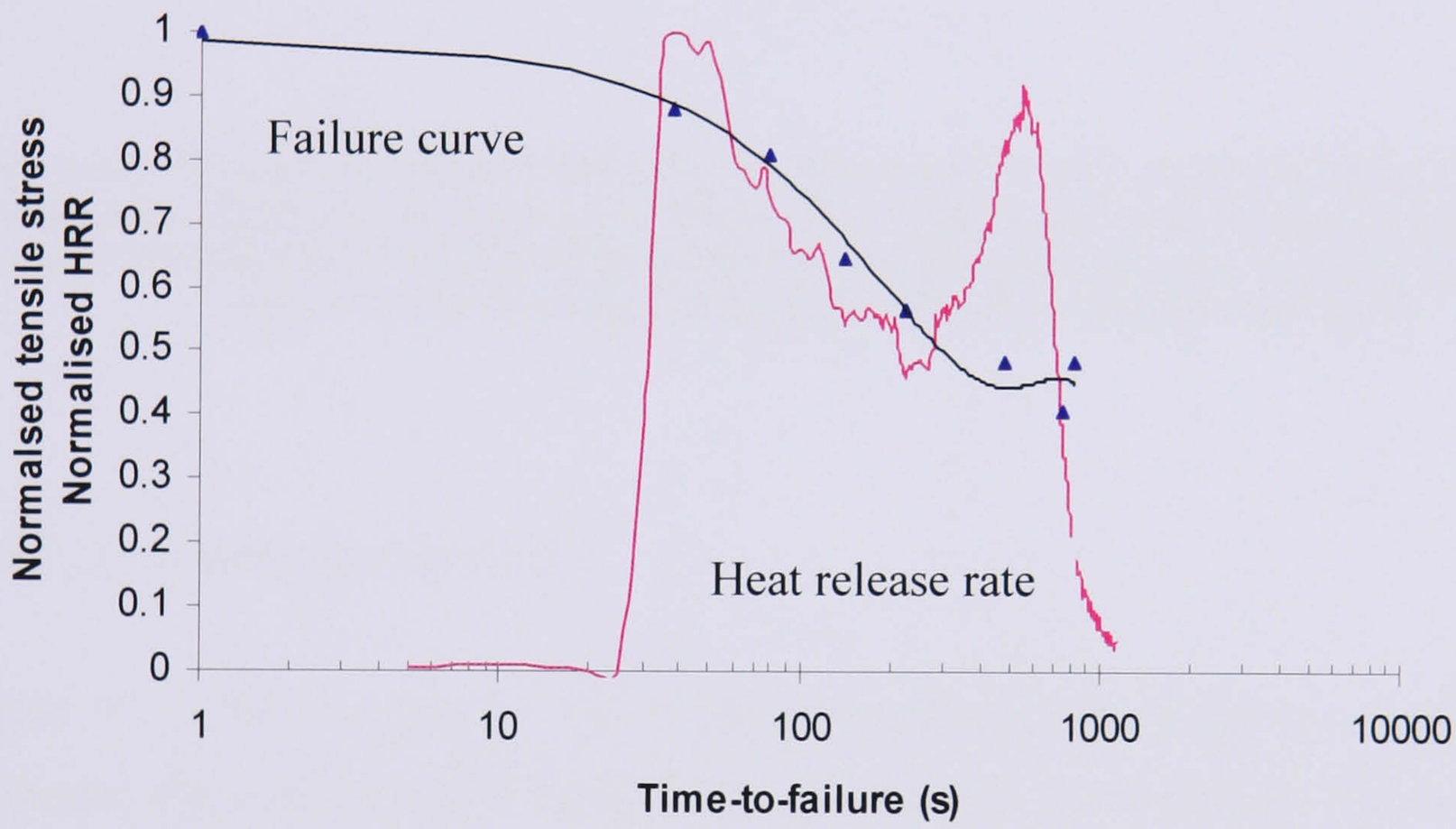


Figure 4.21 Comparison of the failure time vs applied tensile stress curve with the normalised heat release rate of vinyl ester laminate at 75 kW/m^2. The normalised tensile stress is the applied tensile stress of the laminate divided by its tensile strength at room temperature and the normalised heat release rate is the instantaneous heat HRR divided by the peak HRR

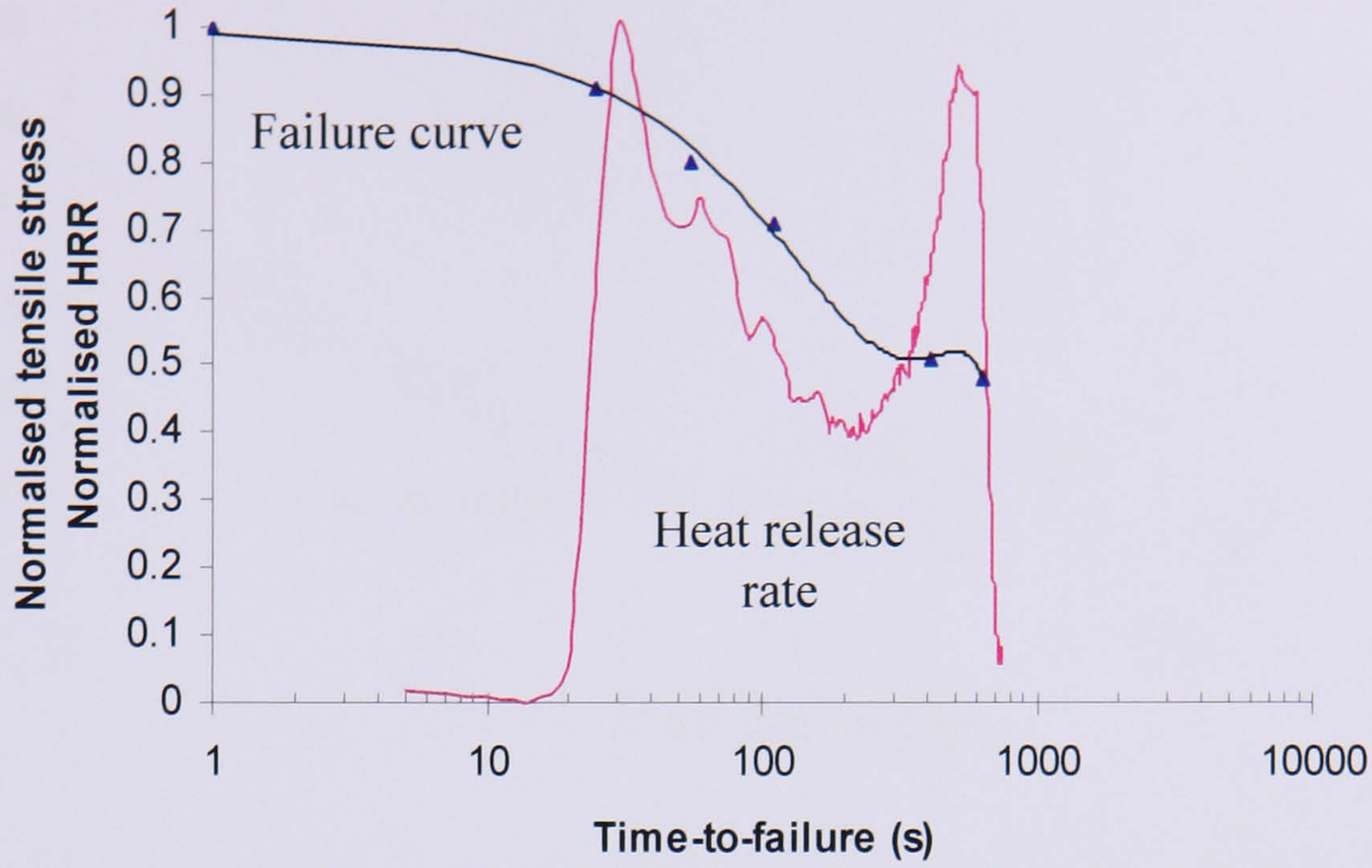


Figure 4.22 Comparison of the failure time vs applied tensile stress curve with the normalised heat release rate of polyester laminate at 75 kW/m^2. The normalised tensile stress is the applied tensile stress of the laminate divided by its tensile strength at room temperature and the normalised heat release rate is the instantaneous heat HRR divided by the peak HRR

4.3.2.2 Compression tests

Figure 4.23 shows a plot of time-to-failure against the compressive stress for glass polyester and vinyl ester at 75 kW/m^2. It can be seen that failure times are shorter when the applied load is increased. This response has been reported for other types of polymer laminates loaded in compression when exposed to fire or one side heating [34, 106]. Due to the fact that the applied heat flux was fairly high, failure always occurred regardless of the magnitude of the applied load, which shows that resin degradation must further reduce compression strength properties due to the increased heating rate and faster decomposition rate of the polymer matrix. This reinforces the fact that glass transition temperature controls the compressive behaviour of fibre reinforced polymers.

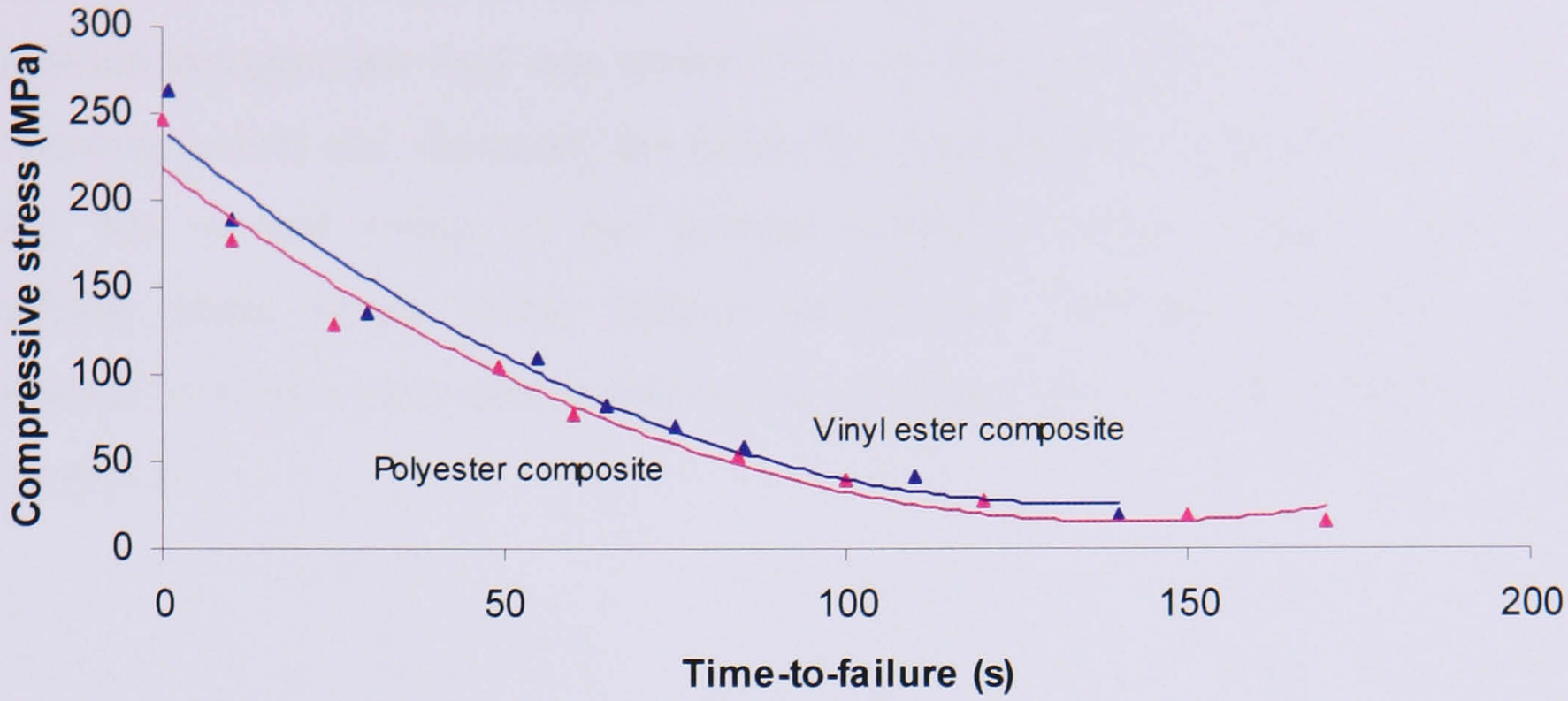


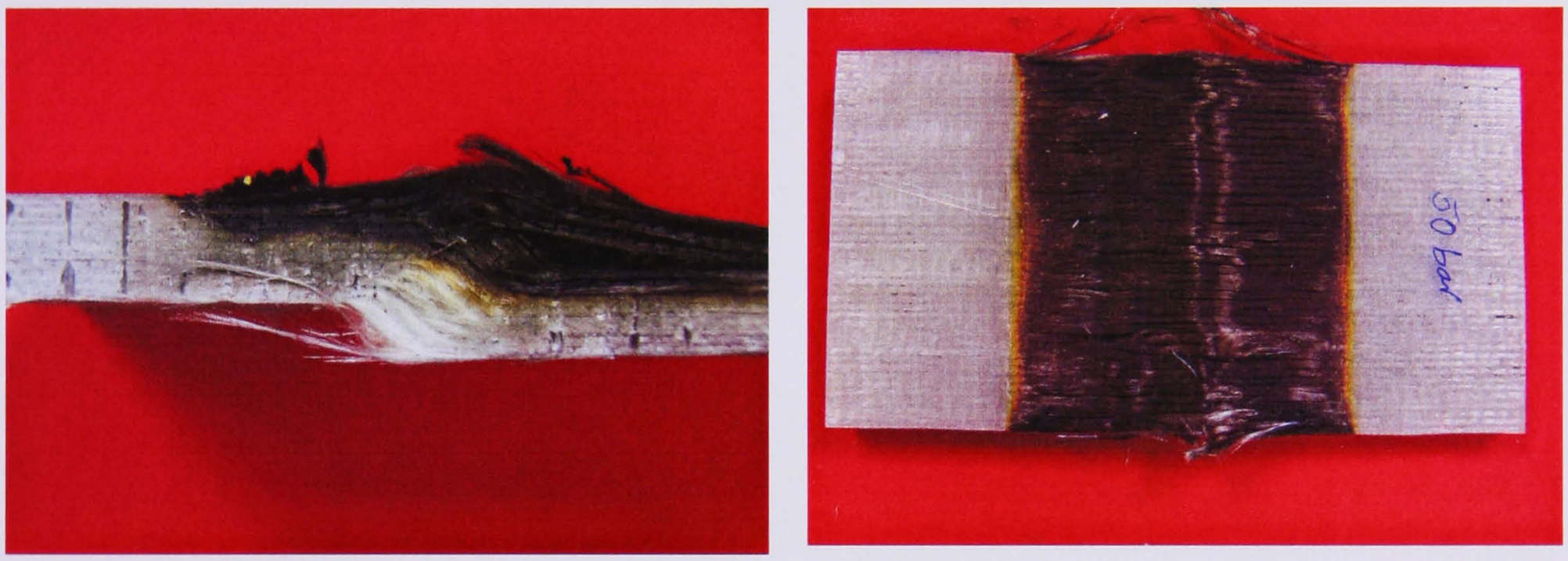
Figure 4.23 Glass polyester subjected to compressive loading and a constant radiant heat flux of 75 kW/m^2. The curve shown is the best fit

Again close inspection of the failed samples, Figure 4.24 revealed that the compressive failure mode occurred by plastic kinking of the glass tows [123, 124]. Delamination cracks between layers near the hot surface spread through the laminate with time. The delaminated plies have little capacity to carry the applied load, which has led to the transmission of this load to the underlying layers that were free of cracks. It is believed that the sample failed when the retained compressive strength dropped below the applied compressive stress. This conclusion explains the failure behaviour, which was sudden and catastrophic.

Mouritz et al. [104] found that the tows rotate for a maximum rotation angle of 60° from the load direction before the failure of vinyl ester laminates due to low shear stiffness of the hot resin matrix (Figure 4.25). It is found in this research that the kink band width is ≈ 6 mm, which is considered as large value compared with the band width of 0.2 mm at ambient temperature.

Again Figure 4.26 and Figure 4.27 show graphs of normalized HRR and compressive strength against time-to-failure. The time period over which the polymer matrix was thermally decomposed has occurred between approximately 25 and 800 seconds. The

failure curve shows that the laminate failed in fewer than 25 seconds when the normalised compressive load was above 50%. At this value failure occurred prior to resin decomposition and, therefore, the failure by delamination cracking and plastic tow kinking was caused solely by the thermal softening of the polymer matrix. At normalized loads below 50%, failure times were sufficient to allow matrix decomposition to take place and, in this occasion, failure is mainly due to both softening and pyrolysis.



(i) (ii)

Figure 4.24 Typical compressive failure of polyester laminate exposed to heat flux of 75 kW/m^2 and compressive stress of 20 MPa. (i) Kinking in the cold face. (ii) Delamination cracking in hot face

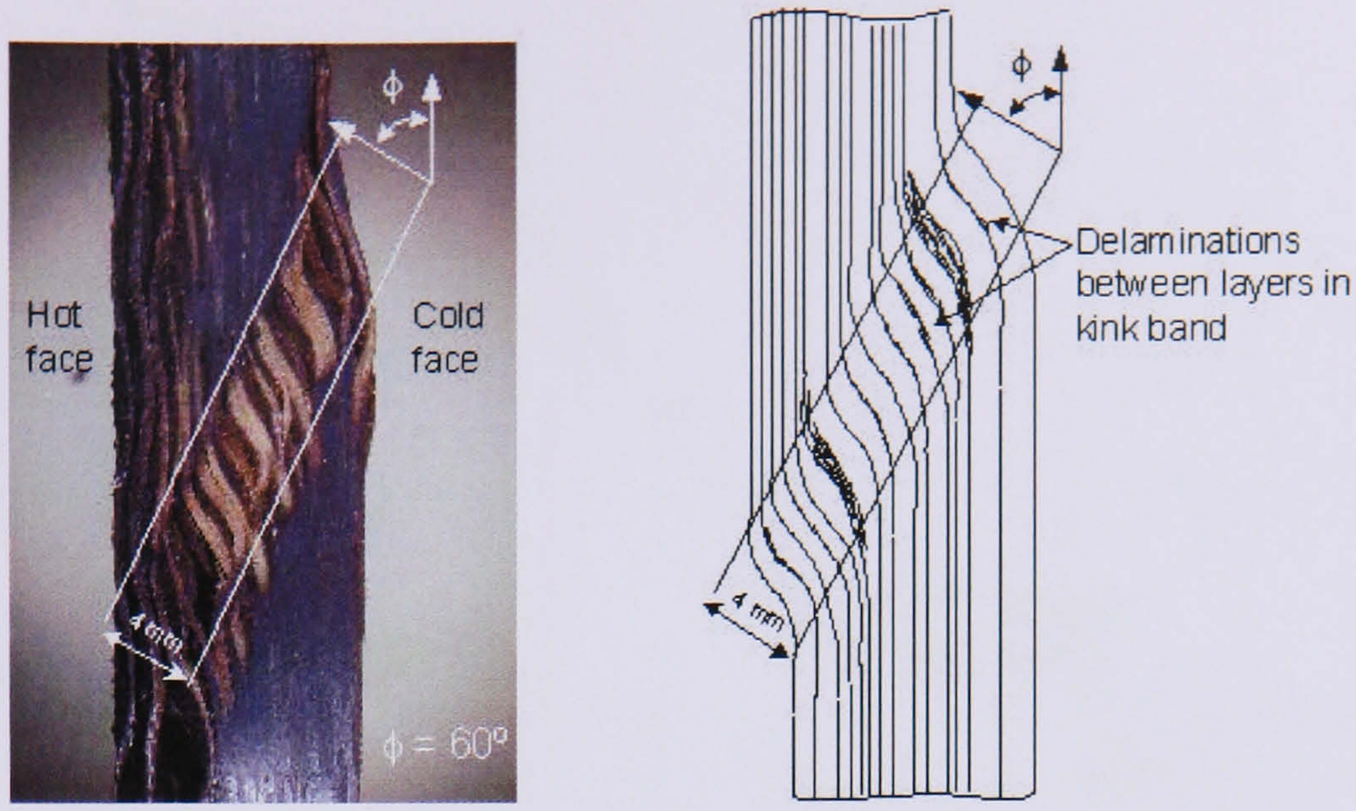


Figure 4.25 Photograph and schematic of plastic tow kinking of a laminate under compressive loading [15, 104]

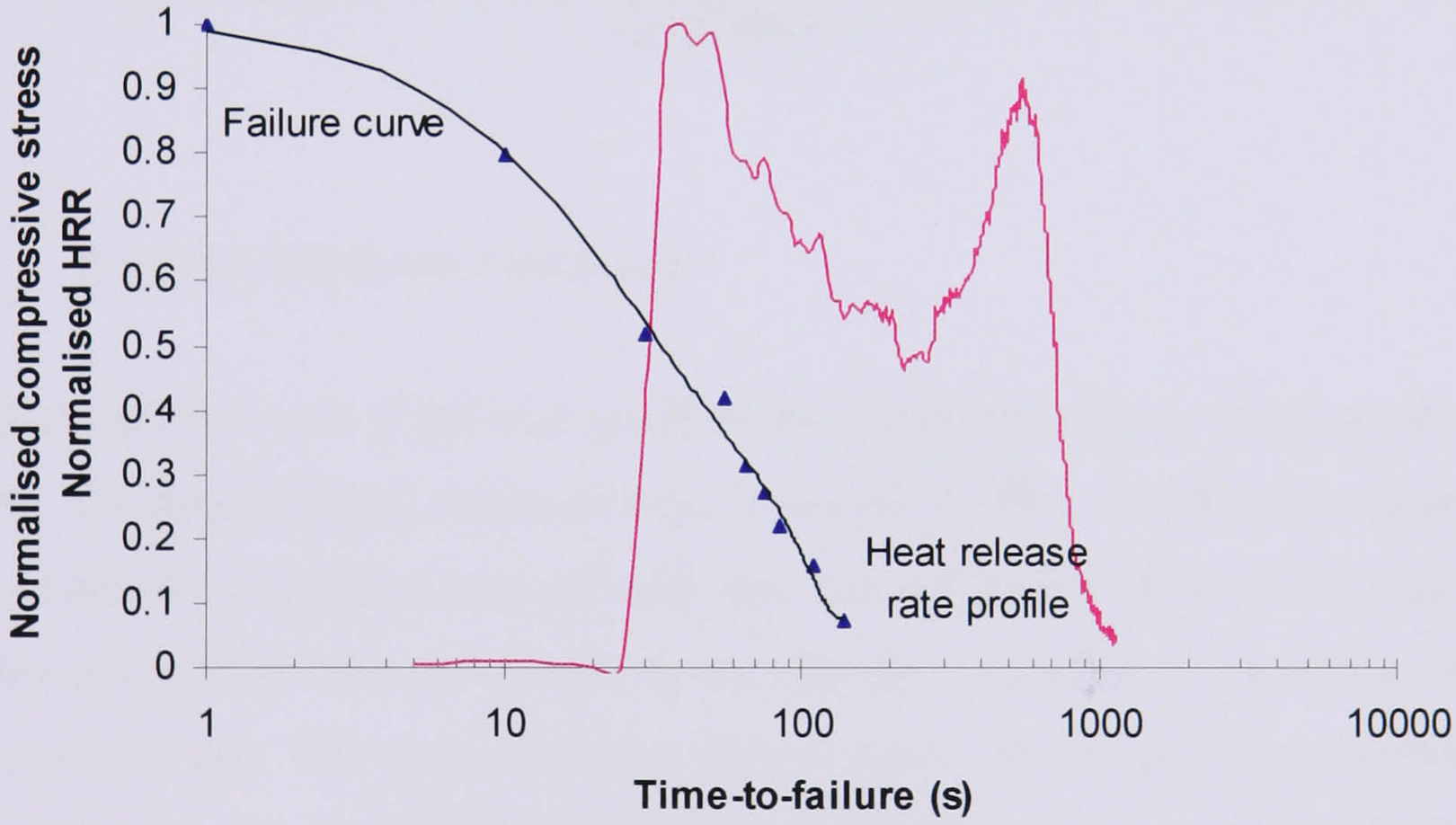


Figure 4.26 Comparison of the failure time vs. normalizes compressive stress curve with the normalised heat release rate of vinyl ester laminate at 75 kW/m^2. The normalised compressive stress is the applied compressive stress of the laminate divided by its compressive strength at room temperature and the normalised heat release rate is the instantaneous heat HRR divided by the peak HRR

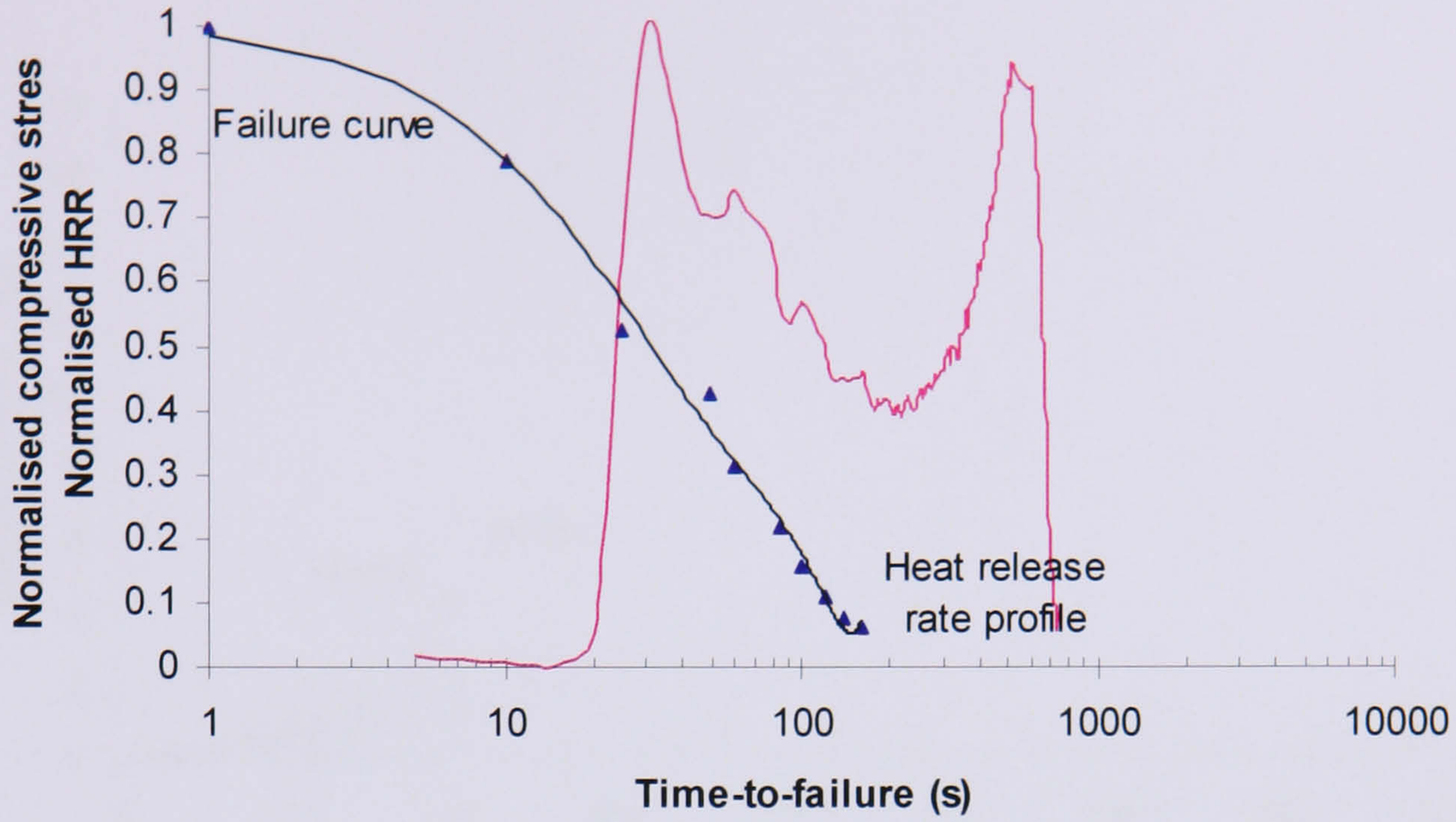


Figure 4.27 Comparison of the failure time vs normalizes compressive stress curve with the normalised heat release rate of poly ester laminate at 75 kW/m^2. The normalised compressive stress is the applied compressive stress of the laminate divided by its compressive strength at room temperature and the normalised heat release rate is the instantaneous heat HRR divided by the peak HRR

4.3.2.3 Thermal forces and moments

Thermal expansions took place as a result of the exposure to heat, which results in the generation of thermal forces and moments. In tensile loading, the thermal expansion is directly related to the applied load and heat flux. From Figure 4.28, it can be noticed that the higher the applied load, the steeper is the thermal extension curve, which indicates more expansion rate. The expansion rate slows rapidly as the applied load decreases. This effect is not very clear between 95 MPa and 64 MPa but it is clear between 95 MPa and 32 MPa.

The effect of the compression stress is shown in Figure 4.29. The compression load counteracts the axial thermal expansion (tensile force). This effect increases with increasing the compressive stress. Eventually the laminate looses its stiffness, which resulted from thermal softening and progressive ply failure.

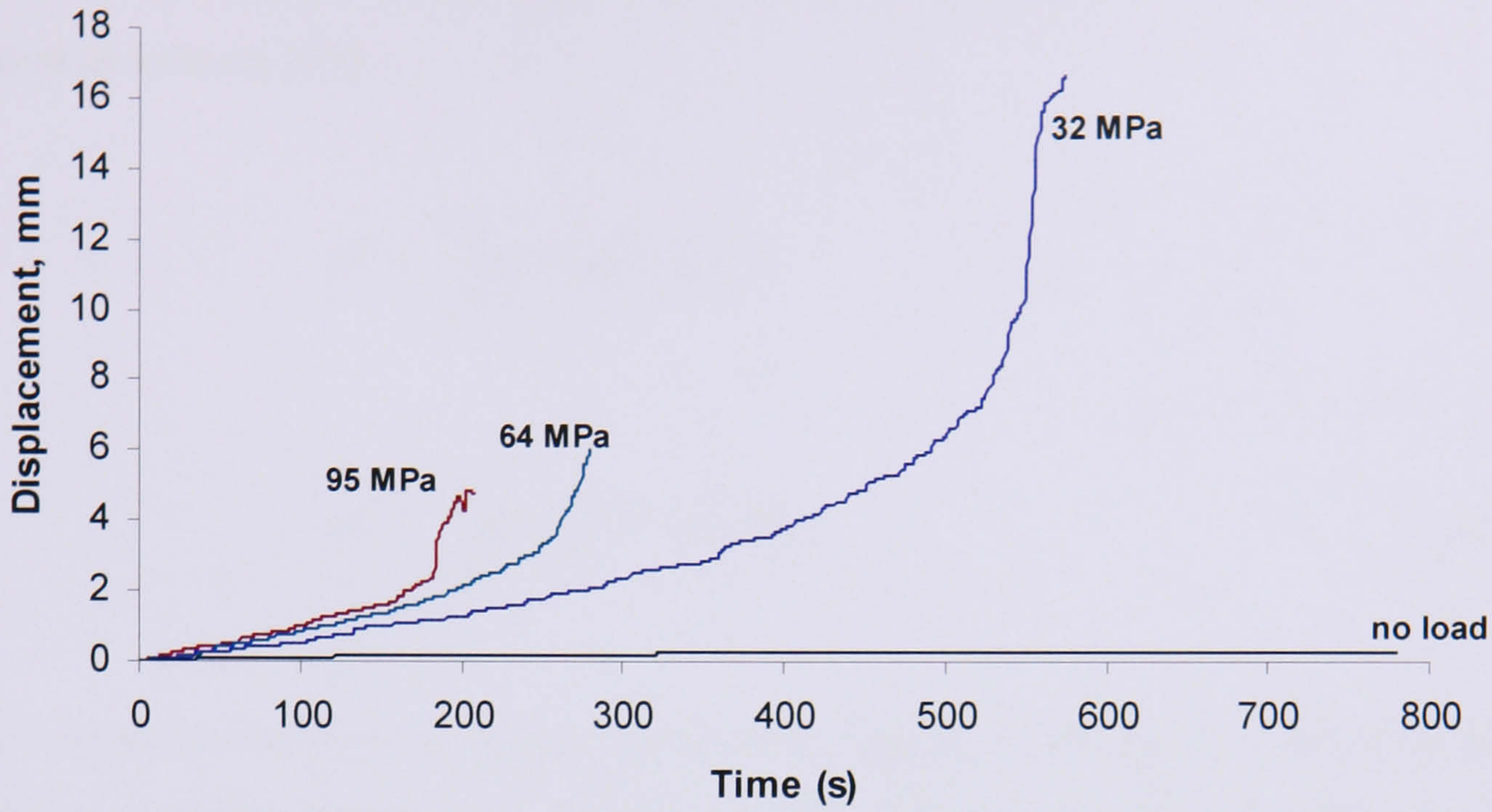


Figure 4.28 Effect of tensile loading on the axial displacement of glass vinyl ester composite exposed to a heat flux of 75 kW/m^2

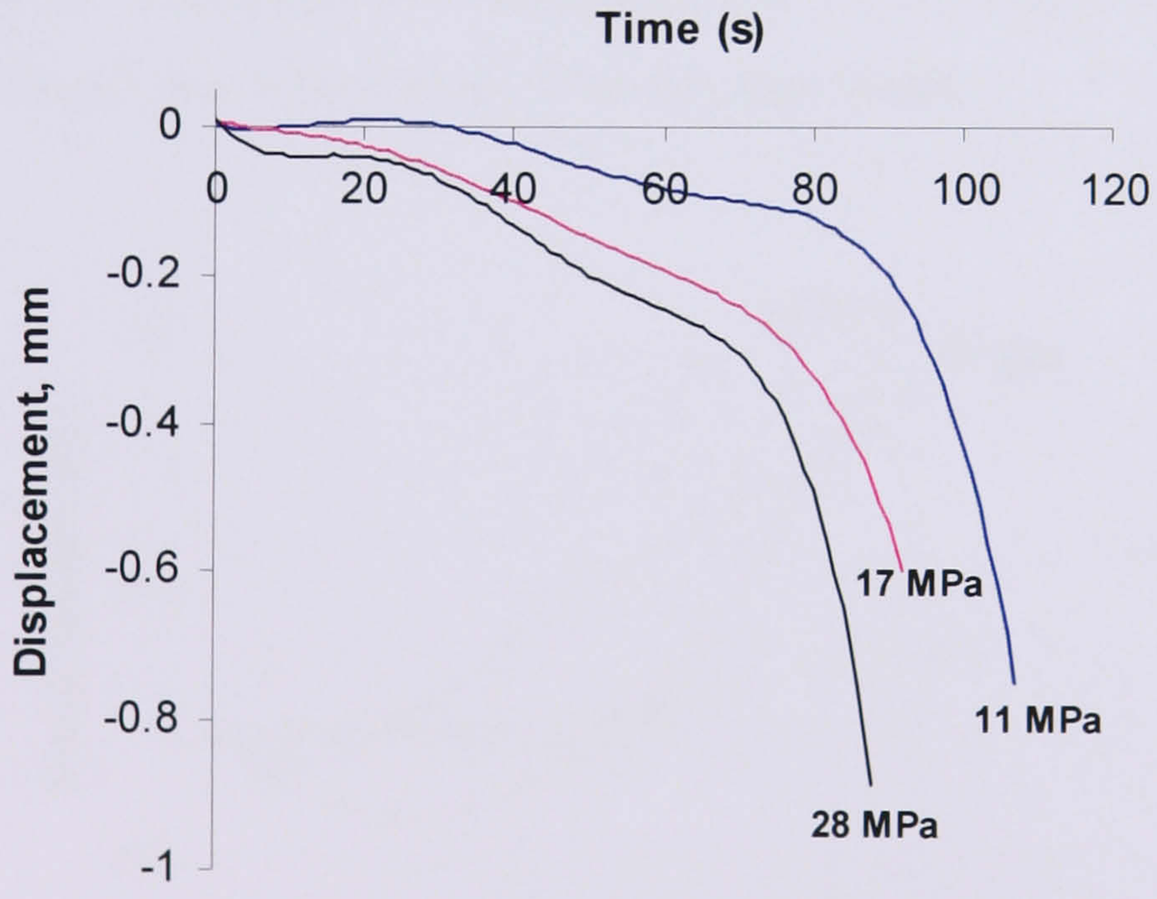


Figure 4.29 Effect of compressive loading on the axial displacement of glass vinyl ester composite exposed to a heat flux of 75 kW/m^2

The thermal forces and moments initiate from the longitudinal expansion and the temperature gradient in the through-thickness direction, respectively and they can be expressed as follows [23]: -

$$N^T = \int_{-h/2}^{h/2} E(T)\alpha(T)\Delta T.dz \qquad \textbf{(4.1)}$$

$$M^T = \int_{-h/2}^{h/2} E(T)\alpha(T)\Delta T.zdz \qquad \textbf{(4.2)}$$

.

Figure 4.30 shows the vertical displacement at the centre of the sample's rear face when exposed to a constant heat flux 75 kW/m^2 and different compressive stresses. The sample initially bends out-of-plane towards the heat source (negative displacement) because the upper face becomes hotter than the rear face. Due to the fact that the applied heat flux was quite high, the thermal expansion of the hot surface increases accordingly and results in higher thermal strains. As a consequence, the sample must bend towards the heat source. But, due to the decomposition of the sample's hot surface, the bending direction changes and moves away from the heat source.

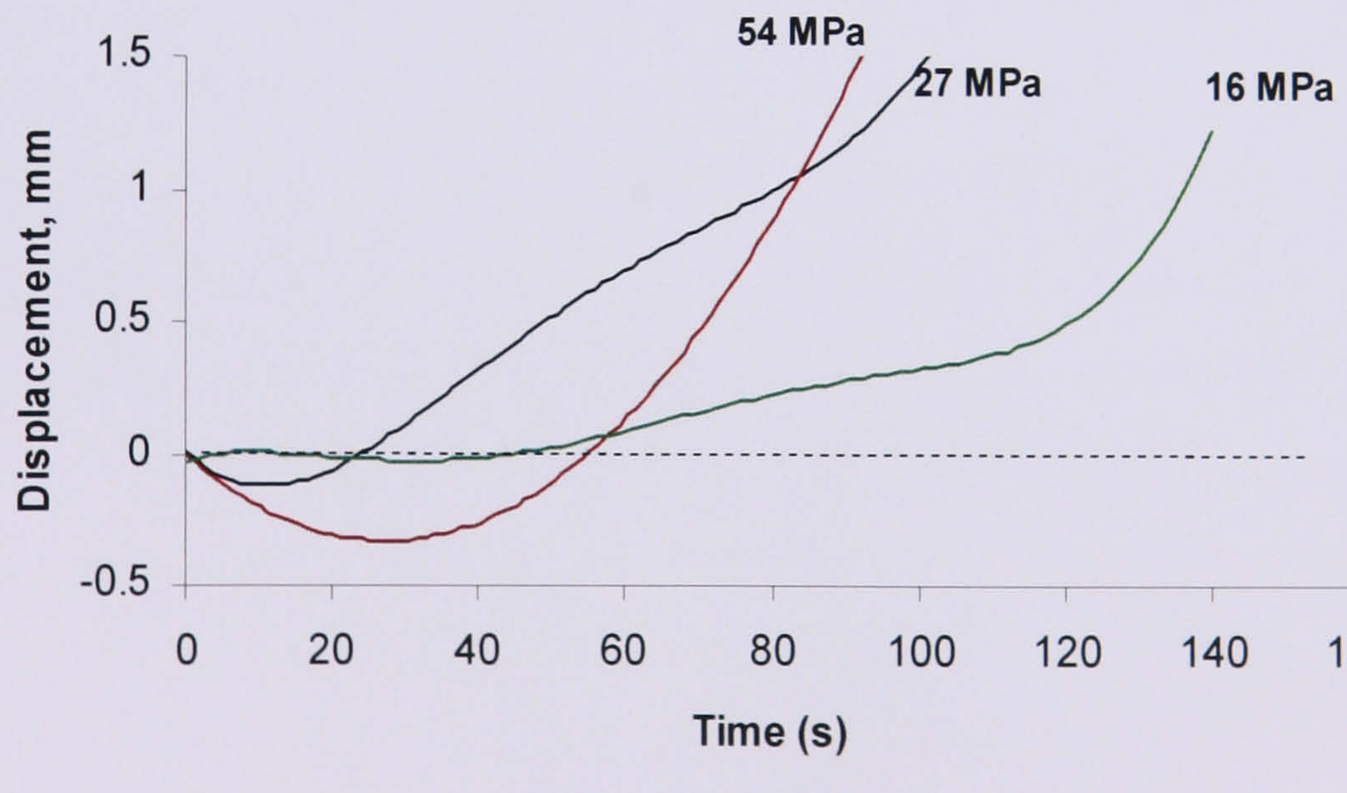


Figure 4.30 Out-of plane displacement of glass polyester composite exposed to a heat flux of 75 kW/m^2

It has been demonstrated [125. 126] that the term M^T in Equation 4.2 is responsible for the out of plane response towards or away from the heating source in the case of zero load. However, in the loaded condition, three terms interact to produce structural equilibrium [126]: -

$$M^T + Pv + Pe = 0 \qquad \textbf{(4.3)}$$

where:

M^T is the thermal moment, P is the applied load at the specimen's centre.

v is the current out-of-plane deformation in either direction and e is the shift in neutral axis caused by the asymmetric thermal softening.

The term, Pv, counts for the increase in out–of-plane deformation either towards the heating source or in the opposite direction because the specimen is not concentric with applied load direction. The reversal of the sample curvature away from the heating source is also due to the effect of the eccentric loading moment, Pe, as a result of the larger stiffness loss in the hot side.

Chapter 5 Modelling

5.1 Preparation for thermal modelling

In order to run the thermal model and to predict the thermal response and the remaining resin content of the composite material, it was necessary to determine the glass volume fraction, and the kinetic thermal degradation parameters such as the pre-exponential factor, A, and the activation energy, E, for the resin system using the thermo-gravimetric analysis.

5.1.1 Volume fraction determination

The methodology described in ASTM D 792-00 standard [107] was used to determine the fibre volume fraction, weight fraction and the void content, as shown in Table 5.1, following the steps outlined in Section 3.2.

Table 5.1 Percentage of glass fibre weight fraction (W_f), volume fraction (V_f) and void content

Composite system	W_f (%)	V_f (%)	Void content (%)
E-glass / Vinyl ester	64	46	4
E-glass / Polyester	62	44	2

5.1.2 Thermo-gravimetric Analysis (TGA)

The TGA test data is usually obtained in the form of remaining mass (mg) as a function of time (s) and temperature (°C) in order to study the decomposition processes of fibre reinforced plastic composites. The normalized experimental mass loss curves (relative mass m/m_o) for vinyl ester and polyester resins at two different heating rates are shown in Figure 5.1 & Figure 2.2, respectively as function of temperature. The fibre mass for each resin system was subtracted from the composite mass and therefore only the resin mass has been shown in each graph. It can be observed that for vinyl ester the resin started to decompose at 420°C at 25°C/min heating rate and was at slightly higher temperature at heating rate of 40°C/min. In the case of polyester resin the decomposition temperature started at 370°C for 25°C/min heating rate and also was slightly higher at

40°C/min heating rate. Above the start of decomposition temperature, the resins rapidly decomposed in an endothermic process that is dominated by random chain scission of the polymeric chain leaving approximately 2-4% of the mass as a residual char [30, 127]. This is because at this stage styrene and other volatiles are released. Both curves for the two resins have the same shape, with the exception that the vinyl ester curve is slightly steeper than polyester, which means that vinyl ester has a faster decomposition rate over a narrower temperature range. This behaviour results in higher rate factor (A), and higher activation energy (E). Also, increasing the heating rate resulted in a shift in the decomposition temperature for both cases.

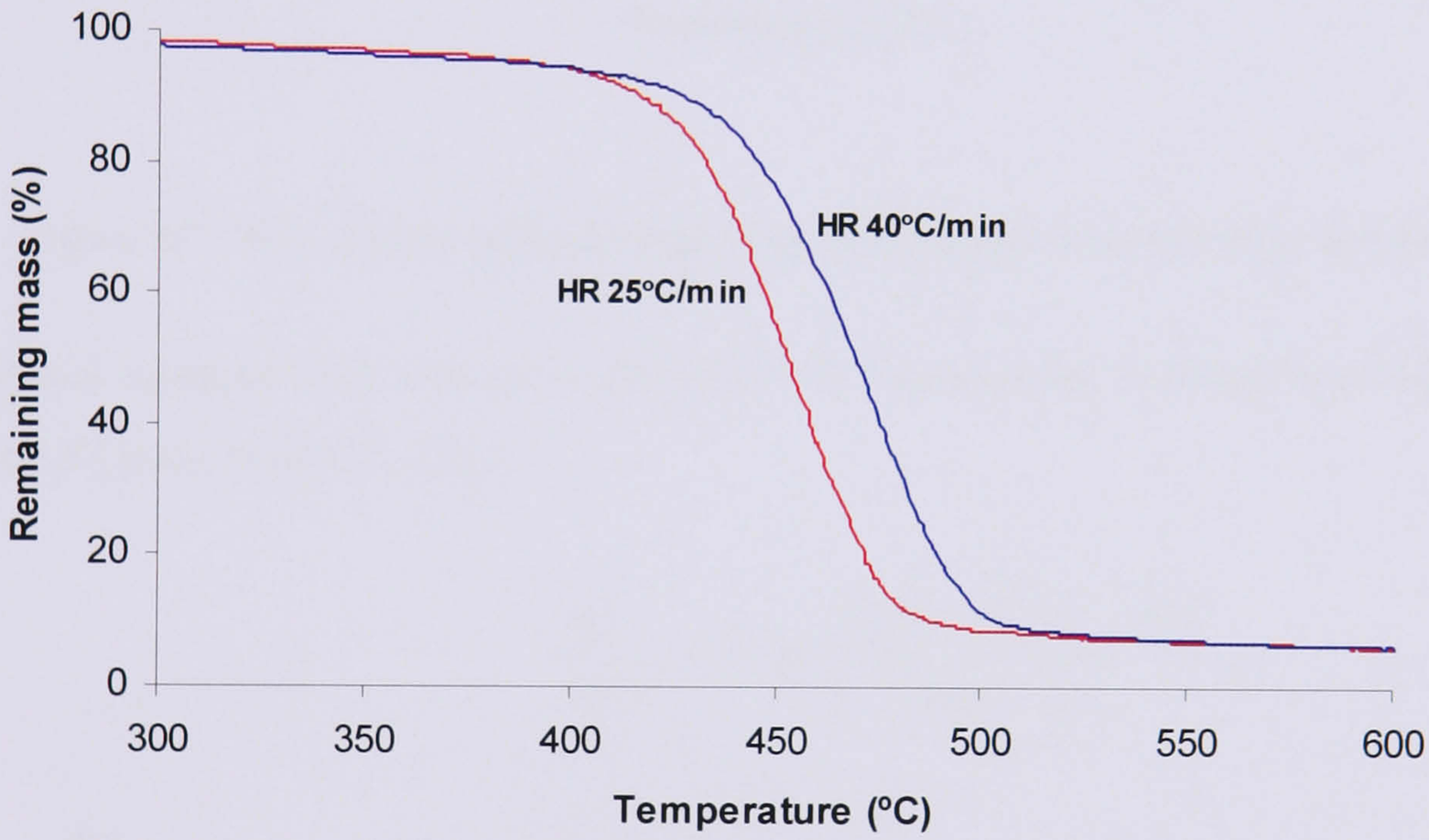


Figure 5.1 TGA test for vinyl ester rein using two heating rates 25°C/min and 40°C/min

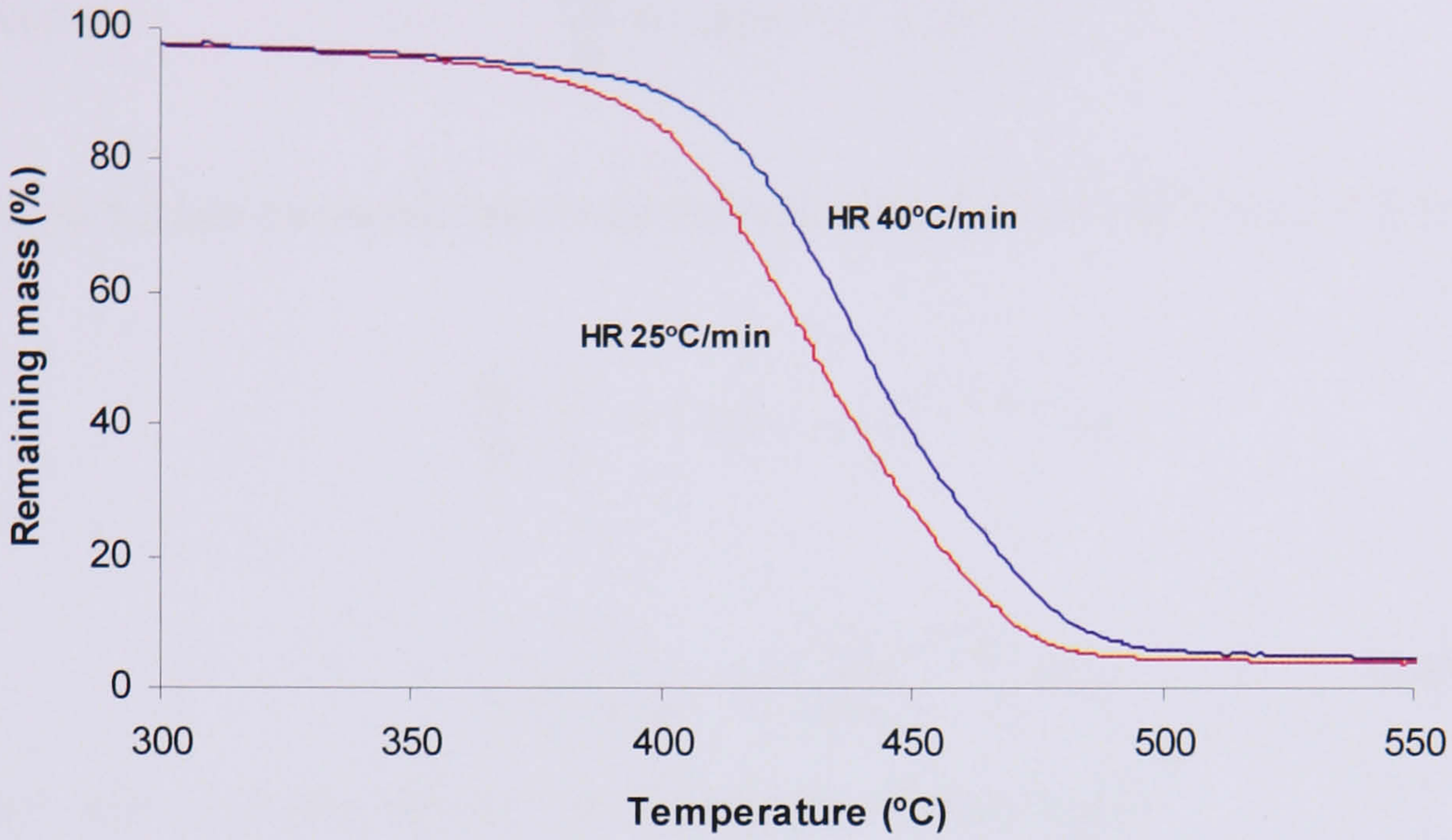


Figure 5.2 TGA test for polyester rein using two heating rates 25°C/min and 40°C/min

Arrhenius equation was used to model the resin decomposition reaction of fibre reinforced polymers [11, 128].

$$\frac{\partial M}{\partial t} = -A \cdot M_o \left[\frac{M - M_f}{M_o} \right]^n e^{\left(\frac{-E}{RT}\right)} \qquad \textbf{(5.1)}$$

where: $\frac{\partial M}{\partial t}$ is the rate of mass change (kg/s),

A is the rate constant (1/s),

M_o, M *and* M_f are the original, instantaneous and final mass of the polymeric resin, respectively (kg),

E is the activation energy (J/kgmol),

R is the universal gas constant (8.314 J/mol.K)

T is the temperature (K),

n is the order of the reaction.

The mass in Equation 5.1, M, can be replaced by $w = \frac{M}{M_\circ}$, and Equation 5.1 is reduced to:

$$\frac{\partial w}{\partial t} = -A(w - w_f)^n e^{(-E/RT)} \qquad \textbf{(5.2)}$$

Equation 5.2 can be transformed into the following form to make the integration easy:

$$\frac{\partial w}{\partial T}\frac{\partial T}{\partial t} = -A(w - w_f)e^{(-E/RT)}, \text{ or}$$

$$\frac{dw}{(w - w_f)^n} = -\frac{A}{HR}e^{(-E/RT)}dT \qquad \textbf{(5.3)}$$

Where, $HR = (\partial T / \partial t)$ denotes the heating rate of the reaction.

Equation 5.3 can be integrated to give an explicit function $w = w(T)$, which is similar to the data format obtained from TGA analysis: at T_o, the weight fraction is 1 and at any instantaneous temperature T, the weight fraction is w. The integration depends on the value of n:

$$\int_1^w \frac{dw}{(w - w_f)^n} = -\int_{T_0}^T \frac{A}{HR}\left(e^{-E/RT}\right)dT \qquad \text{or} \qquad \int_w^1 \frac{dw}{(w - w_f)^n} = \int_{T_0}^T \frac{A}{HR}\left(e^{-E/RT}\right)dT \qquad \textbf{(5.4)}$$

For n = 1, which is commonly used for this type of resins, the integration leads to:

$$\ln\left(\frac{1 - w_f}{w - w_f}\right) = \int_{T_0}^T \frac{A}{HR}\left(e^{-E/RT}\right)dT \Rightarrow w(T) = w_f + (1 - w_f)e^{\left[-\int_{T_0}^T \frac{A}{HR}\left(e^{-E/RT}\right)dT\right]} \qquad \textbf{(5.5)}$$

Feih S. [129] used the following forms of approximation to implement the exponential integral $G(T)$.

$$G(T) = \int_{T_0}^T \frac{A}{HR}\left(e^{-E/RT}\right)dT \approx \frac{A}{HR}\int_{T_0}^T \left(\frac{T}{T_m}\right)^2 \left(e^{-E/RT}\right)dT = \frac{A}{HR}\left|\frac{T_m^2 R}{E}e^{-E/RT}\right|_{T_0}^T \qquad \textbf{(5.6)}$$

$$G(T)=\int_{T_0}^{T}\frac{A}{HR}\left(e^{-E/RT}\right)dT\approx\frac{A}{HR}\int_{T_0}^{T}\left(\frac{T}{T_m e}\right)^{-E/RT_m}dT=\frac{A}{HR}\frac{1}{T_m e}\frac{1}{E/(RT_m)+1}\left|T^{E/RT_m+1}\right|_{T_0}^{T} \quad \textbf{(5.7)}$$

where: T_m, is the temperature of the maximum decomposition rate (loss rate) and it has to be evaluated from the experimental data sets by plotting *dw/dT* as shown in Figure 5.3 and Figure 5.4.

From the experimental data, the derivative *dw/dT* can be determined as it is shown in Table 5.2.

Table 5.2 Values of T_m and (*dw/dT*), derived from experimental data for vinyl ester and polyester resins at the specified heating rates

HR (°C/min)	Vinyl ester		Polyester	
	T_m (°K)	$(dw/dT)_m$ ($°K^{-1}$)	T_m (°K)	$(dw/dT)_m$ ($°K^{-1}$)
25	725	0.01769	703.3	0.01421
40	750	0.01643	713.3	0.01457

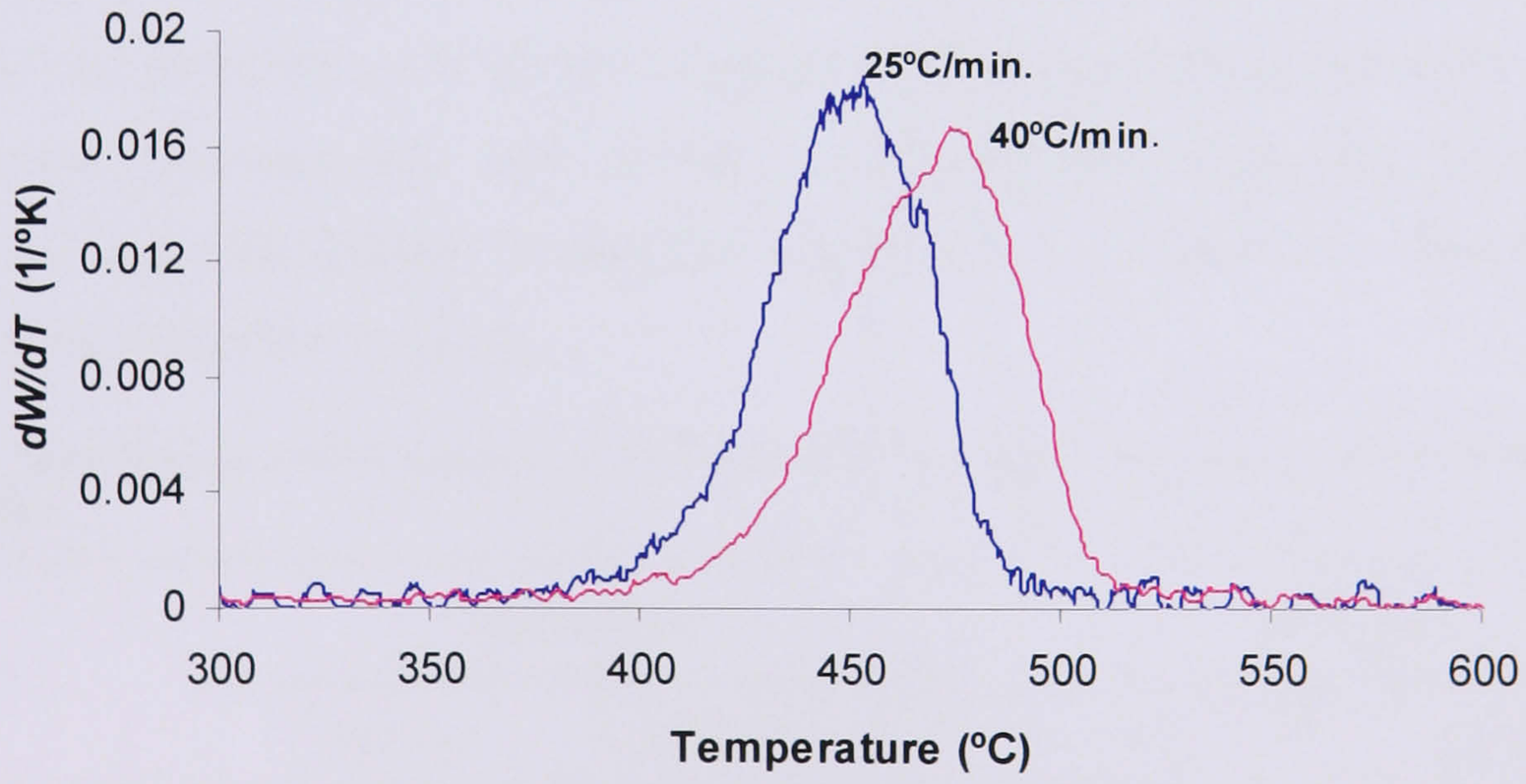


Figure 5.3 The derivative dW/dT for vinylester resin against temperature at 25 C/min and 40 C/min heating rates

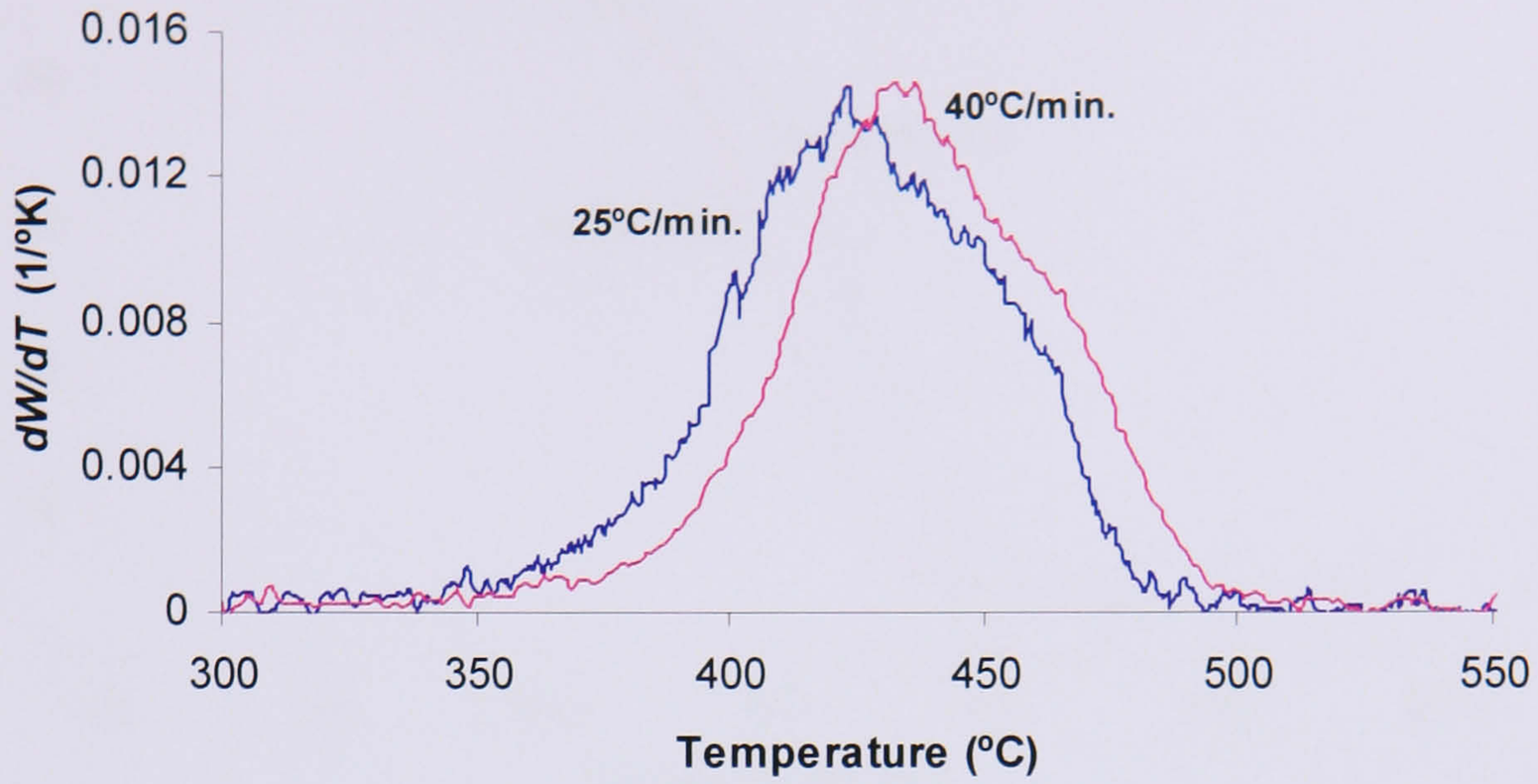


Figure 5.4 The derivative dW/dT against temperature for polyester resin at 25 °C/min and 40 °C/min heating rates

Gnuplot [130] software has been used to achieve this. It allows fitting the data independently or simultaneously using multi-branch fitting. The main inputs to the model are the different heating rates HR_1 and HR_2, and the values of maximum decomposition temperatures T_{m1} and T_{m2}. The starting values for, A, and, E, for both vinyl ester and polyester were chosen based on previous literature values [35]. The two functions are simultaneously fitted to the two heating rates' data sets. The resulted values from the multi-branch fittings are listed below in Table 5.3. The input file example is shown in the Appendix.

Table 5.3 Simultaneous fitted parameters for vinyl ester and polyester resins using a multi-branch fitting option

	Vinyl ester		Polyester	
	A (1/s)	E [(J/(K mol)]	A (1/s)	E [(J/(K mol)]
Multi-branch fitting	1×10^{12}	192861	1×10^{10}	160386

Figure 5.5 and Figure 5.6 show comparisons between the measured and modelled mass loss curves for the two laminate systems

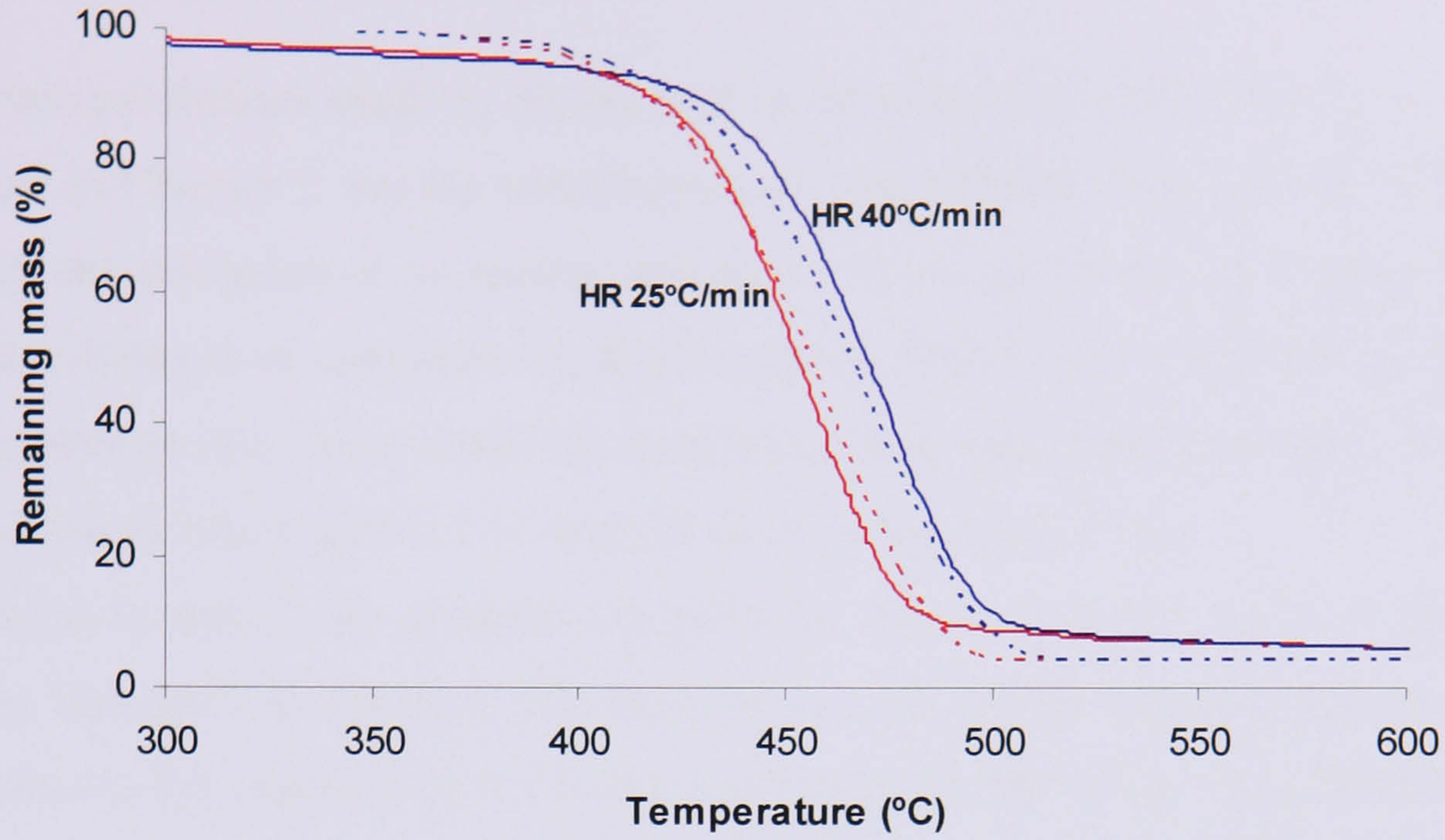


Figure 5.5 Measured and modelled mass loss curves for vinyl ester at 25°C/min and 40°C/min. The solid line is the measured curves and the dashed line is the modelled curves

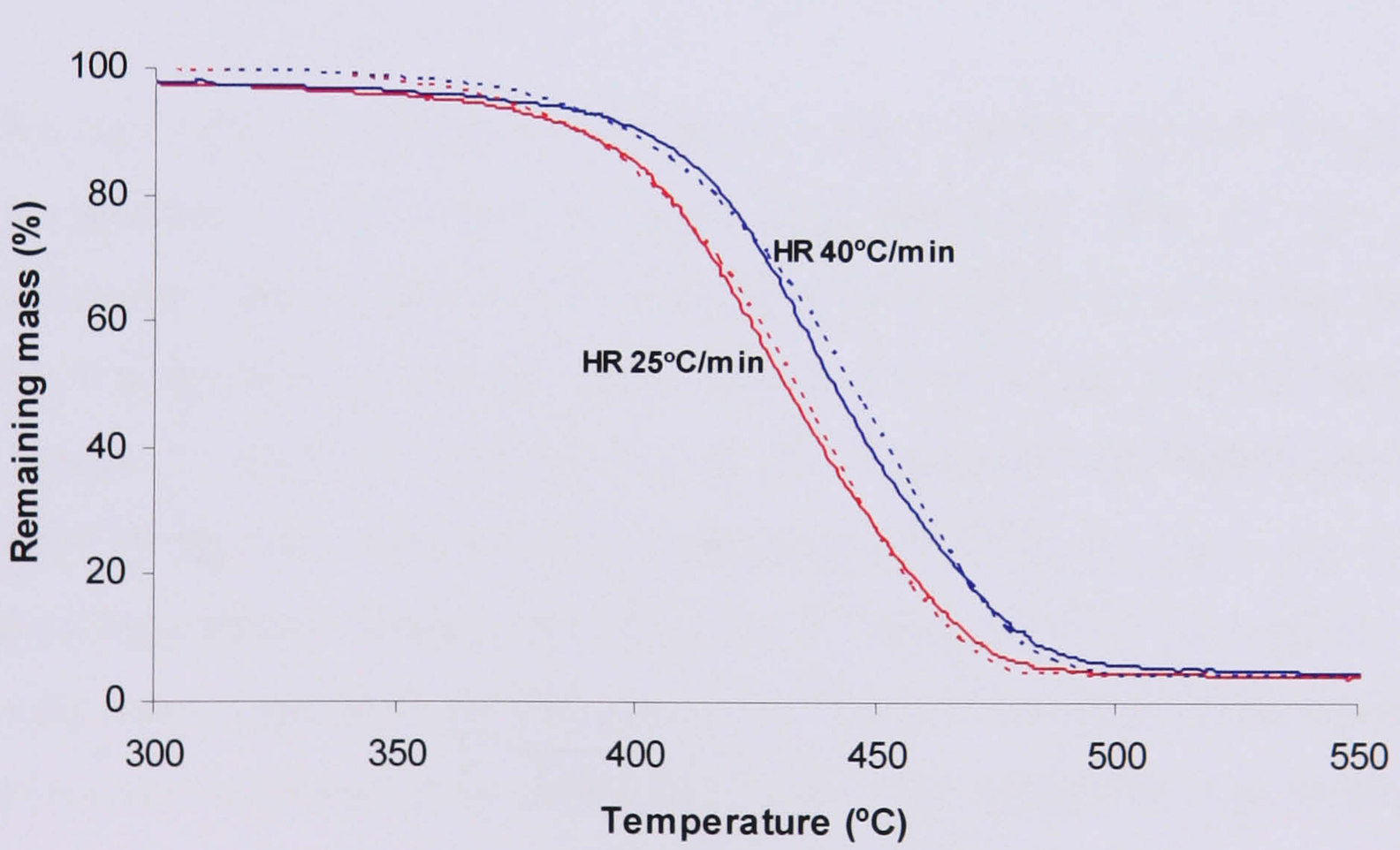


Figure 5.6 Measured and modelled mass loss curves for polyester at 25°C/min and 40°C/min. The solid line is the measured curves and the dashed line is the modelled curves

5.2 Thermal model

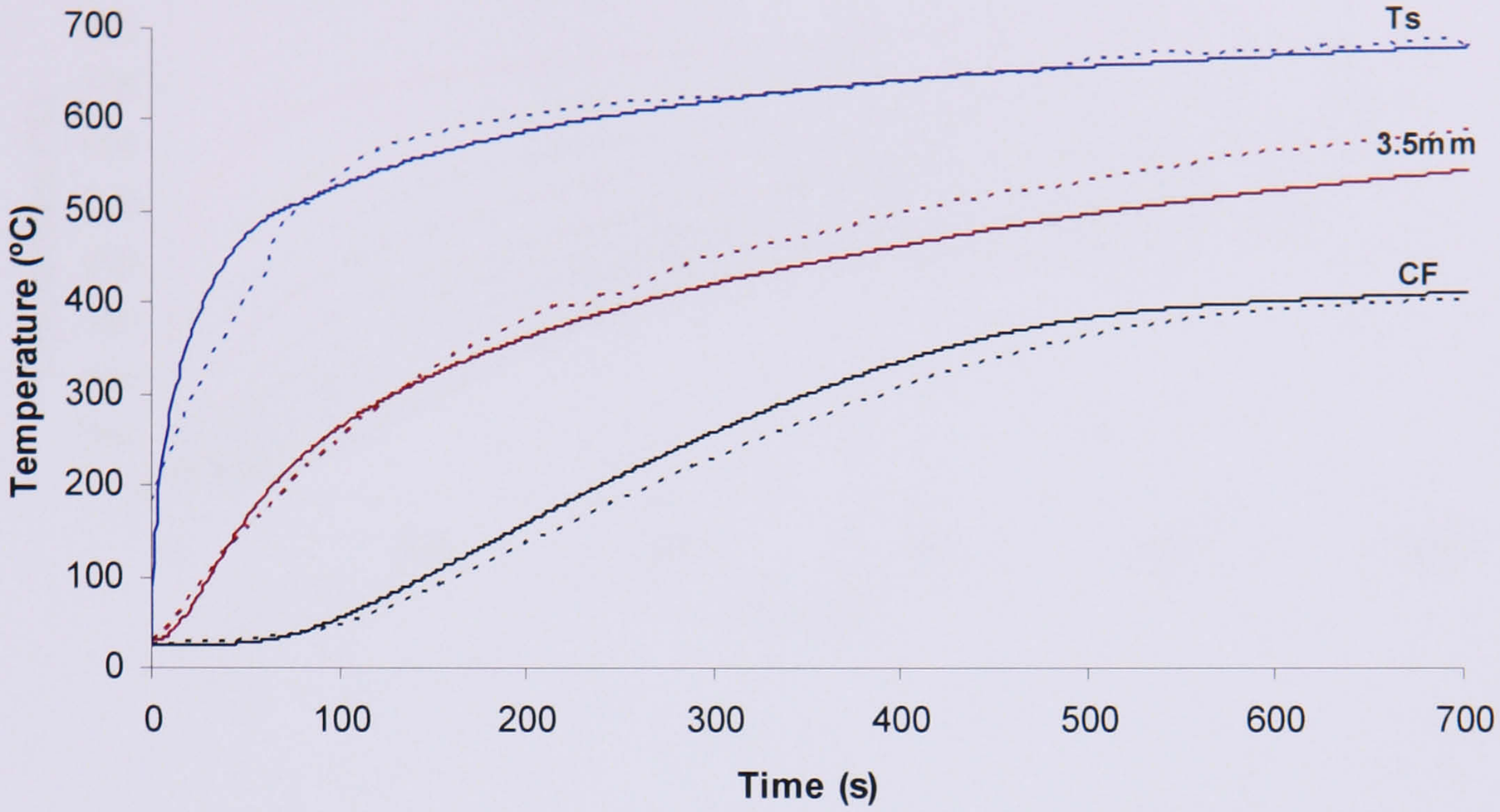
The main predictions made by the thermal model (Equation 2.10), which were described in detail in Chapter 2, are the temperature and the residual resin content (RRC) profiles through the thickness of composite laminates. These profiles were employed to model the fire resistance of composite laminate systems. Before doing this, the accuracy of the temperature profiles were tested by comparing them with some measured profiles at the same depth points. Figure 5.7 (i) and (ii) show these comparisons.

It is believed that if the modelled temperature profile is within 10°C of the measured profile, especially for the first 300 seconds, then the model accuracy can be considered as sufficient for mechanical modelling [35]. In addition, if the modelled TGA curves discussed in the previous section and the modelled temperature profiles are accurate enough, then it is legitimate to assume that the modelled (RRC) is of a reasonable accuracy because of the dependence of the resin decomposition on the temperature. Mouritz and Mathys [1, 2] validated the RRC prediction of the thermal model by visually inspecting composite laminates subjected to fire for a given exposure time.

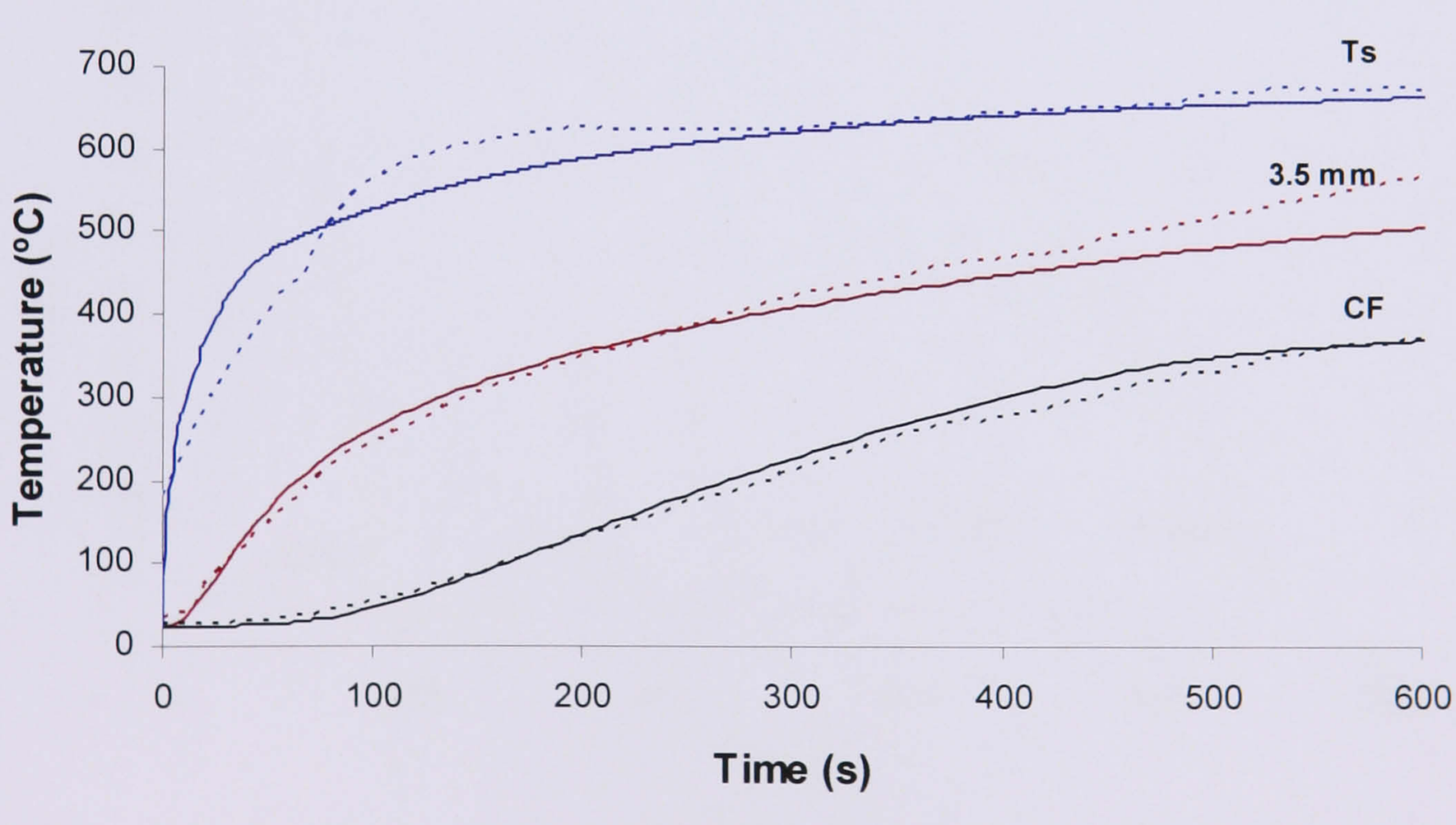
The hot face field temperature was measured using a type (k) metallic thermocouple and the temperature in the other positions was measured using a type (k) normal thermocouples. From Figure 5.7 (i) and (ii), it can be seen that at 3.5mm below the hot surface, the discrepancy between the measured and modelled profiles started at around 200 seconds, which was mainly due to the detachment of thermocouple from the specimen as the resin decomposed. The temperature of the hot face was approximated by measuring the field temperature (T_s) at about 5mm above the hot surface.

The responses of the three profiles shown in Figure 5.7 (i) and (ii) for glass vinyl ester and polyester laminates were nearly the same. This behaviour was expected as both systems have similar glass volume fractions and physical structure.

Figure 5.8 and Figure 5.9 show the modelled temperature and residual resin content profiles for glass/vinyl ester and glass/polyester composites, respectively, at constant heat flux of 75 kW/m^2.

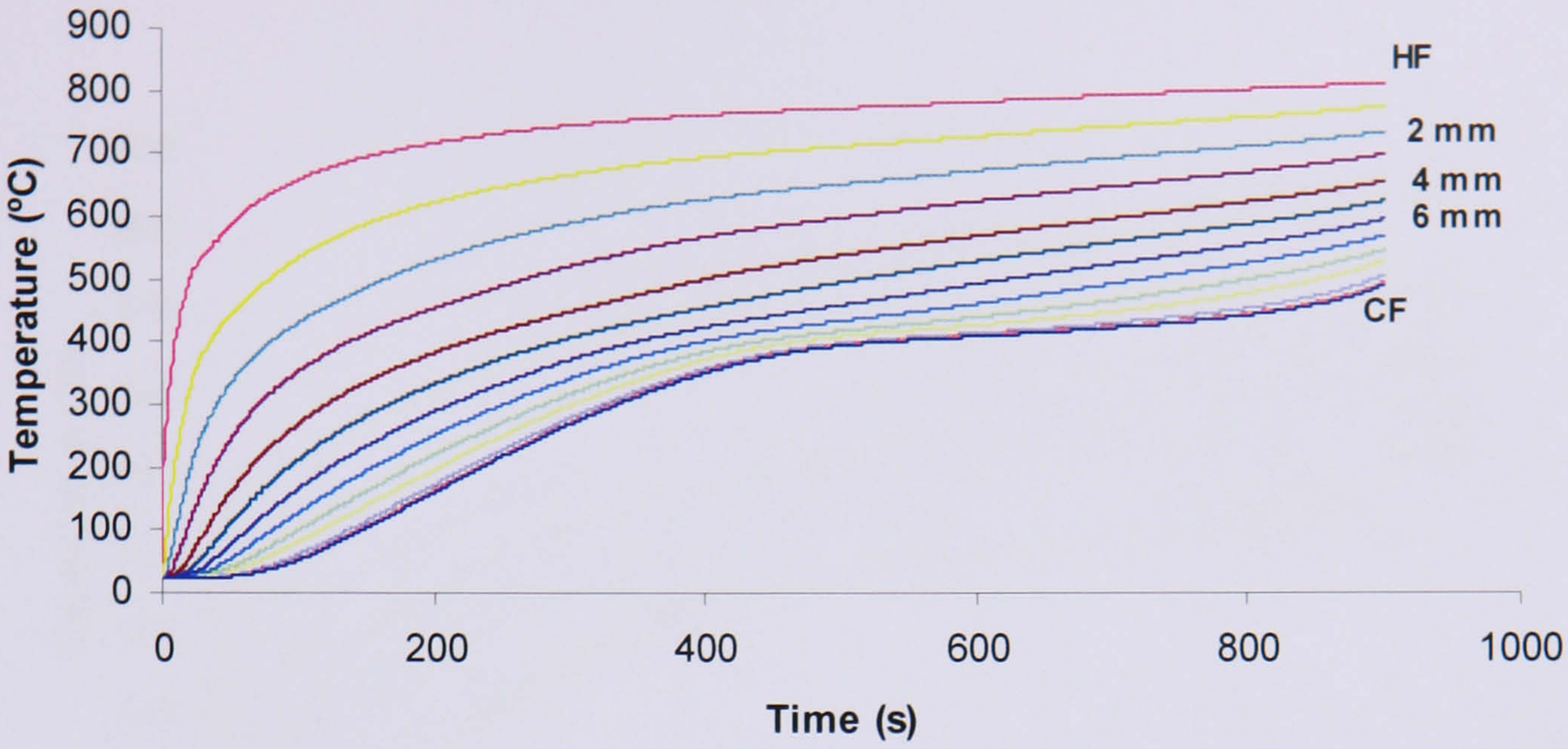


(i)

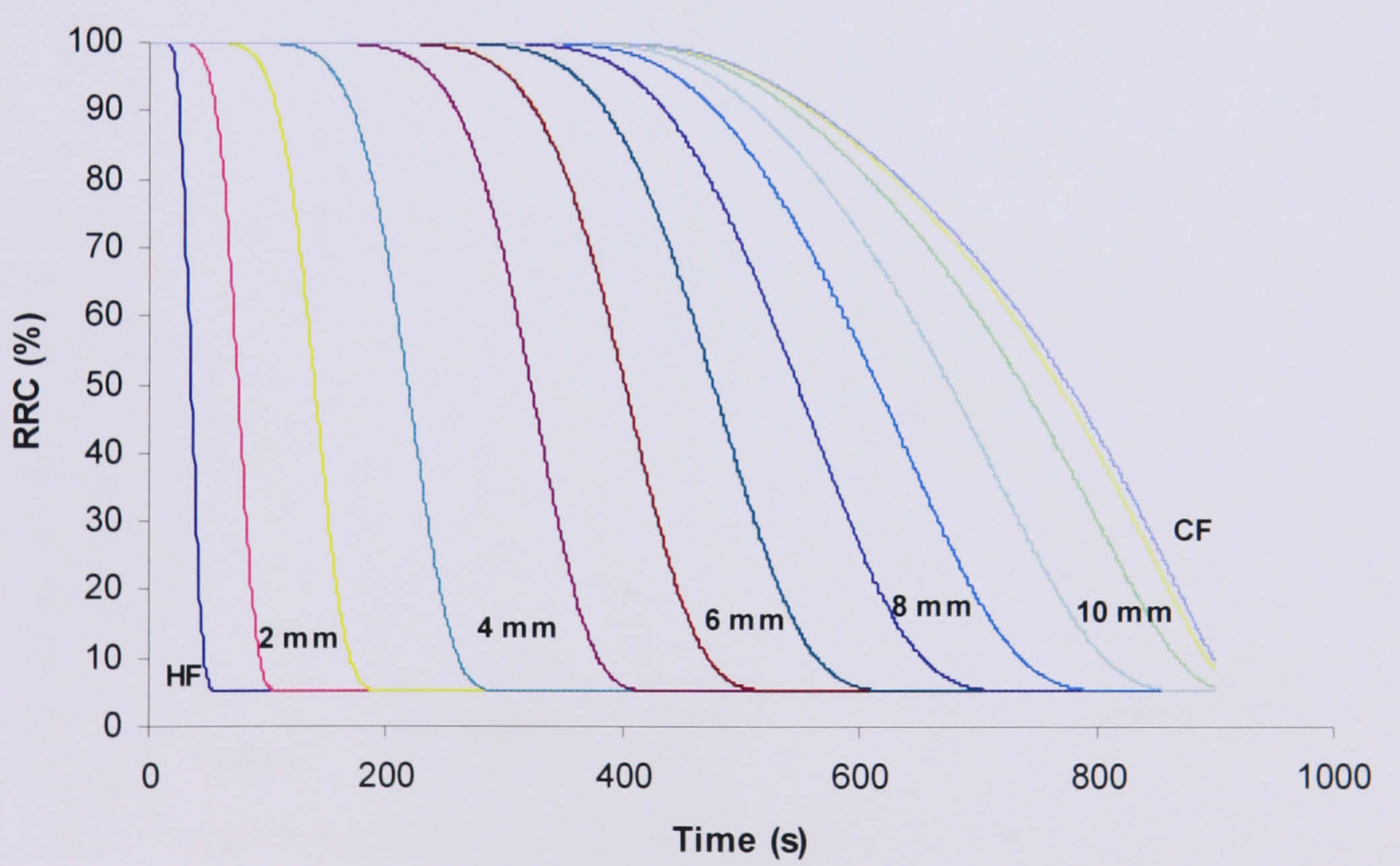


(ii)

Figure 5.7 Measured (dashed line), and modelled (continuous line) temperature profiles at field temperature (Ts), 3.5mm below the hot face and at the cold face for (i) an 11.8mm glass/vinyl ester, and (ii) a 11.6mm glass/polyester. The applied heat flux was 50 kW/m^2

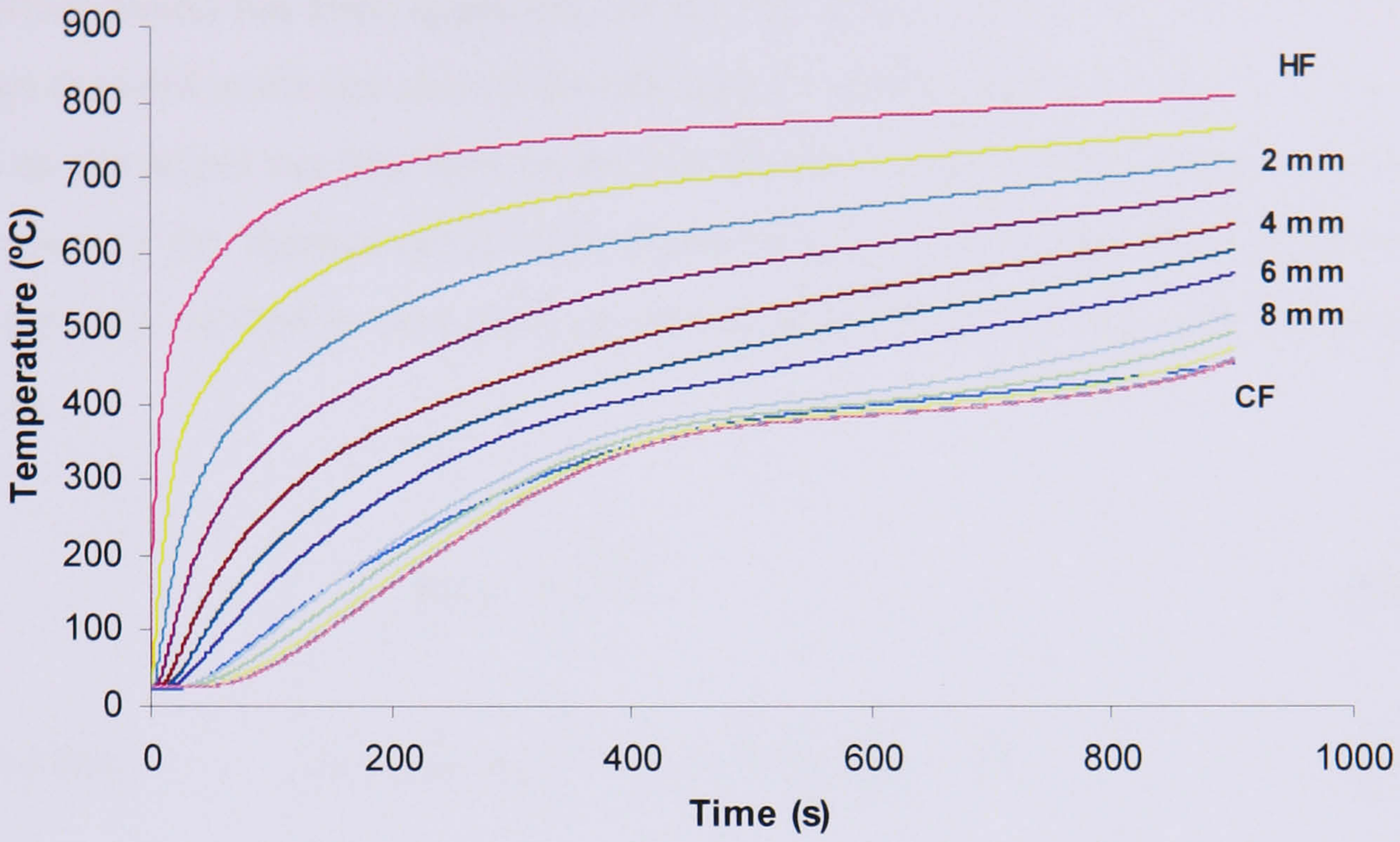


(i)

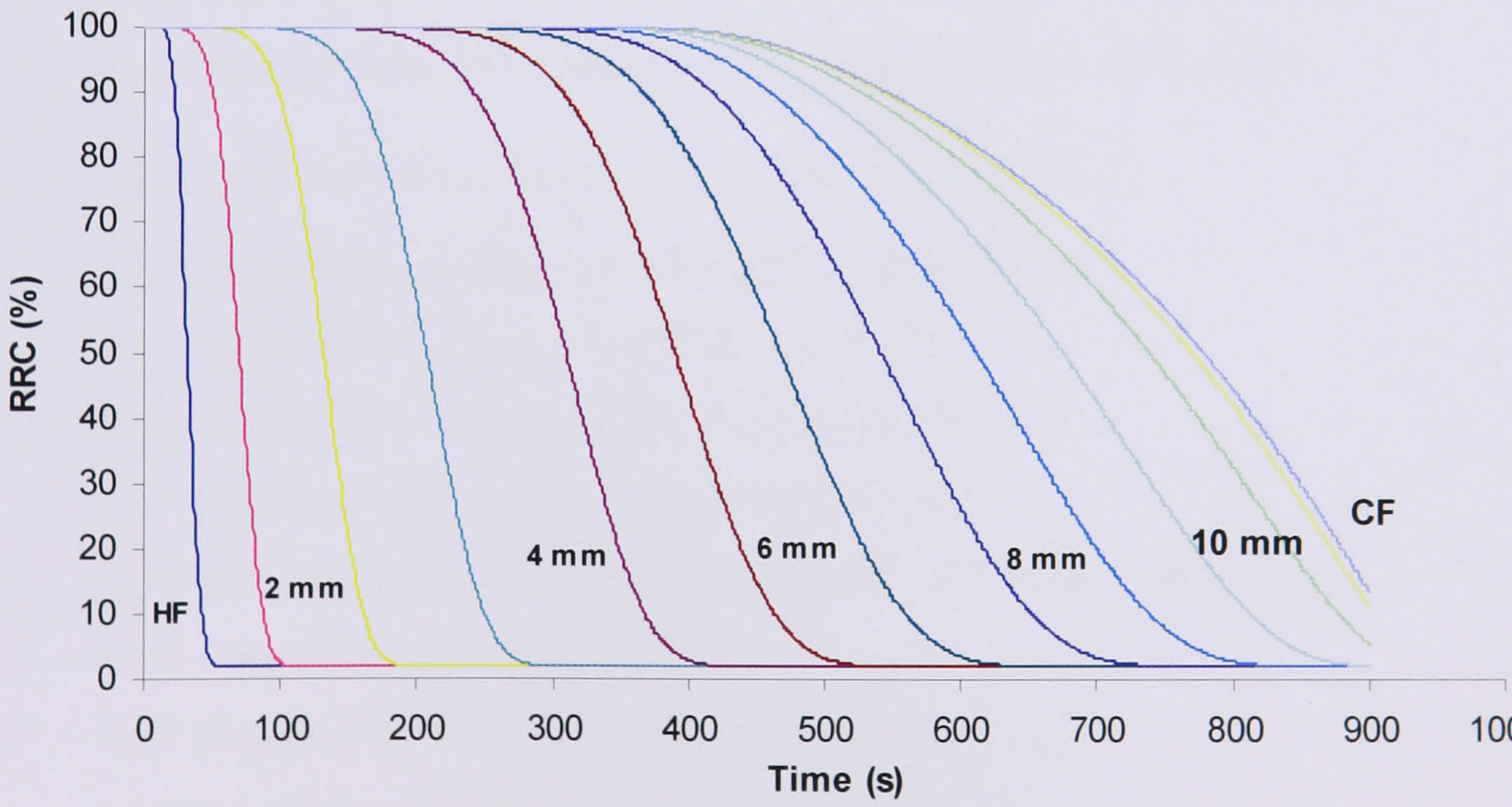


(ii)

Figure 5.8 Thermal model output for the case of 11.8 mm thick glass/vinyl ester laminate. Predictions are shown for a one-sided heat flux of 75 kW/m^2, with rear face insulated. (i) Temperature profile through the laminate thickness. (ii) Residual resin content (RRC) as %



(i)



(ii)

Figure 5.9 Thermal model output for the case of 11.6 mm thick glass/polyester laminate. Predictions are shown for a one-sided heat flux of 75 kW/m^2, with rear face insulated. (i) Temperature profile through the laminate thickness. (ii) Residual resin content (RRC) as %

5.3 Effect of mass flux on the hot face at flashover

The thermal model has been upgraded, for the first time, to study the effect of gas flow rate from the cold to the hot side of the laminate on the total energy at the hot face. This is because the actual net heat flux on the hot face at flashover is no longer constant. A new version of the thermal model was produced to consider these new changes. This novel approach resulted in very good prediction of fire reaction properties of composite laminates.

$$q = q_{\circ} \pm k\dot{M}_g \tag{5.8}$$

Knowing that,

$$q_{\circ} = \sigma\left(\varepsilon_s \alpha_m T_s^{\,4} - \varepsilon_m T_k^{\,4}\right) + h_{nc}\left(T_{sc} - T_c\right) \tag{5.9}$$

Where: -

q = heat flux into the hot face of the sample (W/m^2);

$q_{\circ}$ = original heat flux without the effect of gaseous mass flow rate (W/m^2);

k = constant depends on the resin type and probably heat flux also;

$\dot{M}_g$ = gas mass flow rate towards the hot face (kg/m^2s);

T_{sc} = surrounding temperature of heating source (^oC);

T_c = temperature on hot face of the sample (^oC);

T_s = surrounding temperature of heating source (^oK);

T_k = temperature on hot face of the sample (^oK);

h_{nc} = heat transfer coefficient through natural convection ($W/m^2/C$);

ε_s = emissivity of heating source (-);

α_m = absorptivity of the HF material of the sample (-);

ε_m = emissivity of the HF material of the sample (-);

σ = Stefan-Boltzmann constant (56.7×10^{-12} $W/m^2/K^4$).

The second term in Equation 5.8 accounts for the mass flow rate towards the hot surface and the first and second terms in Equation 5.9 are the radiation and natural convection

effects, respectively. They represent the thermal interaction between the heating source and the hot face of the composite.

It has been reported that at the onset of ignition, the applied incident heat flux is increased by 15 kW/m^2 [112, 131]. This increase in incident heat flux will result in an increase in the material's hot face temperature due to the flame feed back on the surface.

Figure 5.10 compares the measured temperature profile in the vicinity of the hot face and the modelled temperature profiles using a value for "k" for glass vinyl ester composite at 75 kW/m^2. Table 5.4 show different values for "k" for both resin systems at 50 and 75 kW/m^2, which represent the effects due to the gas flow rates at flashover.

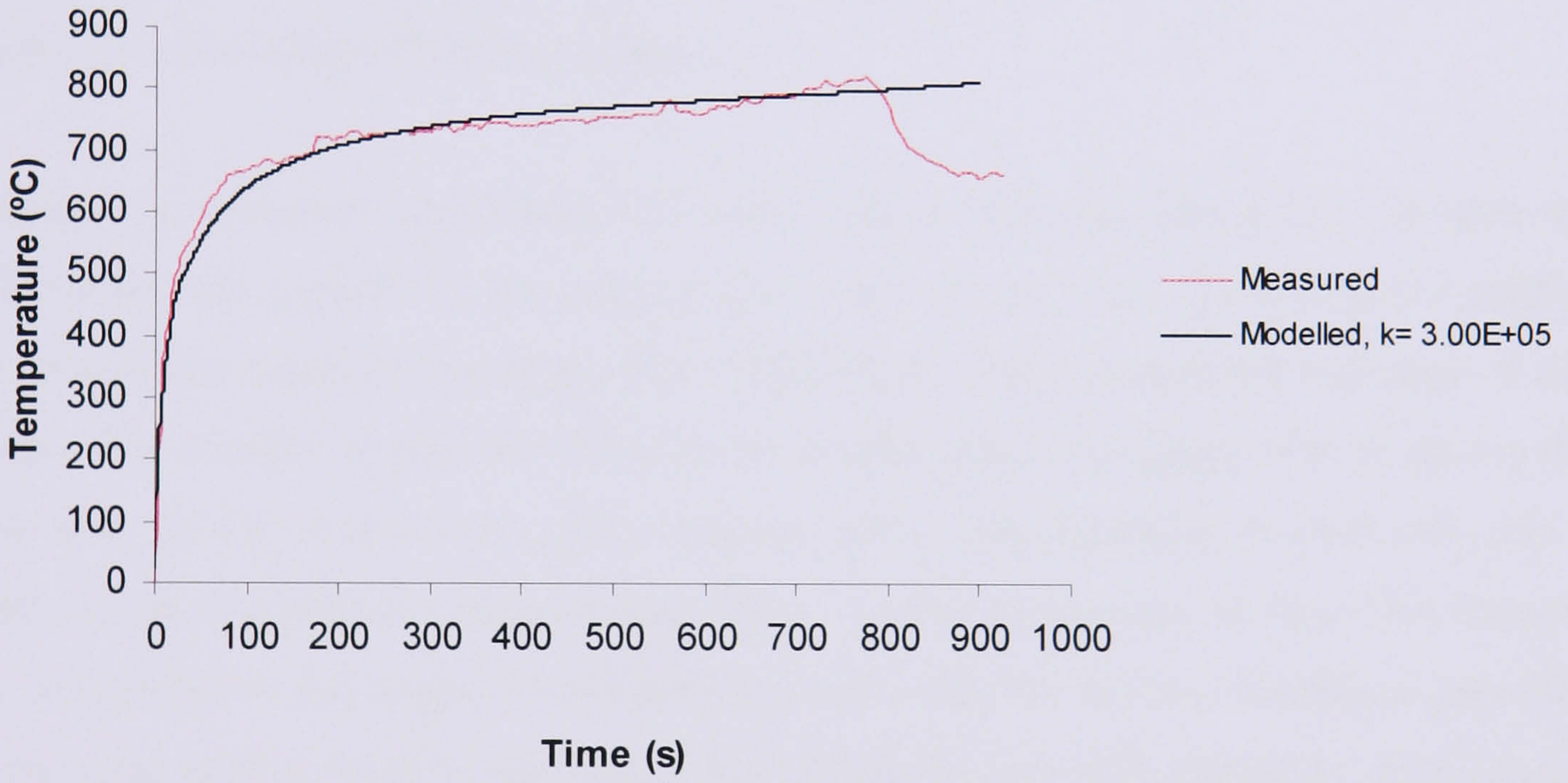


Figure 5.10 The measured and modelled field temperature profiles for glass vinyl ester composite at 75 kW/m^2

Table 5.4 Values for the constant "k" to count for the gas flow effects

Composite	Heat Flux (kW/m^2)	Value of "k"
Glass Vinyl ester	50	2E06
	75	3E05
Glass polyester	50	1E06
	75	4E05

5.4 Fire reaction modelling

5.4.1 Mass loss

Mass loss reflects the decomposition behaviour of composites in fire. Therefore, modelling the amount of decomposition is an important factor in calculating the loss in load capacity and the time-to-failure. The thermal model has been employed to model the mass loss, and this was compared to the actual mass loss measured by the cone calorimeter. The predicted mass flux of the gaseous flow from the cold to the hot side of the laminate during fire exposure has been used to calculate the remaining mass against time.

The measured and modelled mass loss behaviour of woven glass vinyl ester and polyester composites at constant heat flux of 50 and 75 kW/m^2 is shown in Figure 5.11-Figure 5.14. Good agreement was found.

Initially, the composite experiences no loss in mass when exposed to fire, because the material has not reached the decomposition reaction temperature of the polymer matrix. The model is capable of describing this initial delay with a reasonable accuracy. It can be seen that at times around 500 seconds, the model starts to slightly overestimating the mass loss. At this stage, most of the polymer matrix has degraded to char and only a small region of composite near the back-face remains undamaged by fire. It is thought that, the model at this stage did not precisely calculate the thermal insulation provided by the char surface layer to the underlying composite material, therefore calculating a little higher mass loss. Also, the carbonaceous char residue is modelled as a void and its contribution to the overall thermal conductivity is not considered. In fact, the thermal conductivity within the char region approaches that of the reinforcing fibers as the burning proceeds.

It is important to point out that the mass loss rate is not constant and this is because mass loss is affected by several thermal processes that change with time, including ignition, combustion, char formation and the transition from thermally thick to thermally thin

behaviour. A thermally thick material ensures that ignition takes place before the thermal wave has reached the back surface.

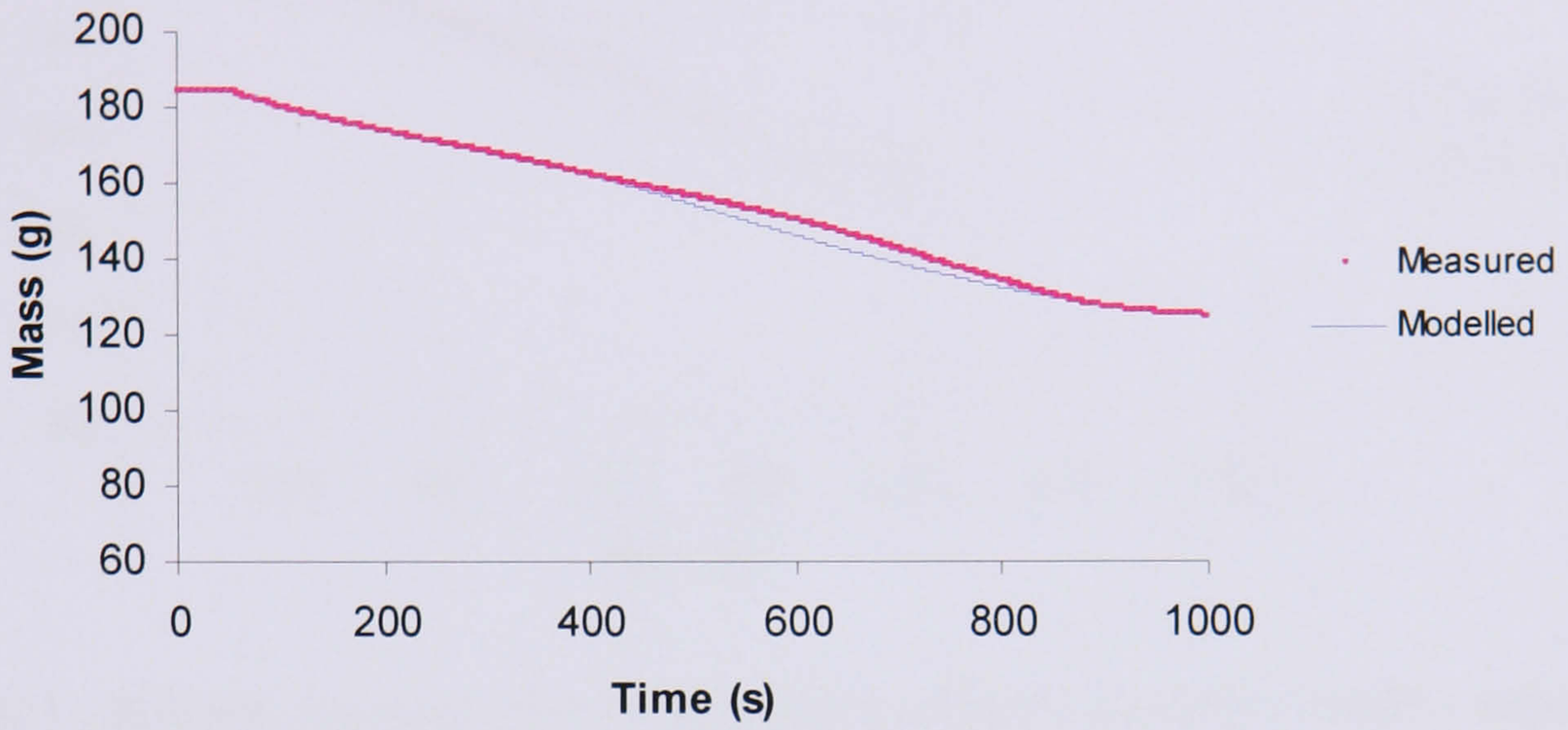


Figure 5.11 Modelled and measured mass loss of the woven glass vinyl ester composite at heat flux of 50 kW/m^2

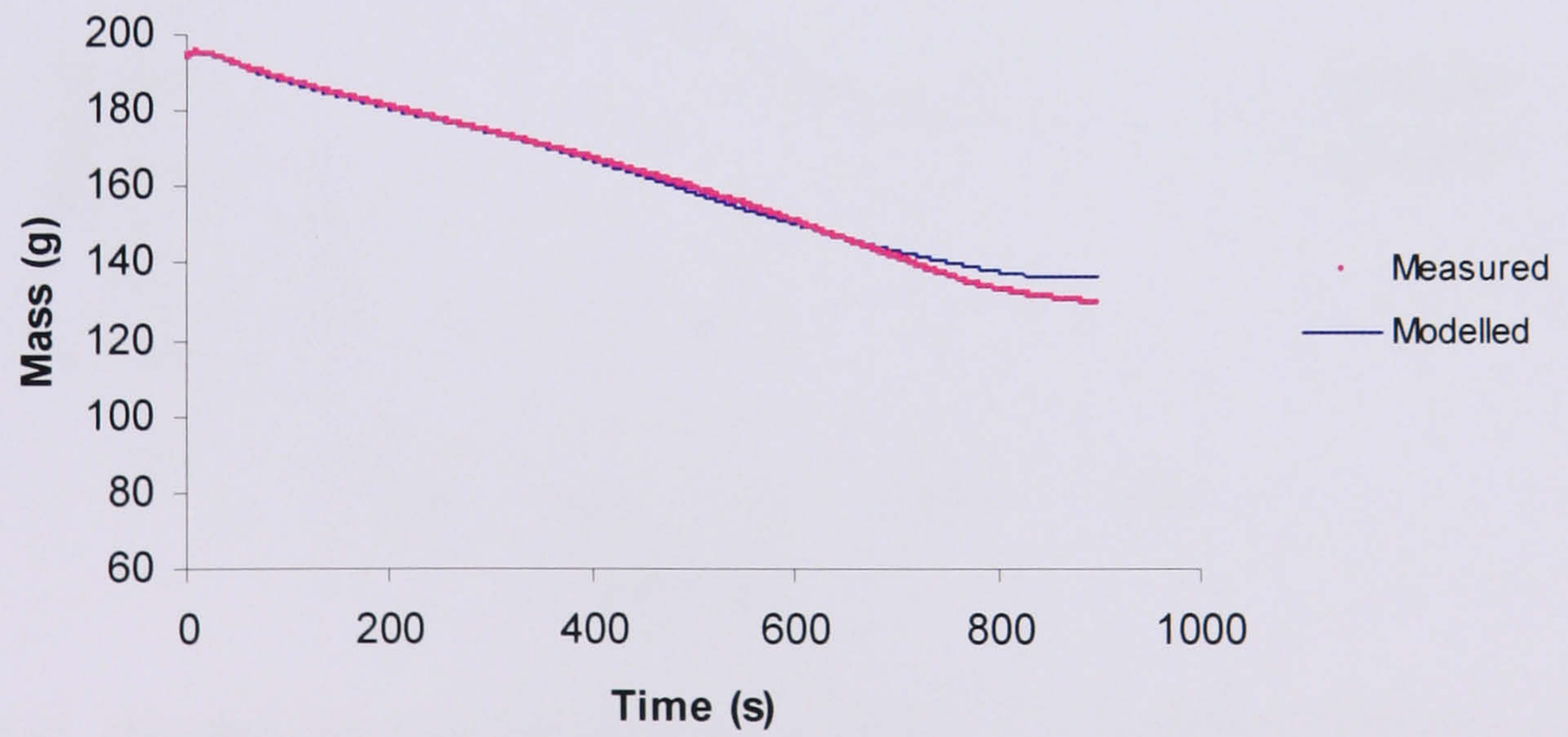


Figure 5.12 Modelled and measured mass loss of the woven glass vinyl ester composite at heat flux of 75 kW/m^2

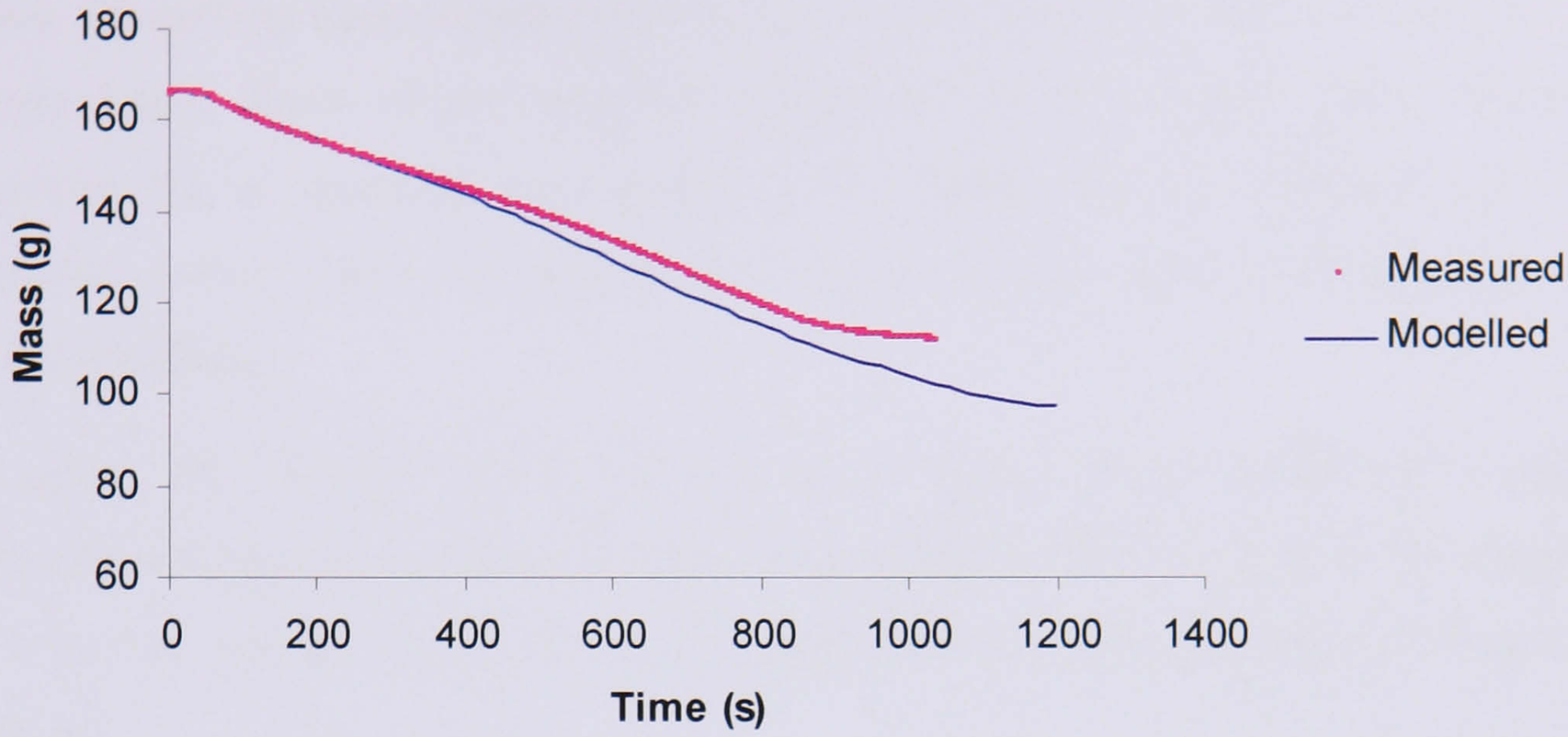


Figure 5.13 Modelled and measured mass loss of the woven glass polyester composite at heat flux of 50 kW/m^2

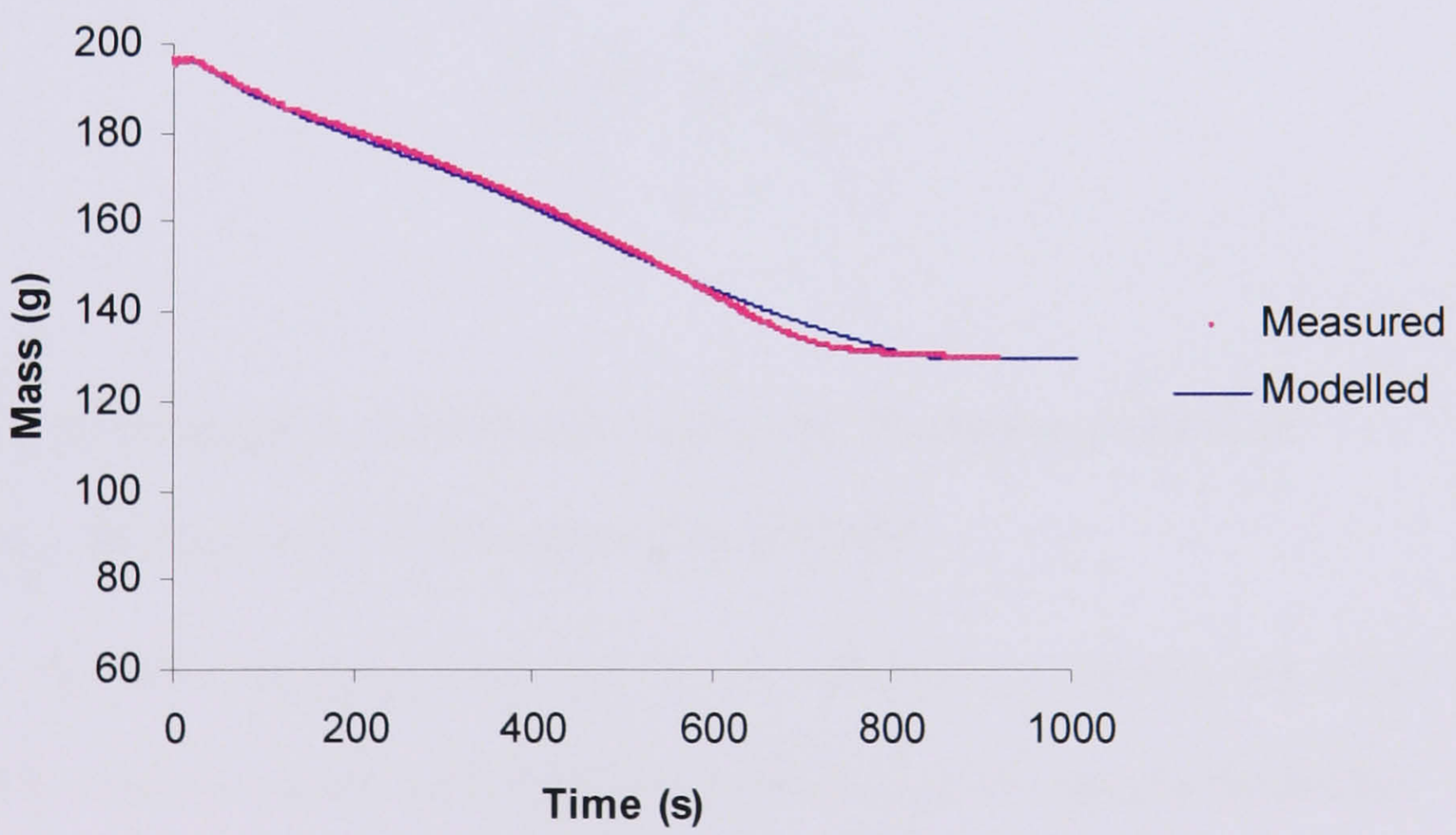


Figure 5.14 Modelled and measured mass loss of the woven glass polyester composite at heat flux of 75 kW/m^2

5.4.2 Heat release rate

The heat release rate is the liberated heat during the combustion of hydrocarbon volatiles. Modelling heat release rate is based on the definition that it equals the mass loss rate (mass flux) of the material multiplied by its average effective heat of combustion for a specified time period [64], which can be obtained from cone calorimeter testing. Table 4.4 shows the average effective heat of combustion values used for modelling.

Once again, the thermal model [5] was used, after a minor rectification and the incorporation of gas flow effects into the energy inputs of the hot face of the sample, to model the heat release rate as shown in Figure 5.15 to 5.18 using the calculated mass flux values.

By considering mass conservation over the finite difference element in the through-thickness direction, the following equation may be considered:

$$\frac{\partial}{\partial x}\left(\dot{M}_g\right) = \frac{\partial \rho_{com}}{\partial t} \qquad \textbf{(5.10)}$$

where:

$\dot{M}_g$ is the gaseous mass flux, or is the rate of gaseous mass flow.

$\partial \rho_{com}$ is the density of the composite material.

Therefore, the gaseous mass flux, $\dot{M}_g$ at any position, x, and at any time, t, can be calculated by integrating the rate of density change over the sample thickness:

$$\dot{M}_g = \int_{coldface}^{x} \frac{\partial}{\partial t}(\rho_{com})dx \qquad \textbf{(5.11)}$$

The heat release rate graphs show that the thermal response of these two materials changes with exposure time. The initial spike in heat release rate is due to the rapid

decomposition of resin rich surface layer. After this, a steady decrease is observed, which probably occurs as a result of the increase in thermal insulation provided by the growth of a char surface layer. Then another increase in heat release occurs and this is believed to happen because of the increase in decomposition reaction rate as the materials' behaviour change from thermally thick to thermally thin.

It can be concluded that the thermal model is able to capture, with good accuracy, different oscillations of heat release rate resulting from the change of thermal response with time. The precision in modelling the peak heat release rate value was improved compared with the published heat release rate models [131, 132]. Again there is a little disagreement, especially in modelling the second peak heat release rate due to the fact that the model did not consider the change in behaviour from thermally thick to thermally thin. Also, the uncertainties bout thermal and transport properties affect the modelling results.

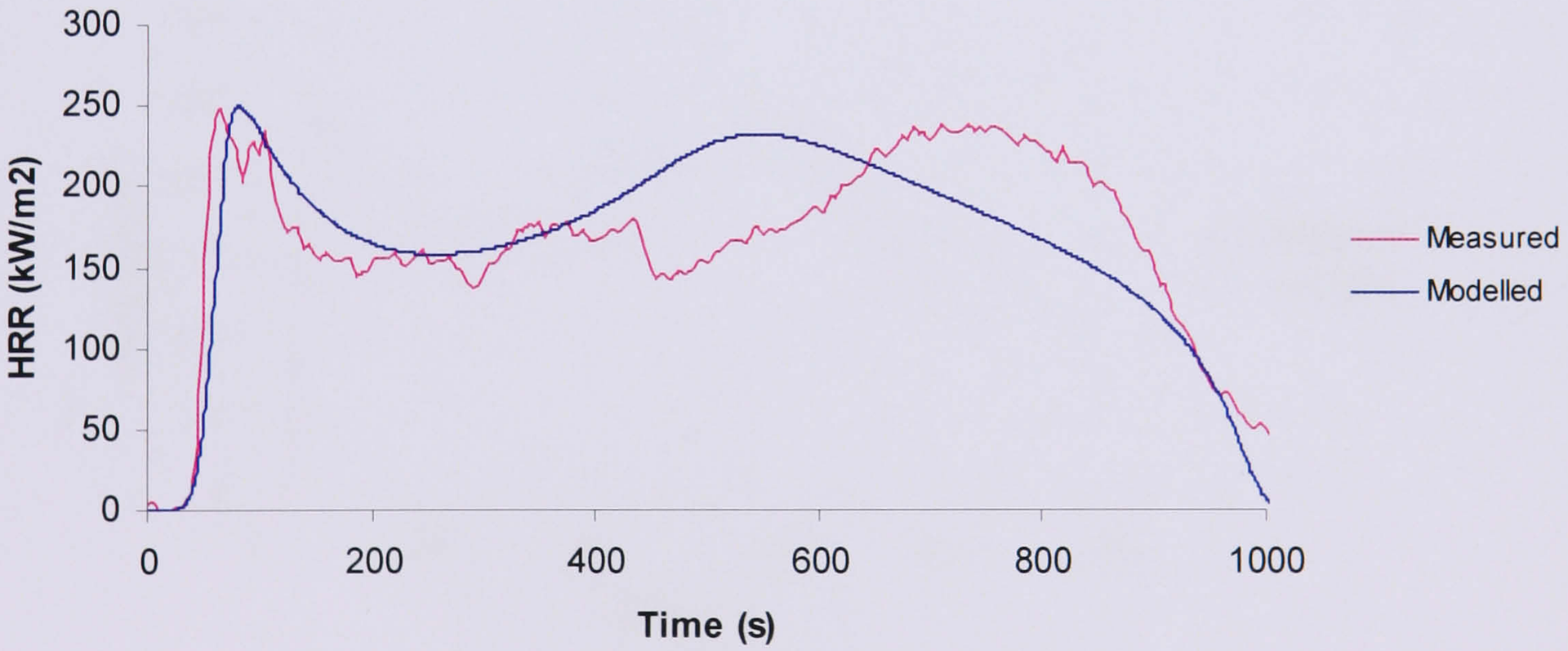


Figure 5.15 Modelled and measured heat release rate of the woven glass vinyl ester composite at heat flux of 50 kW/m^2

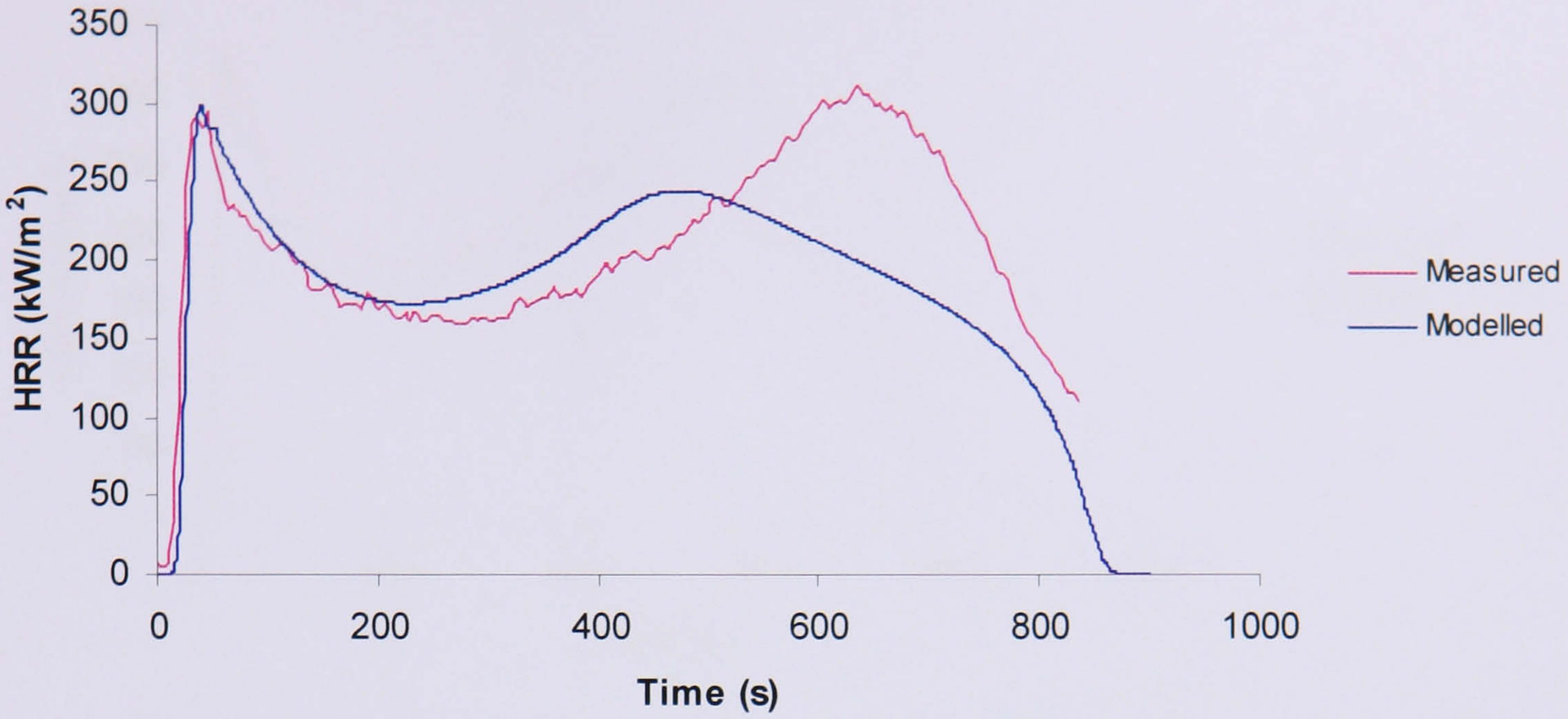


Figure 5.16 Modelled and measured heat release rate of the woven glass vinyl ester composite at a heat flux of 75 kW/m^2

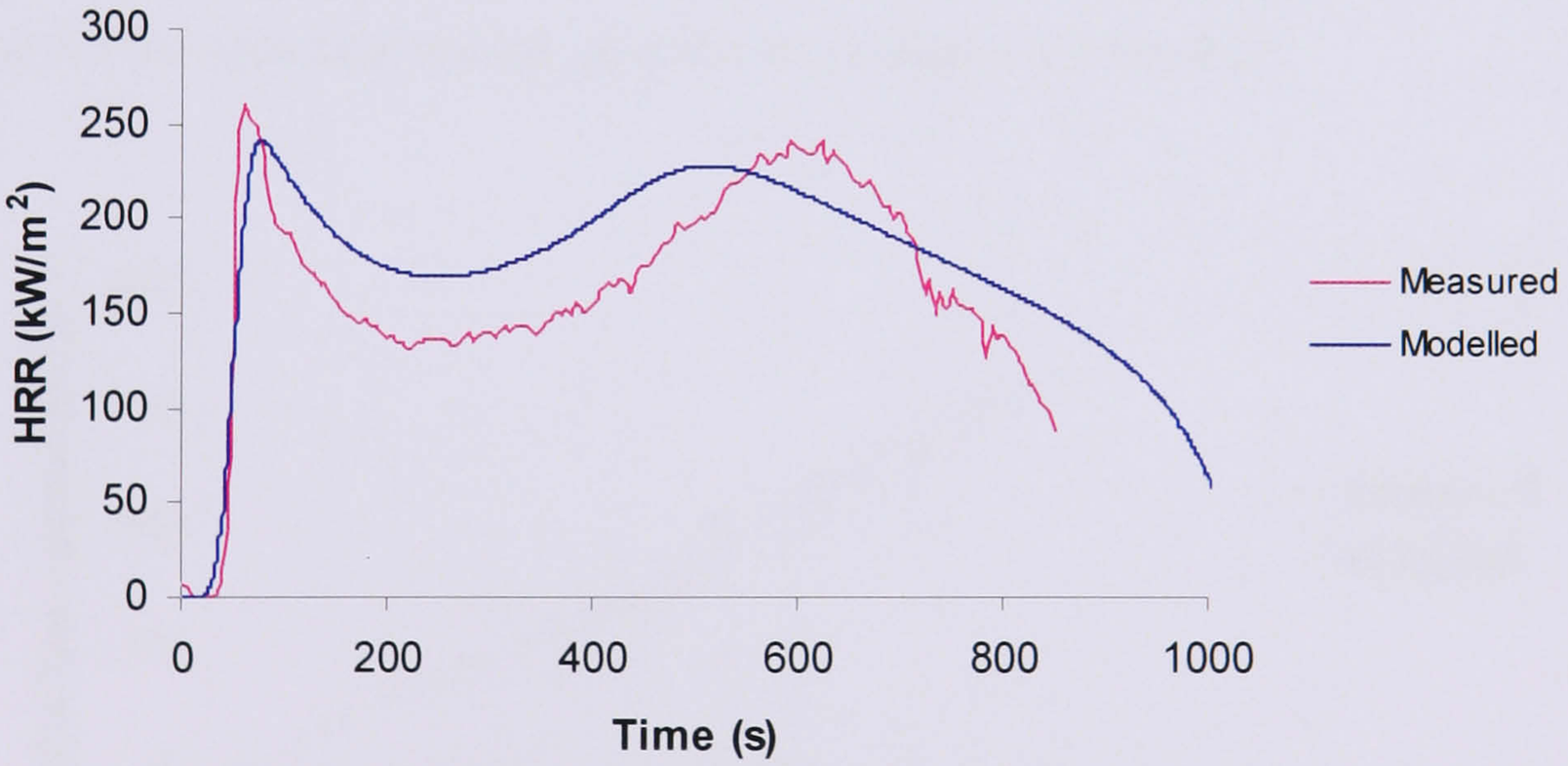


Figure 5.17 Modelled and measured heat release rate of the woven glass polyester composite at a heat flux of 50 kW/m^2

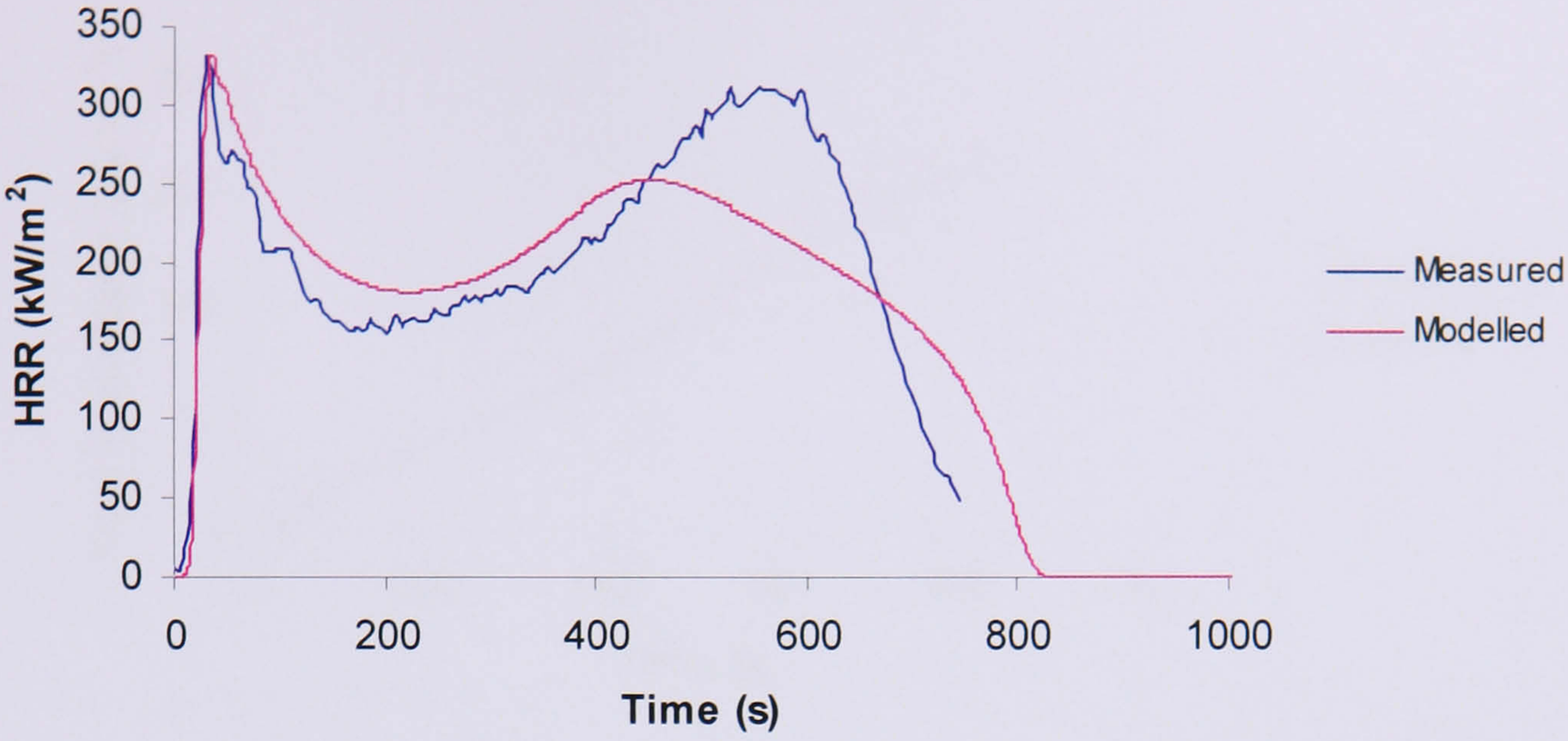


Figure 5.18 Modelled and measured heat release rate of the woven glass polyester composite at heat flux of 75 kW/m^2

Generally, the slight difference between the experimental and modelled heat release rate for the rest of profiles can be attributed to the uncertainties of the material thermal and transport properties, which are the main modelling inputs. However, the agreement is very good for the total heat release as it shown in Figure 5.19 to 5.23.

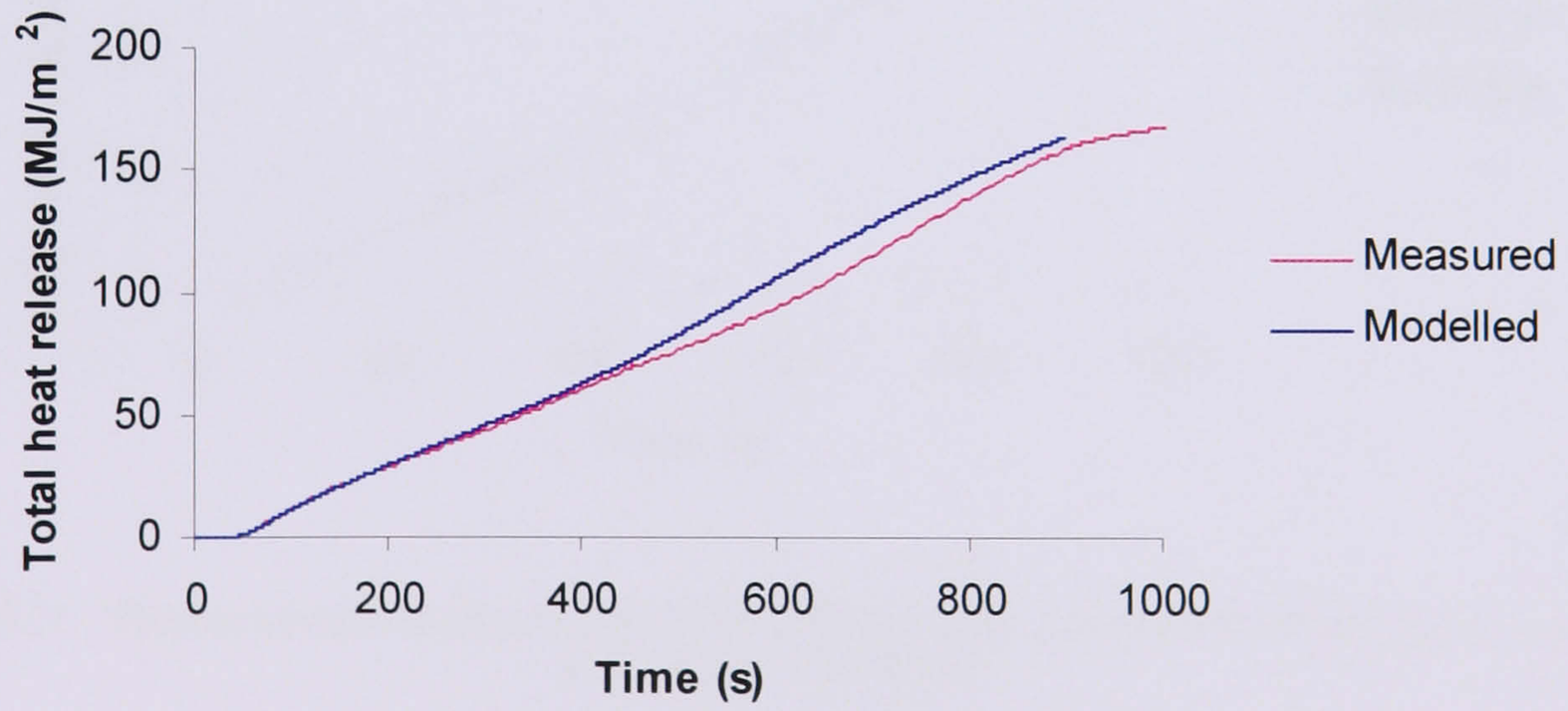


Figure 5.19 Measured and modeled total heat release of glass vinyl ester composite at a constant heat flux of 50 kW/m^2

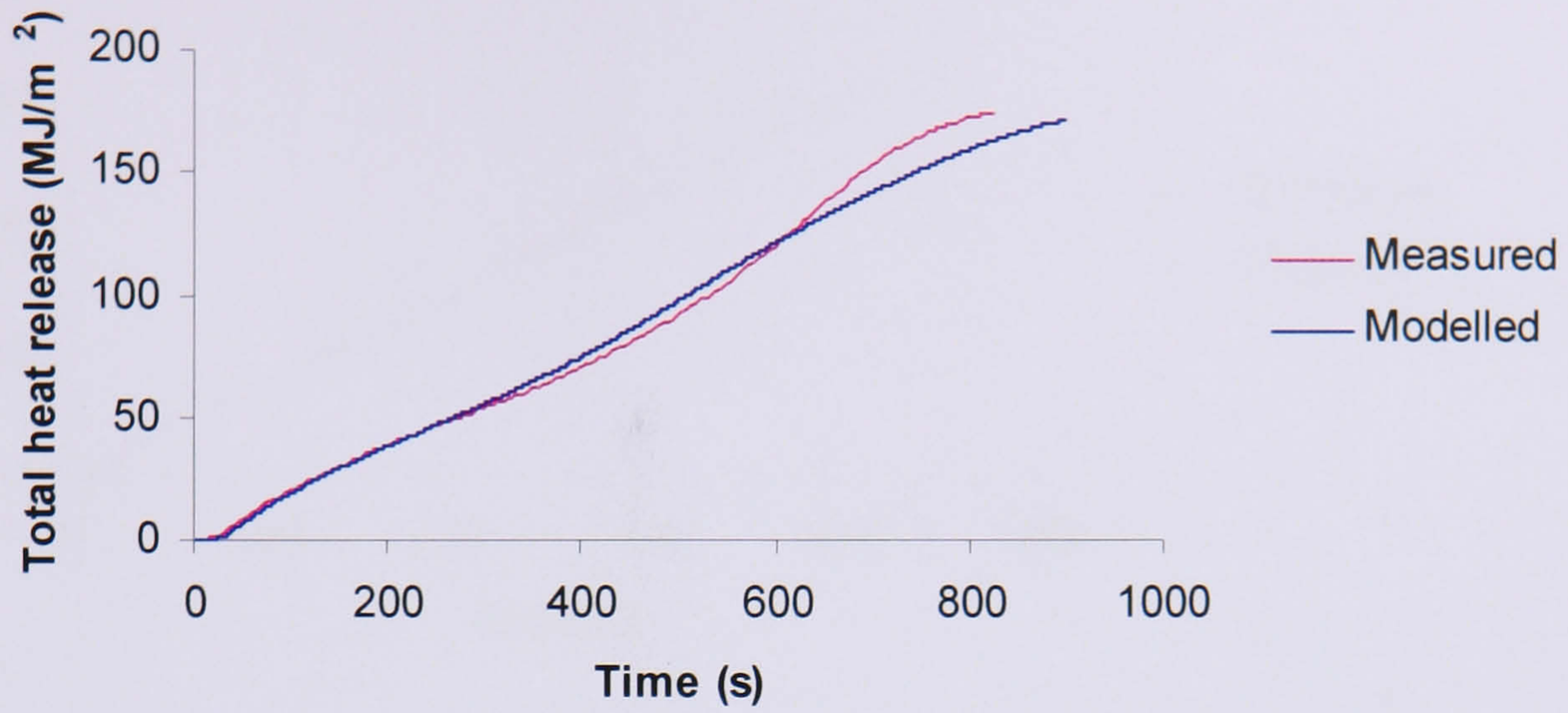


Figure 5.20 Measured and modeled total heat release of glass vinyl ester composite at a constant heat flux of 75 kW/m^2

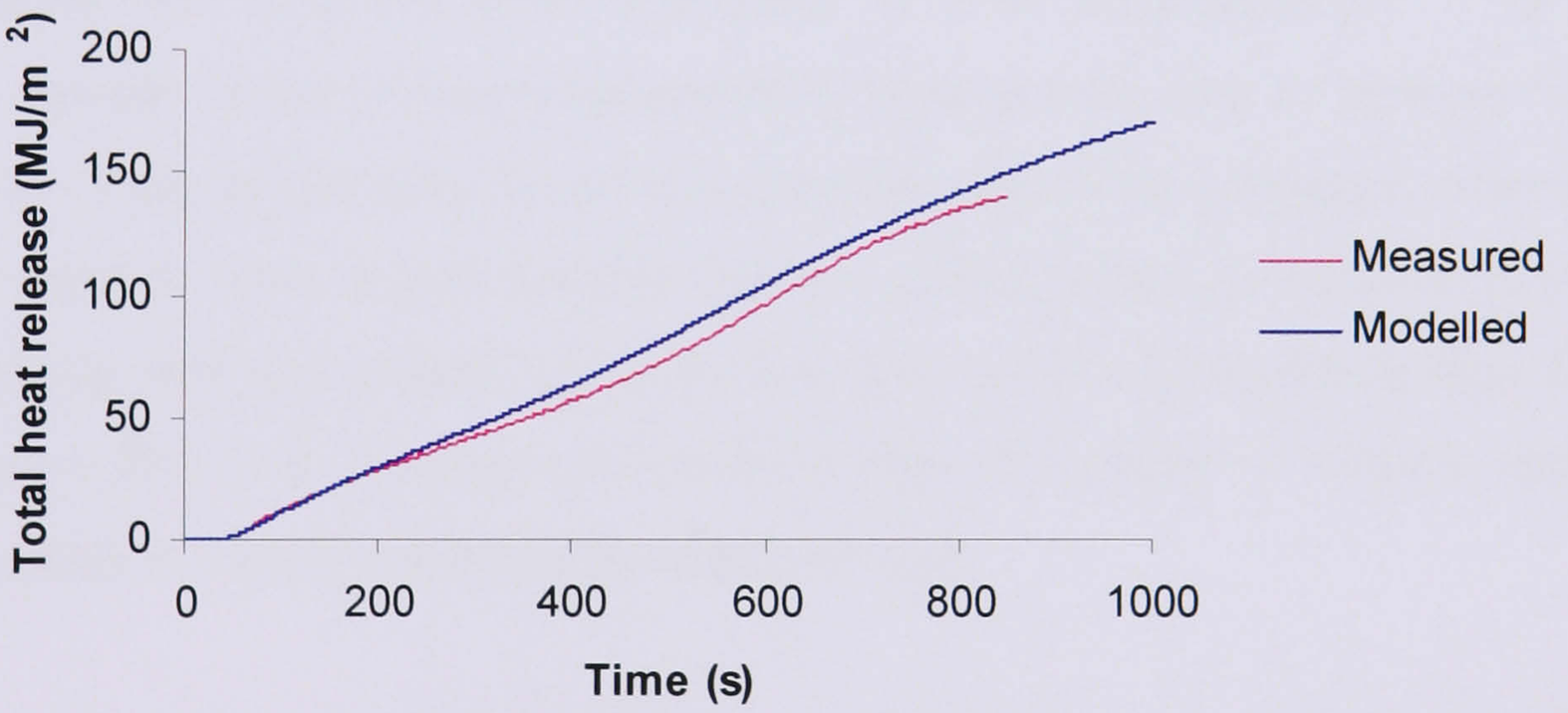


Figure 5.21 Measured and modeled total heat release of glass polyester composite at a constant heat flux of 50 kW/m^2

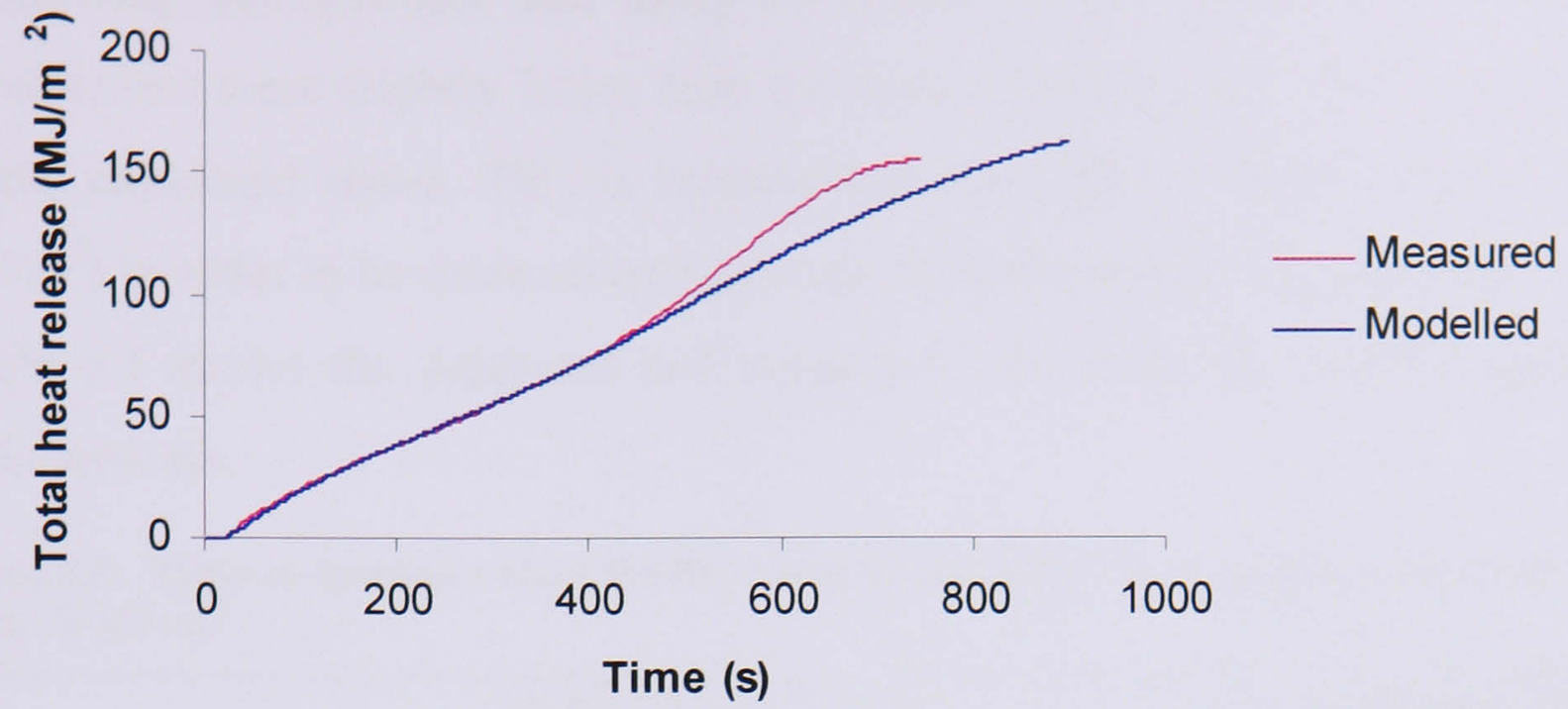


Figure 5.22 Measured and modeled total heat release of glass polyester composite at a constant heat flux of 75 kW/m^2

5.4.3 Time-to-ignition

It has been found in the literature that the mass flux at sustained ignition of fibre glass reinforced composites is ≈ 4-5 g/m^{2}s [25] and this was independent of the resin type. General agreement with this result was made by other researchers [29, 133]. In this study the thermal model [5] has been employed to model the time to ignition. This was achieved by firstly determining the critical mass loss rate of the composite at the onset of sustained ignition when experimentally exposed to fire, which is found to be 4 g/m^{2}s, approximately, and then relating this mass loss rate to the corresponding time from the model output file. This is because the concentration of flammable volatiles required to initiate ignition is mainly controlled by mass loss rate.

Lattimer [131] modelled the time–to ignition by predicting the mass loss rate of the material for every time step and then determining the potential heat release rate of the material using the heat of decomposition. This potential heat release rate was related to the fire point. If it is greater than the fire point, it was assumed that ignition would occur, otherwise not. Lyon [134] defined the fire point as the critical heat release rate at sustained ignition and demonstrated that it was 66±17 kW/m^2.

Following this approach and using the thermal model (com_fire), we found that the predictions were slightly lower than the ones obtained using the output of the thermal model explained above. This is because Lattimer used the lower end of the range (50 kW/m^2) in order to be more conservative in determining the time-to-ignition.

Table 5.5 shows the predicted and measured values for the time-to-ignition for both resin systems.

Table 5.5 Time-to-ignition values for fibre reinforced polyester and fibre reinforced vinyl ester at 50 & 75 kW/m^2

	flame-out time (min.) 50 kW/m^2			**flame-out time (min.) 75 kW/m^2**		
	Modelled	Modelled*	Experimental	Modelled	Modelled*	Experimental
Glass Polyester	42	36	39	19	17	17
Glass vinyl ester	51	43	46	22	19	18

* Modelled using the critical heat release value.

Table 5.6 below summarizes the measured and modelled values of the main fire reaction properties. A reasonable agreement between these values can be observed.

Table 5.6 Comparison of the measured and modelled fire reaction properties for fibre reinforced vinyl ester and polyester composites at constant heat flux of 50 & 75 kW/m^2

	Glass reinforced vinyl ester				**Glass reinforced polyester**			
	50 kW/m^2		**75 kW/m^2**		**50 kW/m^2**		**75 kW/m^2**	
	Measured	**Modelled**	**Measured**	**Modelled**	**Measured**	**Modelled**	**Measured**	**Modelled**
Time-to-ignition (s)	46	51	18	22	39	42	17	19
$AHRR_{(300s)}$ (kW/m^2)	145	151	183	187	140	156	182	200
$PHRR_{(300s)}$ (kW/m^2)	249	250	296	299	269	253	330	331
Time-to-PHRR (s)	65	73	35	36	65	75	40	38
AMLR (g/s)	0.053	0.061	0.075	0.084	0.051	0.057	0.075	0.085

5.5 Fire resistance modeling

The output of the thermal model, temperature profile and residual resin content, coupled with the material temperature dependent properties using the transition fitting relationship allowed modelling time-to-failure for glass polyester and vinyl ester composites. This approach is based on two assumptions. The first assumption is that the laminate is evenly heated at a constant radiant heat flux. The second assumption is that the applied tensile and compression loads are applied evenly in the axial (lengthwise) direction. Hence, this system can be considered as one dimensional whose temperature and strength differ through the laminate thickness.

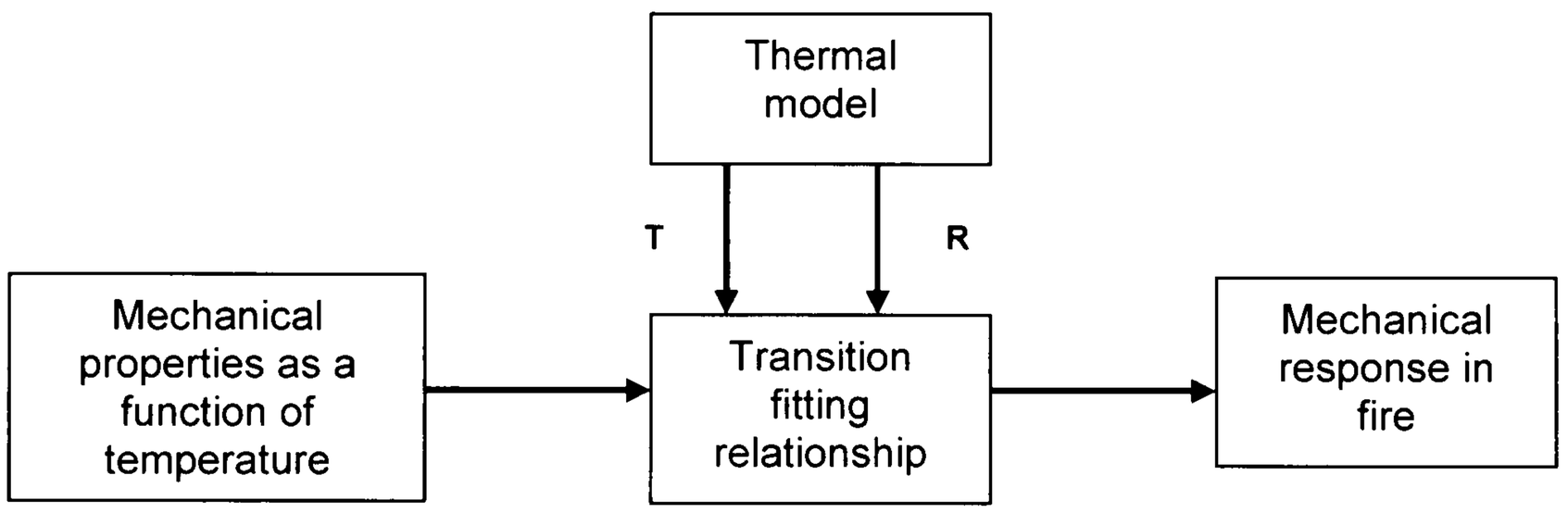


Figure 5.23 Mechanical response model

5.5.1 Temperature dependent properties

In order to study the mechanical behaviour of composite laminates in fire, it was useful to express different mechanical properties as a function of temperature. The data used in this research was obtained from the previous test results made by previous researchers [15, 35, 106]. Summary of the materials' properties are provided below in Table 5.7 and Table 5.8.

Table 5.7 Polyester parameters: A summary of the relevant parameters required for modelling the temperature dependent properties of glass/polyester laminates [35]

	P_U	P_R	k	T'
σ_c	250 MPa	23 MPa	0.025	70°C
σ_T	330 MPa	150 MPa	0.033	70°C

Table 5.8 Vinyl ester parameters: A summary of the relevant parameters required for modelling the temperature dependent properties of glass/vinyl ester laminates [35]

	P_U	P_R	k	T'
σ_c	260 MPa	24 MPa	0.035	83°C
σ_T	375 MPa	170 MPa	0.03	103°C

Where: σ_c refers to the modelled compressive strength.

σ_T refers to the modelled tensile strength.

P_U and P_R are the un-relaxed property value at room temperature and the relaxed value at elevated temperature, respectively.

k is a constant describing the temperature range across which softening occurs.

T' is is the mechanically determined glass transition temperature around which fall in property value occurs (often similar in value to T_g).

The hyperbolic *tanh* function (Equation 2.2) was used to fit the relationship between the mechanical property and temperature cross the transition region.

5.5.2 Modelling time-to-failure

In most cases, fire resistance is quantified as the time by which an element can meet certain failure criteria during exposure to fire [74]. The first step in predicting time-to failure under tensile and compressive loading was to determine temperature profile and the residual resin content through the laminate thickness. The next step was to calculate the tensile or compressive strength at each point through the thickness for every time step. Equation 2.2 was deployed to achieve this using the property data as a function of temperature outlined in Table 5.7 and Table 5.8.

The bulk strength was obtained by averaging the residual strengths through the laminate thickness using Simpson's rule [135]. The time component came from the thermal

model (Equation 2.10) to allow the prediction of failure time. The time to failure is the time taken for the residual strength of the composite laminate to become equal to the applied stress where failure must occur. Tensile strength is not affected by RRC. In tensile loading the value of "n" in Equation 2.6 is considered to be of zero, whereas, in compressive loading the value of "n" is assumed to be one [19, 106]. This is because when the resin has decomposed at high temperatures, the tensile stress is supported solely by the glass fibres. The resin has a negligible tensile strength compared to the fibres, and so the RRC is not included in the function. Simultaneous failure of all the plies was assumed in this model. With the used averaging method, it was assumed that the sample failed unstably with all the plies collapsing at the same time. This has led to slight underestimation of the failure load when using the thermal-mechanical model.

Figure 5.24 and Figure 5.25 show the measured and modelled tensile strength against time-to-failure for fibre glass polyester and vinyl ester, respectively.

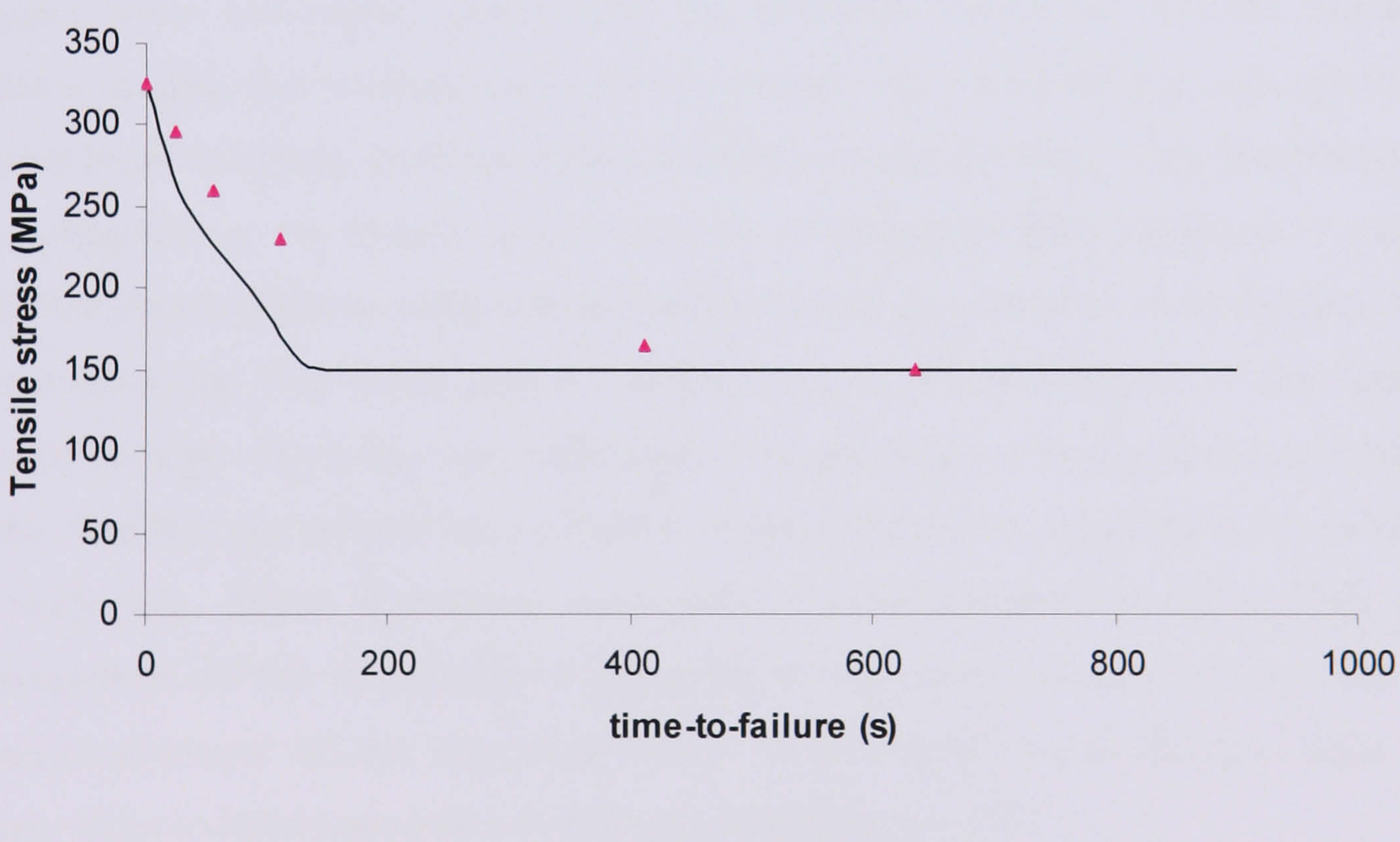


Figure 5.24 Comparison of the predicted (solid line) and measured (data points), time-to-failure for the glass/Polyester laminate under tensile loading and heat flux of 75 kW/m^2

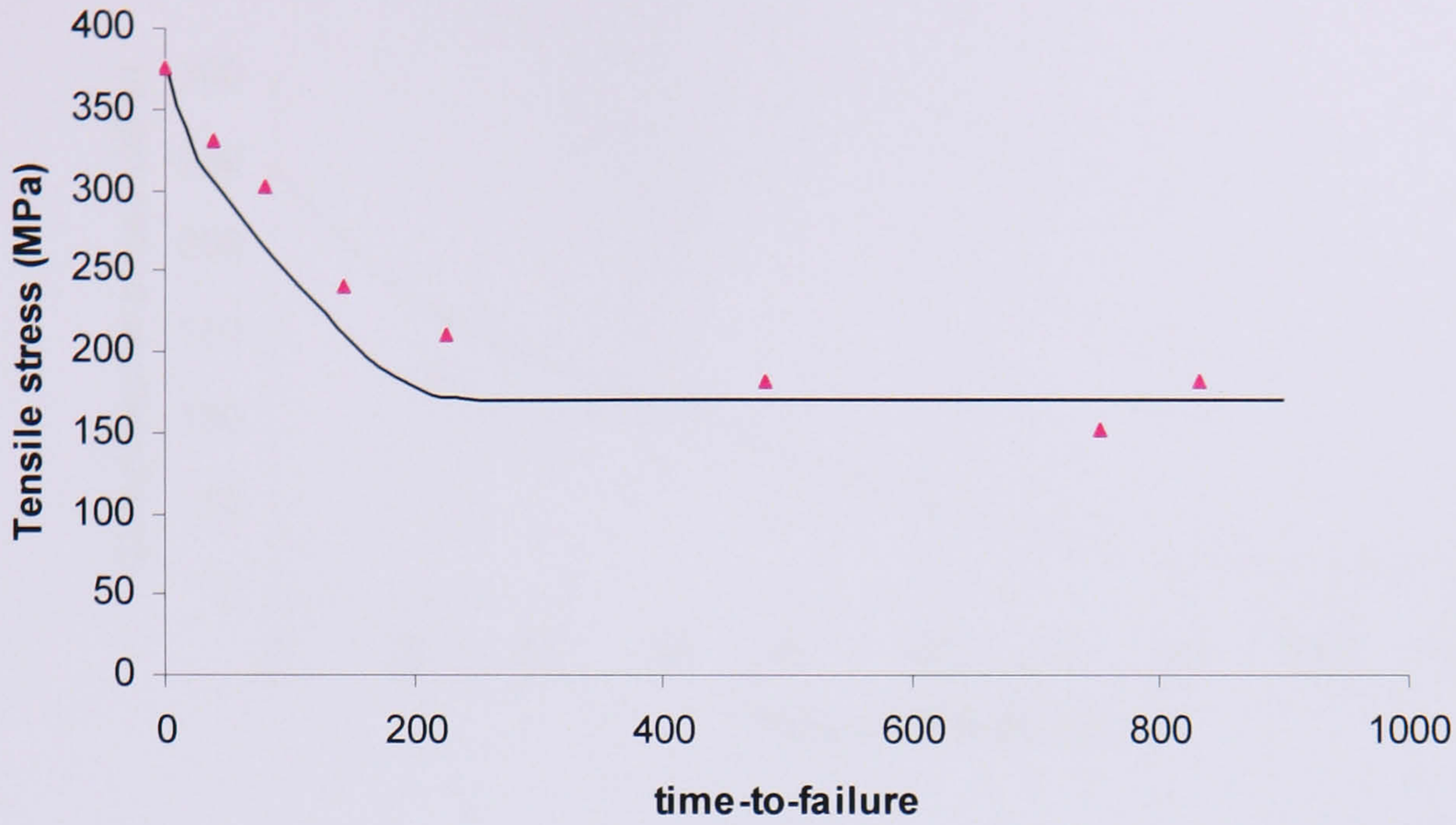


Figure 5.25 Comparison of the predicted (solid line) and measured (data points), time-to-failure for the glass/Vinyl ester laminate under tensile loading and heat flux of 75 kW/m^2

Regarding the compressive failure previous researchers [35, 36] tested composite samples using constrained compression test apparatus and found that the specimens failed at slightly lower compressive failure stresses. They believed that although the jig limited Euler buckling, it still permitted a degree of local buckling. This phenomenon is also observed in our results despite the use of relatively short rectangular samples (200mm length×100mm width×12mm thickness) and the provision of insert slots in the compression jig. One other reason could be due to the architecture of the laminate (woven roving), which has resin rich layers. The resistance to buckling in these regions is less than the rest, and this may initiate a compressive failure. In addition, the existence of voids and fibres' undulation could have a major pronounced effect [38]. As a consequence, all this would lead to deterioration of compressive strength. The thermal-mechanical model did not take these factors in consideration and therefore calculated higher times to failure as shown in Figure 5.26 and Figure 5.27.

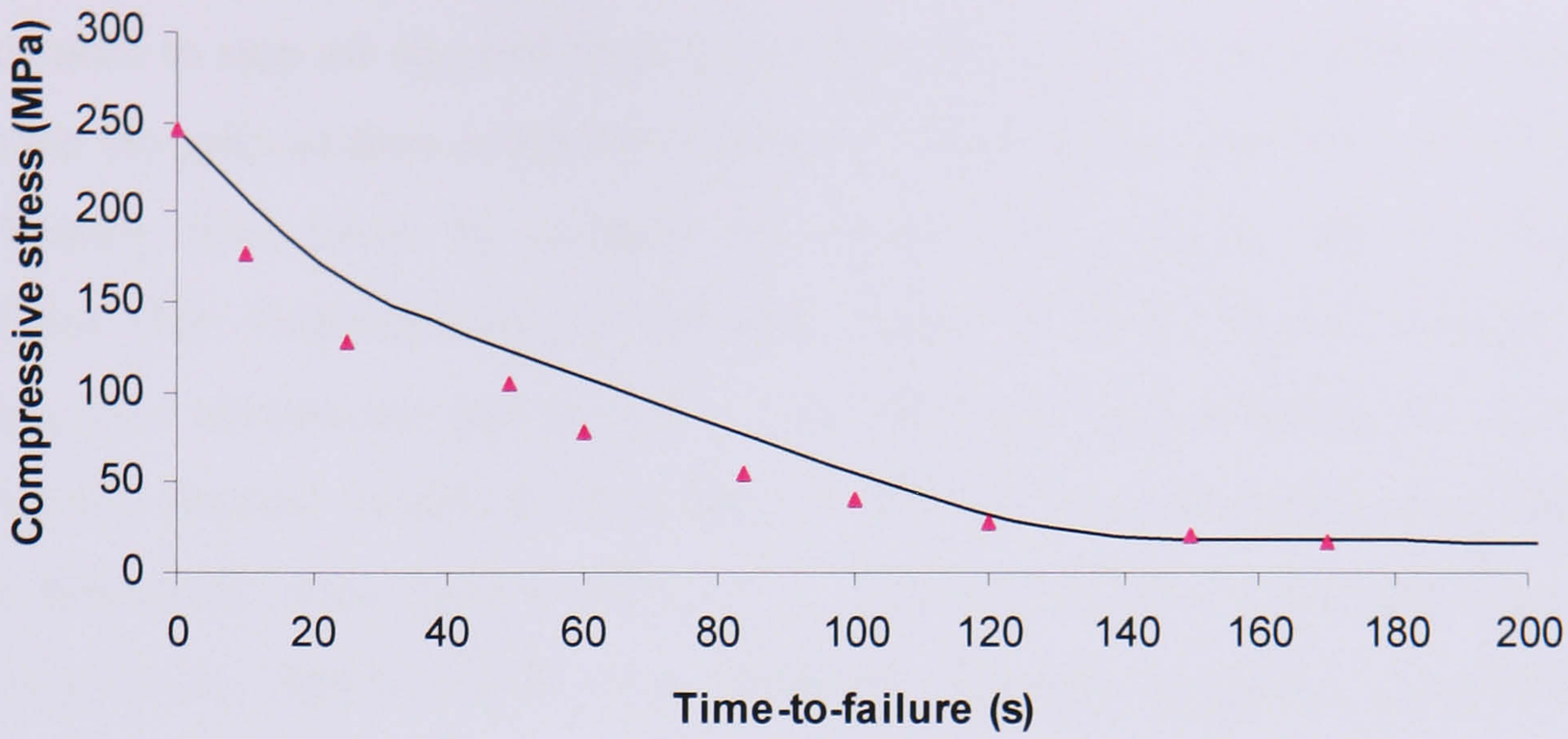


Figure 5.26 Comparison of the predicted (solid line) and measured (data points), time-to-failure for the glass/Polyester laminate under Compressive loading and heat flux of 75 kW/m^2

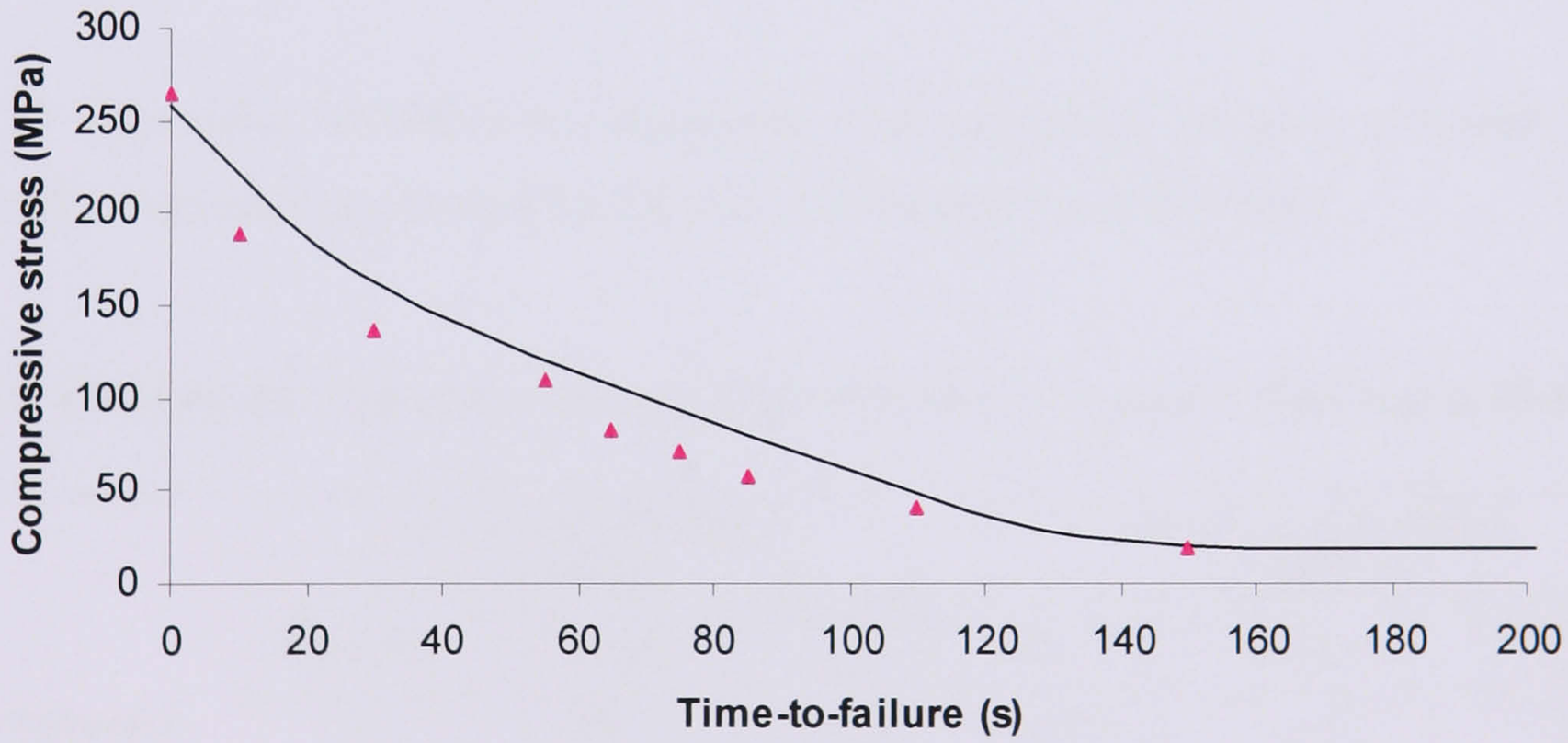


Figure 5.27 Comparison of the predicted (solid line) and measured (data points), time-to-failure for the glass/vinyl ester laminate under Compressive loading and heat flux of 75 kW/m^2

5.5.3 Prediction of flame-out time

The time taken to stop all signs of flaming combustion is one of the properties required to assess the integrity of fibre reinforced polymers. In this thesis the flame-out is defined by the heating time taken to degrade the whole resin content into volatiles and carbonaceous char. Experimentally it was determined by measuring the time of flame out during cone calorimeter testing. Due to the difficulty in estimating the flame-out time using the thermal model, it was approximated by considering the time taken to bring the remaining resin content (RRC) to 2% and 4% for polyester and vinyl ester resins, respectively. These values were based on thermogravimetric analysis results (TGA) mentioned before. This assumption has led to slight overestimation of the calculated burning times because the composite might have stopped burning well before the time required to reach the above mentioned resin values due to the difference in degradation conditions and also due to the influence of char formation.

Flame-out time values were also calculated based on the concept of critical heat release rate value (50 kW/m^2) [131, 134]. Good agreement was found.

Table 5.9 shows the calculated and measured flame-out times for glass polyester and vinyl ester composites at constant heat fluxes of 50 kW/m^2 and 75 kW/m^2.

Table 5.9 Flame-out times for fibre reinforced polyester and fibre reinforced vinyl ester at 50 & 75 kW/m^2

	flame-out time (min.) 50 kW/m^2			**flame-out time (min.) 75 kW/m^2**		
	Modelled	Modelled*	Experimental	Modelled	Modelled*	Experimental
Glass Polyester	20	16	15	16	16	15
Glass vinyl ester	20	13	17	15	14	14

* Modelled using the critical heat release value.

Chapter 6 Conclusions

6.1 Fire reaction measurements

Fire reaction measurement using the cone calorimeter (ASTM E1354 and ISO 5660) is a very useful tool to characterize, classify and model fibre reinforced composites. It provides an indication on how the material behaves in real fires. Therefore, flammability assessment is an essential requirement for product selection and development.

6.2 Fire reaction properties as function of stress

A loading frame fitted to the cone calorimeter allowed 100mm × 30mm rectangular glass vinyl ester and polyester laminate samples to be tested under tension and compression, while being exposed to a constant heat flux.

It was found that there was a small but significant effect of stress on the fire reaction properties; heat release and smoke generation. Tensile stress increased heat release and smoke generation peaks, whereas compressive stress had the opposite effect. Tensile stress also shortened the time-to-ignition, with compressive stress having the opposite effect. The effect was attributed to an increased tendency for cracks to form when the laminate was subjected to tension, the opposite being true for compression.

The crack formation hypothesis is further supported by the observation that applied stress has the greatest effect on the early heat and smoke release peaks, with a lower effect on the final 'run-out' values.

6.3 Fire under load tests

Experimental fire under load tests revealed that the time-to-failure of the laminate decreases with increasing the applied load or heat flux. The failure times of compressive loading are much shorter, by approximately an order of magnitude, than for tensile loading. This is because compressive failure is dependent on thermal softening and

pyrolysis of the matrix, which results in plastic kinking of fibre tows. The same finding has been established by previous researchers who studied the mechanism of composites compressive failure [35, 123-125]. Delamination cracks between layers near the hot surface propagate through the laminate with time. The delaminated plies have little capacity to carry the applied load, which leads to the transmission of this load to the underlying layers that were free of cracks. This conclusion explains the sudden and catastrophic nature of the compressive failure of fibre reinforced polymers. Tensile failure on the other hand, depends on the decomposition of the matrix and premature failure of the fibres, which occurs at higher temperatures. This indicates that fibre reinforced polymers retain a considerable residual tensile strength even when exposed to high temperature untill the applied stress is higher than the retained tensile strength. It is believed that stress corrosion on the surface of glass fibres was behind the deterioration of their strength. This mechanism is not fully understood, but the presence of water in the air may provide an aqueous environment required to initiate this process.

It is shown that composites laminates elongate and bend due to thermal forces (expansion) and thermal moments (bending). The amount of elongation and degree of bending are dependent on the level of heat flux, applied load and time of exposure.

6.4 Modelling

The thermal model was used to model the major fire reaction properties such as time-to-ignition, heat release rate, mass loss rate and flame-out time to simulate the response of the cone calorimeter at constant heat flux. Good agreement was obtained.

The output of the thermal model, especially temperature profile and residual resin content, combined with temperature dependent properties were used to construct ply constitutive equations and hence, predict the reduction to mechanical properties and also the time-to-failure of the laminates under tension or compression loads. The predictions were found to be reasonably accurate.

Chapter 7 Future Work

7.1 Thermal model

A library comprising data files on the change in thermal properties such as thermal conductivity and specific heat as function of temperature is required. This data needs to be incorporated into the existing thermal model to predict the thermal response of laminates and sandwich composite materials in fire more accurately.

Also, it is known that during the decomposition of the composite, delamination cracks are generated. This effect and its consequences on the total energy and on the general integrity of the composite have to be considered in the thermal model by finding a suitable criterion to represent it and then include it in the governing equation.

7.2 Fire protection techniques

There is a need to consider the modelling of different fire protection systems, which have been developed to reduce the effects of high heat flux on the composite structure. The main drawback of the standard fire protection systems such as paints and intumescent coatings when applied to loaded structures is their tendency to fracture. However, metal protection layers can maintain their integrity when subjected to high heat fluxes and loads. The transmission of temperature from the metallic layer to the underlying material can be compensated by low thermal conductivity and endothermic decomposition of matrix, which in turn reduce the transfer of heat through the composite thickness.

7.3 Equipment modification

It would be very useful to remove the pillars, which support the radiant heater in the cone calorimeter and provide an alternative support arrangement in consultation with the equipment manufacturer. This modification will enable the measurement of fire reaction properties as function of in-plane loads for samples with standard dimensions.

7.4 Heat flux measurement

In order to test the accuracy of thermal model predictions for the net heat flux on the hot face of the composite laminate. There is a need to identify or develop a proper measuring instrument suitable for this type of material, especially to cope with the decomposition products like char.

References

1. A. P. Mouritz and Z. Mathys, 1999. *Post-fire mechanical properties of marine polymer composites.* Composite Structures, **47**: pp. 643-653.

2. A. P. Mouritz and Z. Mathys, 2001. *Post-fire mechanical properties of glass-reinforced polyester composites.* Composites Science and Technology, **61**(4): pp. 475-490.

3. A. G. Gibson. *Basic mechanisms of fire damage in organic matrix composites*. In *Composites in Fire 3: 3rd International Conference on the Response of Composite Materials to Fire*, 2003, Newcastle upon Tyne, England.

4. J. B. Henderson and T. E. Wiecek, 1987. *A mathematical model to predict the thermal response of decomposing, expanding polymer composites.* Journal of Composite Materials, **21**: pp. 373-393.

5. A. G. Gibson, Y-S. Wu, H. W. Chandler, J.A.D. Wilcox and P. Bettess, 1995. *A model for the thermal performance of thick composite laminates in hydrocarbon fires.* Revue de l'Institut Français du Pétrole, **50**(1): pp. 69-74 (special issue).

6. J. B. Henderson, J. A. Wiebelt and M. R. Tant, 1985. *A Model for the thermal response of polymer composite materials with experimental verification.* Journal of Composite Materials, **19**: pp. 579-594.

7. M. Kesner and W. D. Vos, 2001. *Teaching about flame retardants. A joint Israeli-Dutch project.* Journal of Chemical Education, **78**(1): pp. 41-45.

8. F. Le Lay and J. Gutierrez, 1999. *Improvement of the fire behaviour of composite materials for naval application.* Polymer Degradation and Stability, **64**(3): pp. 397-401.

9. N. D. Brown and G. Tipping. *Fire safe polyester composites using aluminium hydroxide*. In *Composites in fire 1: 1st international conference on the response of composites to fire.*, 1999, Newcastle upon Tyne, England.

10. T. Grigoriou. *Phenolic composites- The use of fire safe materials*. In *Composites in fire 1: 1st international conference on the response of composites to fire*. 1999, Newcastle upon tyne, England.

11. N. Dodds, A. G. Gibson, D. Dewhurst and J. M. Davies, 2000. *Fire behaviour of composite laminates.* Composites: Part A, **31**(7): pp. 689-702.

12. A. G. Gibson, P. N. H. Wright, Y-S. Wu, A. P. Mouritz, Z. Mathys and C. P. Gardiner, 2003. *Modelling residual mechanical properties of polymer composites after fire.* Plastics, Rubber and Composites, **32**(2): pp. 81-90.

13. A. G. Gibson, P. N. H. Wright, Y-S. Wu, A. P. Mouritz, Z. Mathys and C. P. Gardiner, 2004. *The Integrity of Polymer Composites during and after Fire.* Journal of Composite Materials, **38**(15): pp. 1283-1307.

14. First edition, 1987. *BS 476-20/21: "Fire tests on building materials and structures. Method for determination of the fire resistance of elements of construction ".* British Standards Institution.

15. A. P. Mouritz and A. G. Gibson, *Fire Properties of Polymer Composite Materials*. Springer, Dordrecht, 2006.

16. J. Bausano, S. Boyd, J. Lesko and S. Case, 2006. *Composite Lifetime During Combined Compressive Loading and one-sided simulated fire exposure.* Composites Part A: Applied Science and Manufacturing, **37**(7): pp. 1092-1100.

17. R. C. Easby, S. Feih, C. Konstantis, G. La Delfa. V. Urso Miano, A. E. Elmughrabi, A. P. Mouritz and A. G. Gibson, 2007. *Failure model for phenolic and polyester pultrusions under load in fire.* Plastics Rubber and Composites, **36**(9): pp. 379-388.

18. S Feih, Z. Mathys, G. Mathys, A. G. Gibson, M. Robinson and A. P. Mouritz, 2008. *Influence of water content on failure of phenolic composites in fire.* Polymer Degradation and Stability, **93**(2): pp. 376-382.

19. A. G. Gibson, P. N. H. Wright, Y-S. Wu and J. T. Evans, 2006. *Laminate theory analysis of composites under load in fire.* Journal of Composite Materials, **40**(7): pp. 639-658.

20. A. G. Gibson, Y-S. Wu, A. L. Naas and R. J. McNaught. *A low cost burner technique for the development and modelling of laminates in fire*. In *Composites in Fire 3: 3rd International Conference on the Response of Composite Materials to Fire*, 2003, Newcastle upon Tyne, England.

21. P. G. B. Seggewiß. *Properties of fire damaged polymer matrix composites*. In *Composites in Fire 3: 3rd international conference on composites in fire*, 2003, Newcastle upon Tyne, England.

22. S. Feih, Z. Mathys, G. Mathys, A. G. Gibson, M. Robinson and A. P. Mouritz, 2008. *Influence of water content on failure of phenolic composites in fire.* Polymer Degradation and Stability, **93**(2): pp. 376-382.

23. S. Feih, Z. Mathys, A. G. Gibson and A. P. Mouritz, 2007. *Modelling the compression strength of polymer laminates in fire.* Composites Part A: Applied Science and Manufacturing, **38**(11): pp. 2354-2365.

24. L. Lui, J. W. Holmes, G. A. Kardomateas and V. Birman. *Compressive response of composites under combined fire and compressive loading*. In *Composies in Fire 4: 4th international conference in composites in fire* 2005, Newcastle upon Tyne, England.

25. R. E. Lyon, J. Demario, R. N. Walters and S. Crowley. *Flammability of glass fibre-reinforced polymer composites*. In *Composites in Fire 4: 4th International Conference on Composites in Fire*, 2005, Newcastle upon Tyne, England.

26. J. H. Koo, F. Muskop, R. Venumbaka, R. Van Dine, B. Spencer and U. Sorathia. *Flammability properties of polymer composites for marine applications.* In *proceedings of the 32nd International SAMPE Technical Conference*, 5-9 November 2000.

27. J. R. Brown and Z. Mathys, 1997. *Reinforcement and matrix effects on the combustion properties of glass reinforced polymer composites.* Composites Part A: Applied Science and Manufacturing, **28**(7): pp. 675-681.

28. H. D. B. Fu-Yu Hshieh, 1997. *Flammability testing of flame-retarded epoxy composites and phenolic composites.* Fire and Materials, **21**(1): pp. 41-49.

29. R. E. Lyon, *Plastics & Rubber*. McGraw-Hill New York 2004

30. A. P. Mouritz, Z. Mathys and A. G. Gibson, 2006. *Heat release of polymer composites in fire.* Composites: Part A, **37**: pp. 1040-1054.

31. A. G. Gibson, A. P. Mouritz, Y-S. Wu, C. P. Gardiner and Z. Mathys. *Validation of the Gibson model for the fire reaction properties of fibre polymer composites*. In *Composites in Fire 3: 3rd international conference on composites in fire*, 2003, Newcastle upon Tyne, England.

32. S. Feih, A. P. Mouritz, Z. Mathys and A. G. Gibson, 2007. *Tensile strength modelling of glass fiber-polymer composites in fire.* Journal of Composite Materials, **41**(19): pp. 2387-2410.

33. S. Feih, Z. Mathys, A. G. Gibson and A. P. Mouritz, 2007. *Modelling the tension and compression strengths of polymer laminates in fire.* Composites Science and Technology, **67**(3-4): pp. 551-564.

34. J. Bausano, S. Boyd, J. Lesko and S. Case. *Composite Lifetime During Combined Compressive Loading and one-sided simulated fire exposureo.* In *Composites in fire 3: 3rd international conference on composites in fire*, 2005, Newcastle upon Tyne, England.

35. T. N. A. Browne, *PhD Thesis: Amodel for the structural integrity of composite laminates in fire*, in *School of Mechanical & Systems Engineering*. 2006, Newcastle University: Newcastle upon Tyne.

36. R. C. Easby, *PhD Thesis: Fire behaviour of pultruded composites*, in *School of Mechanical and Systems Engineering*. 2006, Newcastle University: Newcastle upon Tyne.

37. M. Mukhopadhyay, *Mechanics of Composite Materials and Structures.* Universities Press (India) Private Limited Hyderabad 2004

38. D. Hull, *An Introduction to Composite Materials*. Cambridge University Press Cambridge 1981

39. Isaac M. Daniel and Ori Ishai, *Engineering Mechanics of Composite Materials.* Oxford University Press 1994

40. G. Eckold, *Design snd Manufacture of Composite Structures.* Woodhead Publishing Ltd. Cambridge 1994

41. C. L. Scutte, 1994. *Environmental durability of glass-fibre composites.* Material Science and Engineering, **R13**: pp. 256-324.

42. J. M. Hale, B. A. Shaw, S. D. Speak and A. G. Gibson, 2000. *High temperature failure envelopes for thermosetting composite pipes in water.* Plastics Rubber and Composites, **29**(10): pp. 539-548.

43. P. C. Almenara and P. Thornburrow. *A new glass fibre reinforcement for anti-corrosion composites*. In *Advanced Polymer Composites for Structural Applications in Construction*, 2004, University of Surrey, Guilford, England: Woodhead Publishing Ltd.

44. B. D. Agarwal and L. J. Broutman, *Analysis and performance of fiber composites*. John Wiley & Sons, Inc. Chichester 1990

45. *Pictures courtesy of Hongzhou Mingda Glass Fibre Co. Ltd. (http://mingdafibreglass.en.alibaba.com/product).*

46. *Pictures courtesy of Netcomposites (http://www.netcomposites.com).*

47. *Pictures courtesy of Opti-x (http://www.opti-x.dk).*

48. A. H. Charles, *Handbook of Plastics, Elastomers, and Composites*1996

49. *Glass reinforced plastics*. Butterworth & Co. Ltd. London 1970

50. J. Murphy, *The Reinforced Plastics Handbook.* Elsevier Advanced Technology Oxford 1994

51. R. O. Saied, *Failure envelopes for filament wound composite tubes in water at elevated temperatures*, in *School of Mechanical & Systems Engineering.* 2004, Newcastle University: Newcastle upon Tyne. UK.

52. *Resin systems for use in Fibre-Reinforced Composite Materials (http://www.azom.com).*

53. H. Zhang, *Fire-safe polymers and polymer composites*. 2004, Office of aviation research, USA: Washington, DC.

54. V. Babrauskas and U. Wickström. *The rational development of bench-scale fire tests for full-scale fire prediction*. In *Proceedings of the 2nd International Fire Safety Science Symposium*, 1989.

55. V. Babrauskas., 1991. *Effective measurement techniques for heat, smoke, and toxic fire gases.* Fire Safety Journal, **17**: pp. 13-26.

56. V. Babrauskas, 1992. *The cone calorimeter, in heat release in fire.* Elseiver applied science.

57. Second Edition, 2002. *ISO 5660-1: "Reaction-to-fire tests - Heat release, smoke production and mass loss rate - Part 1: (cone calorimeter method)".* International Organization for Standardization.

58. First edition, 1996. *ISO 4589: "Plastics - Determination of burning behaviour by oxygen index".* International Organization for Standardization.

59. E. Greene, *Marine Composites, www.marinecomposites.com*1999

60. . *http://www.fire-proof.co.uk.*

61. V. Babrauskas and R. D. Peacock, 1992. *Heat release rate: The single most important variable in fire hazard.* Fire Safety Journal, **18**(3): pp. 255-272.

62. *Pictures courtesy of Qualitest (http://www.qualitest-inc.com).*

63. *Pictures courtesy of the Bolton Fire Materials Laboratory, University of Bolton, (http://www.bolton.ac.uk/fire).*

64. 2000. *ASTM E 176: "Standard terminology of fire standards".* ASTM International.

65. First edition, 1998. *ISO 5659-2: "Plastics - Smoke generation - Part 2: Determination of optical density by a single-chamber test".* International Organization for Standardization.

66. *Pictures courtesy of the Tin Technology website (http://www.tintechnology.com).*

67. *Pictures courtesy of fire testing technology website (http://www.fire-testing.com).*

68. 2002. *ASTM E 162-02a: "Standard test method for surface flammability of materials using a radiant heat energy source".* ASTM International.

69. R. M. Morchat. and J. A. Hiltz. *Fire-safe composites for marine applications.* In *The 24th International SAMPE Technical Conference.*, 1992.

70. *Pictures courtesy of Govmark Fire Labaoratories (http://www.govmark.com).*

71. First edition, 2002. *BS EN 13823: "Reaction to fire for building products. Building products excluding floorings exposed to the thermal attack by a single burning item".* British Standards Institution.

72. *http://www.sp.se/sv/units/fire/PublishingImages/Material/ISO9705-col-txt.gif.*

73. First edition, 1993. *ISO 9705: "Fire Tests - Full-scale room test for surface products".* International Organization for Standardization.

74. A. H. Buchanan, *Structural Design for Fire Safety*. John Wiley & Sons Ltd Chichester 2001

75. 1988. *ASTM E 199-88 "Standard test methods for fire tests of building construction and materials".* ASTM International.

76. B. R. Kirby, D. E. Wainman, L. N. Tomlinson, T. R. Kay and B. N. Peacock, 1999. *Natural fires in large scale compartments.* International Journal on Engineering Performance-Based Fire Codes, **1**(2): pp. 43-58.

77. First edition, 1999. *ISO 834-3: "Fire resistance tests - Elements of building construction - Part 3: Commentary on test method and test data application".* International Organization for Standardization.

78. M. A. Sultan, 1996. *The effect of furnace parameters on fire severity in standard fire resistance tests.* Fire & Materials, **20**: pp. 245-252.

79. *Pictures courtesy of SINTEF, the Norwegian Fire Resource Centre (http://www.sintef.no).*

80. *Picture courtesy of ULC (http://www.esemag.com).*

81. *Pictures courtesy of the Advantica Ltd. website (http://www.spadeadam.biz).*

82. P. S. Hill and G. C. White. *Jet fire testing and performance of composite materials.* In *Composites in fire 1: 1st international conference on composites in fire*, 1999, Newcastle upon Tyne, England.

83. J. Folkers. *Fire testing and performance of fiber glass pipe.* In *Composites in fire 1: 1st international conference on composites in fire*, 1999, Newcastle upon Tyne, England.

84. A. P. Kulcami and R. F. Gibson. *Non-destructive characterisation of effects of temperature and moisture on elastic moduli of vinyl ester resin and E-glass/vinyl ester resin composite.* In *Proceedings of the American Society of Composites, 18th Annual Technical Conference*, 2003, Florida.

85. J. Bausano, S. Boyd, J. Lesko and S. Case. *Composite Lifetime During Combined Compressive Loading and one-sided simulated fire exposure*. In *Composites in fire 3: 3rd international conference on composites in fire*, 2003, Newcastle upon Tyne, England.

86. J. Lua and J. O'Brien. *Fire simulation for woven fabric composites with temperature and mass dependent thermal mechanical properties*. In *Composites in Fire 3: 3rd international conference on composites in fire*, 2003, Newcastle upon Tyne, England.

87. C. A. Mahieux and K. L. Reifsnider, 2001. *Property modeling across transition temperatures in polymers: a robust stiffness–temperature model.* Polymer, **42**(7): pp. 3281-3291.

88. C. A. Mahieux and K. L. Reifsnider, 2002. *Property modelling across transition temperatures in polymers.* Journal of Materials Science, **37**: pp. 911-920.

89. M. Robinson. *Modelling fire reaction properties of composites for rail applications*. In *Composites in fire 4: 4th International Conference on Composites in Fire*, 2005, Newcastle upon Tyne, England.

90. E. J. Kansa, H. E. Perlee and R. F. Chaiken, 1977. *Mathematical model of wood pyrolysis inlcuding internal forced convection.* Combustion and Flame, **29**: pp. 311-324.

91. H. C. Kung, 1972. *A mathematical model of wood pyrolysis.* Combustion & Flame, **18**: pp. 185-195.

92. C. H. Bamford and D. H. Malan, 1946. *The combustion of wood, Part 1.* Proceedings of the Cambridge Philosophical Society, **42**: pp. 166-182.

93. T. R. Munson and R. J. Spindler, *Transient thermal behaviour of decomposing materials: Part 1 General theory and application to convective heating*. in *RAD-TR-61-10*. 1961, AVCO Corporation.

94. B. Fredlund, 1993. *Modelling of heat and mass transfer in wood structures during fire.* Fire Safety Journal, **20**: pp. 39-69.

95. C. I. Chang, 1986. *Thermal effects on polymer composite structures.* Theoretical & Applied Fracture Mechanics, **6**: pp. 113-120.

96. R. J. Asaro, M. Dao and N. Schultz, 1998. *Fire protection techniques for commerical vessels: structural fire protection modelling.* Flame Retardant Polymers: pp. 113-127.

97. J. Milke and A. J. Vizzini, 1991. *Thermal response of fire-exposed composites.* Journal of Composites Technology & Research, **13**: pp. 145-151.

98. J. A. Charles and D. W. Wilson, 1981. *A model for passive thermal non-destructive evaluation of composite laminates.* Polymer Composites, **2**: pp. 105-111.

99. G. A. Pering, P. V. Farrell and G. S. Springer, 1980. *Degradation of tensile and shear properties of composites exposed to fire or high temperature.* Journal of Composite Materials, **14**: pp. 54-66.

100. M. R. E. Looyeh, P. Bettess and A. G. Gibson, 1997. *A one-dimensional finite element simulation for the fire-performance of GRP panels for offshore structures.* International Journal of Numerical Methods for Heat & Fluid Flow. **7**(6): pp. 609-625.

101. M. R. E. Looyeh and P. Bettess, 1998. *A finite element model for the fire performance of GRP panels including variable thermal properties.* Finite Elements in Analysis & Design. **30**: pp. 313-324.

102. C. P. Gardiner, Z. Mathys and A. P. Mouritz, 2002. *Tensile and compressive properties of FRP composites with localised fire damage.* Applied Composite Materials, **9**(6): pp. 353-367.

103. A. P. Mouritz, 2003. *Simple models for determining the mechanical properties of burnt FRP composites.* Materials Science and Engineering A, **359**(1-2): pp. 237-246.

104. A. P. Mouritz, S. Fieh, Z. Mathys and A. G. Gibson, 2006. *Mechanical property degradation of naval composite materials, In: Modelling of Naval Composite Structures in Fire, ed. L. Couchman and A. P. Mouritz.*

105. G. H. Staab, *Laminar Composites*. Butterworth - Heinemann Woburn 1999

106. A. G. Gibson, Y-S. Wu, T. N. A. Browne and A. P. Mouritz. *Laminate theory analysis of composites under load in fire*. In *Composites in Fire 4: 4th International Conference on Composites in Fire*, 2005, Newcastle upon Tyne, England.

107. 2000. *ASTM D 792-00: "Standard test methods for density and specific gravity (relative density) of plastics by displacement. Method A - For testing solid plastics in water".* ASTM International.

108. V. Babrauskas, 1997. *Why was the fire so big? HRR: The role of heat release rate in described fires.* Fire & Arson Investigator, **47**: pp. 54-57.

109. C. Hugget, 1980. *Estimation of rate of heat release by means of oxygen consumption measurements.* Fire & Materials, **4**: pp. 61-65.

110. M. Janssens and W. J. Parker, *Oxygen consumption calorimetry. In: Heat Release in Fires, ed. Babrauskas V. and Grayson S. J.*London 1992

111. *Pictures courtesy of SpecialChem (http://www.specialchem4polymers.com).*

112. S. J. Ritchie, K. D. Steckler, A. Hamins, T. G. Clearly, J. Yang and T. Kashiwagi, 1997. *The effect of sample size on the heat release rate of charring materials.* Fire safety science: Proceedings of the fifth international symposium. **5**: pp. 177-188.

113. B. Y. Lattimer, S. P. Hunt, M. Wright and U. Sorathia, 2003. *Modeling fire growth in a combustible corner.* Fire Safety Journal, **38**(8): pp. 771-796.

114. J. E. Brown, E. Braun and W. H. twilley, *Cone calorimeter evaluation of the flammability of composite materials. Technical report NBSIR 88-3733.* 1988. National Bureau of standards, Centre for fire research.

115. A. T. Grenier, N. A. Dembsey and J. R. Barnett, 1998. *Fire characteristics of cored composite materials for marine use.* Fire Safety Journal, **30**(2): pp. 137-159.

116. G. T. Egglestone, 1994. *Flammability of GRP for use in ship superstructures.* Fire and Materials, **18**: pp. 255-260.

117. M. M. Hirschler, 1987. *Fire hazard and toxic potency of the smoke of burning materials.* Journal of Fire Sciences, **5**: pp. 289-307.

118. D. Drysdale, *Fire science and combustion. In an introduction to fire dynamics, chapter 1.* John Wiley and Sons New York 1985

119. O. Grexa. *Fundamental thermophysical properties of materials derived from the cone calorimeter measurements.* In *3rd International Scientific Conference: Wood & Fire Safety*, 1996, Technical University Zvolen, Slovakia.

120. J. E. Staggs, 2004. *The heat of gasification of polymers.* Fire Safety Journal. **39**(8): pp. 711-720.

121. J. G. Quintiere, 1993. *A simulation model for fire growth in materials subject to a room-corner test.* Fire Safety Journal, **20**: pp. 313-339.

122. B. K. Kandola, A. R. Horrocks, P. Myler and D. Blair, 2001. *Thermal characterisation of thermoset matrix resins. In: ACS Series 797 Fire and Polymers, Eds G. L. Nelson and C. A. Wilkie, American Chemical Society, PP344-360*

123. B. Budiansky and N. A. Fleck, 1993. *Compressive failure of fibre composites.* J. Mech. Phys. Solids, **41**(1): pp. 183-211.

124. B. Budiansky, N. A. Fleck and J. C. Amazigo, 1998. *On kink-band propagation in fiber composites.* J. Mech. Phys. Solids, **46**(9): pp. 1637-1653.

125. S. Feih, Z. Mathys, A. G. Gibson and A. P. Mouritz. *Property degradation of fibreglass composites in fire*. In *Composites in Fire 4: 4th International Conference on Composites in Fire*, 2005, Newcastle upon Tyne, England.

126. L. Liu, J. W. Holmes, G. A. Kardomateas and V. Briman, 2006. *Compressive response of composites under combined fire and compression loading, In: Modelling of Naval Composite Structures in Fire, ed. L. Couchman and A. P. Mouritz, [chapter 3].*

127. N. Regnier and B. Mortaigne, 1995. *Analysis by pyrolysis/gas chromatography/mass spectromy of glass fibre/vinyl ester thermal degradation products.* Polymer Degradation and Stability, **49**: pp. 419-428.

128. H. L. Friedman. *Kinetics of thermal degradation of char-forming plastics from thermogravimetry: Application to a phenolic plastic*. In *Proceedings of the 136th American Chemical Society meeting*, 1959, Atlantic City, NJ.

129. S. Feih, A. P. Mouritz and Z. Mathys, *Finding kinetic parameters from TGA curves with a multi-branch least squares fit. TR05002, CRC-ACS.* 2005.

130. *http://www.gnuplot.info*.

131. B. Y. Lattimer. *Predicting cone calorimeter data using heat and mass transfer decomposition models*. In *Composites in Fire 5:5th International Conference on the Response of Composite Materials to Fire*, 2008, Newcastle upon Tyne, England.

132. J. Gutierrez. *Use of fire safety Engineering for the design of marine composite structures*. In *Composites in Fire 5:5th International Conference on the Response of Composite Materials to Fire*, 2008, Newcastle upon Tyne, England

133. V. Babrauskas, *Ignition Handbook*. Fire Science Publishers WA 2003

134. R. Lyon. *Piloted igntion of some solids*. In *Fire and Materials: 9th International conference and exhibition* 2005, San Francisco, California, USA: Interscience Communications.

135. K. A. Stroud, *Engineering Mathematics: programs and problems*. The Macmillan press ltd London 1987

List of Publications

- T. N. A. Browne, R. C. Easby, A. Elmughrabi, A. G. Gibson and A. P. Mouritz, *Composite structures under load in fire.* In: Characterisation and Modelling Procedures of DURACOSYS (Durability of Composite Systems), 2006. Virginia Tech., Blacksburg VA, USA.

- R. C. Easby, S. Feih, C. Konstantis, G. La Delfa, V. Urso Miano, A. Elmughrabi, A. P. Mouritz and A. G. Gibson, 2007. *Failure model for phenolic and polyester pultrusions under load in fire*. Plastics, Rubber and Composites, 2007. **36**(9): pp. 379-388.

- A. Elmughrabi, M. Robinson and A. G. Gibson, 2008. *Effect of stress on the fire reaction properties of polymer composite laminates*. Polymer Degradation and Stability, **93**(10): pp. 1877-1833.

Appendix

1 Fitting with Gnuplot, Multi-branch fitting procedure

```
#Functions to be fitted (two different heating rates) Tm1-Tm2 and HR-HR2, var1 and
var2.
f1(x)=wf+(100 - wf)*(exp(-((var1)/HR1)*((exp(1)*Tm1)/(var2/(R*Tm1) +
1))*((x/(exp(1)*Tm1))**(var2/(R*Tm1) + 1) - (T0/(exp(1)*Tm1))**(var2/(R*Tm1) +
1))))
f2(x)=wf+(100 - wf)*(exp(-((var1)/HR2)*((exp(1)*Tm2)/(var2/(R*Tm2) +
1))*((x/(exp(1)*Tm2))**(var2/(R*Tm2) + 1) - (T0/(exp(1)*Tm2))**(var2/(R*Tm2) +
1))))

FIT_LIMIT = 1e-9
#Final resin content - FIXED
#Needs to be adjusted according to experimental data
wf=4.2

#Room temperature in Kelvin
T0=273.0

#Gas constant
R=8.3143

#Experimental heating rates (in C/sec)
#25C/min, 40C/min
HR1=0.4166
HR2=0.6667

#Temperature at which fastest mass loss occurs.
#Needs to be adjusted according to experimental data
Tm1=723
Tm2=750

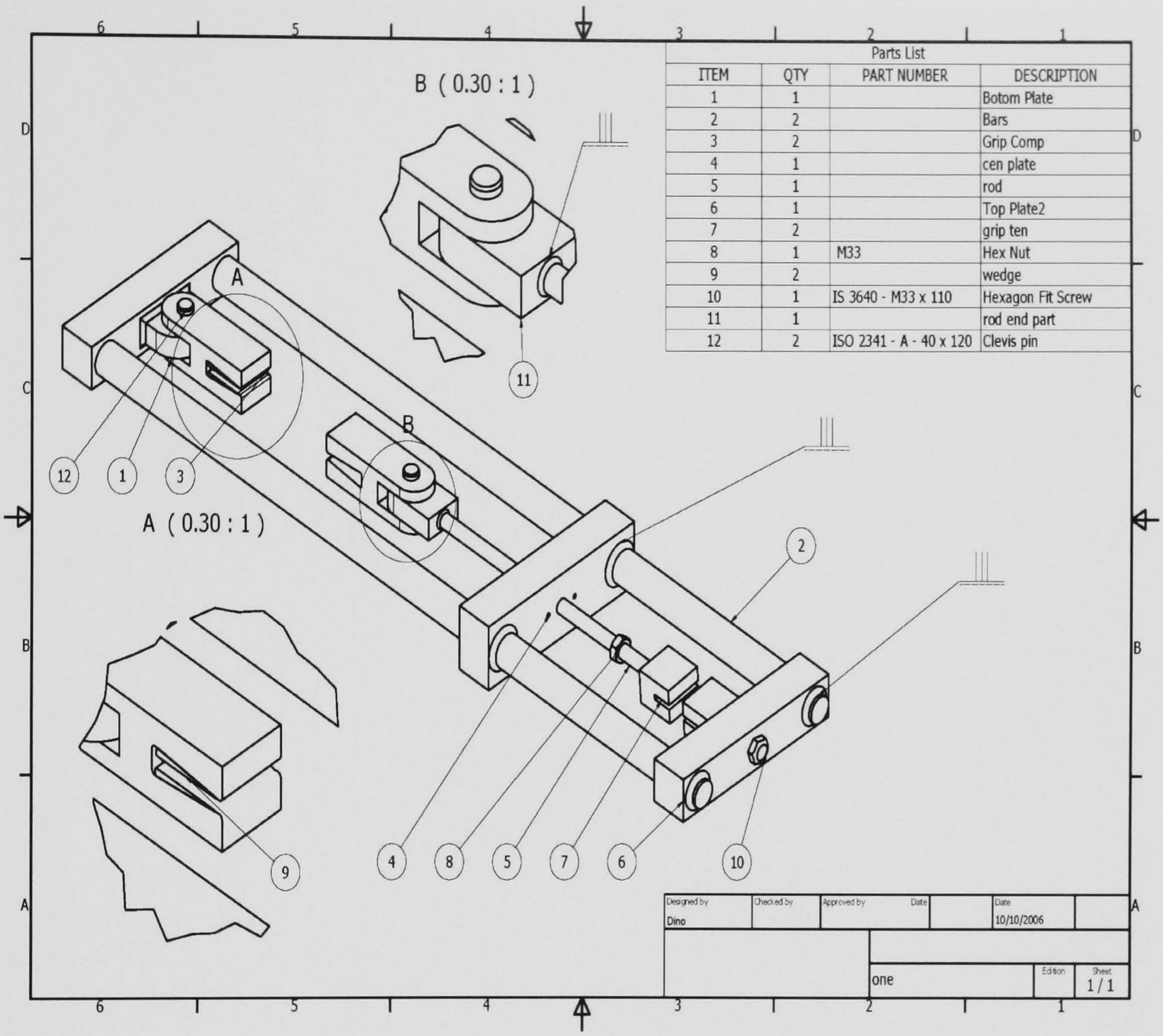
#Starting values. Can most likely remain for common resin systems
var1 = 9e10
var2 = 1.8e5

#Fit function. y is a dummy variable determining which data set to use (see Gnuplot
help).
h(x,y) = (y == 0) ? f1(x) : ((y==1) ? f2(x) : f3(x))
fit [500:850] h(x,y) 'TGA DATA.txt' using 1:-2:2:(1) via var1, var2
```

2 Thermal properties data for glass vinyl ester and glass polyester composites

Property	Glass vinyl ester		Glass polyester	
	Value	**Method**	**Value**	**Method**
Volume fraction, V_f	0.456	Burn off test	0.437	Burn off test
Rate constant, A (1/s)	1×10^{12}	TGA	1×10^{10}	TGA
Activation energy, E (J/mol)	1.93×10^{5}	TGA	1.61×10^{5}	TGA
Remaining resin mass fraction, m_f (%)	4	TGA	2	TGA
Specific heat, $C_{Pe\text{-}glass}$ (J/kg.K)	760	Literature [5]	760	Literature [5]
Specific heat resin, C_{Presin} (J/kg.K)	1800	Literature [5]	1600	Literature [5]
Specific heat gas, C_{Pgas} (J/kg.K)	2386.5	Literature [5]	2386.5	Literature [5]
Thermal conductivity, $k_{e\text{-}glass}$ (W/m K)	1.09	Literature [15]	1.09	Literature [15]
Thermal conductivity composite, k (W/m K)	0.43	Rule of mixture	0.43	Rule of mixture
Density glass, ρ_{glass} (g/cm^3)	2.54	Literature [44]	2.54	Literature [44]
Density resin, ρ_{resin} (kg/m^3)	1120	Manufacturer	1200	Manufacturer

3 Engineering drawing of the small scale testing rig



Parts List			
ITEM	QTY	PART NUMBER	DESCRIPTION
1	1		Botom Plate
2	2		Bars
3	2		Grip Comp
4	1		cen plate
5	1		rod
6	1		Top Plate2
7	2		grip ten
8	1	M33	Hex Nut
9	2		wedge
10	1	IS 3640 - M33 x 110	Hexagon Fit Screw
11	1		rod end part
12	2	ISO 2341 - A - 40 x 120	Clevis pin